Evaluation of tridactyl theropod tracks in southern Africa: quantitative morphometric analysis across the Triassic–Jurassic boundary

By

Miengah Abrahams

Supervisor: Associate Professor Emese M. Bordy

Co-supervisor: Dr Fabien Knoll

A thesis submitted in fulfilment of the requirements for the degree of Doctor of Philosophy in the Department of Geological Sciences, Faculty of Science, University of Cape Town

April 2020

Declaration

I declare that this thesis is my own original work and where I have been aided, it is noted in the text. This thesis is submitted for the degree of Doctor of Philosophy at the Faculty of Science, University of Cape Town and has not been submitted in the past for a degree or examination at any other University.

Signed by candidate

(Signature of Candidate)

11 April 2020

Acknowledgements

Special thanks to my main supervisor Associate Professor Emese Bordy for all her support and encouragement throughout my years of study. Thank you for your undying belief that I could achieve this dream of mine.

I would like to thank my co-supervisor Dr Fabien Knoll for kind words of encouragement and swift replies even though we are 12 000 km apart. Special thanks for planning a memorable fieldtrip, my first European tracking experience.

A heart felt thank you to my family and close friends who went on this journey with me. I appreciate you all for grounding me during this rollercoaster adventure. Special thanks to my Mother and elder Brother who understand, among other things, the true value of a cold coke. My sincere admiration and gratitude go to Berts, Lucre and Dr Rob for cheering me on.

Thank you to my friends in the 'fifth floor seds-palaeo group' for making the years fly by! Thanks to the members of the UCT dino-tracking team with whom I shared too many good memories to simply name one here. Special shout outs to Lara, Mhairi, Howard, Akhil and Chad for the good chats, advice and overall support. Thanks to Team Zircon for all things U-Pb.

Sincere thanks are also due to my academic mentor, Dr Alastair Sloan, with whom conversations over the last year have been precious for both my academic and personal growth.

Thank you to various colleagues whom I've met at conferences for insightful discussions and probing questions that have helped me better this body of work.

The warmest of Thank yous to all the southern Africans I encountered in the field, particularly the Basotho children for their curiosity, overall joy of life, and genuine enthusiasm for visitors.

The research component of this project was supported from the following research grants obtained by my supervisor, A/Prof Emese Bordy: National Research Foundation (NRF) of South Africa Competitive Programme for Rated Researches (CPRR) and African Origins Programme (AOP) [grant numbers 93544, 113394, 98825] and DST-NRF Centre of Excellence in Palaeosciences [CoE PAL 2015, 2019]. I would also like to acknowledge the following financial support that I personally received as postgraduate bursaries from the:

- Centre of Excellence in Palaeosciences in 2016, 2017 and 2018
- National Research Foundation of South Africa in 2016 and 2017
- University of Cape Town, Association of Sedimentologists (IAS) and the Society for Sedimentary Geology (SEPM) for funding various conference attendances in 2017 and 2019.

Abstract

In the Mesozoic, dinosaur abundance and diversity steadily increased from the Carnian to the Triassic booming soon after the end Triassic Mass-Extinction event (ETE), marking a key period in archosaur history. In southern Africa, the Triassic–Jurassic Boundary (TJB) is contained in the richly fossiliferous, fluvio-lacustrine-aeolian Upper Triassic to Lower Jurassic strata of the Stormberg Group. More specifically, the middle Norian – Pliensbachian Elliot and Clarens formations (upper Stormberg Group) of main Karoo Basin, host a diverse tetrapod osteological and ichnite record. Due to an absence of high resolution radioisotopic age determinations, the exact stratigraphic placement of the TJB remains unknown. Although diverse ichnofossils attributed to Saurischians and Ornithischians are preserved in the Stormberg Group, the record is dominated by isolated tridactyl tracks that can be assigned to common ichnogenera like *Grallator, Eubrontes* and *Kayentapus*. Ideally, these track morphologies would reflect the trackmaker's autopod morphology, but complex interactions between the trackmaker and tracking substrate may affect the final footprint shape. Tracks with a high morphological preservation grade may be used to infer information (e.g., body length, hip height, weight) about the trackmaker, which is especially useful when skeletal remains are scarce, as is the case with theropod body fossils in the Elliot and Clarens formations. Herein, we present the findings of an extensive southern African field-based study to quantify the morphological variation of *Grallator, Eubrontes* and *Kayentapus* tracks across the TJB in the upper Stormberg Group. Furthermore, this study produced the first detrital zircon Uranium–Lead (U-Pb) LA-ICPMS ages of the major ichnosites from this region, and confirmed that the TJB is within the Elliot Formation, near the boundary of the lower and upper Elliot Formation (i.e., near the contact of the informal lEF and uEF). Across this contact, the considered tridactyl tracks become more abundant, larger and have a less pronounced medial digit projection. These morphological changes are gradational, with tracks from the Clarens Formation being distinct to tracks from the lEF, while the uEF tracks being intermediate between the lEF and Clarens Formation. A decrease in the mesaxony (Dp/TS ratio) and a decrease in medial digit projection relative to track length can be detected in both small and large tridactyl tracks. These apparent trends in the upper Stormberg Group are consistent with global tridactyl trends, which suggest an overall increase in theropod abundance and body size across the Jurassic. Moreover, the reason for the less prominent medial pedal digit is linked to a better weight distribution across the autopod in the increasingly larger theropods. Last but not least, *Grallator, Eubrontes* and *Kayentapus* ichnogenera which may be attributed to at least three different groups of theropod-like trackmakers, suggest a higher palaeo-diversity and abundance of tridactyl dinosaurs in southern Africa than is known from the osteological record.

Table of Contents

1 Introduction

The main Karoo Basin of southern Africa (Lesotho and South Africa) is globally recognised for containing one of the world's thickest successions of continental sedimentary rocks (i.e., the Karoo Supergroup) that records ~117 Ma of geological history and at least three major mass extinction events that occurred approximately ~260, ~250 and ~200 million years ago. The fluvio-lacustrine and aeolian Triassic–Jurassic rocks of the Stormberg Group, the youngest sedimentary group in the Karoo, encapsulates the end-Triassic Mass Extinction event (ETE) and preserves a broad suite of vertebrate body and trace fossils. These rocks, their ancient life remains, including their taphonomy, thus hold important messages about the dynamics of the palaeoecological system in southern Gondwana in the early Mesozoic. In spite of this recognized biogeological potential and the several high-quality outcrops of the Molteno, Elliot and Clarens formations in the Stormberg Group, critical contextual information concerning the sedimentology, stratigraphy, rate and magnitude of the continental biotic turn-over across the Triassic–Jurassic Boundary (TJB), and the dynamics of biotic changes and recovery after the ETE have only been outlined in a handful of preliminary and regional-scale studies (e.g., Ellenberger, 1970; Kitching and Raath, 1984; Bordy *et al*., 2004a, b, c; Knoll, 2005; Sciscio *et al*., 2017a; McPhee *et al*., 2017).

The ETE has long been considered as one of the five largest mass extinctions in the Phanerozoic (Raup and Sepkoski, 1982; McElwain *et al*., 1999). The validity of the hypothesis, that there was a single rapid, severe ETE, has repeatedly been questioned by some authors who propose that the latter part of the Triassic, instead, records a series of extinctions that are stratigraphically poorly resolved (e.g., Lucas *et al*., 2011; 2015, 2018). In the marine realm, the ETE is recorded by the extinction of conodonts, the disappearance of many ammonoids and a sudden shift in the size and composition of various marine families (e.g., Palfy *et al*., 2007), while in the continental realm, the evidence for a distinct event is more tenuous and has primarily focused on tetrapod vertebrates, which do not illustrate a sudden or severe extinction (e.g., Lucas *et al*., 2011, 2015). Because the ETEs occurred both in the marine and continental realms, correlation of these events across the TJB in both environments, is paramount to understanding the chronology of the extinction events. This is made more difficult by a deficiency of continuous Norian (Late Triassic) to Hettangian (Early Jurassic) continental successions, such as the Karoo Supergroup, which adequately preserve the information needed to evaluate these events as they occurred in continental settings. However, the chronostratigraphy of the Triassic–Jurassic Stormberg Group has historically relied on biostratigraphic arguments (e.g., Ellenberger, 1970; Anderson and Anderson, 1983, 1984; Kitching and Raath, 1984; Lucas and Hancox, 2001; Knoll, 2004, 2005), and to date, lacks high resolution radiometric dating, which may hinder global correlations.

Since the coining of the term Dinosauria in 1841 by Sir Richard Owen, this group of archosaurs has enraptured the imagination of most naturalists. To date, controversy still surrounds the evolutionary history of early dinosaurs, their phylogenetic relationships, the overall dinosaur family tree (Baron *et al.*, 2017), and even the timing of their origin is hotly contested as the osteological and ichnological records are incongruent (e.g., Marsicano *et al*., 2007; Brusatte *et al*., 2011). During the first 30 million years of their evolution, dinosaurs constituted a relatively morphologically non-diverse group of land-dwelling vertebrates compared to contemporaneous crurotarsans with which they shared many ecosystems in the Late Triassic (Brusatte *et al.*, 2008). It has been hypothesised that events associated with the end-Triassic Mass Extinction event, which removed the competitors of dinosaur, played a vital role in the global evolutionary radiation of Dinosauria at the start of the Jurassic (e.g., Olsen *et al.,* 2002, 2011). The earliest Jurassic records an important increase in dinosaur diversity and abundance (Brusatte *et al.,* 2008) and is thus a period of interest because it encompasses a post-extinction recovery period during which dinosaurs continued to thrive and diversify globally. Furthermore, it has been hypothesised that an abrupt, significant increase in body size occurred after the TJB due to "ecological release" post-dating the extinction of dinosaur competitors (Olsen *et al.,* 2002) but this view remains contested (e.g., Lucas *et al.*, 2006, Lucas and Tanner, 2006).

Historically, the dinosaurian osteological record has been favoured over the trace fossil record, despite documentation of dinosaur tracks dating back to the 1800s (e.g., Hitchcock, 1836; Degenhardt, 1839; Dieterlin, 1885). It was not until the 1970s, when a "dinosaur renaissance" of footprints occurred and the number of global studies began to flourish. In southern Africa, macrovertebrate ichnofossils, especially dinosaur tracks and trackways, were intensely studied and classified by Ellenberger (1955, 1970, 1972), Ellenberger and Ellenberger (1958) and Ellenberger *et al.* (1963) from the Karoo strata of Lesotho. In addition to a wealth of information detailing the ichnology, palaeontology and palaeobotany of the upper Karoo Supergroup, Ellenberger also established the first crude biozonation of this unit (e.g., Molteno and lower Elliot formations encompassing zones A1–A7, the upper Elliot and Clarens formations comprising zones B1–B7, and the Drakensberg Group consisting of zones C1–C7). Ellenberger's extensive ichnotaxonomy was reviewed by Olsen and Galton (1984), who significantly reduced the number of southern African ichnotaxa through synonymisation.

Aims

The ichnological study presented herein focuses on tridactyl tracks with a theropod affinity from the Elliot and Clarens formations of southern Africa (upper Stormberg Group). The aim of this study is to quantify the morphological variation of these tracks. The specific objectives of this study are to:

a) Generate an extensive, high-resolution track database[1] (including standardised measurements, 3D models of tracksites and individual tracks, and revised ichnotaxonomy),
b) Produce the first chronostratigraphic framework[2] for the upper Stormberg Group using Uranium–Lead (U-Pb) radioisotopic dating of detrital zircons via LA-ICPMS techniques,
c) Quantify track morphological variations across the TJB,
d) Quantify track morphological variations across the *Kayentapus-Grallator-Anchisauripus-Eubrontes* (K-GAE) plexus, which are some of the most well-documented and defined tracks attributed to theropod trackmakers, and
e) Compare the southern African tracks and trends to global data.

Theropod osteological remains are scarce in the Stormberg Group (Kitching and Raath, 1984; Smith and Kitching, 1997; Chinsamy, 2002; Yates, 2005. Therefore, the high abundance of theropod tracks preserved offer much needed evidence to understand the palaeodiversity, palaeoabundance and evolutionary history of southern African theropods.

---

1. *Track measurements, interpretative track outlines and ichnotaxonomic assignments obtained during the course of this PhD, have contributed to the ichnological publications listed below:*

Sciscio, L., Bordy, E.M., Reid, M., **Abrahams, M.** 2016. Sedimentology and ichnology of the Mafube dinosaur tracksite (Lower Jurassic, eastern Free State, South Africa): a report on footprint preservation and palaeoenvironment. *PeerJ*, DOI 10.7717/peerj.2285

Abrahams, M., Bordy E.M., Sciscio, L., Knoll, F. 2017. Scampering, trotting, walking tridactyl bipedal dinosaurs in southern Africa: ichnological account of a Lower Jurassic palaeosurface (upper Elliot Formation, Roma Valley) in Lesotho. *Historical Biology*, DOI: 10.1080/08912963.2016.1267164

Bordy, E.M., **Abrahams, M.,** Sciscio, L. 2017. The Subeng vertebrate tracks: stratigraphy, sedimentology and a digital archive of a historic Upper Triassic palaeosurface (lower Elliot Formation), Leribe, Lesotho (southern Africa). *Bollettino della Societa Paleontologica Italiana*, 56: 181 – 198. doi:10.4435/BSPI.2017.12

Sciscio, L., Bordy, E.M., **Abrahams, M.**, Knoll, F., McPhee, B.W. 2017. The first megatheropod tracks from the Lower Jurassic upper Elliot Formation, Karoo Basin, Lesotho. *Plos One* 12 (10): e0185941. https://doi.org/10.1371/journal.pone.0185941

Rampersadh, A., Bordy, E.M., Sciscio, L., **Abrahams, M.** 2018. Dinosaur behaviour in an Early Jurassic palaeoecosystem – uppermost Elliot Formation, Ha Nohana, Lesotho*. Annales Societatis Geologorum Poloniae*, 88: https://doi.org/10.14241/asgp.2018.010

Abrahams, M.,Sciscio, L., Reid, M., Haupt, T., Bordy, E. M. 2020. Large tridactyl tracks from the Early Jurassic of southern Gondwana – uppermost Elliot Formation, Upper Moyeni, Lesotho. *Annales Societas Geologorum Poloniae*, 90: doi: https://doi.org/10.14241/asgp.2020.07

Sciscio, L., Bordy, E.M., Lockley, M.G., **Abrahams, M.**, Reid, M. In review. Basal sauropodomorph locomotion: lessons on bipeds and early quadrupeds from two Late Triassic ichnosites (Elliot Formation) in Lesotho.

An additional paper, based on the Tiskoane ichnosite, is presented in Chapter 5 of this thesis:

Abrahams, M., Brody, E.M., Knoll, F. 2020. Hidden for one hundred years: a diverse theropod ichnoassemblage and cross-sectional tracks preserved from the historic Early Jurassic Tsikoane ichnosite (Clarens Formation, northern Lesotho, southern Africa). *Historical Biology*, DOI: 10.1080/08912963.2020.1810681

2. *A detailed assessment of the geochronological data obtained during the course of this PhD is integrated into the following review paper, which was recently published:*

Bordy, E.M., **Abrahams, M.**, Sharman, G.R., Viglietti, P.A., Benson, R.B.J., McPhee, B.W., Barrett, P.M., Sciscio, L., Condon, D., Mundil, R., Rademan, Z, Jinnah, Z., Clark, J.M., Suarez, C.A., Chapelle, K.E.J., Choiniere, J.N. 2020. A chronostratigraphic framework for the upper Stormberg Group: implications for the Triassic Jurassic boundary in southern Africa. *Earth Science Reviews*, 203: doi.org/10.1014/j.earscirev.2020.103120

2 Background

2.1 Geological Background: The main Karoo Basin

The asymmetrical, northward thinning main Karoo Basin predominantly preserves clastic sedimentary rocks and minor igneous rocks, which together make up the Karoo Supergroup. With a maximum preserved thickness of ~6 km in the south (Johnson, 1976; Lindeque *et al*., 2011; Tankard *et al.,* 2012*;* Scheiber-Enslin *et al.,* 2015), the Karoo Supergroup spans in age from the Late Carboniferous to the Early Jurassic. Clastic sedimentation stopped soon after the initial extrusion of the Karoo flood basalts and accompanying dolerite sills and dykes ~183 Ma ago (Johnson *et al.*, 1997, Duncan *et al.,* 1997; Hanson *et al*., 2009). Today, the basin covers approximately two-thirds of southern Africa (700 000 km^2) but it was more extensive in the pre-Cretaceous (Fig. 2.1; e.g., Visser, 1987; Hanson *et al*., 2009; Muir *et al*., 2020).

The ~117 million-year rock record in the Karoo preserves a rich heritage of body and trace fossils, including, but not limited to, pseudosuchians, lepidosaurs, dinosaurs, turtles, temnospondyl amphibians, mammiliaforms, as well as diverse Permo-Triassic plant assemblages dominated by *Dicroidium* (e.g., Anderson and Anderson, 1970; Ellenberger, 1970, 1972, 174; Kitching and Raath, 1984; Anderson *et al*., 1998; Hancox and Rubidge, 2001; Damiani, 2004; Knoll, 2004, 2005; Marsicano *et al*., 2009; Prevec *et al.,* 2010; McPheee *et al*., 2017; Chapelle *et al*., 2019; Bordy *et al*., 2020a). The Karoo Supergroup also encompasses the geological record of several mass extinction events, of which the most renowned ones are the end Permian (PTE) and the end Triassic (ETE) Mass Extinction events. In addition to the wealth of palaeobiological information, the Karoo rock record played a key role in supporting the theory of plate tectonics and has high economic importance in southern Africa due to its various natural resources (e.g., groundwater, coal, shale gas, uranium; e.g., Cadle *et al*., 1993; Cairncross, 2001; Geel *et al.*, 2013, 2015).

2.1.1 Tectonic Setting

Karoo-aged sedimentary rocks are preserved throughout southern Africa (e.g., main Karoo Basin, Springbok flats, Ellisras, Tshipise and Tuli basins) and formed under different tectonic regimes (Fig.2.1; Catuneanu *et al*., 2005). In the north, extensional/transtensional stress propagated southward from the divergent Tethyan margin of Gondwana, whilst in the south, accommodation space was generated via flexural dynamic loading in response to the Palaeo-Pacific plate convergence (Fig. 2.2A; Catuneanu *et al*., 1998; 2005). The compressional regime along the southern margin of Gondwana resulted in the formation of a 6 000 km long Pan-Gondwanan fold-thrust belt, which in South Africa is preserved as the Cape Fold Belt (CFB; Figs. 2.1, 2.2A; Catuneanu *et al*., 2005; Blewett *et al*., 2019).

The main Karoo Basin is generally considered to be a retro-arc foreland basin established to the north of the Cape Fold Belt (Fig. 2.2; Cole, 1992). According to Catuneanu *et al*. (1998), the low-angle subduction of the Paleo-Pacific plate beneath the Gondwana plate during the Late Palaeozoic – Early

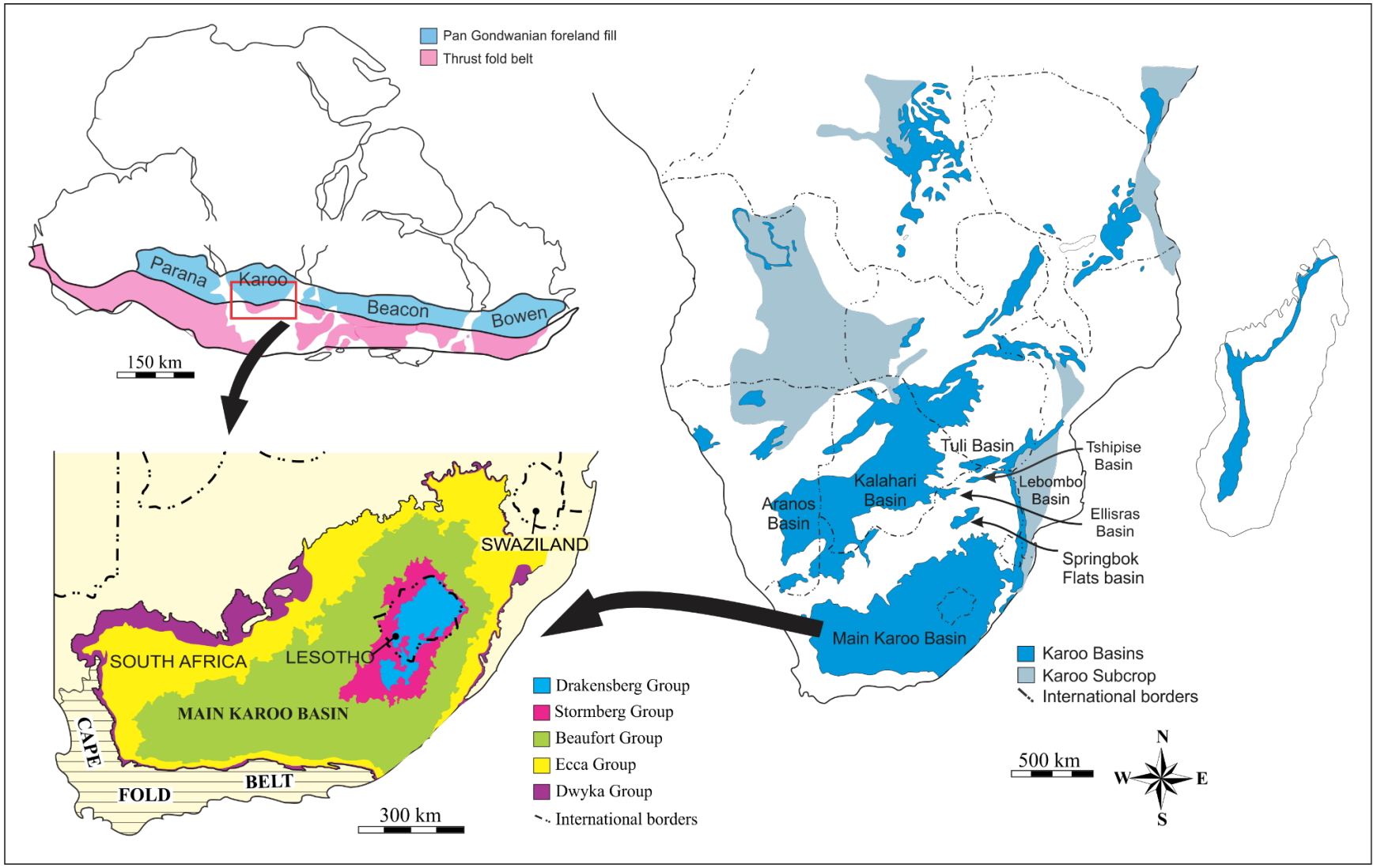

Figure 2.1: Overview of the outcrop distribution of the Karoo Supergroup and its equivalents within southern Africa (modified after Johnson et al., 1997 and Catuneanu et al., 2005). Geological map has been modified from the Simplified Geology ma under a CC BY license, with permission from the Council for Geoscience, original copyright (2003).

Mesozoic resulted in the Cape orogenic event, which triggered the formation of the CFB and consequently the main Karoo Basin. The orogenic load, resulting from the compressional tectonic regime, caused the sagging of the lithosphere, and created a depression in which sediments could accumulate (Fig. 2.2). An east-west trending belt, immediately north of the orogenic load, experienced the greatest subsidence and resulted in the asymmetry of the main Karoo Basin (Fig. 2.2; e.g., Johnson, 1976; Catuneanu *et al*., 1998).

It is important to note that others argue that a purely retro-arc foreland basin model does not adequately explain the evolution of the main Karoo Basin (e.g., Turner, 1999; Tankard *et al*., 2009, 2012; Lindeque *et al*., 2011). For example, an alternative basin formation model in Lindeque *et al*. (2011) involves arc-continent collisional tectonics, which resulted in the formation of the thick CFB and southward subduction taking place in the distant south. Turner (1999) only accepted the foreland basin model for the pre-Triassic evolution of the basin and proposed that a thermal anomaly induced by a mantle plume created crustal deformation, volcanism and an extensional regime from the mid-Triassic onwards. Moreover, Tankard *et al*. (2009, 2012) suggested that the

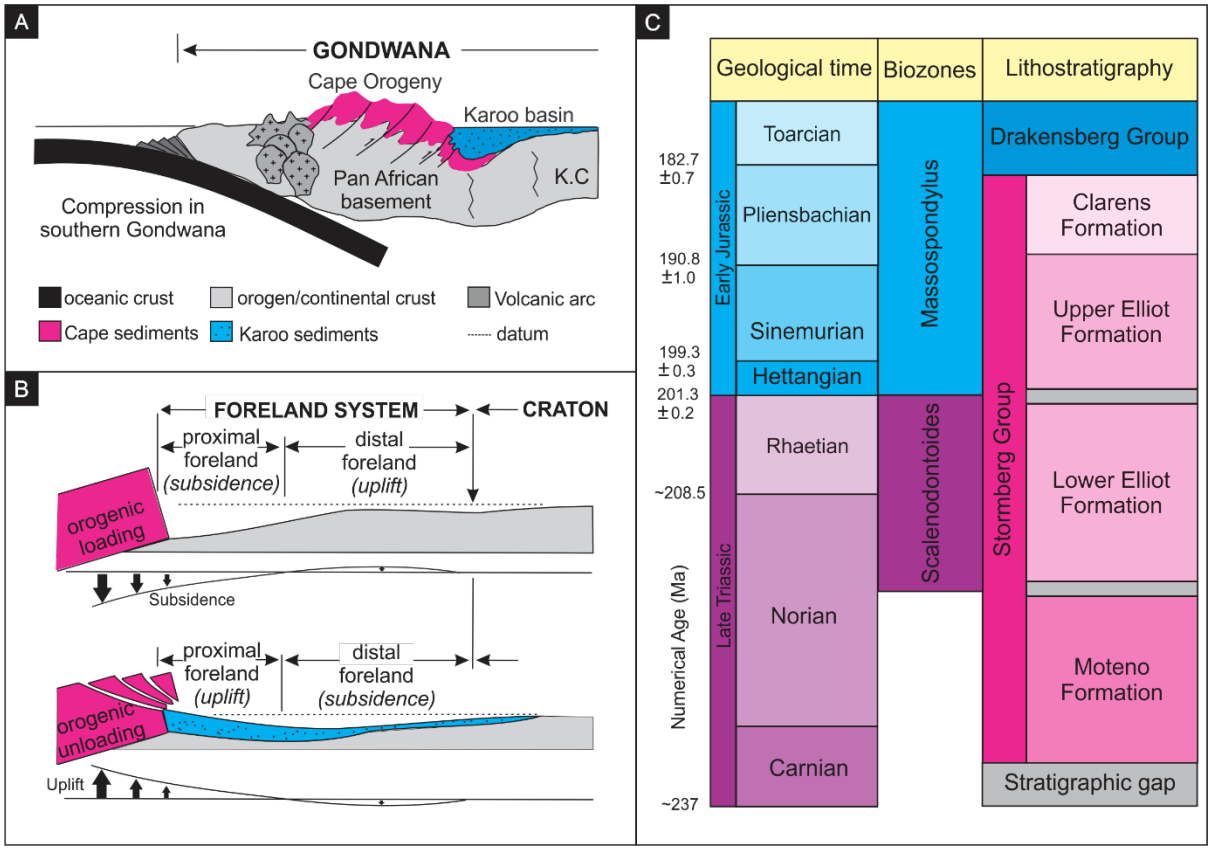

Figure 2.2: *Basin formation and dynamics of the main Karoo Basin. A) Key geodynamic elements of the compressional tectonic setting of southern Gondwana; modified after Catuneanu et al., (1998); B) Flexural and surface profile showing the evolution of a foreland system during phases of orogenic loading and unloading; modified after Catuneanu et al., (1998); C) Stratigraphy of the Stormberg Group which was deposited in the distal foreland during a period of first-order orogenic*

unloading; Modified after McCarthy and Rubidge (2005), geological time scale based on the International Chronostratigraphic Chart (v2018/08; ICS, 2018) . See text for details.

Cape Orogeny only started playing a role in the main Karoo basin evolution from the Early Triassic, and attributed the initial basin formation to rigid basement block movement associated with crustal faults and lithospheric deflection due to subduction-driven mantle flow. Given that the focus of this study is to document tridactyl tracks from the upper Stormberg Group, evaluating the scientific merits of these models is beyond the scope of this work. One of the main disputes in the debate surrounding these models for the Karoo basin is the timing of the onset of the flexural tectonics. Here, the retro-arc foreland basin model of Catuneanu *et al*. (1998) is considered most plausible as deposit distributions and trends from the Dwyka to Stormberg groups can be attributed to flexural tectonics (e.g., Catuneanu, 2004; Bordy *et al*., 2004a; Isbell *et al.,* 2008; Rutherford *et al*., 2015; Rubidge *et al*., 2016; Viglietti *et al*., 2017). Efforts in constraining ages of deformation in the Cape Fold Belt (e.g., Hansma *et al.,* 2015) and dating the deposition in the Karoo Supergroup (e.g., Rubidge *et al.,* 2013) further aid the correlation of tectonic paroxysm with periods of sedimentation in the Karoo basin. Evaluating the scientific methods of existing models and contributing to solving the geological issues of the main Karoo basin is beyond the scope of this thesis and is left to future research.

In the retro-arc foreland basin model, the main Karoo Basin is characterised by two first-order flexural tectonic events: orogenic loading mostly in the pre-Triassic and orogenic unloading from the Middle Triassic onwards (Fig. 2.2B; Catuneanu *et al*., 1998). The orogenic loading event generated the accommodation space in which the early Karoo sediments were deposited from the later Carboniferous to the Early Triassic. During the unloading event, a distal Karoo basin foresag was formed in the north in response to proximal uplift in the south. The latter lead to the erosion, and northward sediment transport (Figs. 2.2B, C). Clastic sedimentation terminated essentially when magma extruded and intruded on and into the sedimentary units of the Karoo Basin as continental flood basalts and associated dolerite dykes and sills ~183 Ma ago (i.e., Drakensberg Group; Duncan *et al.,* 1997). Finally, an extensional tectonic regime was initiated and ultimately led to the break-up of Gondwana (Muir *et al*., 2020).

2.1.2 Lithostratigraphy of the Stormberg Group

The Karoo Supergroup consists of five main groups namely, in chronological order from oldest to youngest, the Dwyka (Permo-Carboniferous), Ecca (Early to Middle Permian), Beaufort (Middle Permian to Early Triassic), Stormberg (Middle Triassic to Early Jurassic) and Drakensberg Groups (Early Jurassic). These primary lithostratigraphic units outcrop, as erosional remnants, concentrically within the main Karoo Basin (Fig. 2.1). The Karoo strata were deposited in an array of palaeo-environments

and climates, and illustrate a general aridification trend over ~117 million years of depositional history. In part, this may be attributed to the migration of Gondwana from higher to lower palaeo-latitudes over this time span (i.e., Permo-Carboniferous glacial Dwyka Group versus Early Jurassic mostly aeolian Clarens Formation; Visser, 1991; Johnson, 1976; Catuneanu *et al*., 2005). Furthermore, due to the asymmetric foreland basin tectonics (see Catuneanu *et al*., 1998), characteristics of the various groups also differ from south to north.

The focus of this study is within the Stormberg Group, which comprises the Molteno, Elliot and Clarens formations (Fig. 2.2C). The current preservation area of the Stormberg Group is a post-Karoo erosional remnant of a much larger, original basin (e.g., Bordy *et al*., 2004a; Hanson *et al*., 2009; Muir *et al*., 2019).

The Molteno Formation forms a wedge-shaped, siliciclastic unit with a maximum thickness of ~600 m in the south and a minimum thickness of<10 m in the north (Johnson *et al.*, 1997; 2006). It consists primarily of laterally continuous, tabular sheet sandstones that are coarse- to medium-grained and are dominated by horizontal- and cross-bedding (Turner, 1975, 1983; Bordy *et al*., 2005). The sandstones are interbedded with plant- and insect fossil rich mudstones and coal deposits. The depositional environment of the Molteno Formation has been interpreted to be broad, shallow braided rivers and floodplains with abandoned channels, swamps and ponds (e.g., Turner, 1975, 1983; Cairncross *et al*., 1995; Anderson *et al*., 1998; Labandeira *et al*., 2018). Fossil plant and insect assemblages within the Molteno Formation are indicative of cool and wet palaeoclimatic conditions, but the appearance of maroon and green mudstones towards the top of the formation has been taken as evidence for increasingly warm, arid conditions in the late Middle Triassic (e.g., Johnson *et al.,* 1997; Anderson *et al.*, 1998). Bone fossils are rare in the Molteno Formation, with fossil fish being the only vertebra found. Vertebrate traces, e.g., tracks and possible tail marks, have also been reported (Raath *et al.*, 1990; Raath, 1996; Anderson *et al*., 1998).

The Elliot Formation has a sharp, regionally traceable unconformable contact with the underlying Molteno Formation and a gradational, conformable contact with the overlying Clarens Formation (Bordy *et al*., 2004b; 2005*)*. It attains a maximum thickness of ~460 m in the south and declines to approximately 70 m in the north (Bordy *et al*., 2004b). Within the Elliot Formation, there are major sedimentary facies differences that allow the subdivision of the formation into two informal units, namely the lower Elliot Formation (lEF) and upper Elliot Formation (uEF; characteristics of the lEF and uEF are summarised in Table 2.1; Fig. 2.2C; Bordy *et al*., 2004a, b, c). The subdivision of the Elliot Formation can easily be noted in the field, as the two units are separated by an obviously detectable plateau which is the product of differential weathering between the lower and upper parts (Bordy *et*

al., 2004a). The large grain size difference between the medium-fine grained sandstones and intermittent mudstones of the lEF give it a terraced morphology, which contrasts the smooth hill slopes of uEF which results from a moderate grain size difference between the uEF fine-very fine silty sandstones and intermittent mudstones. Bordy *et al*. (2004a, 2005) proposed that the boundary between the lEF and uEF represents a second order sequence boundary that was generated by tectonic activity linked to the final orogenic loading of the CFB. The Elliot Formation was deposited in a fluvio-lacustrine environment, with the uppermost part of the formation containing evidence of aeolian processes (e.g., Visser and Botha, 1980; Johnson *et al*., 1997; Smith and Kitching, 1997; Bordy *et al*., 2004b, 2005; Bordy and Head, 2018). This aridification within the formation can also be seen by a change in fluvial style from stable, moderately meandering perennial rivers to broad, shallow ephemeral watercourses (Bordy *et al*., 2004b).

Fauna that typify the lEF and uEF are listed in Table 2.1, and these include amphibians, fish, turtles, crocodilians, ornithischians, prosauropods, sauropodomorphs, theropods and therapsids (e.g., Ellenberger, 1970; Kitching and Raath, 1984; Knoll, 2004, 2005; Abdala *et al.*, 2007; Bordy et al., 2020b). In addition, petrified wood, conchostracans, invertebrate and vertebrate trace fossils are found within the Elliot Formation. The lEF and uEF lithostratigraphic units were historically thought to coincide with the biostratigraphic zones of Kitching and Raath (1984), namely the *Euskelosaurus* and *Massospondylus* Range Zones, and Ellenberger's trace fossil-based zones A3–A6 and A7, B1–B3, respectively (Fig. 2.2C). Subsequent workers have shown the invalidity of these zones and the need for their revision (e.g., McPhee *et al.,* 2017; Knoll, 2005), which was recently published Bordy *et al.* (2020b).

The contact between the Elliot and Clarens formations is gradational, and generally uneven, and is marked by the first appearance of large- to very large scale cross-bedding. The Clarens Formation characteristically comprises cream very fine- to medium-grained sandstones (primarily arenites) with minor mudstones (Eriksson, 1981; Bordy and Head, 2018). These sandstones typically preserve interbedded large-scale cross-bedding and massive units with less abundant planar and trough cross-bedding, horizontal lamination, ripple-cross lamination and desiccation cracks that are associated with lenticular sandstones and mudstones (Bordy and Catuneanu, 2001; Bordy *et al*., 2009; Bordy and Head, 2018). The Clarens Formation can be subdivided into three zones. The lower and upper zones reflect wetter depositional conditions and include deposits of ephemeral streams and shallow playa lakes, while the central zone reflects more arid conditions and is dominated by large-scale cross-bedding of aeolian origin (Beukes, 1970; Body and Head, 2018). In addition to vertebrate tracks (Ellenberger, 1970, 1972; Mukaddam, 2019) and invertebrate traces (e.g., termite nests - Bordy et al., 2009), the Clarens Formation preserves various body fossils including freshwater fish,

crocodylomorphs, ornithischians, basal sauropodomorphs, mammaliaforms and plant fossils, including sphenophytes and conifers (e.g., Broom, 1911; Haughton, 1924; Ellenberger, 1970; Tasch, 1984; Kitching and Raath, 1984; Bordy and Catuneanu, 2002; Bamford, 2004; Bordy and Eriksson, 2015; McPhee et al., 2017).

2.1.3 Age of the Stormberg Group

Various relative dating methods from the past four decades suggest that the Stormberg Group is Late Triassic – Early Jurassic in age. More specifically, the Molteno Formation is assumed to be Carnian based on age diagnostic palynomorphs and palaeoflora that primarily comprise the seed fern *Dicroidium* (Anderson and Anderson, 1983, 1984; Anderson *et al*., 1998; Labandeira *et al*., 2018). The Elliot Formation preserves rich, diverse body and trace fossil assemblages, which are comparable with other Late Triassic – Early Jurassic faunas (e.g., Kitching and Raath, 1984; Lucas and Hancox, 2001; Knoll 2004, 2005). The informally subdivided lEF and uEF, respectively, are thought to represent Norian–Rhaetian (e.g., Hopson, 1984; Lucas and Hancox, 2001; Knoll, 2004; McPhee *et al.,* 2017) and Hettangian–Sinemurian (e.g., Olsen and Galton, 1984; Smith and Kitching, 1997; Lucas and Hancox, 2001; Knoll, 2005) deposits. Using magnetostratigraphy, Sciscio *et al*. (2017a) determined a Norian–Sinemurian age for the Elliot Formation and assigned a more refined age of ~214–213 Ma to ~195–190 Ma for the Elliot Formation, with the lower limit possibly extending to ~218–219 Ma. The age of the Clarens Formation was inferred to be Sinemurian– Pliensbachian based chiefly on the vertebrate biostratigraphy as the Formation contains taxa similar to those of the underlying uEF and an isotopic radiometric date of 181–183 Ma for the conformably overlying Drakensberg Group (Duncan *et al*., 1997; Svensen *et al., 2012,* Moulin *et al*., 2017) signals the minimum depositional age of the Stormberg Group.

Though tuffaceous strata within the Elliot Formation have been reported on from South Africa and Lesotho, there are no published radiometric dates associated with these deposits (Botha and Theron, 1967; Johnson, 1971; Schmidt, 1976; Heckroodt, 1991). Relocation and dating of these deposits have proven tough (Sciscio, 2016). Abrahams (2015) attempted radiometric dating of a bentonite layer from the middle part of the uEF from Pronksberg but found that the deposit was reworked (see Bordy and Abrahams, 2016), and the maximum depositional age derived from its absolute dating was incompatible with the local and regional stratigraphic considerations.

Table 2.1: Summary comparing the facies characteristics, palaeoenvironments and vertebrate fossil assemblages of the lEF and uEF (modified Ellenberger et al. 1964; Bordy et al. 2004a,b,c,d, 2005; Bordy and Head, 2018).

	lower Elliot Formation	upper Elliot Formation
Kitching and Raath (1984)	*Eusekelesaurus* Range Zone	*Massospondylus* Range Zone
Viglietti et al. (in press)	*Scalendontoides* Acme Zone	*Massospondylus* Acme Zone
Ellenberger (1970)	A3-A7	B1-B3
Conglomerate characteristics	Mud-pebble conglomerates	Carbonate-nodule conglomerates with bone fragments
Sandstone body characteristics	Primarily medium-grained sandstones; Predominantly asymmetric channel fills (20-25 m thick); Multi-storey, lenticular geometry; Point bars and lateral accretion surfaces present; Lateral extent < 100-150 m Sedimentary structures: trough and planar cross-bedding, massive beds and less commonly low angle cross-bedding, horizontal lamination and bioturbation structures Composition: Sublitharenites	Primarily fine-grained sandstones; Predominantly tabular with minor channel fills (5 m thick); Multi-storey, sheet geometry; Absence of point bars and lateral acrcetion surfaces; Lateral extent > 100-150 m; Sedimentary structures: massive beds, trough and planar cross-bedding, horizontal lamination ripple cross-lamination, bioturbation structures, soft sediment deformation, desiccation cracks, common pedogenic overprinting including root traces, calcic palaeosols and *in situ* carbonate nodules Composition: Subarkoses - arkoses
Mudstone characteristics	20-30 m thick; Rare pedoegnic overprinting, desiccation cracks and invertebrate traces;	<10 m thick; Common pedogenic overprinting including root traces, calcic palaeosols, desiccation cracks, in situ carbonate noduels, bioturbation structures
Colour	Red-purple heterogenous mudstones with green-grey mottling	Brick red-maroon deep with sporadic light grey mottling
Palaeoenviornment	Moderately meandering rivers, perenial lakes, vegetation along channel banks	Shallow, broad, ephemeral rivers, ephemeral lakes, vegetation on floodplain
Sediment Supply	Northwards and north-eastwards	Northwards, north-eastwards and eastwards
Provenance	Recycled orogen	Continental interior and rarely recyled orogen
Palaeoclimate	Humid-semi arid	Semi-arid
Vertebrate fossil content	Sauropodomorpha, synapsida, temnospondyli, therapsids, dicynodonts and possible Theropoda	Sauropodomorpha, Theropoda, Ornithischia, crocodyllomorpha, synapsia, temospondyli and possible testudinata, sphenodontia, actinopterygii and cynodontia

2.2 Understanding tracks

Trace fossils, or ichnofossils, offer a wealth of information into animal behaviour, life habits, biocenoses, plant presence and even climate. Despite having the potential to provide insights into animals daily lives, vertebrate trace fossils (or ichnites), in particular dinosaur trace fossils, were grossly understudied, relative to their body fossil counterparts, until interest in the topic of tracking was rejuvenated in the 1970s (e.g., Demathieu, 1970; Ellenberger, 1970, 1972, 1974; Sarjeant, 1970; Farlow, 1981; Hay and Leakey, 1982; Padian and Olsen, 1984 ; Warren *et al.*, 1986; Lockley, 1998). The vertebrate trace fossil record complements the osteological record of tetrapods, and in stratigraphic units lacking skeletal remains, trace fossils may provide the only evidence that vertebrates existed at a given location and time (Currie, 1989; Thulborn, 1990). The preservation of body and trace fossils are both controlled by syn- and post-depositional processes, which are often referred to as 'facies control'. For example, fossil bones and traces are not normally preserved together, because the former is often biased towards rapid burial (Kuban, 1994). Unlike body fossils, which can be exhumed and redeposited far away from their original site of burial, trace fossils cannot be transported. Consequently, vertebrate ichnites indicate the exact environment that an organism inhabited during a short window of time, which can be as brief as a moment, needed to leave behind tracks while moving over a sediment surface i.e., *in situ* and in *vivo* evidence of living animal (Thulborn, 1990).

The first written accounts of dinosaur tracks, attributed to theropods, ornithopods and possible ankylosaurs, are from the 1800s and were described from North America (Hitchcock, 1836; Hitchcock, 1866), Central and South America (Degenhardt, 1839), Europe (Tagart, 1846) and Africa (Le Meste and Peron, 1881; Dieterlin, 1885). Interest in tracksites persisted to the early 1900s (e.g., Lull, 1904; Dornan, 1908; von Huene, 1932; Buckland, 1928), but essentially abruptly halted until the 1970s when there was, again, an increase in interest in dinosaur track investigations (see Bakker, 1975 who termed this period as 'Dinosaur Renaissance').

2.2.1 How tracks are formed and deformed

Footprint morphology is the dynamic product of three interlinked variables: the trackmakers anatomy, the substrate conditions upon which the trackmaker crosses and its locomotory style at the time of limb impression (Fig. 2.3A; Padian and Olsen, 1984; Milan and Bromley, 2006; Avanzini *et al*., 2012). The most extreme variations in track morphology can often be attributed to differences in substrate conditions particularly relating to grain size and water content. The porosity of a medium is complex and is affected by the sorting and grain shape of the sediment particles, the particle packing, and the degree of compaction and cementation of the sediments e.g., coarser grains and spherical shapes have a lower porosity. The tracks that best reflect a trackmakers foot are made in finer-grained substrates, that are neither too soft nor too firm and have ~10 % moisture content (Fig. 2.3B; Scrivner

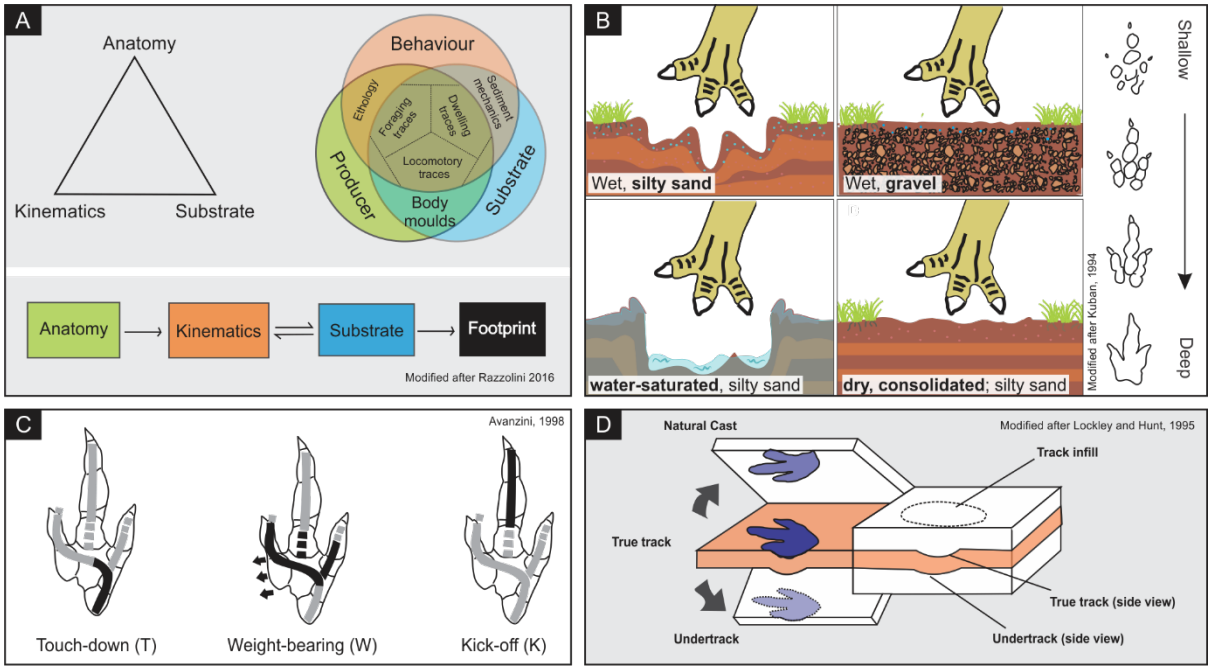

Figure 2.3: Factors controlling track morphology. A) three variables interacting during track formation; B) varying substrate conditions; C) weight distribution during a step; D) tracking surfaces and types of track preserved.

and Bottjer, 1986; Kuban, 1994; Jackson *et al*., 2010). In more water-saturated sediments, the trackmaker may sink creating a deeper track, possibly introducing additional parts of its anatomy [e.g., raised hallux (digit I)] and/or metatarsal for a digitigrade theropod pes; Fig. 2.3B; Lockley, 1998; Gatesy *et al*., 1999; Romano and Citton, 2017; Rampersadh *et al*., 2018). Footprints generated in water-saturated sediments (>30 % moisture content) preserve few anatomical details (Jackson *et al*., 2010), and are at risk of being deformed by sediment collapse features due to the overly malleable nature of the substrate. In dry sediments, shallow impressions are likely to be made, possibly with minimal morphological details (Fig. 2.3B).

Both deep and shallow tracks can be informative for understanding the interaction between the trackmaker and the substrate. Deep tracks have the potential to preserve traces of additional limb features such as hallux and metatarsal impressions. Consequently, they can be used to illustrate the path the foot travels through a medium, providing kinematic information (Gatesy *et al*., 1999). Using deep tracks, Gatesy *et al.* (1999) reconstructed theropod foot movements and were able to show that the digits converged beneath the surface. The presence of metatarsal impressions indicates that, unlike birds, theropods did not lift their ankles during the stance phase i.e., when the foot is in contact with the sediment (Fig. 2.3C). To capture skin impressions or scale drag marks, the substrate typically needs to be in a quasi-solid state. Consequently, skin features are typically associated with shallow tracks (Gatesy, 2001; Paik *et al.,* 2017; Kim *et al.,* 2019). Skin impressions and scale drag marks can shed light on the angle at which the foot initially contacted the substrate and the angle at which it

subsequently removed its foot (e.g., Gatesy *et al*., 1999; Gatesy 2001; Avanzini *et al*., 2012; Paik *et al.,* 2017). Skin impressions have also played a pivotal role in understanding foot dynamics as the impression distribution is not consistent across the track surface area (i.e., certain areas, like sides and 'heel' region of the track preferentially record skin impressions; Currie *et al*., 1991; Gatesy, 2001;).

It is important to note that a track is not the product of one distinct movement but rather a series of movements which take place almost instantaneously (Avanzini, 1998; Falkingham, 2014). This series can be divided into three discrete phases: 1–touch down (T), 2–weight-bearing (W) and 3–kick-off (K) (Fig. 2.3C; Avanzini, 1998). Within the step cycle maximum weight is shifted from the 'heel' region of the track to primarily digit III. Consequently, the load will vary in position, magnitude and direction ultimately affecting track formation and morphology. Decelerations and accelerations will respectively impact on the T and K phases with deceleration increasing the force at the rear of the foot and acceleration increasing the force anteriorly i.e., at higher speeds digit tips are more deeply impressed because the trackmaker exerts greater pressure on the substrate (Fig. 2.3C; Thulborn, 1990; Milan, 2006; Falkingham *et al.,* 2011). A trackmaker is likely to use differing gaits when interacting with a firm or squidgy medium (Fig. 2.3A).

Because track formation is a complex process, dependent of various, interlinked parameters, it is difficult to reconstruct which parameter contributed most to the track morphology (Fig. 2.3A). The fact that most foot-sediment and sediment-sediment interactions occur within, and not on, the subsurface adds to this complexity (Ellis and Gatesy, 2013). To have a better understanding of autopod morphology and possible extramorphological processes involved in track registration, statistical approaches to understand track variability prove useful (e.g., Razzolini *et al.,* 2017). A track may be subjected to modifications during exposure after its initial formation and after it is exhumed as a trace fossil. Unconsolidated tracks may potentially be altered by wind or water or may be disturbed by invertebrates or overgrown by plants or algal mats (e.g., Thulborn, 1990; Sciscio *et al*., 2016). Fossil tracks may have their preserved morphology deformed by partial erosion. Early on in erosion, narrow and angular features (e.g., claw marks, raised hypices) are removed or rounded, which can, for example, limit the distinction between theropod and ornithopod tracks (Henderson, 2006b). Tracks exposed to varying degrees of erosion may present an array of morphologies (Milan and Bromley, 2006). Understanding the effects of erosion limits the misidentification of tracks and erection of new ichnotaxa (Milan and Bromley, 2006). While partially-preserved tracks are suboptimal for taxonomic assignment, Henderson (2006b) erosion models suggest that tracks subjected to erosion maintain their basic shape, at least with respect to the track length to track width ratio. Therefore, these parameters (section 3.2) can be used to quantitatively describe the track morphology and assign ichnogenera.

2.2.2 Types of tracks

Tracks made on a tracking surface, where the trackmaker's autopodia make direct contact with the substrate, are termed *true tracks* (Fig. 2.3D), and have the highest potential to preserve morphological details such as claw marks, skin and scale features, and digital pad impressions. However, the sediment beneath the tracking surface is also subjected to deformation when the trackmaker's load is placed on unconsolidated, moist substrates (Milan *et al*., 2004; Avanzini *et al*., 2012). The pressure exerted by the foot is transferred outwards radially, with the magnitude of the force decreasing away from the true track. The underlying deformed sediment will resemble the impressing autopodia (depending on the substrate conditions, etc.) but will typically have less morphological detail and their dimensions may not reflect the true track (Lockley, 1998). These tracks that form in horizons beneath the tracking surface are called *undertracks (or transmitted or ghost tracks;* Fig. 2.3B, D). Statistically, more undertracks would be preserved in the rock record than true tracks (Thulborn, 1990; Nadon, 2001; Milàn and Bromley, 2006). Larger, heavier trackmakers are also more likely to produce undertracks because of their greater weight (Lockley, 1986; Platt and Hasiotis, 2006). Additionally, trackmakers with larger total digit divarication angles (section 3.2) may be able to better distribute their weight reducing the odds of them producing undertracks (Falk *et al*., 2011). A true track is a negative feature (a natural mould of the impressing extremity) and may by infilled by sediments. The infilling sediment, acting as a natural cast (Fig. 2.3D), will form an exact copy of the true track at the time the infilling occurs. If claw marks, skin impressions or digital pad impressions are present at the time of infilling, the infilling sediment may record these biological features. Natural casts may be preserved on overhang surfaces (e.g., cave ceilings) if the original tracks were made in relatively less-competent sediments (e.g., silt overlain by sand) or may be eroded away completely when the tracking surface is re-exposed. During the partial erosion of a tracksite, remnants of the natural cast can obscure original features of the true track (Kuban, 1994) and multiple generations of tracks and various track types may be exposed (Thulborn, 1990). Therefore, it is important to understand track types and variations in preservation, especially for ichnotaxonomic purposes, because new ichnotaxa should only be erected based on the morphological features of the highest quality tracks available at any given tracksite (e.g., Sarjeant, 1989; Belvedere and Farlow, 2016; Marchetti *et al.,* 2019).

Table 2.2 Preservation grade criteria and the usefulness of the tracks of a specific grade as defined by Belvedere and Farlow (2016) and Marchetti et al. (2019).

Preservation grade	Description (Belvedere and Farlow, 2016)	Use	Additional Description (Marchetti *et al* ., 2019)	Additional Uses
3	All digit impressions sharp and clear; well-defined digit wallks, claw impressions and digital pads preseved; for quadrupeds, both the manus and pes are perfectly preserved.	Can be used to base new ichnotaxa, even at ichnospecies level; can be used for reliable landmark identifications for shape analyses.	Palm/sole present if taxonomically relevant; secondary features such as tail impressions, digit skin impressions may be preserved; absence of super-imposition or erosion; no directional deformation of anatomy-related morphology	May be used to recognise morpho-functional characters which are useful for trackmaker attribution
2	Digit impressions are fairly clear and sharp, for the most part; claw marks and some digital pads are observed	More information on the trackmaker; higher, generic level ichnotaxonomy is possible; can be used for shape comparisons; can be used to determine precise heteropody for quadrupeds.	Palm/sole present and nearly complete if taxonomically relevant; track walls are reasonably defined; secondary features such as tail impressions, digit drag marks etc may be preserved; low occurrence of directional deformatin of anatomy-related morphology	
1	Faint or distorted digit impressions that are recognizable; claw marks are recognizable; general outline is observed; for quadrupeds pes and manus impressions are distinguishable	Good information about the kind of trackmaker but poor information about the shape of the autopodium; can determine direction of movement and possible body carriage posture; may be assigned to existing ichnogenera.	Incomplete; claw marks and digital pads may be missing; undefined track walls; may be preseverved with secondary features such as tail and digit drag impressions; considerable directional deformation of anaotmy-related morphology; lots of superimposition/erosion	
0	No visible morphological details	Indicates the passage of the animal; if it is a trackway, some parameters such as direction of travel and print alignment may be determined.	Digit impressions and palm/sole unrecognisable; track completely distorted; track walls may not be defined; for quadrupeds, manus is distiughed from pes based purely on size; possible preservation of secondary features like tail impressions and drag marks; significant directional deformation of the anatomically-related morphology; superimposition or erosion	

Additional details (Marchetti *et al* ., 2019)	
p	Partial preservation (e.g., missing digits)
c	Morphology cut (e.g., superimposition)
w	Anomolous width (e.g., very broad digits)
f	Flattened footprint
a	Anomolous morphology (multi-directional deformation)
m	Anomolous morphology (mono-directional deformation)
s	Skin/scale impressions
d	Drag marks
b	Digit tip bifurcations

2.2.3 Why study tracks

Tracks are biogenic sedimentary structures and can therefore be used to elucidate not only about the trackmaker's biology but also the substrate conditions at the time of track formation (Fig. 2.3A, B). For example, extra-morphological features such as expulsion rims and wall-collapse features are indicative of water-saturated media, while autopodia-related morphological features such as digital pad and claw mark impressions are made in firmer substrates. Track morphology is also controlled by the anatomical features of the trackmaker's manus (hands) or pes (feet). Therefore, the track size and shape of well-preserved tracks can be used for trackmaker identification but only in a broad, non-generic sense (e.g., theropod, iguanodon; e.g., Thulborn, 1990). The trackmaker can only be identified with more confidence under exceptional conditions such as when associated body fossils are also found (Soergel, 1925; Baird, 1980). Even in cases where skin textures, metatarsal impressions, resting traces, and tail drag marks are associated with tracks (e.g., Gatesy, 2001; Romano and Citton, 2017; Kim and Lockley, 2013), the generic level identification of the exact tracemaker is almost impossible. Trackways, a series of at least three consecutive tracks made a by a single trackmaker, provide insight into the animal's movement, including locomotory style (e.g., Wilson *et al*., 2009), gait (e.g., Day *et al*., 2004; Henderson, 2006a),speed (e.g., Alexander, 1976; Day *et al*., 2004) and behaviour (Lockley *et al.*, 2003). For example, trackway evidence shows that dinosaurs were not habitual tail draggers (contrary to earlier reconstructions) and did not commonly walk with sprawling gaits (Lockley, 1986).

Because tracks represent a snapshot in time and are the product of living animal activities (Lockley, 1986), they may represent the behaviour of, and interactions in, ancient animal communities (e.g., courtship: Lockley *et al*., 2016; gregarious behaviour: Barco *et al*., 2006). Large ichnological discoveries may yield additional palaeoecological information over osteological accumulations, because fossil bone graveyards may simply be protracted amalgamation of remains in taphonomic traps (e.g., in a meander bend) and may not be a true reflection of past living communities. However, tracksites (surfaces with numerous tracks) need to be treated with caution, because they are also subjected to time averaging (i.e., parallel trackways may be interpreted as gregarious behaviour but may simply represent unrelated individuals crossing the surface at different times while the substrate was still moist while walking next to physical barrier such as a shoreline; Lockley, 1991; Getty *et al*., 2012, 2017), and may preserve juxtaposed tracks from different and partially exhumed tracking surfaces (the surface on which an animal interacted; Fig. 2.3D; Fornos *et al*., 2002). Furthermore, preservation of ichnofossils is subjected to multiple biases (e.g., a threshold weight may be required to leave impressions on a substrate; Falkingham *et al.,* 2011), which may mislead palaeoecological reconstructions.

Because of their relatively high taxonomic diversity and evolutionary history, Dinosauria present with various distinct foot morphologies that can be linked to various size quadrupeds and bipeds (Falkingham *et al.,* 2011). This, coupled with the fact that dinosaurs had a global distribution in the Mesozoic (e.g., Lockley *et al*., 1998; Day *et al*., 2004; Huh *et al*., 2006; de Valais and Melchor, 2008; Belvedere *et al*.,2013; Xing *et al*., 2013, Thulborn, 2017), makes the group ideal for studying diversification and evolution. The utility of tracks for inferences about palaeobiology, palaeoecology and palaeoenvironments depends on the quality and detail of the tracks both at the time of registration and the present day. At the time of track registration, tracks may have only been partially imprinted due to substrate conditions: e.g., tridactyl tracks may be preserved as didactyl in firm substrates such as damp sand (Milan, 2006). After the initial track formation, existing tracks may be disturbed/overprinted by the initial trackmaker or other animals e.g., a quadrupedal trackmaker may disturb its manus impressions with its pes impressions (Lockley, 1998; Klein *et al*., 2015). The preservation style and extent to which a footprint has been eroded will determine its preservation quality. The preservation quality, or anatomical fidelity, of tracks has received a lot of attention recently (Belvedere and Farlow, 2016; Falkingham and Gatesy, 2017; Marchetti *et al.,* 2019). The conversation has particularly focused on what the term preservation means and how to quantify "grades" or "levels" of preservation quality i.e., can one ascribe a number to a track to indicate it's higher quality relative to another track? Marchetti *et al*. (2019) define two preservation categories: "morphological preservation" and "physical preservation". The former is defined as preservation linked to the degree of congruency between the autopodial anatomy and its associated track, and the latter is defined as the potential of a track to be preserved and not altered or destroyed by taphonomic processes. Given that the aims of this study relate to track morphology (and ichnotaxonomy), we simply use the term "preservation" to mean "morphological preservation". A scale to quantify the morphological preservation grade of tracks was recently erected to standardise the description of the amount of detail a given track preserves and to assess the ichnotaxonomic and morphological usefulness of a track (Belvedere and Farlow, 2016). The scale ranges from 0 to 3, with increasing morphological detail where tracks classified as "0" have no morphological detail and simply illustrate a trackmakers presence and "3" represents pristine tracks which may be used for landmark-based morphological studies and from which new ichnotaxa may be erected. This simple scale was subsequently refined (Marchetti *et al*., 2019). For detailed descriptions of the morphological scales, see Table 2.1.

2.3 Dinosaur origins and diversification

The rise of dinosaurs in the Middle Triassic and their dominance until the end-Cretaceous represents a remarkable evolutionary radiation as well as a critical event in history of life on Earth (Brusatte *et al.*, 2010). Dinosaurs originated approximately 230 million years ago as minor ecological components, which had limited body sizes and low diversity, before reaching a global distribution, morphological diversity and some of the largest body sizes to have evolved. Additionally, their extant representatives, birds, constitute a significant proportion of modern ecosystems. However, early dinosaur history is still poorly understood, with the timing and cause of the dinosaur ascent being highly debated (Furin *et al.,* 2006; Irmis, 2011; Padian, 2012; Baron *et al.*, 2017; Langer *et al.,* 2017; Bernadi, 2018).

Dinosaurs form part of a larger radiation, Dinosauromorpha, which emerged 1-5 million years after the Permian–Triassic Extinction (Brusatte *et al.,* 2011). During the Mid to Late Triassic, the ornithodiran archosaur lineage split into multiple distinct groups, which included pterosaurs, silesaurids and dinosaurs (Baron *et al*., 2017). By the end Norian, some dinosaur lineages became abundant and species rich (Baron *et al.*, 2017). There are two commonly used measures to quantify biodiversity: morphological disparity and taxonomic diversity. These measures do not follow the same trend in dinosaur history: a significant jump in dinosaur disparity occurred during the Carnian – Norian, while diversity increased steadily with an important increase in diversity and abundance during the Early Jurassic (Fig. 2.4; Brusatte *et al*., 2008).

Dinosaurs diversified into three main lineages: Theropoda, Sauropodomorpha and Ornithischia. Theropoda and Sauropodomorpha have a classic reptile-like pelvic anatomy and were recognized as forming a natural group, Saurischia. Ornithischians are classically distinguished from saurischians by their bird-hipped anatomy (e.g., Langer *et al*., 2010; Baron *et al*., 2017). Initially, it was thought that saurischians and ornithischians were unrelated, each the descendent of a different primitive archosaur (e.g., Romer, 1966). However, during the 1980s, it became consensus that Saurischia and Ornithischia were monophyletic sister-taxa (e.g., Bakker and Galton, 1974; Gauthier, 1986; Langer, 2014). Recently, this longstanding paradigm has been scrutinized (Baron *et al*., 2017), shedding doubt on our understanding of the basic structure of the dinosaur family tree. Baron *et al*. (2017) proposed that theropods and ornithischians form a sister-group, Ornithoscelida, with sauropodomorphs forming a separate, monophyletic branch. However, when examining the data of Baron *et al. (*2017), checking and correcting the scoring if necessary, Langer *et al*. (2017) were able to observe the more classical saurischian and ornithischian clades.

2.3.1Timing

The hypothesis about the timing of the origins and diversification of dinosaurs is also contentious, not only because the body and trace fossil records are incongruent but also because the key fossiliferous

strata hosting these early dinosaurian remains are poorly dated with radioisotopic methods on a global scale. Historically, only the osteological record was considered for understanding the timing of dinosaur origins. Body fossils of dinosaur relatives, the dinosauromorphs, are sparse but suggests that the dinosaur stem lineage originated by the late Anisian, Middle Triassic (e.g., *Asilisaurus* – Nesbitt *et al.,* 2010 and possibly *Nyasasaurus parringto*n – Nesbitt *et al.*, 2012). The skeletal record implies that basal dinosaurs and their close relatives appeared suddenly in the Carnian (early Late Triassic) with a low degree of diversity and a restricted abundance (Fig. 2.4). Although early dinosaur fossils are scarce, they indicate a geographically widespread distribution of the group in the Upper Triassic of both Laurasia and Gondwana, with the oldest occurrences being recorded in South America and east Africa (Marsicano *et al*., 2007). Theropod and sauropodomorph remains are confidently known from several Upper Triassic deposits (see Irmis, 2011 for a review), but Late Triassic ornithischian remains are still controversial: an alleged heterodontosaurid jaw was reported from Norian Laguna Colorada Formation of Patagonia (Baez and Marsicano, 2001) but is too poorly preserved for a confident identification. On re-evaluation of additional *Revueltosaurus* material from the Chinle Formation it was shown that this taxon is more related to crocodylomorphs rather than dinosaurs (Parker *et al.,* 2005); and the southern African *Eocursor* (Butler *et al*., 2007) comes from strata that are likely Early Jurassic in age (see McPhee *et al*., 2017). Now, all evidence for Late Triassic ornithischians has been removed from the global osteological record (e.g., Irmis *et al.,* 2007; Olsen *et al*., 2010; Baron, 2019). The absence of Late Triassic ornithischians may be attributed to their late derivation from within Theropoda (Padian, 2013; Baron, 2019) or a lack sampling.

Contrary to the osteological record, the ichnological record suggests that the dinosaur stem lineage dates to the Olenekian (Early Triassic, Fig. 2.4; Brusatte *et al.,* 2011). However, evidence for these tracks having been made by dinosauromorpha is debated (Irmis, 2011). Tridactyl, digitigrade pes impressions of a bipedal trackmaker with a parasagittal posture are observed in mid-Triassic strata throughout Pangea (e.g., Avanzini, 2002). Although early tracks, and their interpretation, are negatively impacted by poor preservation and the uncertainty of their age and stratigraphic position, the early track record should not be disregarded. If the osteological and ichnological records are considered in conjunction, the fossil record demonstrates that the ascent of dinosaurs was a protracted event, beginning during the PTE ecological recovery (e.g., Langer *et al*., 2010; Brusatte *et al*., 2011, Benson *et al*., 2014).

In addition to the timing, the locus of dinosaur origin is also contested. Many authors have repeatedly proposed that Dinosauria originated in southern Gondwana (e.g., Nesbitt *et al*., 2009; Brusatte *et al*., 2010; and more recently Michael *et al*., 2019) though a Laurasian origin has also been proposed (Baron *et al*., 2017).

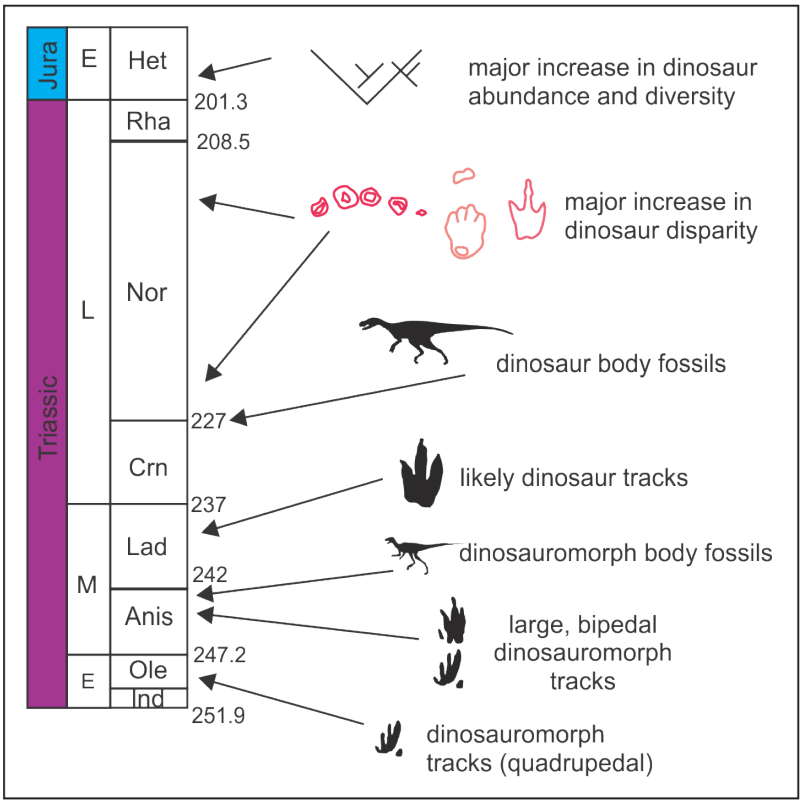

Figure 2.4: A general timeline for early dinosaur history modified from Brusatte et al. (2011). Pink dinosaur track outlines are from the IEF Subeng ichnosite (Ellenberger, 1790; Bordy et al., 2017).

2.4 The Grallator-Anchisauripus-Eubrontes (GAE) plexus

Theropod tracks from the Late Triassic – Early Jurassic are some of the most well-known tridactyl tracks; and have commonly been assigned to 3 ichnogenera: *Grallator* (Hitchcock, 1856) – *Anchisauripus* (Lull, 1904) – *Eubrontes* (Hitchcock, 1836) which form the so called GAE plexus (Olsen, 1980). The ichnotaxonomic diagnoses for each of the three ichnogenera of the GAE plexus are amongst the earliest recognised and formally documented, and are summarized below largely based on a review by Olsen *et al.* (1998):

Grallator tracks are defined as the smallest on the spectrum and have a Track length (TL) < 15 cm with a high Track length/Track width (TW) ratio (TL/TW > 2), total interdigit angle between 10^{o} and 30^{o} and a digit III with a large anterior projection (Fig. 2.5). A hallux is rarely preserved.

Anchisauripus tracks have a 15 < TL < 25 cm with an intermediate TL/TW ratio (~2), total interdigit angle ranging from 20^{o} to 35^{o} and a digit III projection between 1.3 and 1.8 (Fig. 2.5). A hallux is rarely preserved.

Eubrontes tracks are the largest tracks defined within the plexus and have TL > 30 cm with a relatively weaker TL/TW of 1.4-1.5, total interdigit divarication of 30^{o} – 40^{o} and digit III projection of 2.2 (Fig. 2.5). A hallux is rarely preserved.

In addition to these characteristics, *Grallator* appears to be more gracile than *Eubrontes*, which has more robust digits (Fig. 2.5). Furthermore, digits II and IV in *Eubrontes* and *Anchisauripus* tracks have an equal anterior projection, while in *Grallator* digit IV projects further than digit II (Olsen *et al*., 1998). Smaller theropod tracks also tend to have a narrower total digit divarication (Olsen, 1995; Smith and Farlow, 1996). The GAE plexus is a morphological continuum and tracks should not solely be assigned to an ichnotaxon based on the randomly chosen track length parameters. Additional morphological features, such as digit widths and mesaxony, should also be considered. Unfortunately, the characteristics that most clearly distinguish GAE vary similarly in theropod tracks across different size groupings.

The validity of having three distinct ichnotaxa to describe these track morphologies has received a lot of attention in the literature (e.g., Olsen, 1980; Weems, 1992; Olsen *et al*., 1998; Rainforth, 2005; Weems, 2019). *Anchisauripus* is probably the most dubious of the three ichnotaxa. As Rainforth (2005) highlighted, Lull (1904) erected the taxa by assuming its trackmaker, which he incorrectly identified as the basal sauropodomorph *Anchisaurus*. Weems (1992) reassessed the tracks that Lull (1904) described and concluded that the hallux Lull associated with *Anchisauripus* was in fact a mudcrack. *Anchisauripus* is often regarded as a wastebasket taxon and most recently, Weems (2019) synonymised it with *Grallator*. However, as mentioned above, Olsen *et al*. (1998) illustrated that the three ichnotaxa are indeed distinct from one another. This is contrary to Olsen's (1980) earlier view, which considered *Eubrontes* and *Anchisauripus* to be junior synonyms of *Grallator*. Synonymizing the three ichnotaxa has been supported in the last two decades. For example, Rainforth (2005) proposed that *Grallator* and *Anchisauripus* should be junior synonyms of *Eubrontes*. Lucas *et al*. (2006) assigned tracks that were described as *Anchisauripus* to the umbrella term *Eubrontes*. It is their opinion that *Grallator* and *Eubrontes* represent the same ichnogenus as they are often only reliably differentiated from each other by their size. To date, many authors still use the discrete ichnotaxa names and assign tracks as being either *Grallator* or *Eubrontes* (e.g., Lockley and Gierlinski, 2014; Castanera *et al*., 2016; Sciscio *et al*., 2016), and only a few recent publications identify tracks as *Anchisauripus* (e.g., Gierlinski and Nieszwiedzki, 2005; Gallagher and Hanczaryk, 2006). It was proposed, based on a reduction in digit III projection, decrease in track elongation (TL/TW) and widening of total interdigit angles with increasing track lengths, that the GAE plexus (or morphological continuum) represents different ontogenetic stages of, possibly, a single trackmaker species (Olsen, 1980; Olsen, 1995). However, recent rigorous statistical analysis suggests that two distinct taxa may be assigned as the trackmakers of small *Grallator-Anchisauripus* and large *Anchisauripus-Eubrontes* (Farlow, 2018).

The debate regarding the "splitting" and "lumping" of ichnotaxa is not restricted to the GAE plexus. This debate arises because there is a strong degree of convergence and conservatism in footprint

morphology for tridactyl dinosaurs and birds, which may be attributed, in part, to functionality Farlow, 2018). The morphological continuum that is linked to track size, described above, s, are also observed for ornithischians (Lockley, 2009). Given this convergence and conservatism, many other ichnotaxa have been proposed to be synonymous with *Grallator, Anchisauripus* and *Eubrontes*. For example, although *Atreipus*, described by Olsen and Baird (1986), has a distinct manus print morphology, Weems (2019) regards the ichnotaxon as *Grallator* because the pedal proportions are indistinct from one another. *Dilophosauripus* was considered to be a separate ichnotaxon from *Eubrontes* because it preserves long claw marks but authors have proposed that this distinction is purely an artifact of claws dragging in the substrate rather than a true reflection of the trackmakers foot (Fig. 2.5; Weems, 2003; Rainforth, 2005; Lucas *et al*., 2006; Milner *et al*., 2009; Lockley *et al*., 2011). *Gigandipus caudatus* tracks have indistinguishable pedal proportions to *Anchisauripus* and *Eubrontes*. The main morphological variation from the GAE plexus is that *Gigandipus* preserves a medially orientated hallux impression (Fig. 2.5; Milner *et al*., 2009). Some authors suggested that the hallux impression is an extra-morphological feature, produced when the

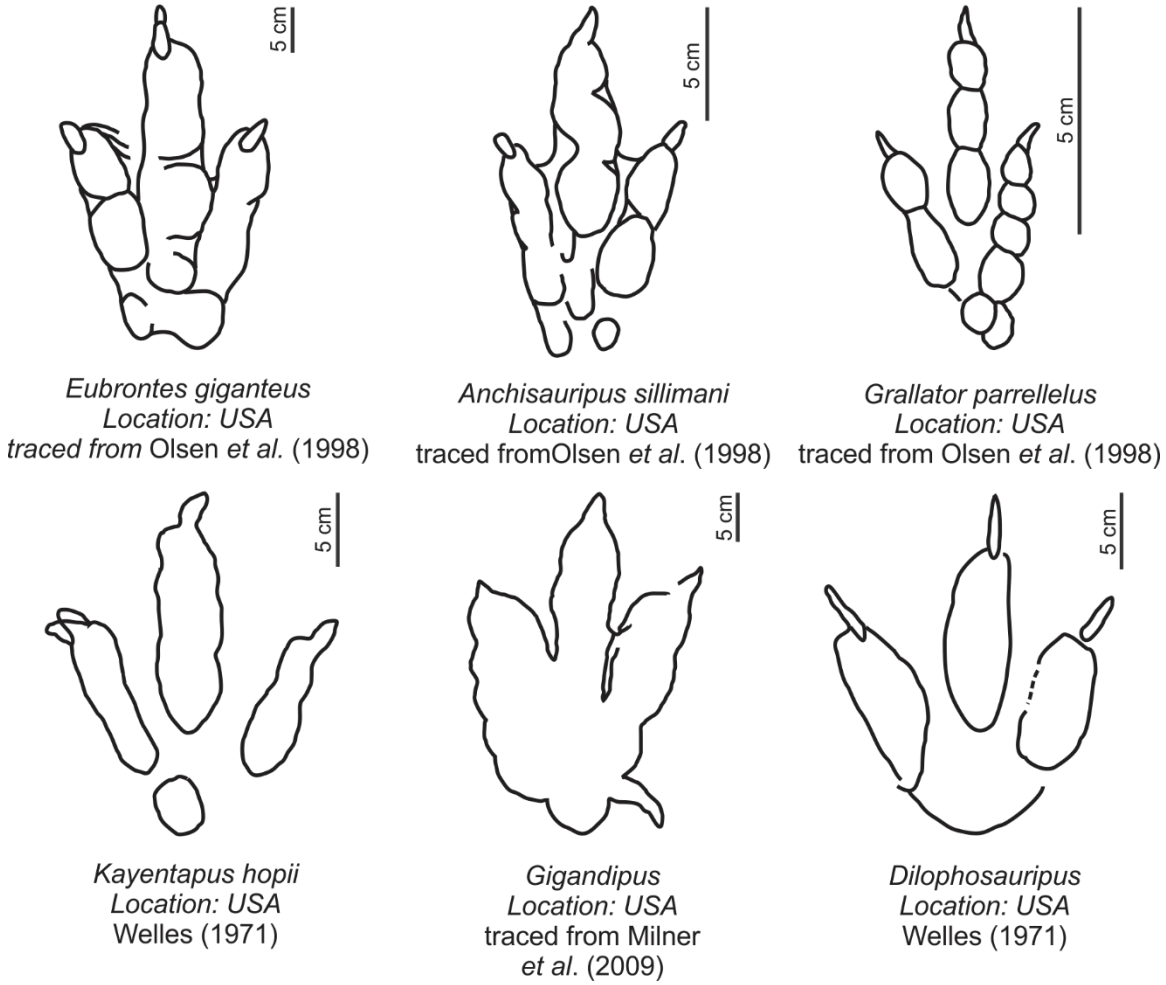

Figure 2.5: Tracings of holotype outlines of GAE plexus tracks and various ichnogenera that have been proposed to be synonymous with ichnogenera in the GAE plexus.

trackmaker sinks into the substrate and the raised hallux interacts with the medium and therefore, *Gigandipus* should be synonymized with *Eubrontes* (Weems, 2003; Rainforth, 2005; Lucas *et al*., 2006; (Milner *et al*., 2009). However, some *Eubrontes* tracks, which are apparently deeper than *Gigandipus* tracks, do not preserve a hallux impression. *Kayentapus*, a gracile tridactyl morphotype with large divarication angles, was erected as a distinct morphotype by Welles in 1971 (Fig. 2.5). Many authors regard the ichnotaxon as a discrete theropod track morphology with a global distribution (e.g., Puibelli *et al*., 2005; Lockley, 2009; Xing *et al*., 2009; Sciscio *et al*., 2017b). Weems (1992) even showed that *K. minor* and *K. soltykovensis* plotted separately from other known ichnotaxa. However, some propose that it should be synonymised with tracks of the GAE plexus – Olsen *et al*. (1998) consider *Kayentapus* to be a junior synonym of *Anchisauripus*, while Lucas *et al*. (2006) consider *Kayentapus* to be a synonym of *Eubrontes*. Many of the ichnogenera erected in southern Africa and China have been synonymized with the GAE plexus (see Olsen and Galton, 1984 and Lockley *et al*., 2013 for a comprehensive list). Piubelli *et al*. (2005) proposed that some southern African tracks may also be assigned to the ichnogenus *Kayentapus*.

In this thesis, we retain the GAE plexus and regard the ichnotaxa as morphologically distinct. Although features such as track elongation and digit projection (and mesaxony) are linked to increasing TL, *Grallator* and *Eubrontes* do present with differing morphologies including variations in digit widths and relative projections of digits II and IV. Furthermore, the recent assertion by Farlow (2018) that two trackmakers are responsible for *Grallator-Anchisauripus* and *Anchisauripus-Eubrontes* warrants further investigation into them as distinct ichnotaxa in this thesis. The GAE plexus also allows for easier comparison of the southern African tracks with global equivalents.

2.4.1 K-GAE Trackmaker

It is generally assumed that the trackmaker of all *Kayentapus* and GAE tracks is a theropod (Olsen *et al*., 1998; Li *et al*., 2006). While the idea of a gracile theropod trackmaker for *Kayentapus* (e.g., *K hopii, K. ambrokolohali*) and *Grallator* is essentially undisputed, the identity of the *Eubrontes* trackmaker is contested (for: Baird, 1957; Olsen, 1980; Olsen *et al*., 1998; Lockley, 1991; against: Bock, 1952; Miller *et al*., 1989; Weems, 1992, 2009). The idea that the *Eubrontes* trackmaker may have been herbivorous rather than carnivorous is not a new thought: Lull (1904) proposed a herbivorous trackmaker for *Eubrontes* although later he again suggested a large, bipedal theropod as the trackmaker. In the case of large, tridactyl tracks from southern African, von Huene (1932) attributed some of them to basal sauropodomorphs ("prosauropods"). It is noteworthy that, in general, very few authors provide robust evidence for assuming a theropod trackmaker other than the tracks being large, elongate tridactyl impressions with fairly sharp claws. Olsen *et al*. (1998) compared GAE tracks to the osteological record and showed similarity between theropod bones and the tracks: the digit lengths III/IV vs III/II of GAE

tracks from the Newark Supergroup are comparable with theropod osteological remains (Olsen *et al*., 1998). Recent revision of these ratios suggests that the relative length of digit II and III are consistent with theropods while the digit III and IV ratio has some ambiguity (Farlow, 2018). Additional features that support a theropod trackmaker are the claw mark lengths and medial digit projection of *Eubrontes.* The claw lengths are short and the digit III impression length is the longest of all digits, which is consistent with a theropod trackmaker (Farlow, 2018). The robust nature of *Eubrontes* digits is atypical from what we expect for theropod feet. However, when considering the soft tissue surrounding the digits, *Eubrontes* digit widths are within the range for theropods (Farlow, 2018). *Kayentapus* is unanimously attributed to a theropod trackmaker (Weems, 2006 a, b; Lockley *et al*., 2011); therefore, authors who regard *Kayetanpus* and *Eubrontes* as synonymous ichnotaxa attribute *Eubrontes* to a theropod (Lucas *et al*., 2006). The bipedal, tridactyl nature of *Eubrontes* may lean towards a theropod trackmaker but does not exclude sauropodomorphs. Weems, who has been a vocal advocate for a non-theropod saurischian trackmaker for *Eubrontes* (e.g., Weems, 1992, 2003), has recently revisited his earlier argument for a basal sauropodomorph (such as *Plateosaurus)* trackmaker for *Eubrontes* (Weems, 2019). In his view, basal sauropodomorphs were probable habitual bipeds and their foot morphology and gait patterns only minimally diverged from primitive saurischians. In addition to Weems (2006) numerous workers have shown that *Plateosaurus* was primarily or entirely bipedal based on its forelimb and hand designs (Reisz *et al*., 2005; Bonnan and Senter, 2007; Mallison 2010a, b, 2011). Basal sauropodomorphs such as *Massaurus patagonicus* and *Massospondylus* were also bipedal, the former as an adult (Otero *et al.,* 2019) and the latter through all life stages (Chapelle *et al.,* 2019). Basal sauropomorphs may also have been functionally tridactyl *at least* during walking locomotory styles (Cooper, 1981; Weems, 2003; Mallison, 2010b). Weems (2003) proposed that the metatarsal attached to digit I in *Plateosaurus* lie at an acute angle, close to the other metatarsals, so that digit I could swing 180^{o} behind metatarsals II and II, off the ground. Cooper (1981) argued that the pedal digit I of the *Massospondylus* was permanently held in an extended position similar to modern mammals "dew claw". The southern African ichnite *Kalosauropus*, which has recently confidently been attributed to *Massosspondylus* (Mukkadam, 2019), consistently preserves a tridactyl pes impression comprising of digits II-IV with simply the claw impression of digit I, suggesting that the hallux barely made contact with the tracking surface.

An overall similarity of *Eubrontes* with prosauropod and ornithischian feet, highlighting the convergence and conservatism of footprint morphologies, was noted by Olsen *et al*. (1998) and Farlow (2018). Unlike later in the Mesozoic, Early Mesozoic dinosaur pedal forms were not so different.

3 Methods

Dinosaur tracksites from the upper Stormberg Group of South Africa and Lesotho have primarily been reported on by Dornan (1908), Ellenberger and Ellenberger (1958), Ellenberger *et al.* (1966), Ellenberger (1970, 1972, 1974) and Ambrose (2003). Tracksites described by these authors form the basis of this morphological dinosaur track study. In recent years, these tracksites, and additional new discoveries, have been re-examined and reported on using modern techniques and understanding (e.g., Smith *et al*., 2009; Sciscio *et al*., 2016; Bordy *et al*., 2017; Sciscio *et al*., 2017b; Rampersadh *et al*., 2018). Ten of the twelve ichnosites considered in this study are known from the literature, primarily from the works of Paul Ellenberger and David Ambrose (Fig. 3.1). During the duration of this PhD (2016 – 2020), these sites were revisited and redocumented by the UCT-dino tracking research team, which includes the current PhD candidate (MA), and some sites have been published on (see section 1 for co-authored publications which include MA). Two ichnosite included in this study were not known from earlier literature (Lephoto and Upper Moyeni ichnosites) and were first reported on by the UCT dino-tracking team (Abrahams *et al*., 2017 and Abrahams *et al*., 2020a, respectively). All track data, photographs and models included in this PhD thesis were generated first-hand and analysed by MA during these research trips. For most of the tracksites, notably excluding Tsikoane, only field data collected during this study has been included. Cast material collected by the Ellenbergers and illustrations from Ellenberger (1970, 1972, 1974) are not included in the Stormberg Group track database.

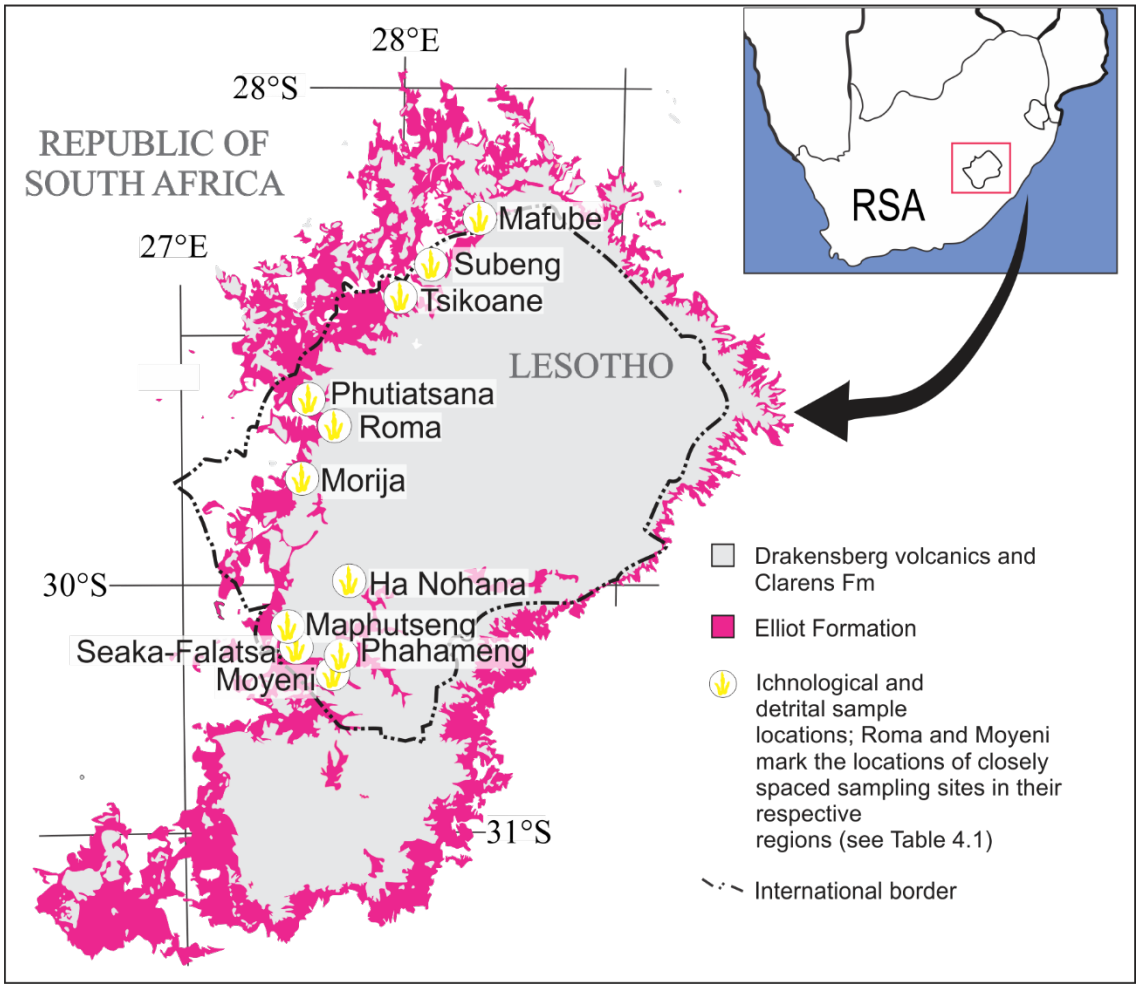

Figure 3.1: Simplified geological map of the study area, marking the location of studied ichnosites and detrital zircon-bearing rock samples. For a regional overview of southern Africa, refer to Fig. 2.1. Geological map has been modified from the Simplified Geology ma under a CC BY license, with permission from the Council for Geoscience, original copyright (2003).

3.1 Outcrop data

Macroscopic observations of the sedimentary track-bearing rocks were recorded following a slightly modified version of the facies analysis method fully described in Miall (1996). Extensive photographs of the ichnosites were taken to record the morphology of individual tracks and to generate 3D photogrammetric models of tracks and tracksites (section 3.3). Representative, fresh sandstone samples from the track-bearing strata at each ichnosite (Fig. 3.1) were collected for Uranium-Lead Laser Ablation Inductively Coupled Plasma Mass Spectrometry (U-Pb LA-ICPMS) dating of detrital zircons ($ZrSiO_4$; section 3.6).

3.2 Track data

While numerous track types e.g., tridactyl, tetradactyl and pentadactyl, are preserved at the ichnosites evaluated during this study, only tridactyl tracks with a theropod affinity are considered for the morphological analysis. Whether tracks potentially have a theropod affinity is determined in the field:

theropod tracks are generally elongate and asymmetrical, with digits II and IV having subequal lengths, mesaxonic and typically possess gracile digits that taper to V-shaped tips/claw impressions. Because the focus of this study are tracks with a theropod affinity, the term "tridactyl track" from this point on can be assumed to mean "tracks with a theropod affinity" unless otherwise stated. At some ichnosites considered herein, tridactyl tracks that are not attributable to theropods are also preserved (e.g., *Anomoepus* at Lower Moyeni, *Trisauropodiscus* at Lephoto and Maphutseng) and are mentioned in the site overviews provided in section 4.1.

Objectively defining the margin of a track, especially those with grading walls, is one of the key problems faced in vertebrate ichnology. This is due to the continuous nature between the impression and the surrounding sediments. Therefore, the track outline an operator produces is an *interpretation* of the track morphology. There has been a shift in practice from qualitative to quantitative descriptions of ichnites, and this extends to incorporating technological advancements to aid objectively defining track boundaries (Falkingham *et al.,* 2018). Recently, Lallensack (2019) developed software utilizing mathematically-defined criteria to produce a track outline. However, the computed outline cannot always be used independently because it loses most of the internal structures and cannot discriminate extramorphological detail. Therefore, it should still be considered in conjunction with an operator's interpretative outline as anatomical features may be disregarded by the program. Belvedere *et al*. (2018) proposed the use of mediotypes and stat-tracks: combining 3D models to generate a composite track of ichnotypes, which is useful for ichnotaxanomic comparisons and to explore track variations, respectively. The importance of standardizing the morphological outline can be seen quite simply in the significant difference in linear measurement values obtained for a single specimen by different operators (e.g., Castanera *et al*., 2012). These inconsistencies have ramifications for ichnotaxanomic assignments, track comparisons and inferences such as trackmakers' speeds, body sizes, masses, etc. which are based on track parameters. To mitigate the variability in track morphology outlines (and subsequent track measurements), a single operator (MA) outlined and measured the tracks sometimes with the aid of depth models (section 3.3).

Standard track measurements are recommended to quantify vertebrate track dimensions and ultimately assign them to established or new ichnotaxa (Thulborn, 1990; Lockley, 2009; Falkingham *et al.,* 2018). These basic measurements include the track length (TL), track width (TW) and track span (TS), which are measured directly in the field (Fig. 3.2A). Additional track parameters such as digit divarication (II^III, III^IV and II^IV), digit III projection beyond digits II and IV (Dp) and digit lengths (LII, LIII, LIV) are measured from field photographs using Image J software (a public domain image processing programme – Schneider *et al*., 2012; Fig. 3.2A). Track measurements are presented in Appendix Table A.1.

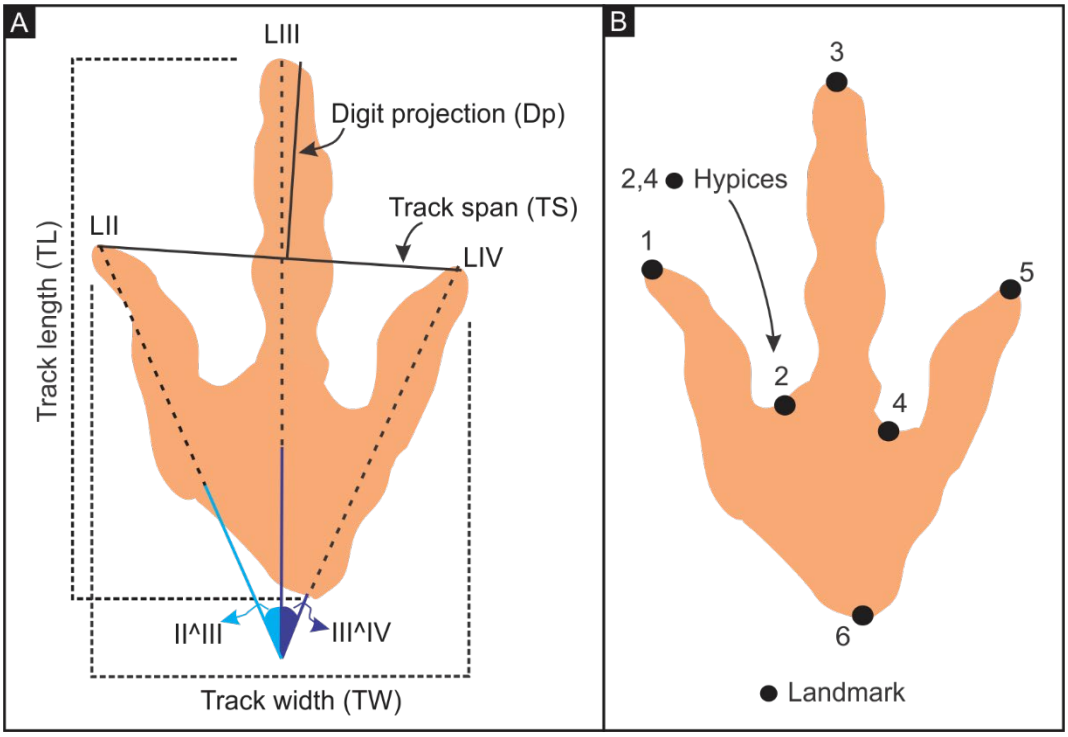

Figure 3.2: Measurements taken on the tridactyl bipedal ichnite. A) Outlines for linear measurements taken in the field and using ImageJ. B) Placement of landmarks used for principal component analysis (PCA; section 3.5).

Estimates of a trackmaker's hip height (*h*) and body length (BL) are calculated from TL (Fig. 3.2A; Equations. 1–5 listed below). Equations 1 to 4, which determine the hip height, are in fair agreement with the theropod osteological record, especially for smaller theropods (e.g., Avnimelech, 1966; Alexander, 1976; Lockley *et al.,* 1983; Thulborn, 1984, 1989, 1990; Henderson, 2003).

Hip height was estimated using morphometric and allometric ratios for theropods (Thulborn, 1990):

Where TL < 25 cm (1) $h = 4.5 \times TL$ [morphometric ratio]

(2) $h = 3.06 \times TL^{1.14}$ [allometric ratio]

Where TL > 25 cm (3) $h = 4.9 \times TL$ [morphometric ratio]

(4) $h = 8.60 \times TL^{0.85}$ [allometric ratio]

Hip height is considered the most convenient estimate of bipedal dinosaur size (Thulborn, 1990). Although morphometric and allometric formulae are popular in ichnological work, they are estimates; therefore, the results they yield need to be cautiously interpreted (for a discussion, see Rainforth and Manzella, 2007).

Body lengths (BL) for theropod dinosaurs were calculated using Thulborn's (1990) equation:

(5) $BL = 4 (h)$

3.3 Photogrammetry

Photogrammetric digital 3D models are accurate replicas of the tracks, and allow digital gathering of depth information, track measurements, fossil preservation and remote sharing of tracks. Photogrammetry is an affordable simple and popular technique for successfully documenting vertebrate tracksites (e.g.,Petti et al., 2008; Razzolini *et al*, 2014; Lallensak *et al*., 2016; Bordy *et al.,* 2016; Rampersadh *et al.,* 2018).

Photogrammetric 3D models of individual upper Stormberg Group tracks were generated using 20–35 individual track photographs that were taken at acute, right and obtuse angles, relative to the tracking surface, using a Canon PowerShot EOS D1200 (Focal length 28 mm, 5184 x 3456 resolution) camera. The methods described by Mallison and Wings (2014) and Mathews *et al*. (2016) were applied using Agisoft Photoscan (version 1.1.4) software. Here, the main steps are highlighted. Tracks were photographed from multiple vantages with 2/3 overlap between photographs. The relative position of the object in the photographs was determined by the software, allowing for the production of 3D information. The input photographs were filtered, to remove low quality images (e.g., blurry, out of focus) and foreign, unwanted objects (e.g., foot of photographer), as these introduce errors and reduce the overall quality of the final model. The software then aligned the photographs and determined camera positions by identifying and matching various repetitive or overlapping features in the photograph dataset, generating a sparse point cloud, where each point represents x, y and z dimensional data, of the surface. Subsequently, a dense cloud was generated and a "height field" type 3D polygonal mesh, which is applicable for planar surfaces, was added. This step correlates geometric shapes to build a mosaic of photographs without any vacancies across the surface. The meshes generated in Photoscan were exported as Stanford PLY files (.ply) and processed using Cloud Compare (version 2.6.1) to produce false depth maps. Given the irregularities of the modeled surface, meshes are orientated in Cloud Compare by fitting a plane which intersects the mesh. The fitted plane generates a matrice that is then applied to rotate the mesh. Coloured false depth maps are produced by the "export the co-ordinate(s) to the SF(s)" function in the z-direction.

3.4 Casting

Casts of select tracks, which preserve morphological detail or are unique at a given ichnosite, were made using Mold Star R 15 Smooth On Inc, low viscosity, platinum cure silicone rubber following the method described by Sciscio *et al.* (2016). Non-curing modelling clay retaining walls were built around cleaned tracks to prevent spilling of the liquid casting material. The casting material consists of equal measurements of part A and part B components of the RTV silicone rubber. This mixture was poured

into, and slightly above, the track. The casts (individual tracks and trackways) are stored at the Evolutionary Science Institute at the University of the Witwatersrand (Johannesburg, South Africa; accession numbers: Mafube - BP/6/733, Roma: 2 Lephoto - BP/6/734, Roma 3: Matobo - BP/6/735, Upper Moyeni - BP/6/752-3,).

3.5 Principal Component Analysis

Principal component analysis (PCA) is fast becoming a common way to analyse track data (e.g., Demathieu and Wright, 1988; Moratalla, 1998; Acevedo *et al.,* 2002; Demathieu *et al.,* 2002; Belvedere, 2008; Osi *et al*., 2011; Castenara *et al.,* 2015, 2016; Lallensack *et al.,* 2016, Romano and Citton, 2017; Farlow, 2018). It can be used to describe variation in track morphology, refine ichnotaxonomy, and even distinguish the trackmakers of similar looking tracks. Principal component analysis, in this study, was performed using two methods: 1) a geometric morphometric (GM) approach using landmark placement and 2) a traditional approach using linear measurements. Landmark-based and traditional PCA were performed from placed landmarks and track linear measurements, respectively, using Past V3.18 (Hammer *et al.,* 2001).

Geometric morphometric PCA requires digitised landmarks. Six landmarks were selected to define the general shape of the tracks (Fig. 3.2B). The landmarks are placed as follows: 1) The most distal position of digit II, 2) centre of the digit II and III hypice, 3) the most distal position of digit III, 4) centre of the digit III and IV hypice, 5) the most distal position of digit IV, 6) positioned at the "heel" or posterior end. Claw marks were avoided during the placement of landmarks 1, 3 and 5. Therefore, for tracks which preserve claw mark impressions the distal most placement of the landmark is an approximation which be marginally offset. This consideration needs to be kept in mind when interpreting landmark-based PCA results. Landmarks 2 and 4 carry the most uncertainty with their placement as the centre of the hypice carries significant interpreter biases. Furthermore, some tracks are preserved as distinct digit impressions with no hypice preserved; therefore, the landmark placement for these tracks is entirely interpretative. Landmarks 2 and 4 are, consequently, expected to show high variability and cannot confidently be used in landmark-based PCA interpretations. Placement of additional landmarks to better define the track outline, classically linked to nodes (digital pads) within tracks (e.g., Castanera *et al*., 2015), could not be placed due to a lack morphological detail in the tracks. However, using only 6 landmarks to express the morphology of a tridactyl track is acceptable (Lallensack *et al.*, 2016)

Although landmark-based geometric morphometrics is recommended exclusively for tracks with a high anatomical fidelity (*sensu* Gatesy and Falkingham, 2017) or morphological preservation grade (*sensu* Belvedere and Farlow, 2016; Marchetti *et al.,* 2019), we have employed these techniques for lower grade tracks as well. Tracks are selected for landmark-based analysis if they preserve a complete

morphology and do not have obvious substrate controls on their morphologies (i.ee, sediment-collapse features). Where landmark-based PCA is used for ichnotaxonomy or morphological assessment, the measured parameters outlined in section 3.2 are also considered. Therefore, the tentative landmark-based analysis is not the only tool used for ichnotaxonomic interpretations but it is tentatively used an additional method.

In order to place landmarks, Tps files were generated from photographs taken perpendicular to tracks using TpsUtil 1.75 (Canon PowerShot EOS D1200 -Focal length 28 mm, 5184 x 3456 resolution camera; http://life.bio.sunysb.edu/morph/). Tps files were imported into Tps Dig software to digitally place 6 landmarks on each track photograph (Fig.3.2; http://life.bio.sunysb.edu/morph/). Claw marks and extramorphological features were excluded during landmark placement. To exclusively analyse the track morphology, no scale was considered during the placing of landmarks. The landmark data was exported into PAST V3 software (Hammer *et al.,* 2001) and a Procrustes fitting transformation was applied to the data to standardise the alignment of the landmarks (accounting for size and orientation variations between tracks). Principal component analysis and accompanying loadings were obtained on PAST V3. Following the above outlined method, PCA was performed on published holotype, paratype or high anatomical fidelity tridactyl tracks for a morphometric comparison (*Dinehichnus-, Eubrontes-, Gigandipus-, Grallator-, Hispanisaurus-, Irenesauripus-, Jialingpus-, Jurabrontes-, Kayentapus-, Megalosaurids-, Megalosauripus-, Moyenisauripus-, Stenonyx- isp.* from Gierlinski, 1990;Welles, 1991; Lockley *et al*., 1998; Olsen *et al*., 1998; Niedzwiedzki and Remin, 2008; Gierlinksi *et al*., 2009; Smith *et al*., 2009; Lockley *et al*., 2011; Niedzwiedzki, 20111; Xing *et al*., 2014; Forster, 2015; Gierlinksi *et al*., 2017; Razzolini *et al*., 2017; Marty *et al*., 2017; Rauhut *et al*., 2018; see reference list for more details; Fig. 3.3.). From now on, these tracks are referred to as the "comparative ichnogenera database". The tracks from the relevant literature were additionally selected because they included 90^{o} photographs or false depth maps on which landmarks could be placed. Using these published tracks, an ichnogenus morphospace (when considering two principal components) may be generated, allowing one to use the PCA for ichnotaxonomic refinement of unnamed tracks. Because these morphospaces consider high anatomical fidelity tracks, they do not account for natural morphological variation attributable to trackmaker-substrate interactions and/or preservation (see section 2.2). Consequently, unnamed tracks which do not lie within a given morphospace cannot confidently be excluded from the ichnogenus based solely on the landmark-based PCA and would require further investigation i.e., their measured parameters and a visual assessment of their morphologies may be considered.

Traditional PCA was performed using the measured parameters on the upper Stormberg Group dataset as well as on published track data with a global distribution for comparison (Fig. 3.3). The

published track data includes tracks assigned to *Grallator*, *Anchisauripus* and *Eubrontes* from Australia, China, France, Poland and the USA and are also termed the "comparative ichnogenera database" (Weems, 1992; Olsen *et al*., 1998; Cook *et al*., 2009; Demathieu *et al*., 2014; Xing *et al.,* 2014; Xing et al., 2017; see reference list for more details). These data were also used for additional statistical comparison e.g., box and whisker and scatter plots.

3.6 U-Pb Laser Ablation Inductively Coupled Mass Spectrometry

Uranium-Lead (U-Pb) geochronology has become a key tool in Earth sciences for resolving geological time (Spencer *et al.,* 2016). The two primary reasons that U-Pb geochronology is viewed as the gold standard of chronology is that: a) of all the decay schemes, the U decay constants are the most precisely determined, and b) the dual U-decay schemes (Equations. 6 and 7) can be used as an internal check, since ^{238}U and ^{235}U have different half-lives (Jackson *et al*., 2004; Bowring *et al*., 2006; Schoene, 2014). The radioactive decay of ^{238}U and ^{235}U, respectively produces ^{206}Pb and ^{207}Pb (Schoene, 2014).

$$\left(\frac{Pb^{206}}{Pb^{204}}\right) = \left(\frac{Pb^{206}}{Pb^{204}}\right)_0 + \left(\frac{U^{238}}{Pb^{204}}\right)^{e\hat{}(\lambda 238t)-1} \quad (6)$$

$$\left(\frac{Pb^{207}}{Pb^{204}}\right) = \left(\frac{Pb^{207}}{Pb^{204}}\right)_0 + \left(\frac{U^{235}}{Pb^{204}}\right)^{e^{\lambda 235t}-1} \quad (7)$$

Using the two decay schemes, Wetherill (1956) introduced the Concordia diagram, a plot of $^{206}Pb/^{238}U$ vs $^{207}Pb/^{235}U$. Data that lie on the Concordia curve have a $^{206}Pb/^{238}U = {}^{207}Pb/^{235}U$ and are termed "concordant". Data that lie above or below the Concordia curve are interpreted to have experienced open-system behaviour and are termed "discordant". Non-analytic reasons to which discordancy can be attributed include mixing, Pb loss and the incorporation of initial Pb (Gehrels, 2012; Schoene *et al*., 2014). The concordance (or discordance) is expressed as the percentage of agreement (or disagreement) between the two isotopic systems (Spencer *et al*., 2016). Data that have been determined to be significantly discordant are omitted from the data set and subsequent interpretations. The level of acceptable discordancy is arbitrary and has received limited discussion to date and acceptable discordancies range from 1–30 % (Jackson *et al*., 2004; Hietpas *et al*., 2011; Gehrels, 2012; Spencer *et al*., 2016). Here, we apply the commonly used concordance filter of 10% (Spencer *et al.,* 2016). It should be noted that the chosen discordance filter can dramatically influence data interpretation.

In addition to the above-mentioned factors, the abundance of high U-minerals, such as zircon, monazite, apatite, titanite, rutile, in most rock types has contributed to the popularity of U-Pb

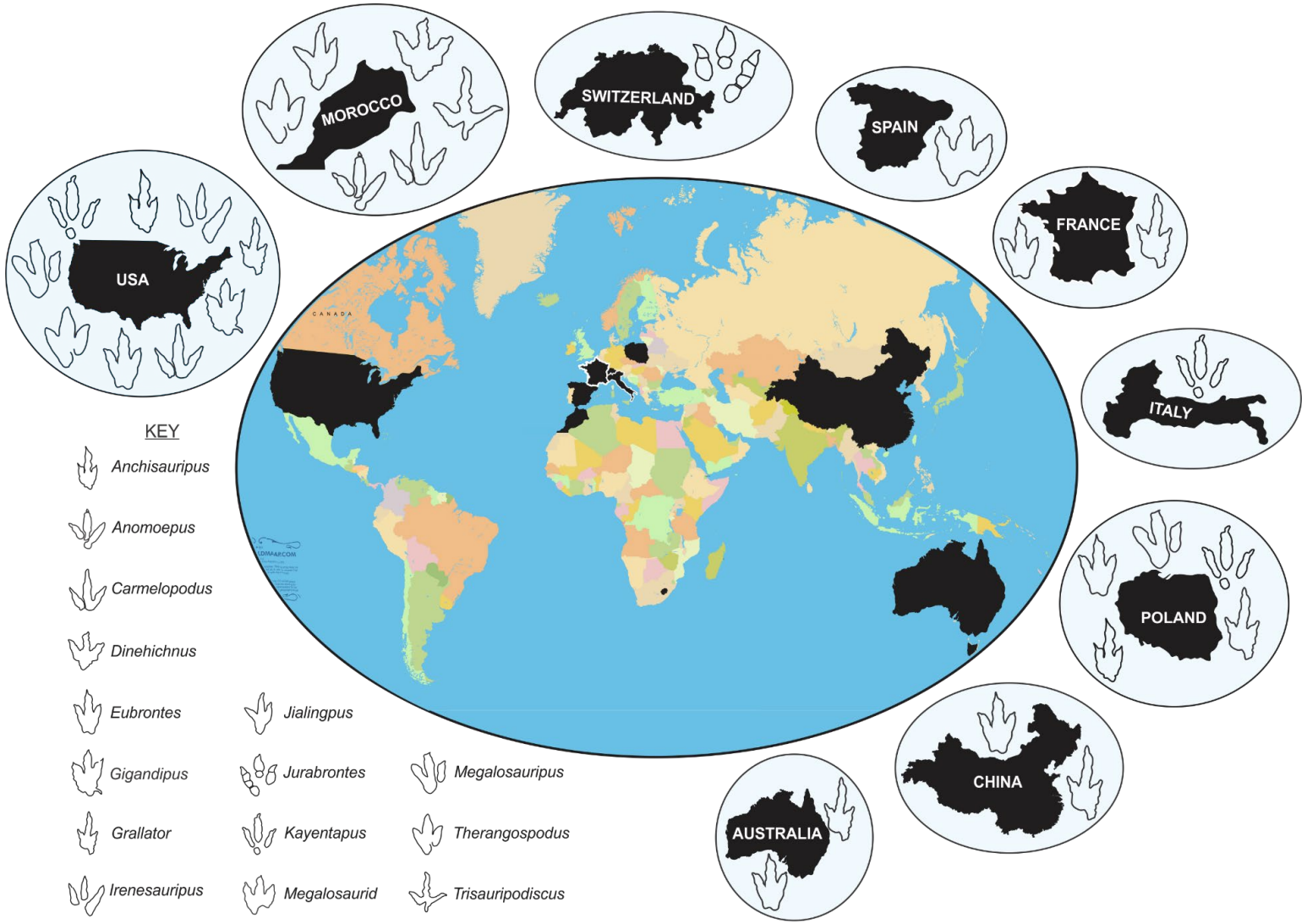

Figure 3.3: Global distribution of published tracks considered for comparison with the upper Stormberg Group tracks in this study i.e., the comparative ichnogenera database defined in section 3.5

geochronology. Of the U-bearing minerals, zircon ($ZrSiO_4$) is most commonly used because a) zircon is ubiquitous within the Earth's crust and is a common accessory mineral, b) zircon contains little to no initial Pb, and c) zircon is a robust, refractory mineral (Cawood and Nemchin, 2000; Bowring *et al*., 2006). Detrital zircon studies can shed light on denudation, exhumation, palaeodrainage systems and, most commonly, provenance, correlation of sedimentary units, and determining maximum depositional age (Burret *et al*., 2014 and references therein; Spencer *et al*., 2016). Dating can be executed via various methods e.g., ID-TIMS, SHRIMP, LA-ICPMS. The latter, also used in this study, has become increasingly popular due to its reduced cost, easy availability and short analysis times (Gehrels, 2012). Relative to ID-TIMS and SHRIMP, LA-ICPMS is subordinate in precision and spatial resolution, respectively (Paton *et al*., 2010).

3.6.1 Sample Preparation

Thirteen fresh, unweathered sandstone samples were primarily collected from the track-bearing palaeosurfaces considered in this study for U-Pb LA-ICPMS dating to obtain their maximum depositional age (MDA; Fig.3.1). At some sites, additional samples from underlying or overlying strata were also collected. Sample locations were selected away from the main tracksite where fresh material could easily be collected.

The sample preparation to extract zircon grains is largely standardised with precautions aimed at preventing biases and contamination. The method followed here is described by Roberts *et al*. (2012) and Tucker *et al*. (2013), and was performed at the Central Analytical Facility at Stellenbosch University. All samples were scrubbed with a brush and washed with water to ensure finer, foreign material was removed from the surface prior to further processing. The rock samples were dried and crushed into cm-chips in a jaw crusher and subsequently disc-milled at 1 cm and 0.5 cm disc-spacings to produce a fine powder. The powder was then sieved using a 350 µm hand-held sieve, and all particles >350 µm were discarded. The remaining powder was then vigorously washed for multiple cycles, until the suspended clay fraction was decanted. As the clay particles tend to agglomerate, the sediment in the beaker needs to be worked between one's fingers to release the mud. When all the finer sediment is removed, and the decanted water is clear, the sediment is spooned onto an oscillating Super panner 2000, which has a stream of water flowing down it, to re-organise the sediment by density. High density minerals, such as zircon, become concentrated proximal to the water source and were pipetted off the panner and dried to undergo additional processing. Within this dense fraction, magnetic minerals were removed using a hand-held magnet prior to further separation in a tetrabromethane heavy liquid. After overnight separation, the dense material was removed and approximately 120 zircon grains within it were randomly picked using a Leica binocular microscope and mounted onto a 25 mm epoxy resin puck. The mounted puck was then polished for a

few minutes to expose the mid-sections of the zircon grains and carbon coated as preparation for cathodoluminsence (CL) imaging (Fig. 3.4). It is important to take care while polishing as zircons can

easily be lost during this step. Under-polishing would not reveal the zircon midsections, while over-polishing could remove zircons in the upper layers of the resin.

A Carl Zeiss MERLIN high resolution field emission scanning electron microscope with attached cathodoluminescence detector and a scan speed of 12 was used to detect complexities such as zoning, cores, inclusions and cracks within the zircon (Fig. 3.4; Appendix Fig. B.1). This is made possible by varying uranium concentrations within the zircon grain, where higher U content areas are darker. This helps to select areas within the zircon crystal to avoid, i.e., cores and cracks, and to focus on, i.e., zoning, during laser ablation.

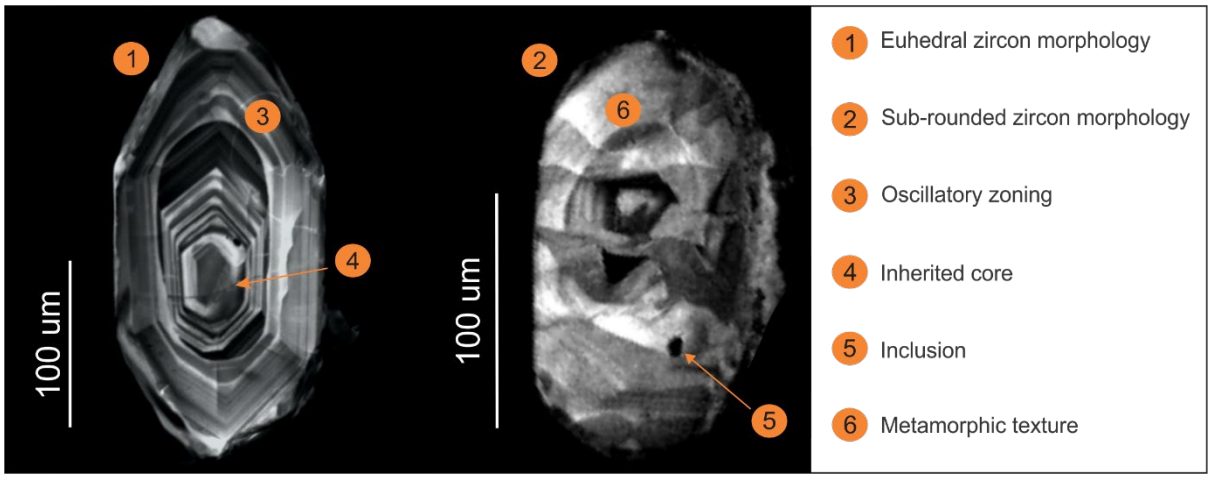

Figure 3.4: Cathodoluminescence images highlighting individual features that may be observed within a zircon crystal (zircons from - left: Subeng ichnosite; right: Maphutseng ichnosite) .

However, it should be noted that CL images are 2D representations so there may be unexpected complexities in the unseen third dimension. CL imaging exposes the internal structures of zircons, which reflect episodes of growth, dissolution and crystallisation (Cawood and Nemchin, 2000). For example, well-developed oscillatory zoning is interpreted to have developed during crystallisation from a magma, while bright zones, particularly rims, are interpreted as being related to metamorphic processes (Fig. 3.4). Given that the aim of this study is determine the MDAs of ichnosites, magmatic textures are preferentially selected for laser ablation.

3.6.2 LA-ICPMS

The measurements with LA-ICPMS were performed using a Thermo Finnigan ELEMENT 2 mass spectrometer coupled to a 193 nm wavelength ASI Resolution laser ablation system at the Central Analytical Facility, Stellenbosch University (Stellenbosch, South Africa). Approximately 100 zircon grains were ablated per sample, in a total of 6 separate analytical sessions or “runs”. The conditions

and instrument specifications were constant between "runs". A spot size of 30 µm, with a crater depth of approximately 15 to 20 µm, was used across an ablation period of 16 seconds per zircon. The spot size was carefully considered to avoid catastrophic ablation of the zircon grains. The ablated isotopic material was transported to the ICP-MS in an Ar and He carrier gas. GJ1, Plešovice and M127 standards were ablated after 30 sample ablations to correct for instrumental mass bias and fractionation. It is assumed that the fractionation effects are the same in the standards as in in the unknowns (Jackson *et al*., 2004). For this correction to be meaningful, the standards and samples require the same ablation conditions. Maintaining constant laser ablation conditions throughout "runs" is vital as elemental fractionation is sensitive to laser pulse energy and focus (Jackson *et al*., 2004). This was, in part, achieved by continuously firing the laser throughout a "run" and initiating and terminating ablation by obstructing the laser beam path, and having a pre-ablation warm-up to set the "run" conditions. All isotope data needed to calculate the U-Pb age and associated uncertainty of a sample were analysed. This U, Pb and Th isotopic data is presented in Appendix Table B.1.

3.6.3 Data reduction and display

Data reduction refers to the conversion of electrical signals detected by the mass spectrometer to useable data (Spencer *et al*., 2016). This reduction corrects for laser induced fractionation, mass discrimination and matrix effects. In this study, a commercial data reduction software package "Iolite" (Paton *et al*., 2011) was used in conjunction with "VizualAge" (Petrus and Kamber, 2012). The dispersed zircon standards were used for data calibration, drift corrections and quality control. Therefore, reduction of these reference materials was performed first.

The isotopic data is acquired as function of time (or ablation depth). Therefore, a) isotopic heterogeneities and discrepancies possibly arising from cracks, cores etc. can be detected; and b) optimal integration periods of the background and signal can be selected for individual zircon grains. This allows common Pb contributions and Pb loss signals to be reduced and concordance to be improved (Jackson *et al*., 2004). Background periods were selected for the GJ1 and Plešovice standards and deducted from the overall reading for all analysis. Integration periods of the standards were selected carefully so that concordant and weighted mean ages obtained for Plešovice (Sláma *et al*., 2008) and M127 (Nasdala *et al*., 2016; Mattinson, 2010) agreed with the published ID-TIMS ages of 338 and 527 Ma, respectively.

Integration periods for the unknowns were cautiously selected after taking the following considerations into account:

1. If all isotopic readings appear normal, the beginning of a signal is favoured over the end;
2. Congruent U^{238} and Pb^{206} signals indicate a continuous reading within a single domain;

3. Crossing of U^{235} and Pb^{206} isotopic readings indicate a change in domains; and
4. Where possible, common lead (Pb^{204}) spikes should be avoided.

The integrated periods of unknowns were chosen based on the level concordancy and/or degree of clustering. Errors associated with U/Pb ages were aimed at less than 10 Ma. A mass common Pb correction was not applied to the "runs".

The final age and visual presentation of the reduced data were produced in MS Excel using the IsoplotEX insert developed by Ludwig (2003). For each sample, a concordia diagram was plotted to illustrate the spread of the data and the degree of concordance associated with individual ages. The isotopic data collected provides 3 different date ratios: $^{207}Pb/^{235}U$, $^{206}Pb/^{238}U$ and $^{207}Pb/^{206}Pb$ (Appendix Table B.1). The measurements of ^{235}U and ^{207}Pb are imprecise, as ^{235}U is not directly measured by the mass spectrometer and is instead calculated using the fixed ~137.8 ratio for the two U isotopes (Steiger and Jäger, 1977). As a result, the $^{207}Pb/^{235}U$ age is rarely used (Spencer *et al*., 2014). $^{206}Pb/^{238}U$ dates are used for ages < 1.2 Ga while $^{207}Pb/^{206}Pb$ dates are used for ages > 1.2 Ga (Spencer *et al*., 2014). Given that the data in this study is chiefly young - i.e., <1.2 Ga, all dates and interpreted ages quoted refer to $^{206}Pb/^{238}U$. The following metrics, described in increasing statistical reliability (1–4), outlined by Dickson and Gehrels (2009) and further discussed by Coutts *et al*. (2019), were employed to ascribe a maximum depositional age (MDA) to samples (see Table 4.2):

1. Youngest single grain (YSG) – the date of the youngest concordant grain is interpreted to be the MDA.
2. Youngest peak age – a graphical peak age determined from a probability plot.
3. Youngest Cluster comprising 2 or more grains overlapping at 1σ error (YC1 σ (2+)) – A weighted mean age obtained from x or more grains that overlap within 1σ error.
4. Youngest Cluster comprising 3 or more grains overlapping at 2σ error YC2σ(3+)) – A weighted mean age obtained from 2 or 3 and more grains, respectively, with dates that overlap within 2σ error.

Two additional metrics were used:

5. Youngest cluster comprising 2 or more grains overlapping at 2s error
6. Concordia age – the MDA is interpreted form the Concordia diagram and is produced by a built-in function in Isoplot 4.15 software. Grains overlap at 2s error on the concordia plot.

The preferred MDA for each sample was assigned after the chronological data was compared to existing age estimates based on litho- (Bordy *et al*., 2004; Bordy and Eriksson 2015), bio- (Kitching and Raath, 1984; McPhee *et al*., 2017), ichno- and magnetostratigraphy (Siscio *et al*., 2017).

3.7 Exploratory statistics

Numerous statistical methods (Table 3.1) have been employed to: a) visualize the distribution of the track data presented herein and b) test the statistical relevance of trends or observations arising from "a". Each method utilisizes different measured parameters and data groupings. Therefore, the details of each method are presented in Chapter 6 along with their results, for easy referencing, comparison and interpretation. Interdigit angle data is omitted from multiple methods because they are the most interpretive to measure (and are therefore highly variable) and are considered to be secondary contributors to track morphology (Moratalla *et al.,* 1998; Lockley, 2009). Furthermore, interdigit angles may be measured in numerous ways (see Thulborn, 1990) and are therefore difficult to compare between authors.

Table 3.1: Overview of statistical methods and tests performed in Chapter 6: Exploratory statistics.

Statistical Method	Section	Data considered
Pairwise scatterplots	6.1	All track measurements
Correlation matrices	6.1	All track measurements
Frequency distributions	6.2	All linear track measurements (excluding TS)
Box and whisker plots	6.3	All track measurements
Principal component analysis	6.5	Landmark data, all linear track measurements
Cluster analysis	6.6	TL, TW, TS, Dp
Discriminant analysis	6.7	All linear track measurements

Statistical tests	Null hypothesis
Mann-Whitney	H0: The two samples are taken from populations with equal medians
Kolmogorov-Smirnov	H0: The two samples are taken from populations with equal distributions
Anova	H0: The two samples are taken from populations with equal means
Kruskal Wallis	H0: The two samples are taken from populations with equal medians

4 Temporally-based ichnological assessments

4.1 Ichnosites

Ichnosite descriptions are presented alphabetically within their stratigraphic horizon i.e., lower Elliot Formation (lEF), upper Elliot Formation (uEF) and Clarens Formation (CLAR). These tracksite overviews include brief stratigraphic and sedimentological contexts, a review of all ichnites preserved on the palaeosurface and a detailed description (including track measurements, high resolution photographs and 3D photogrammetric models) of the tridactyl tracks with a potential theropod affinity. Tracksites that have recently been published on have only brief overviews (see Table 4.1), and for their detailed sedimentological and track descriptions the reader is referred to the relevant publications, which are cited in the Introduction Chapter (1). A single Clarens Formation ichnosite, "The Early Jurassic Tsikoane ichnosite", does not follow this outline and is instead presented as an independent paper in Chapter 5 and is intended to be submitted for publication.

The ichnotaxonomy of the upper Stormberg Group tridactyl tracks is revisited by considering the tracks overall morphology and linear dimensions, as well using geometric morphometrics to compare the tracks with comparative ichnogenera database defined in section 3.5. The defined morphospaces of these published ichnogenera were generated from photographs of primary field or cast material and are therefore limited and do not account for natural morphological variation of the given ichnotaxon. Therefore, the PCA fields are constrained and outlying tracks may be attributed to track morphological variation due to trackmaker-substrate interactions, morphological preservation grade or erosion (section 2.2). It is important to bear this consideration in mind, because many of the studied tracks do not lie within K-GAE morphospace but are inferred to be K-GAE based on select morphological features and measured parameters. This natural variation is most easily demonstrated for trackways, where some of the tracks lie within K-GAE morphospace and others are outliers. Outlying tracks are still considered for almost all the statistical analyses (Chapter 6). The extensive ichnotaxonomic assessments by Ellenberger (1970, 1972, 1974) and Olsen and Baird (1986) are included herein for comparison.

In addition, the geochronology for each ichnosite is also presented. Because these geochronological results are based on the U-Pb LA-ICPMS dating of detrital zircons, it is important to bear in mind that these results present the *maximum* depositional age (MDA) of the sample and that the true depositional age (TDA) of the studied samples may likely be younger. If syn-depositional zircons, primarily from wind-blown ash or active volcanic sources, are prevalent in the depositional system, the MDA will more closely reflect the TDA. Of the metrics considered to assign MDA, YC2[2+] is predominantly the preferred age for the sample. This metric, which incorporates more zircon crystals, is statistically more robust than YSG. Additional geochronological data obtained during this PhD has recently been published in a review paper (Bordy *et al.*, 2020b).

Table 4.1: Ichnosite locality, stratigraphic position and source information for tracks considered in this study.

Site	GPS co -ordinate	Section	Source (Most recent)	Stratigraphy	Database Track #
Ha Falatsa	30°21'57.43''S 27°34'19.18''E	Section 4.1.1	Ellenberger (1970)	lEF	1 to 6
Maphutseng	30°12'44.98''S 27°28'52.39''E	Section 4.1.2	Ellenberger & Ellenbeger (1956)	lEF	7 to 44
Phuthiatsana	29°21'30.02''S 27°36'35.61''E	Section 4.1.3	Sciscio *et al.* (in review)	lEF	45 to 67
Subeng	28°49'23.53''S 28°4'29.82''E	Section 4.1.4	Bordy *et al.* (2017) Smith *et*	lEF	68 to 76
Lower Moyeni	30°23'42.49''S 27°41'34.66''E	Section 4.1.5	*al.* (2009) Sciscio *et al.*	uEF	91 106
Mafube	28°40'0.04''S 28°16'54.13''E	Section 4.1.6	(2016)	uEF	107 to 115
Roma site 1	29°26'55.67''S 27°42'2.52''E	Section 4.1.7		uEF	77 to 80
Roma site 2: Lephoto	29°26'49.03''S 27°44'18.57''E	Section 4.1.8	Abrahams *et al.* (2017)	uEF	81 to 90
Roma site 3: Matobo	29°27'08.57''S 27°42'08.51''E	Section 4.1.9	Sciscio *et al.* (2017)	uEF	116 to 125
Roma site 4: Tlapana	29°27'13.57°S 27°42'23.01''E	Section 4.1.10	Ambrose (2003) Abrahams	uEF	126 to 141
Upper Moyeni	30°24'9.5''S 27°42'7.1''E	Section 4.1.11	*et al* . (in review) Haupt	uEF	142 to 183
Phahameng	30°22'35.38''S 27°42'7.99''E	Section 4.1.12	(2018)	CLAR	184 to 185
Tsikoane	28°54'4.90''S 27°59'41.67''E	Section 5	Dornan (1908)	CLAR	186 to 216

4.1.1 Ha Falatsa ichnosite

The Ha Falatsa ichnosite was first described by Ellenberger (1970, 1972). This lEF site is an extensive (~650 by ~20 m) palaeosurface with multiple tracking surfaces preserving tridactyl, tetradactyl and pentadactyl tracks and trackways (Fig. 4.1; Ellenberger, 1970). Ripple marks, soft sediment deformation structures and desiccation cracks are preserved on the palaeosurface (Fig. 4.1). The preservation grade across the medium- to coarse-grained sandstone surface is variable (0.5–1; Appendix Table A.1).

4.1.1.1 Ichnology

Herein, we describe the six tridactyl tracks found at Ha Falatsa, of which three tracks form a single trackway (Fig. 4.1). The tridactyl tracks are distributed across the track-bearing surface. The preservation grade of these tracks is low (0.5 to 1) with tracks 1, 2 and 6 preserving morphological features such as claw marks and digital pad impressions (Fig. 4.1; Appendix Table A.1). Tracks 1 to 3, which make up the trackway, are preserved purely as digit impressions with the preservation grade of the tracks decreasing along the trackway - i.e., track 3 digits II and IV are more incomplete (Fig. 4.1). Tracks 1 and 2 are elongate (TL/TW of 1.43 and 1.4, respectively) and have an intermediate-high Dp/TS (0.79 and 0.7, respectively; Appendix Table A.1). Tracks 4 and 5 have faint impressions but an interpretation of their morphology is illustrated (Fig. 4.1). Track 5 is the shallowest and most indistinct of the six tracks (lowest Pm of 0.5; Appendix Table A.1).

The morphological variation of the Ha Falatsa tracks, assessed by traditional PCA, is accounted for by two principal components (where PC1 accounts for 76% of the variation). Principal Component 1 is most strongly controlled by TW (and TS), and clearly separates track 6 (which has a larger TW) from tracks 1 and 2 (Appendix Fig. A.1; Appendix Table A. 1). Principal Component 2 subdivides the tracks primarily based on their TL. Variation observed in the landmark-based PCA, which considers three tracks from Ha Falatsa, is in agreement with traditional PCA; variation for the Ha Falatsa tracks considered can chiefly be attributed to landmarks 1, 2 and 3 which would relate to TL, TW and TS (Appendix Figs. A.1, A.2).

The tridactyl tracks of Ha Falatsa preserve little morphological detail and/or are incomplete. Using conventional methods, these tracks cannot be confidently assigned to an ichnogenus. The elongate nature of the tracks (1.1<TL/TW<1.43), the narrow digits tapering to V-shaped tips and intermediate mesaxony suggest that these tracks have a theropod affinity. Additionally, the digitigrade posture and narrow trackway width (28 cm) observed, are consistent with theropods. Tracks 1 to 3 have an unusual morphology and appear to be incomplete: the tracks possess exaggerated claw impressions and the

digits, particularly for track 2, appear parallel to one another (Fig. 4.1). This digit morphology resembles those of swim tracks which often preserve irregular morphologies, subparallel-parallel digits and are incomplete (Milner and Lockley, 2016.) Sediment mounds are sometimes preserved at the posterior end of the digits, though this is not observed for the Ha Falatsa trackway. Most dinosaur swimming tracks are attributed to theropods (Milner and Lockley, 2016).

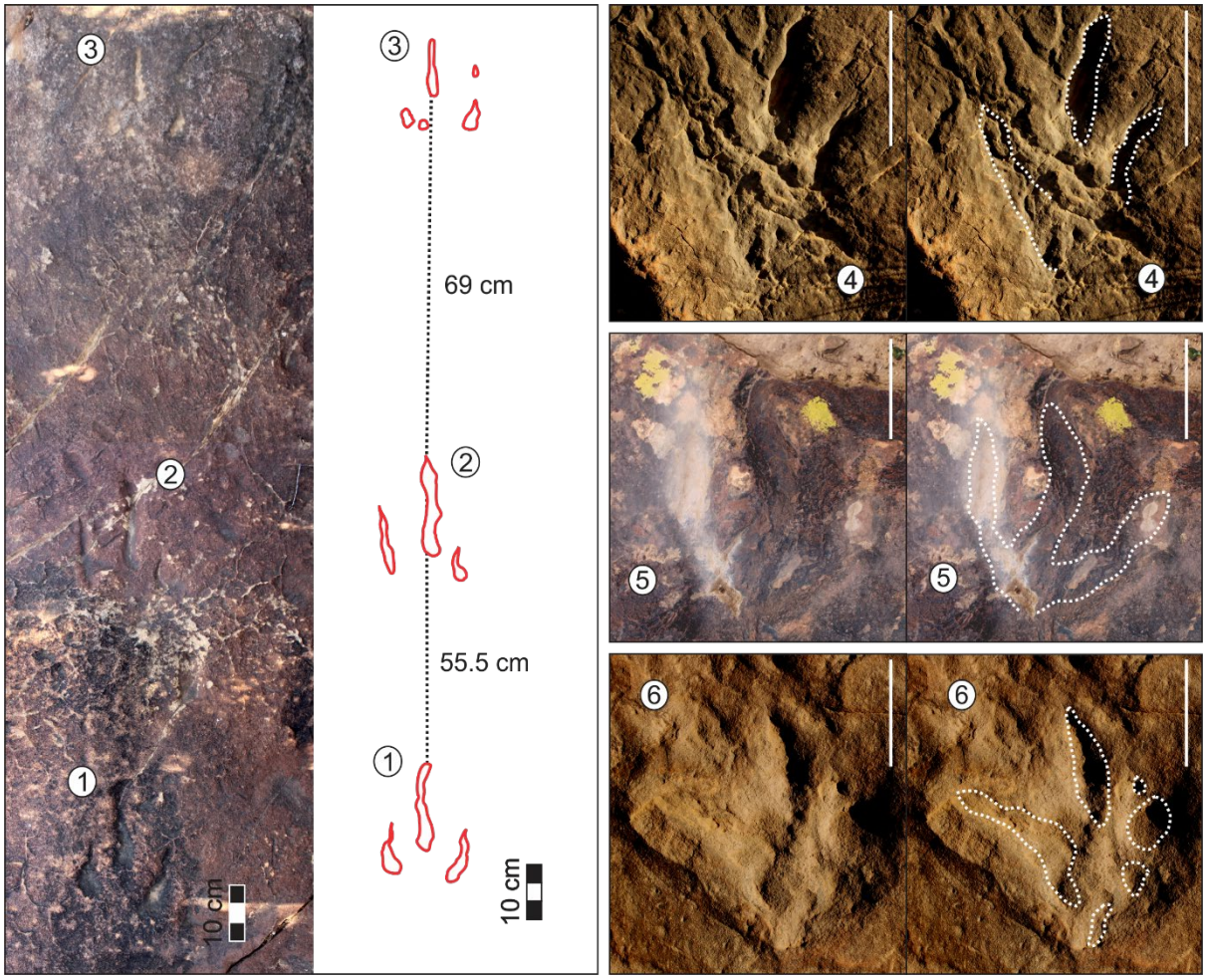

Figure 4.1: Tridactyl tracks and trackways at Ha Falatsa with their interpretive outlines. Scale bar is 10 cm long.

Landmark-based ichnogenera comparisons place tracks 4 and 6 lie within *Grallator-Eubrontes* and *Kayentapus* morphospace, respectively, while track 1 is not within any defined morphospace (Fig. 4.2). This may be due to Track 1 possibly having incomplete digits II and IV which would affect the landmark placement (Fig. 4.1). Given the morphologies, measured track parameters and landmark-based PCA the Ha Falatsa tracks documented herein are considered to be GAE-like.

Of the ichnotaxa illustrated by Ellenberger (1970), two tridactyl ichnotaxa from the Ha Falatsa ichnosite appear to have a theropod affinity: *Prototrisauropus graciosus, Prototrisauropus angustigitus, Prototrisauropus crassidigtus, Seakatrisauripus ungiferus, Seakatrisauripus divergens* and *Paratrisauropus medrezi.* This ichnotaxonomic assignment has since been refined, with

Prototrisauropus synonymised with *Grallator* and *Seakatrisauropus* and *Paratrisauropus* are regarded as indeterminate ichnotaxa by Olsen and Galton (1984).

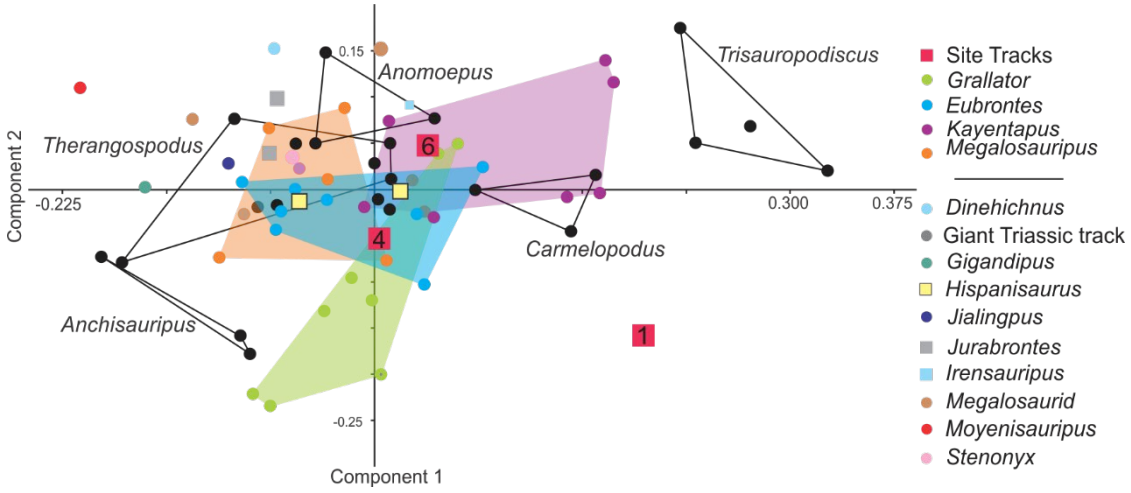

Figure 4.2: PCA morphological comparison between select tridactyl tracks at Ha Falatsa and the comparative ichnogenera database defined in section 3.5.

4.1.1.2 U-Pb Geochronology

A coarse- and fine-grained sandstone samples were collected from the Ha Falatsa ichnosite for U-Pb LA-ICMS dating (HAF_c and HAF_f, respectively). Zircon crystals retrieved from the coarse-grained sandstone sample have a range in length from 88 to 389 µm (average length of 172 µm, Appendix Fig. B.1). The zircons present with two dominant morphologies: larger, elongate, sub-rounded crystals and small, rounded crystals. An array of internal structures is observed, with oscillatory zoning being common (Appendix Fig. B.1). Inclusions and inherited cores are noted within some zircons. Of the 89 successfully ablated zircon crystals, 87 are concordant (Appendix Table B.1). The concordant $^{206}Pb/^{238}U$ dates range between 208±3 and 2084±35 Ma. More than half of the concordant dates are from the Precambrian (55%) and only 15% are from the Mesozoic (Fig. 4.3A, B; Appendix Table B.1). All the concordant zircon crystals have Th/U>0.1 indicative of a magmatic source (0.14<Th/U<2.19). The $^{206}Pb/^{238}U$ MDAs determined from the 6 metrics described in section 3.6.3, ranging from 208±2.9 to 210±2.4 Ma (YSG and Concordia age, respectively; Fig. 4.3; Table 4.2). A Late Triassic (Norian) MDA is likely for the ichnosite, given its lEF stratigraphic position. The fine-grained sample comprises zircon crystals that have a smaller average length (111 µm) than the coarse-grained sample. The crystals are primarily elongate and sub-rounded, and small, rounded zircons are virtually absent (Appendix Fig. B.1). Although complex internal textures are observed, the sample is dominated by zircons with oscillatory and banded zoning internal structures (Appendix Fig. B.1). Inherited cores and inclusions are present in some of the crystals.

Of the 33 successfully ablated crystals, 26 have concordant dates (Appendix Table B.1). Two of the concordant zircons have Th/U ratios < 0.1 suggesting a metamorphic influence on the crystals. The remaining zircons have Th/U ratios ranging between 0.15 and 1.52 (Appendix Table B.1).

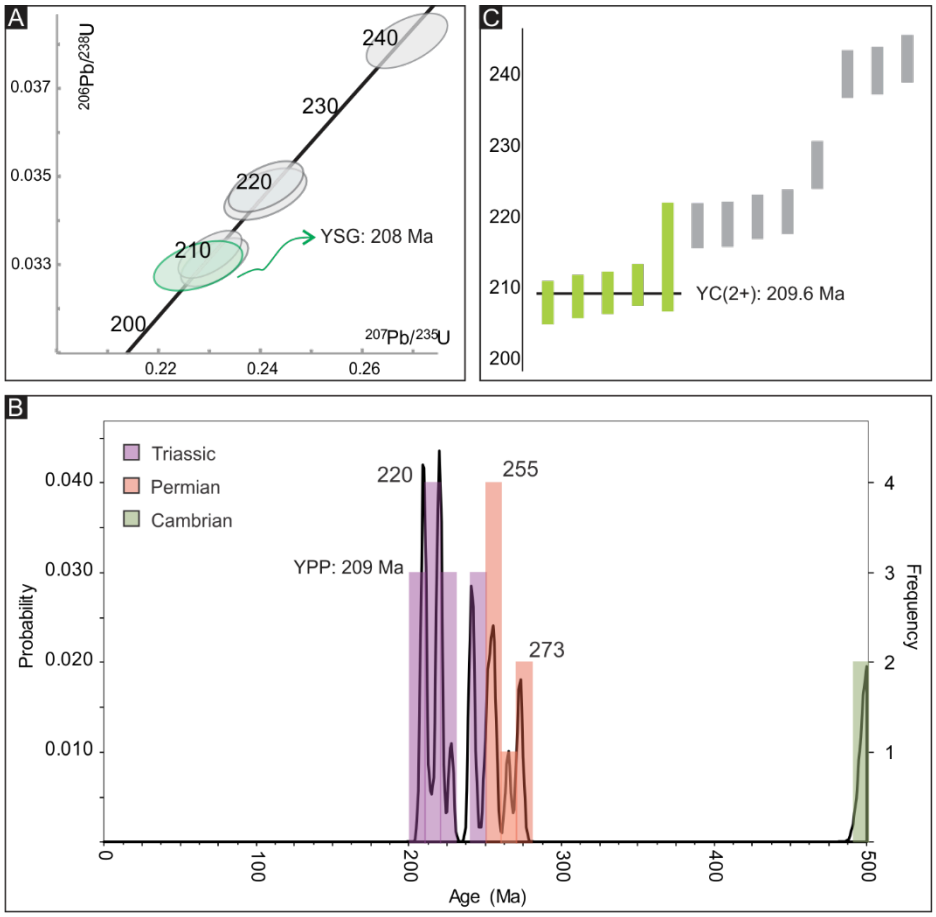

Figure 4.3: Concordant $^{206}P/^{238}U$ date distributions. A) Concordia plot showing the young dates (youngest date highlighted in green); B) Probability density plot for zircon crystals < 500 Ma; C) Weighted mean distribution of young zircons (YC2σ[2+] MDA in green).

The concordant $^{206}Pb/^{238}U$ dates vary between 220±7 and 1595±26 Ma, with a 4% Mesozoic, 34% Paleozoic and 62% Precambrian distribution (Fig. 4.4A, B; Appendix Table B.1). The MDAs calculated using 5 of the metrics described in section 3.6.3 range considerably from 220±7 (YSG) to 556.3±4.4 (YC1σ[2+]) Ma (Fig. 4.4; Table 4.2). Given the lEF stratigraphic position of the sample site, a Permian, Cambrian or Precambrian MDA is significantly older than the interpreted true depositional age of the sample. Therefore, the Late Triassic (Norian) YSG MDA of 220±7 Ma is interpreted as the most likely MDA. Both the coarse- and fine-grained samples collected from Ha Falatsa included Late Triassic MDAs. However, the ages obtained from the coarse-grained sandstone are more robust than the YSG grain age determined from the fine-grained sandstone sample. The YC2σ[2+] MDA of 209.6±1.4 Ma

from the coarse-grained sample is interpreted as the maximum depositional age for Ha Falatsa (Table 4.2).

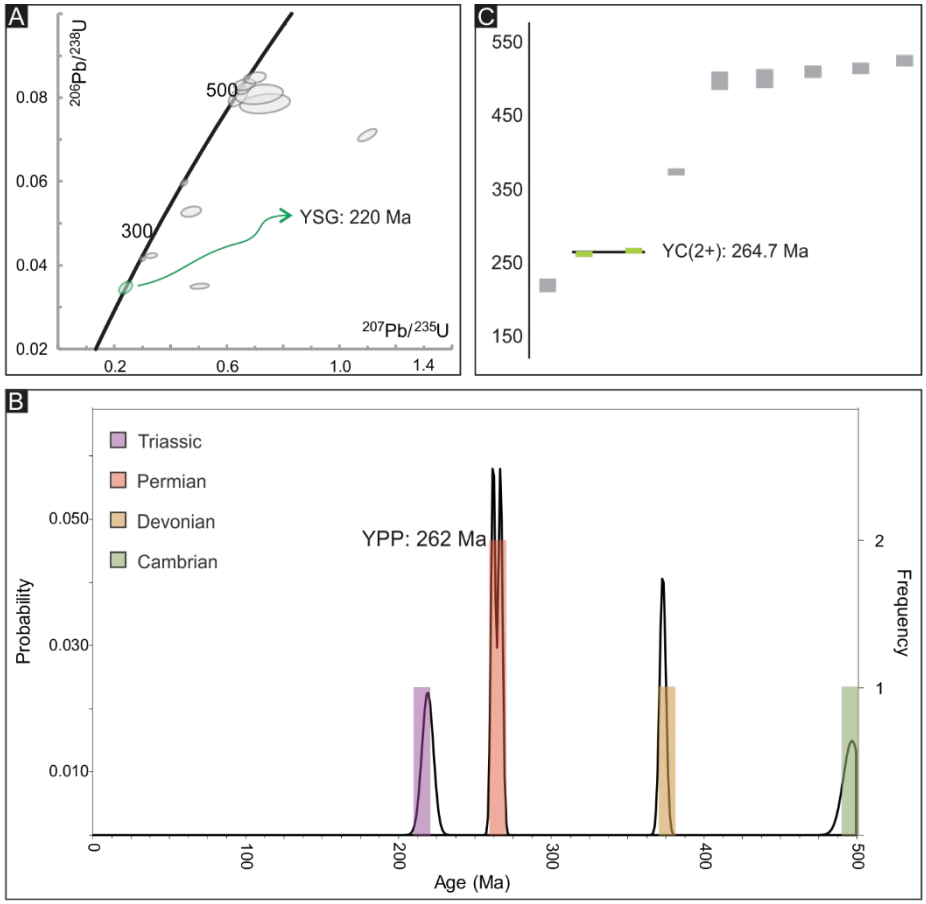

Figure 4.4: Concordant $^{206}P/^{238}U$ date distributions. A) Concordia plot showing the young dates (youngest date highlighted in green); B) Probability density plot for zircon crystals < 500 Ma; C) Weighted mean distribution of young zircons (YC2σ[2+] MDA in green).

4.1.2 Maphusteng ichnosite

The Maphustseng tracksite was first reported on by Ellenberger and Ellenberger (1956; Fig. 3.1). The lEF site preserves numerous tridactyl (both theropod-like and bird-like) and tetradactyl tracks and trackways (Ellenberger, 1970; Bordy *et al.,* 2015) with preservation grades between 0 and 3 (Appendix Table A.1). Since its discovery in the 1950s, some of the tracks have been destroyed by local quarrying of the medium- to coarse-grained track–bearing sandstone. The Maphutseng ichnosite is also remarkable for being situated <20 metres above the largest dinosaur bone bed in southern Africa, where over 1000 fossil specimens were excavated ~70 years ago. For a comprehensive site overview, see van Gend *et al*. (2015).

4.1.2.1 Ichnology

Thirty-eight tridactyl tracks, of which six form two trackways, are considered from the Maphutseng tracksite (Fig. 4.5; Appendix Fig. A.3). The tracks are predominantly extremely shallow, hyporeliefs with tracks 6, 12, 34 and 36 being the deepest (Fig. 4.5; Appendix Fig. A.3). Trackway 2 consists of four

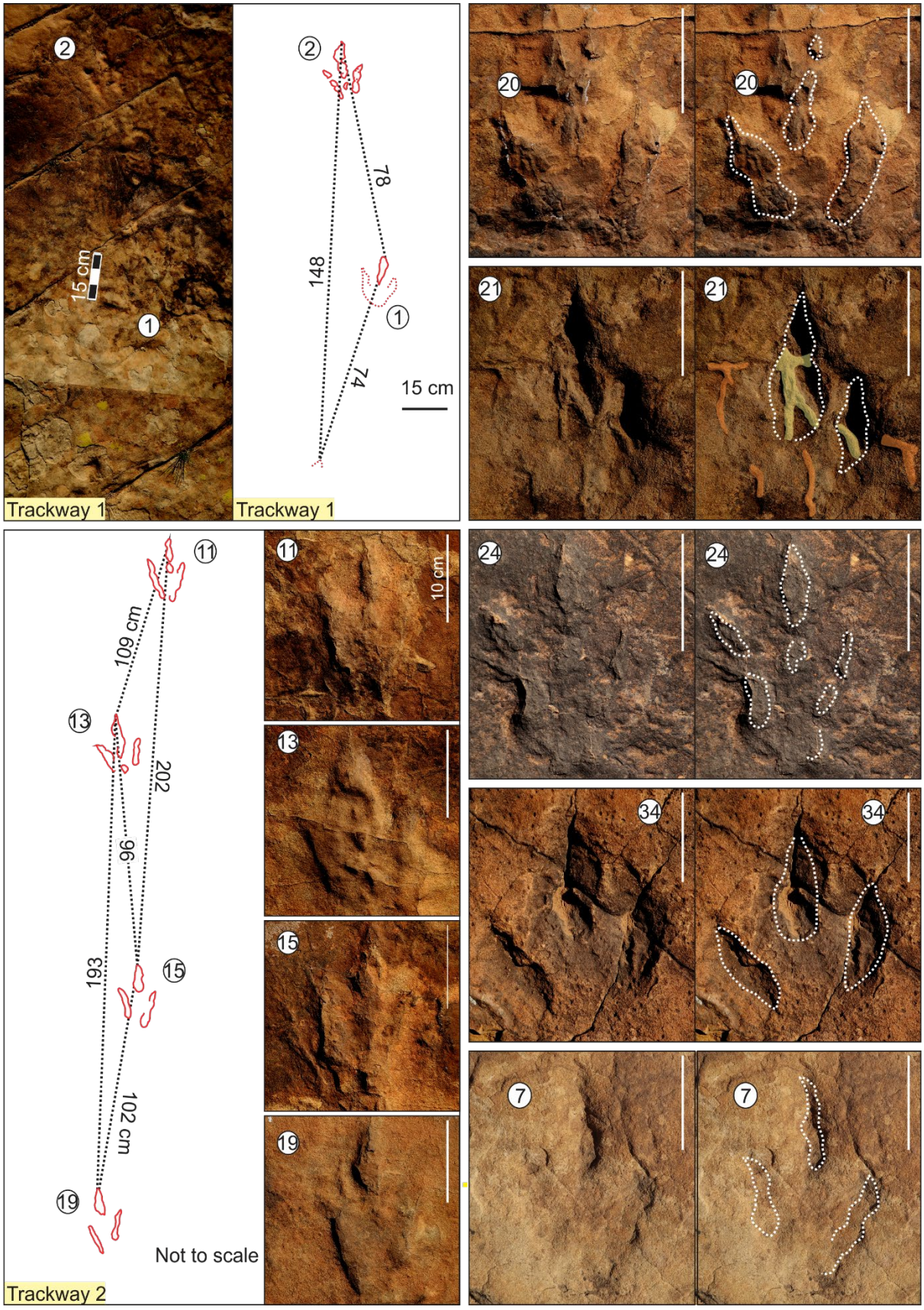

Figure 4.5: Tridactyl tracks and trackways at Maphutseng with their interpretive outlines. Scale bar is 10 cm long unless otherwise stated.

tracks with a preservation grade ranging between 2 and 3 (Fig. 4.5; Appendix Table A.1). The tracks are elongated, have subequal digit II and IV lengths (respective averages of 9.9 and 10.2 cm), with narrow digits that taper to V-shaped tips and in some cases claw mark impressions are preserved (e.g., track 13; Fig. 4.5; Appendix Table A.1). The tracks have an average TL and TW of 19.7 and 11.4 cm, respectively (mean TL/TW of 1.8), an intermediate-high mesaxony (mean Dp/TS of 0.8) and an average digit III projection of 41% (Appendix Table A.1). Digit II and IV are subequal with an average difference of ~1cm, with digit IV being the longest (excluding track 15 which has a ~3 cm difference). Claw impressions are preserved for all the tracks and digital pad impressions are preserved in tracks 11, 13 and 15 (Fig. 4.5).

The remaining individual tracks are variable with TL ranging between 15.8 and 25.4 cm (Appendix Table A.1). Excluding tracks 23, 25, 27 and 35, and incomplete tracks 9 and 10, the tracks have elongate digits and are longer than wide (TL>TW) suggesting a theropod affinity (Fig. 4.5; Appendix Fig. A.3; Appendix Table A.1). Tracks 23, 25, 27 and 35 possibly only preserve partial digit impressions and have a low morphological preservation grade which may be affecting their TLs. Additional morphological features such as claw marks (e.g., tracks 16 and 37; Fig. 4.5; Appendix Fig. A.3) and digital pad impressions (e.g., tracks 7, 8, 20 and 24; Fig. 4.5; Appendix Fig. A.3) are preserved. Tracks 21 and 31 have desiccation cracks within the track impression (Fig. 4.5; Appendix Fig. A.3).

The first three PCs, based on traditional PCA, account for most of the track morphological variation at Maphusteng (55%, 29% and 15%, respectively; Appendix Fig. A.1). Principal Component 1 is most affected by TW and TS (which show a strong association), while PC2 is primarily influenced by Dp/TS (Appendix Fig. A.1). Variation observed from the landmark-based PCA, which considers nineteen tracks, is consistent with traditional PCA; variation is mainly associated with landmarks 1 and 5 which are related to TW and TS (Appendix Figs. A.1, A.2). Trackway 2 tracks are strongly elongate (mean TL/TW of 1.8) with an intermediate – high mean Dp/TS of 0.8 consistent with *Grallator* even though the TL is greater than the TL<15 cm, which defines the ichnotaxon (Olsen *et al*., 1998). Landmark-based PCA of trackway 2, places tracks 11, 15 and 19 in the *Grallator* morphospace (Fig. 4.6). Given that track 13 forms part of trackway 2, it is assumed to also be *Grallator*-like despite plotting as an outlier. Although landmark-based analysis did not assign track 13 to *Grallator*, linear measurements are consistent with *Grallator*: the morphology of track 13 is elongated (TL/TW of 1.45), mesaxonic (Dp/TS of 0.61) and subequal digit II and IV lengths (1:1). The individual tracks at Maphutseng lie within the *Grallator, Eubrontes* and *Kayentapus* morphospace (Fig. 4.6). The outlying tracks which do not lie within any defined morphospace tend to be faint or incomplete impressions (tracks 8, 18), have unusually robust digits (tracks 18, 22, 34) or have a large total digit divarication angle (II^IV of 53 and 65 for tracks 16 and 29, respectively; Fig. 4.6; Appendix Fig. A.3). Given the morphologies, measured

parameters and landmark-based PCA, the tracks documented at Maphutseng are considered to be -GAE-like.

Numerous tridactyl ichnotaxa with theropod affinities, including *Anatrisauropus ginsburgi* and *Qemetrisauropus minor*, were described from various stratigraphic levels at Maphutseng by Ellenberger (1970). Those ichnites that are from the studied tracksite (found in Ellenberger's zone A/4) are *Deuterotrisauropus socialis* and *Mafatrisauropus errans* (his figures 44 and 45), with the former later synonymised with *Grallator* by Olsen and Galton (1984).

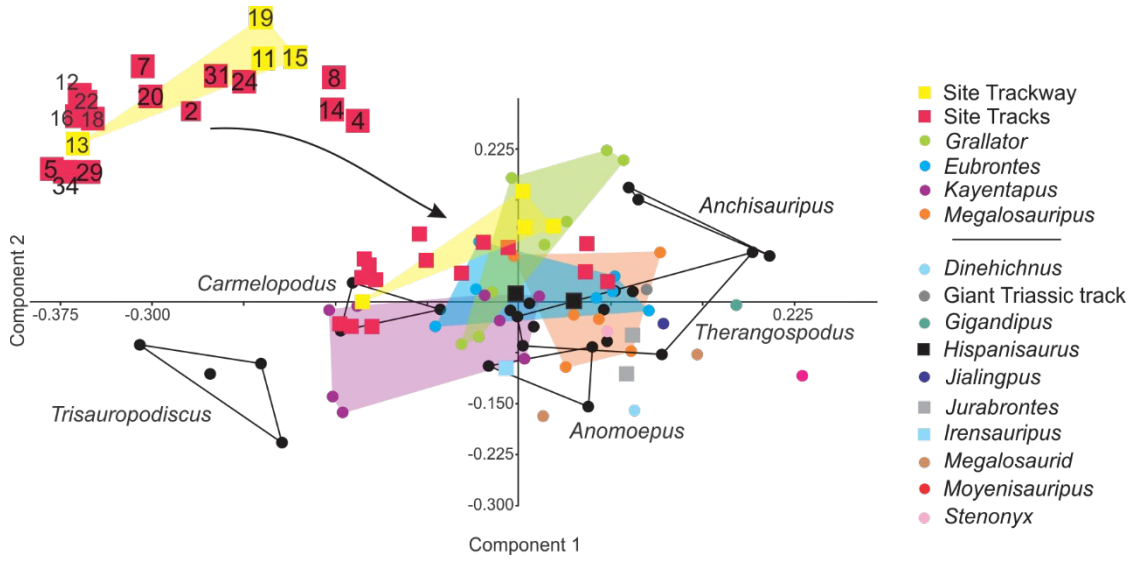

Figure 4.6: PCA morphological comparison between select tridactyl tracks at Maphutseng and the comparative ichnogenera database defined in section 3.5.

4.1.2.2 U-Pb Geochronology

A sample was collected from the track-bearing sandstone for U-Pb LA-ICPMS dating (MAP). The zircon crystals extracted from the sample range in length from 84 to 306 µm (mean length of 170 µm). The crystal morphologies are primarily elongate and sub-rounded with a minor component of small, rounded zircons (Appendix Fig. B.1). Oscillatory zoning is the most commonly observed internal structure. Bright luminescence is noted for a few of the more rounded crystals (Appendix Fig. B.1). Inclusions and inherited cores are present in some crystals.

Ninety-one of the picked zircons were successfully ablated. Of these crystals, 84 are concordant (Appendix Table B.1). All concordant zircons have Th/U ratios consistent with a magmatic origin (Th/U ranges from 0.12 to 2.83; Appendix Table B.1). The concordant $^{206}Pb/^{238}U$ dates vary between 201±2 and 2791±28 Ma. The dates are distributed as follows: 15% Mesozoic, 18% Paleozoic and 67% Precambrian (Fig. 4.7A, B; Appendix Table B.1). The MDAs determined from the 6 metrics outlined in section 3.6.3 range between 201±2.4 and 215.4±1.1 Ma (Fig. 4.7; Table 4.2). Although a MDA of 201

Ma is concluded for 5 of the 6 metrics, it is an unlikely maximum depositional age given the lEF stratigraphic position of the sample site. A Norian YC2σ[3+] MDA of 215.4±1.1 Ma is a more fitting interpretation of the true depositional age.

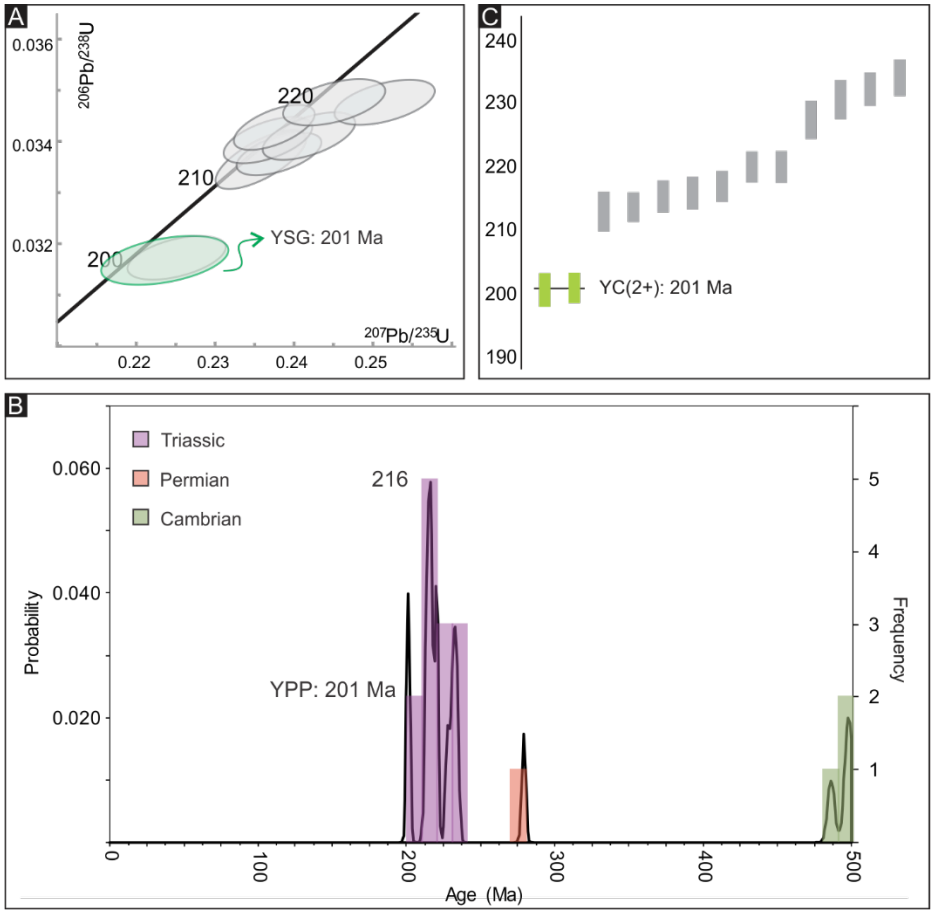

Figure 4.7: Concordant $^{206}P/^{238}U$ date distributions. A) Concordia plot showing the young dates (youngest date highlighted in green); B) Probability density plot for zircon crystals < 500 Ma; C) Weighted mean distribution of young zircons (YC2σ[2+] MDA in green).

4.1.3 Phuthiatsana ichnosite

The Phuthiatsana ichnosite was initially reported on by Ellenberger *et al*. (1963). Ellenberger (1970, 1972) described numerous tridactyl, tetradactyl and pentadactyl tracks and trackways from this lEF site (Fig. 3.1). Recently, Sciscio *et al*. (*in review*) redocumented the ichnosite using modern photogrammetric techniques, refining the ichnotaxonomy, discussing the substrate conditions and commenting on trackmaker behaviour inferred from the tetradactyl trackways. The track-bearing sandstone is massive and trough cross-bedded. The medium-grained, track-bearing sandstone surface preserves asymmetrical ripple marks, desiccation cracks and back-filled invertebrate burrows. The south-western tetradactyl tracks are associated with expulsion rims and soft sediment deformation structures interpreted as slipping/sliding features (Sciscio *et al.,* in review). Herein, only the tridactyl tracks preserved at Phuthiatsana, which were excluded from the reassessment of Sciscio *et al*. (*in*

review), are reviewed. The ichnosurface is large (~80 by ~7 m)and can be subdivided into 3 "sections" with the track preservation grade on each "section" decreasing from SW to NE (Appendix Fig. A.3).

4.1.3.1 Ichnology

More than 50 tridactyl tracks are dispersed across the Phuthiatsana palaeosurface (Appendix Fig. A.3). The abundance of tridactyl tracks increases towards the NE, with only a single defined trackway on "Section 1" in the SW (Fig. 4.8; Appendix Fig. A.3). A second tridactyl trackway, comprising at least 4 tracks across <1.5 m, is observed in the SW but the tracks consistently have an ornithischian-like affinity - e.g., robust, blunt digits with a higher total digit divarication (average II^IV of 88^{o}). Given that the tracks comprise a trackway, and are not isolated tracks, this morphology is assumed to reflect the trackmaker's autopod morphology rather than be a function of substrate interaction or extramorphological features. Consequently, these tracks are omitted from this study.

The Phuthiatsana tridactyl trackway consists of six tracks across ~4.5 m (Fig. 4.8). The tracks are complete, although shallow, and have a high morphological preservation grade (3; Appendix Table A.1). All six of the tracks preserve desiccation cracks throughout the track impression and tracks 3 and 4 preserve partial infillings (Fig. 4.8; Appendix Fig. A.3). Tracks 4 and 6 preserve digital pad impressions in digit III and tracks 1, 2, 3, 4 and 6 preserve claw mark impressions. The average length and width of the tracks are 27.5 and 16.8 cm, respectively (mean TL/TW of 1.6; Appendix Table A.1). They have an intermediate Dp/TS (average of 0.6) and a mean Dp/TL of 34%. Digit II and IV lengths are subequal (12.7±1.3 and 12.6+0.9 cm, respectively) and are shorter than medial digit III (average LIII of 19.3±1.7 cm).

Seventeen of the better preserved (preservation grade of 1 or 2) individual tridactyl tracks at the ichnosite have been recorded in detail (Appendix Fig. A.3). Most of the tracks are preserved as shallow hyporelief features but tracks 8, 14 and 23 are preserved with some of their infilling (Fig. 4.8; Appendix Fig. A.3). Digital pad impressions are preserved in tracks 12, 14, 21 and 22, and claw mark impressions are preserved on tracks 12, 18, 21 and 22 (Fig. 4.8; Appendix Fig. A.3). These seventeen tracks vary in length and width between 18–31 cm and 16.4–22.7 cm, respectively and have an average TL/TW of 1.2 (Appendix Table A. 1). Tracks 7 and 21 have the largest TL/TW ~1.6 and tracks 8, 11, 16 and 19 have TL/TW < 1. The latter tracks are weakly mesaxonic (Dp/Ts < 0.5; Appendix Table A.1).

The first three PCs, from traditional PCA methods, account for most of the track morphological variation at Phuthiatsana (51%, 32% and 16%, respectively). Principal Component 1's variations can be attributed to TL/TW and TW and TS (TW and TS have a strong association; Appendix Fig. A.1). Principal Component 2 mainly differentiates tracks by their Dp/TL ratio. Variation observed in the

landmark-based PCA is congruent with traditional PCA; variation can primarily be attributed to landmarks 3, 5 and 6, relating to differences in TW (and TS) and TL (and digit III, Appendix Fig. A.2).

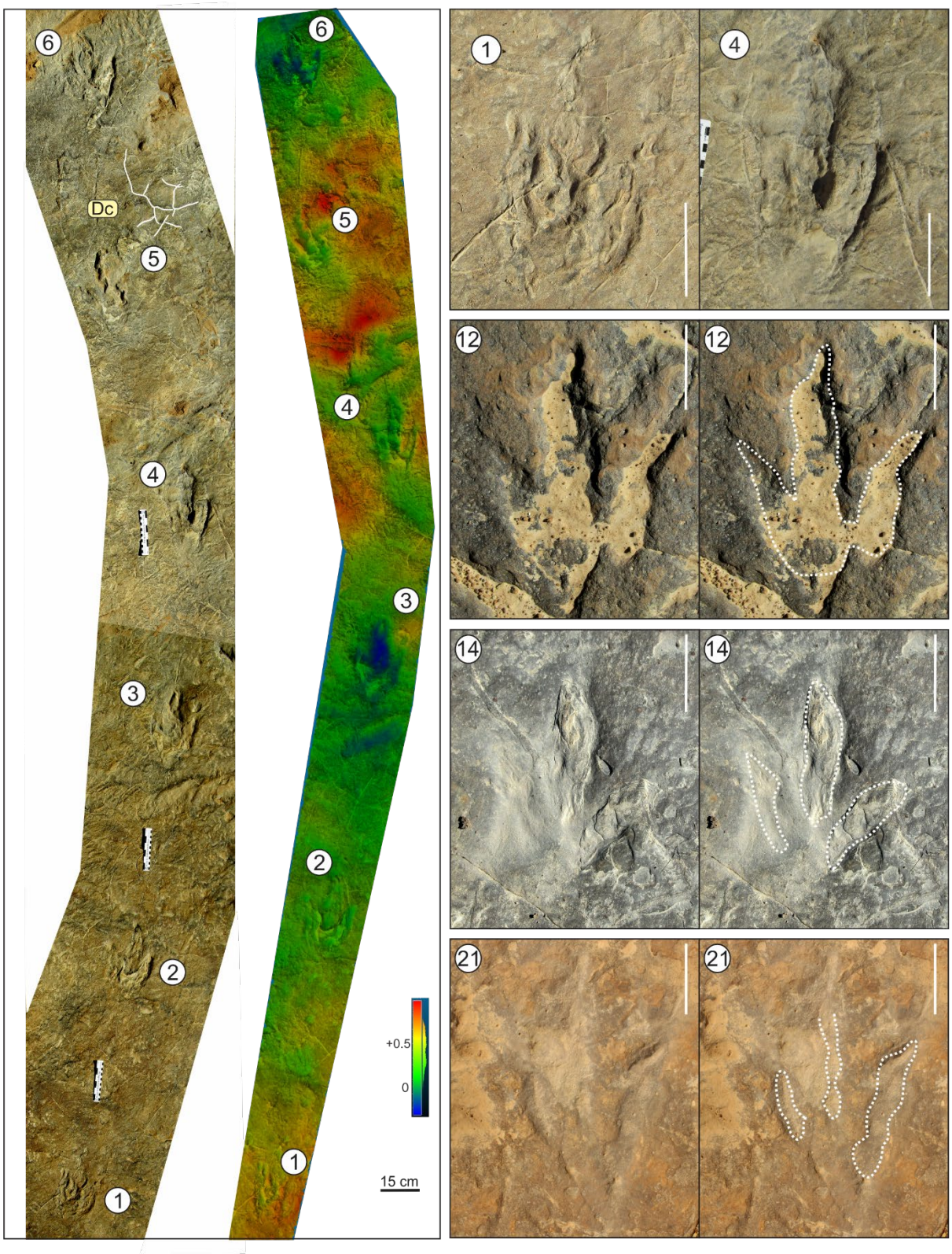

Figure 4.8: Tridactyl trackway and selected individual tracks (tracks 12, 14 and 21) at the Phuthiatsana ichnosite with their interpretive outlines of false depth maps (with a relative depth scale). Scale bar is 10 cm long unless otherwise stated.

All tridactyl tracks at Phuthiatsana (excluding tracks 11, 16 and 23) are elongate, with tapering digits and V-shaped tips, and have U-shaped posteriors (Fig. 4.8; Appendix Fig. A.3). Furthermore, the tracks are mesaxonic (mean Dp/TS of 0.56±0.14) and have an average total digit divarication of 55±11° confirming a theropod affinity. Tracks 11, 16 and 23 have robust, round digits and low TL/TW ratios (0.92–1.12) which is more consistent with an ornithischian trackmaker. Landmark-based PCA comparing the Phuthiatsana tracks to known ichnogenera, primarily assigns the Phuthiatsana trackway to the *Grallator* morphospace (Fig. 4.8). Tracks 1 and 5 do not fall within the *Grallator* morphospace but are assumed to be *Grallator*-like as they form part of the trackway; this variation may be attributed to substrate conditions or behaviour of the trackmaker (section 2.2). The overall morphology (gracile, tapering digits) and dimensions (e.g., average TL/TW and Dp/TS of 1.6 and 0.6, respectively) of the trackway are consistent with those of the ichnogenus *Grallator* (section 2.4).

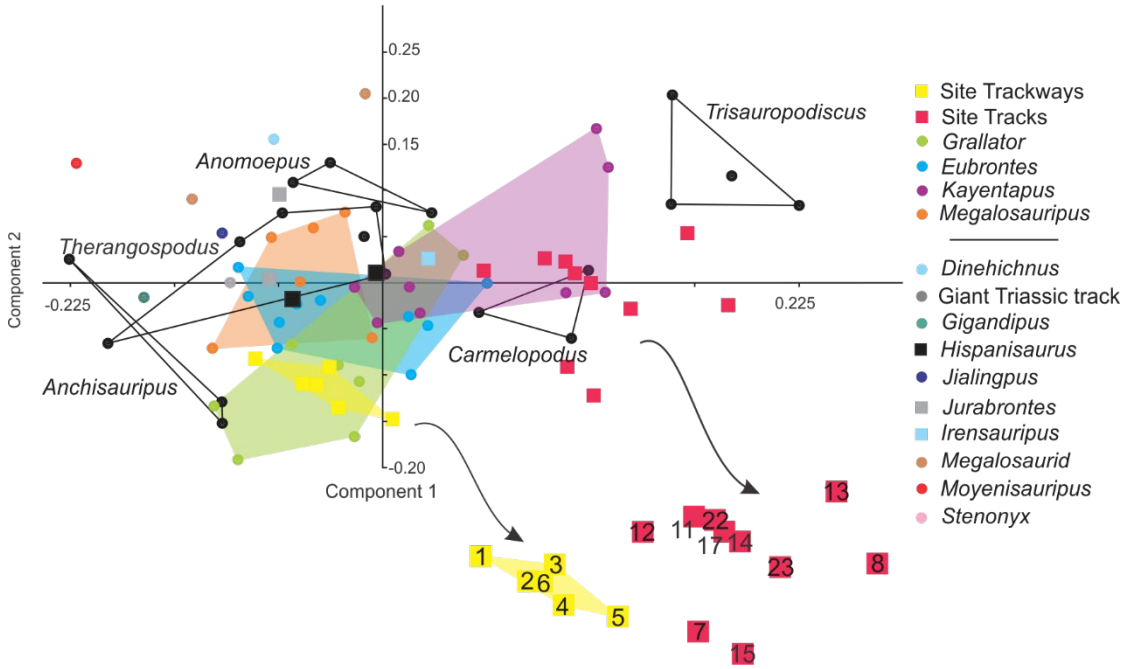

Figure 4.9: PCA morphological comparison between selected tridactyl tracks at Phuthiatsana and the comparative ichnogenera database defined in section 3.5.

Although the TL is large (~28 cm), the gracile, elongate nature of the tracks is more consistent with *Grallator* than *Eubrontes* (Olsen *et al.,* 1998). Individual tracks 11, 12, 14, 17 and 22 lie within the *Kayentapus* morphospace and tracks 7, 8, 13, 15 and 23 are morphospace outliers (Fig. 4.9). The outlying tracks have large total digit divarication (tracks 8, 13, 15 and 23), robust rounded digits (tracks 11, 16 and 23) or low TL/TW (<1.2 for tracks 8, 13, 16 and 23; Figs. 4.7, 4.8; Appendix Fig. A.3).

Interestingly, tracks 11, 16 and 23 which have an apparent ornithischian affinity do not plot near or within the *Anomoepus* morphospace (*Anomoepus* tracks are attributed to ornithischian trackmakers; Olsen and Rainforth, 2003) and instead plot within or near the *Kayentapus* morphospace. However, it must be borne in mind that the limited digital landmarks do not fully capture the morphology of the tracks, such as their digit widths and digit tip shapes which affects their morphospace placement. Furthermore, the ornithischian-like tracks are isolated and it is difficult to assess the effects of the trackmakers' locomotory styles and substrate interactions on the resultant track morphology. Given the morphologies, measured parameters and landmark-based PCA, the tracks documented at the Phuthiasana ichnosite are considered to be K-GAE-like.

Ellenberger (1970) assigned the tridactyl tracks from Phuthiatsana to *Prototrisauropus rectilineus* and *Bosuitrisauropus phuthiatsana*. The trackway tracks described herein, resemble *Prototrisauripus rectilineus* which was later synonymised with *Grallator* by Olsen and Galton (1984).

4.1.3.2 Geochronology

A sample was collected from the ichnite-bearing sandstone for U-Pb LA-ICPMS dating (PHU). The 130 picked zircon crystals, yielded from the sample, have a range in length from 40 to 262 µm (average crystal length of 122 µm; Appendix Fig. B.1). Small, rounded zircons dominate the sample and commonly possess inherited cores or inclusions. Oscillatory and banded zoning are observed internal structures for numerous crystals (Appendix Fig. B.1). Of the 109 successfully ablated crystals, 105 are concordant (Appendix Table. B.1). The concordant $^{206}Pb/^{238}U$ dates range from 218±3 to 2898±36 Ma, with only 7 % of the dates from the Mesozoic (67% of the dates are Precambrian; Fig. 4.10A, B; Appendix Table. B.1). Four zircons have a Th/U ratio < 0.1, suggesting the grains have experienced a metamorphic influence (the youngest crystal is 524±8 Ma). The MDAs obtained from the 6 metrics described in section 3.6.3 vary from Late to Middle Triassic (218±3.4 to 243.1±2 Ma; Fig. 4.10; Table 4.2). Given the lEF stratigraphic position of the ichnosite, a Late Triassic MDA is more likely. Norian MDAs were determined for 3 metrics and are tightly constrained between 218±3.4 and 220±2.5 Ma

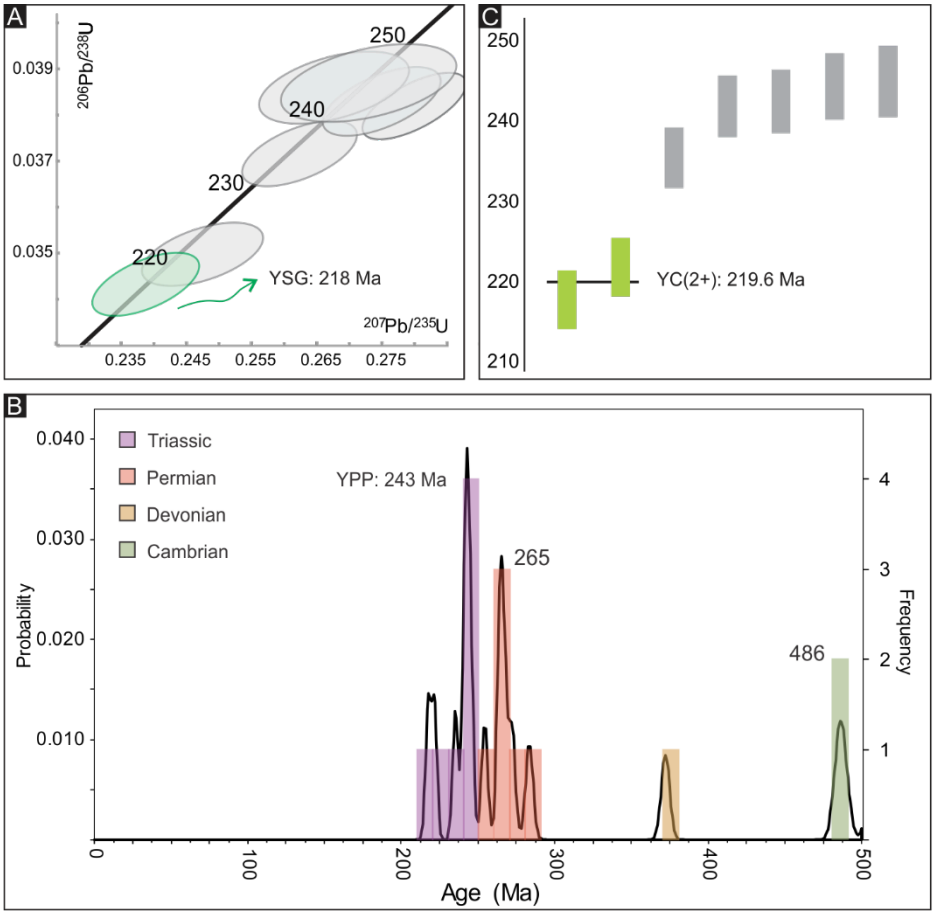

Figure 4.10: Concordant $^{206}P/^{238}U$ date distributions. A) Concordia plot showing the young dates (youngest date highlighted in green); B) Probability density plot for zircon crystals < 500 Ma; C) Weighted mean distribution of young zircons (YC2σ[2+] MDA in green).

4.1.4 Subeng ichnosite

Tracks of the Subeng ichnosite were documented in Ellenberger (1955, 1970, 1972), Ellenberger and Ellenberger (1958), and have recently been revised by Bordy *et al*. (2017). Tridactyl, tetradactyl and pentadactyl tracks and trackways are preserved at this lEF ichnosite. The track-bearing sandstone is fine- to medium-grained, is ripple marked and preserves desiccation cracks. The tridactyl tracks are preserved as isolated tracks across the palaeosurface and do not appear to have a preferred orientation (Appendix Fig. A.3). The morphological preservation of the tracks is variable (1–2; Appendix Table A.1) and some tracks preserve desiccation cracks within the digit impressions - e.g., tracks 8 and 9 (Appendix Fig. A.3).

4.1.4.1 Ichnology

Traditional principal component analysis based on tracks with complete linear measurements (excluding digit lengths) and landmark-based PCA on selected tracks was used to describe the morphological variation at the Subeng ichnosite (Appendix Figs. A.1, A.2). The first three PCs, based on traditional PCA, account for most of the variation at the tracksite (57%, 27% and 15%, respectively). Principal Component 1 is mainly influenced Dp/TS ad TS (TW), while TL is the main parameter

contributing to variation within PC2 (Appendix Fig. A.1). The Dp/TS, Dp/TL and TL/TW ratios have strong associations (Appendix Fig. A.1). The landmark-based PCA variation accounted for by PC1 is primarily linked to landmark 2 (the hypex between digit II and III) and landmark 1 (anterior position digit II). The second PC's variation is chiefly associated with landmarks 5 and 6, which relate to the anterior and posterior of digit IV. The respective position of digit IV would influence a tracks TW and TS.

Landmark-based principal component analysis was used to evaluate the morphology of some of the Subeng tracks to the comparative ichnogenera database defined in section 3.5 (Fig. 4.11). Tracks 1 and 2 lie within the *Grallator–Eubrontes* morphospaces and track 5 lies slightly outside of the *Eubrontes* morphospace (Fig 4.10). Track 4 is a clear outlier but it may not fully preserve digit IV, which affects the proximal landmark placement (Appendix Fig. A.3). Given the morphologies, measured parameters and landmark-based PCA, the tracks documented at the Subeng ichnosite are considered to be K-GAE-like.

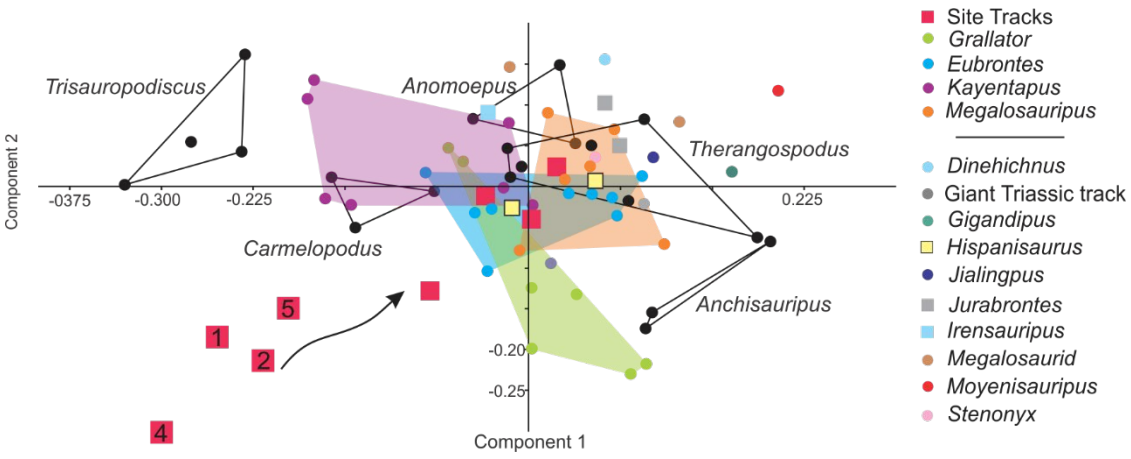

Figure 4.11: PCA morphological comparison between tridactyl tracks at Subeng and the comparative ichnogenera database defined in section 3.5.

Ellenberger (1970) assigned the tridactyl tracks from Subeng to the ichnotaxa *Deuterotrisauropus socialis, Mafatrisauropus errans, Pseudotrisauropus subengensis* (or *Psilotrisauropus subengensis*) and *Pseudotrsauropus dieterleni.* These were later synonymised with *Grallator (D. socialis)* or as intermediate ichnotaxa by Olsen and Galton (1984). In their recent in-depth review of the site, Bordy *et al*. (2017) proposed that *P. dieterleni* also be classified as *Grallator.*

Table 4.2 Summary of maximum depositional ages (metrics outlined in section 3.6).

Sample	Stratigraphic position	YSG	2σ	YC1σ[3+]	2s	YC2σ[2+]	2σ	YC2σ[3+]	2σ	YPP	Concordia	2σ	Preferred MDA	
													Ma	2σ
HAF_c	lEF	208.2	2.9	209	1.6	209.6	1.4	209.6	1.4	209	210	2.4	209.6	1.4
HAF_f	lEF	220	7	556.3	4.4	264.7	2	510.4	4.4	262			262	7
LEP_c	uEF	244	3	469.3	2.3	247	1.9	247	1.9	249	515.6	5.3	244	3
LEP_s	uEF	195.7	3.1	239.6	2.7	197.3	2.3	243	1.5	196	197	2.3	197.3	2.3
LMO	uEF	193.9	2.9	199.8	2.1	199.9	2.3	232	2	194	200	8.6	199.9	2.3
MAF	uEF	199	3	254	2.8	201	2.3	256.4	1.4	256			201	2.3
MAP	lEF	201.1	2.4	201	3.2	201.2	1.6	215.4	1.1	201	201	4.6	215.4	1.1
MAT	uEF	192	3	388.3	4.2	253	2.9	476.6	4.4	251	514.1	4	192	3
PHU	lEF	217.6	3.4	242.6	2.2	219.6	2.5	243.1	2	243	220	2.5	219.6	2.5
SUB	lEF	215.4	3.4	216.4	2.4	216.4	2.4	252	2	216			216.4	2.4
TLA	uEF	205	3	246.1	2	246.1	2	246.1	2	246	264.5	1.9	205	3
UMC	uEF	185.9	2.2	186.7	1.2	187.5	1	187.5	1	187			187.5	1
UMO	uEF	252	3	252.4	1.8	252.4	1.8	252.4	1.8	252	504.7	4.6	252.4	1.8

4.1.4.2 U-Pb Geochronology

A sample was collected from the ichnite-bearing sandstone for U-Pb LA-ICPMS dating (SUB). The zircons extracted from the sample range in length from 31 to 323 µm (mean length of 166 µm). Wide, elongate, sub-rounded zircons are most common, though an array of zircon morphologies are present in the sample (Appendix Fig. B.1). The zircons possess diverse internal structures including oscillatory and banded zoning, and complex metamorphic textures. Inherited cores and a minor component of inclusions are observed (Appendix Fig. B.1).

Of the 105 successfully ablated zircon crystals, 97 are concordant (Appendix Table B.1). The concordant $^{206}Pb/^{238}U$ dates range from 215±3 to 1610±23 Ma and have a 3% Mesozoic, 31% Paleozoic and 66% Precambrian distribution (Fig. 4.12A, B; Appendix Table B.1). Seven of the concordant crystals have Th/U ratios <0.1 suggesting they have experienced metamorphic processes. The Mesozoic concordant zircons have magmatic Th/U signatures between 0.51 and 0.6 (Appendix Table B.1). The MDAs determined from 5 of the metrics outlined in section 3.6.3 vary between 215±3.4 and 252±2 Ma (Fig. 4.12; Table 4.2). Of the 5 MDAs, 4 are tightly constrained between 215 and 216.4 Ma. These Norian MDAs are likely comparable to the true depositional age of this lEF ichnosite.

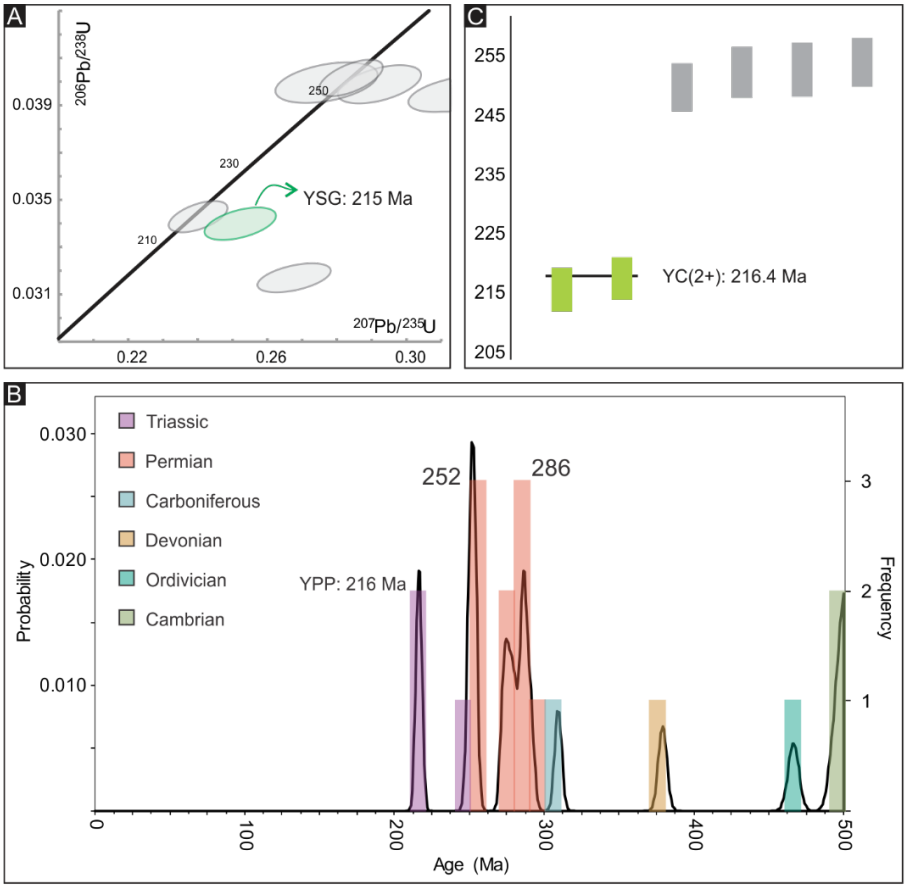

Figure 4.12 (previous page): Concordant $^{206}P/^{238}U$ date distributions. A) Concordia plot showing the young dates (youngest date highlighted in green); B) Probability density plot for zircon crystals < 500 Ma; C) Weighted mean distribution of young zircons (YC2σ[2+] MDA in green).

4.1.5 Lower Moyeni ichnosite

The Lower Moyeni tracksite in the southern Lesotho town of Moyeni (also known locally as Quthing) (Fig. 3.1) was first described by Ellenberger (1970, 1972, 1974) and later revised by Smith *et al.* (2009), Marsicano *et al.* (2009) and Wilson *et al.* (2009). The palaeosurface preserves a high abundance and diverse ichnoassemblage including various tridactyl, tetradactyl and pentadactyl tracks and trackways produced by bipedal and quadrupedal trackmakers. Additionally, unique traces such as belly and toe drag and resting impressions are preserved at Lower Moyeni. The track-bearing surface is ripple marked and has pitted textures interpreted to be algal mat features (Smith *et al.,* 2009). Invertebrate traces, including back-filled meniscate burrows (cf. *Naktodemasis*) and beaded foraging trails (cf. *Hormosoroidea*), are also preserved on the surface (Smith *et al.,* 2009).

4.1.5.1 Ichnology

Herein, we examine a single, extensive Lower Moyeni tridactyl trackway interpreted to have a theropod affinity (Appendix Fig. A.3). Along the trackway, there is evidence for a change in locomotory style by the trackmaker in response to substrate variations (e.g., Smith *et al.,* 2009*;* Wilson *et al.,* 2009). The start of the trackway is associated with biofilm pitted textures and the trackway ends with the tracks overprinting a ripple-marked portion of the surface (Ellenberger, 1974, p. 210). Given the change in substrate conditions and locomotory style, only sixteen tracks of the trackway are considered in this study. The tracks range in length from 22–30 cm, are elongate (mean TL/TW of 1.5) and have mean Dp/TS of 0.53 with an average Dp/TL of 34% (Appendix Table A.1). Most of the tracks preserve digital pad impressions and/or claw marks (Appendix Fig. A.4).

Most of the morphological differences for the Lower Moyeni trackway, determined from traditional PCA, can be accounted for by three PCs (51%, 36% and 12%, respectively). Principal Component 1 is mainly influenced by Dp/TS but is associated with the other measurements (excluding TW and TS). The chief contributors to PC2 variations are TW and TS i.e., tracks in quadrants 3 and 4 have smaller TWs than tracks in quadrant 1 and 2 (Appendix Fig. A.1). Landmarks 2, 5 and 6 account for most of the mean deviations; this agrees with the traditional PCA as landmarks 5 and 6 are linked to digit IV and their movement can relate to TW (TS) and TL, respectively (Appendix Fig. A.2).

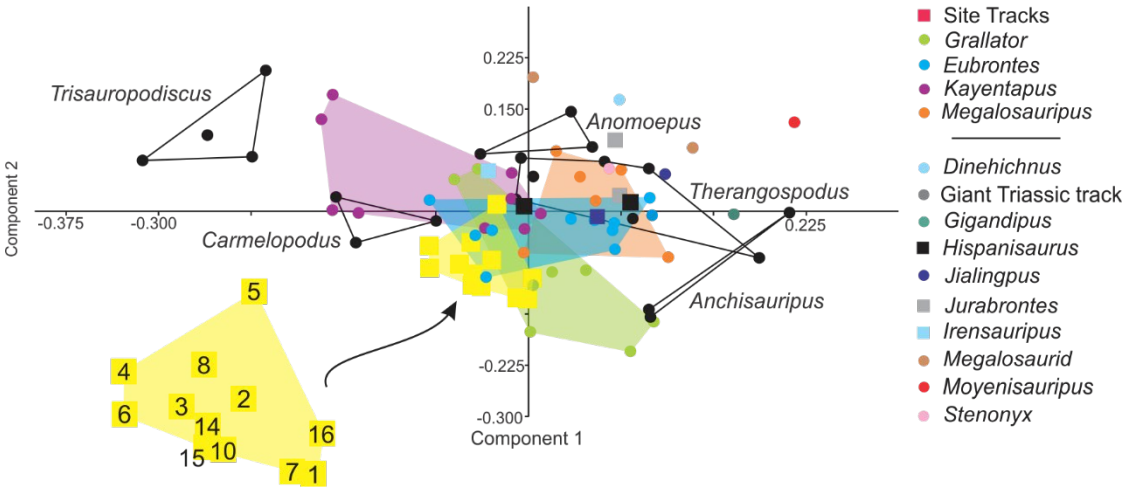

Figure 4.13: PCA morphological comparison between select tridactyl tracks at Lower Moyeni and the comparative ichnogenera database defined in section 3.5.

Landmark-based PCA was used to evaluate the morphology of the Lower Moyeni tracks in comparison to known theropod ichnogenera listed in section 3.5 (Fig. 4.13). The track data points lie within the *Grallator* and *Eubrontes* morphospace or are outliers (Fig. 4.13). Given that all the tracks are part of the same trackway, a *Grallator–Eubrontes* ichnogenus assignment is assumed for the outlying tracks 4, 6, 10, 14 and 15. The elongate, gracile morphology of the tracks is more congruent with *Grallator* than *Eubrontes*, even though the tracks have a TL typical of *Eubrontes* (section 2.4). Given the morphologies, measured parameters and landmark-based PCA, the trackway documented at Lower Moyeni is considered to be K-GAE-like.

Ellenberger (1970) assigned these tracks to *Neotrisauripus* which was later synonymised with *Grallator* by Olsen and Galton (1984). This ichnotaxonomic assignment was accepted by Wilson *et al*. (2009) and Smith *et al*. (2009).

4.1.5.2 U-Pb Geochronology

A sample was collected from the track-bearing lower Moyeni sandstone for U-Pb LA-ICPMS dating (LMO). The zircons retrieved from the sample have a range in length between 29 and 163 µm (mean crystal length of 74 µm). The zircons have diverse morphologies ranging from elongated and sub rounded to small and rounded (Appendix Fig. B.1). Oscillatory and banded zoning are abundantly observed internal structures. Bright luminescent rims are present for many of the more rounded crystals (Appendix Fig. B.1). Inherited cores and a few inclusions are present within the zircons.

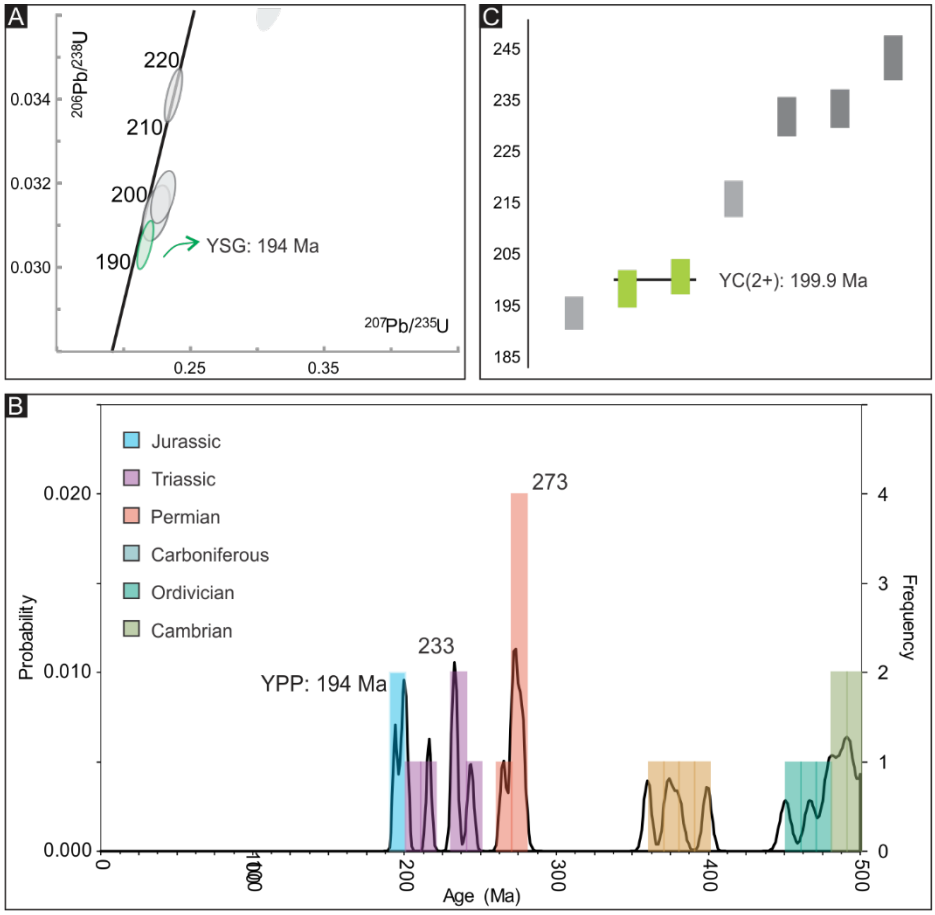

Figure 4.14: Concordant $^{206}P/^{238}U$ date distributions. A) Concordia plot showing the young dates (youngest date highlighted in green); B) Probability density plot for zircon crystals < 500 Ma; C) Weighted mean distribution of young zircons (YC2σ[2+] MDA in green).

Of the 104 ablated zircons, 82 are concordant (Appendix Table B.1). The concordant $^{206}Pb/^{238}U$ dates vary from 194±3 2894±33 Ma and have a 9% Mesozoic, 33% Paleozoic and 58% Precambrian distribution. A single Precambrian crystal has a Th/U<0.1 (Fig. 4.14A, B; Appendix Table B.1). The MDAs obtained from the 6 metrics outlined in section 3.6.3 range from 194±3 to 232±2 Ma (Table 4.2). Five of the metrics are constrained between 194±2.9and 200±8.6 Ma (Sinemurian to Hettangian; Fig. 4.14). An Early Jurassic age is expected for the ichnosite given its position within the uEF.

4.1.6 Mafube ichnosite

The Mafube tracksite is a newly reported ichnosite in the upper Elliot Formation (Fig. 3.1; Sciscio *et al.*, 2016). The palaeosurface substrate conditions vary consistently from a water-saturated substrate (with algal mat textures) to a firm substrate. Tracks preserved on the water-saturated substrate have undefined morphologies and extra-morphological features. Therefore, only nine of the documented Mafube tracks, with the most morphological detail and minimal substrate controls, were considered for this study (Appendix Fig. A.3). Dinosaur body fossils, belonging to a recently described species *Ledumahadi mafube,* have also recently been described from the Mafube region , ~ 30 m stratigraphically below the tracksite (McPhee *et al.*, 2018).

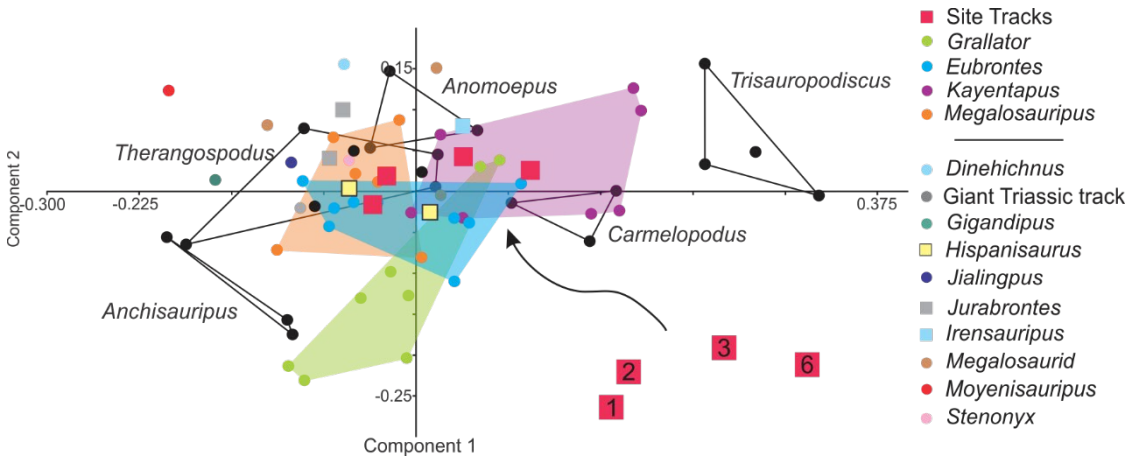

Figure 4.15: PCA morphological comparison between select tridactyl tracks at Mafube and the comparative ichnogenera database defined in section 3.5.

4.1.6.1 Ichnology

The bulk of the morphological variation in the Mafube tracks, determined from traditional PCA, can be accounted for by the first 3 PCs (55%, 29% and 15%, respectively). Principal Component 1 is equally strongly affected by TL, TW and TS while PC2 is predominantly influenced by Dp and Dp/TS (Appendix Fig. A.1). Tracks 2, 4, 5 and 6 in the second, third and fourth quadrants have smaller TL, TW and Dp than other tracks (Appendix Table A.1). Variations in PC1, from landmark-based PCA, are primarily linked to landmarks 4 and 5, the hypex between digit III and IV and the distal point of digit IV, respectively (Appendix Fig. A.2). The main direction of variation for landmark 5 is in the y-plane i.e., the anterior position of digit IV. This reflects variations in Dp and TS measurements. Principal Component 2 shows significant variation in landmarks 2, 3, 4 and 5. The strong x-component associated with landmark 5, shows differences in TW and TS span for the Mafube tracks (Appendix Fig. A.2). The strong y-vector component associated with landmark 6, would reflect differences in digit IV lengths and TL. Therefore, the landmark-based PCA data is consistent with the traditional PCA; the Mafube tracks variations are associated with almost all track parameters.

The considered Mafube tracks fall within *Eubrontes* and *Kayentapus* morphospaces, when compared to known ichnogenera, with track 2 lying just outside of the *Eubrontes* morphospace (Fig. 4.15). Track 1 was the best-preserved track at the Mafube ichnosite and as Sciscio *et al*. (2016) concluded it can confidently be assigned to the *Eubrontes* ichnogenus. Track 2 is preserved with a metatarsal impression; therefore, the landmark placement may have been incorrect for the proximal part of the foot (landmark 6). Given the morphologies, measured parameters and landmark-based PCA, the tracks documented at the Mafube ichnosite are considered to be K-GAE-like.

4.1.6.2 U-Pb Geochronology

A sample was collected from track-bearing sandstone for U-Pb LA-ICPMS dating (MAF). The zircons yielded from the sample have an average length of 94 µm (varies between 36 and 182 µm; Appendix

Fig. B.1). The zircon crystals have an array of morphologies and can broadly be classified into 2 groupings: narrow and elongate, and short and sub-rounded to rounded. Oscillatory and banded zoning are the dominant internal structures observed (Appendix Fig. B.1). Inherited cores are common for the shorter, rounded crystals. Inclusions are present within some zircons.

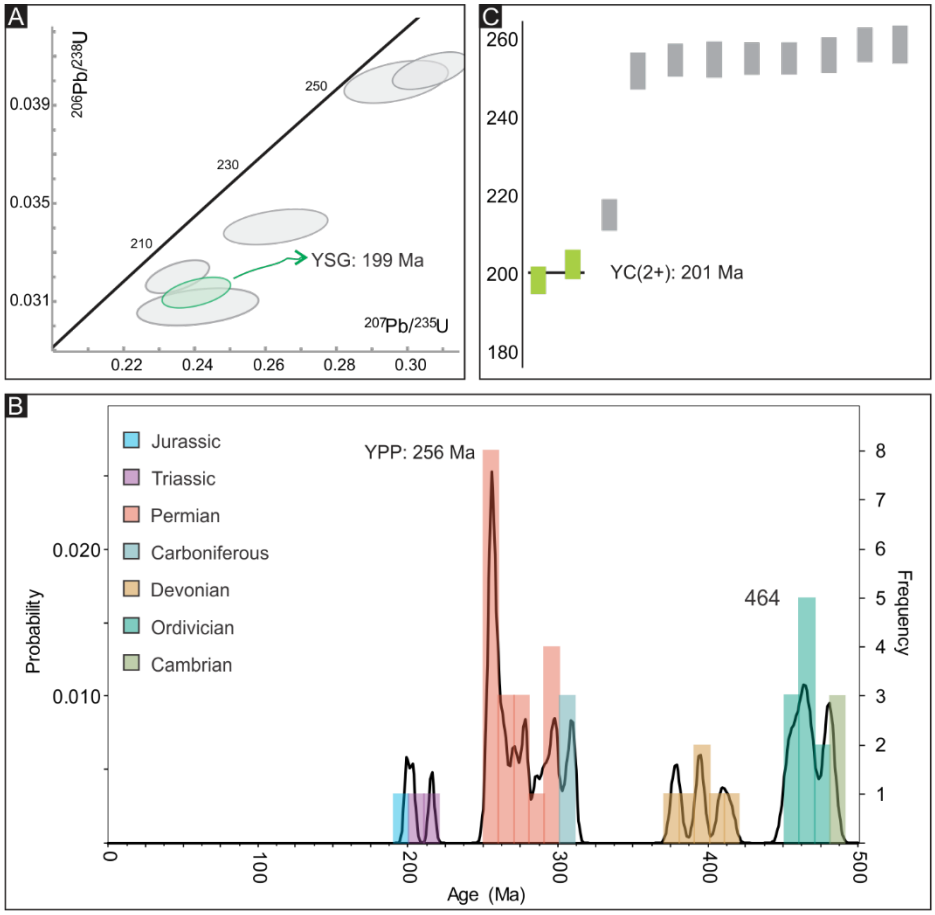

Figure 4.16: Concordant $^{206}P/^{238}U$ date distributions. A) Concordia plot showing the young dates (youngest date highlighted in green); B) Probability density plot for zircon crystals < 500 Ma; C) Weighted mean distribution of young zircons (YC2σ[2+] MDA in green).

Of the 102 successfully ablated zircon crystals, 89 are concordant (Appendix Table B.1). The concordant $^{206}Pb/^{238}$ U dates range from 199±3 to 2059±26 Ma, and are distributed as follows: 3% Mesozoic, 69% Paleozoic and 28% Precambrian (Fig. 4.16A, B; Appendix Table B.1). The Mesozoic zircons have magmatic Th/U signatures between 0.69 and 1.73. Maximum depositional ages, obtained from 5 metrics described section 3.6.3, range from 199±3 to 256.4±1.4 Ma (Fig. 4.16; Table 4.2). Given the stratigraphic position of the ichnosite (uEF) the YSG age of 199±3 and the YC2σ[2+] age of 201±2.3 Ma are more comparable to the expected true depositional age of the sandstone which s interpreted to be Early Jurassic based on magnetostratigraphy and body fossils. It should be noted that a second Sinemurian zircon (195±4 Ma) with 11% discordance (1% out of the applied filter) is present in the data.

4.1.7 Roma Site 1 ichnosite

The uEF and Clarens Formation in the Roma Valley of Lesotho preserves numerous dinosaur tracksites, which were mostly discovered by Professor David Ambrose (Fig. 3.1, Ambrose, 2003; Abrahams *et al*., 2017; Sciscio *et al*., 2017b). Roma Site 1 is preserved on a local footpath on top of an uEF sandstone.

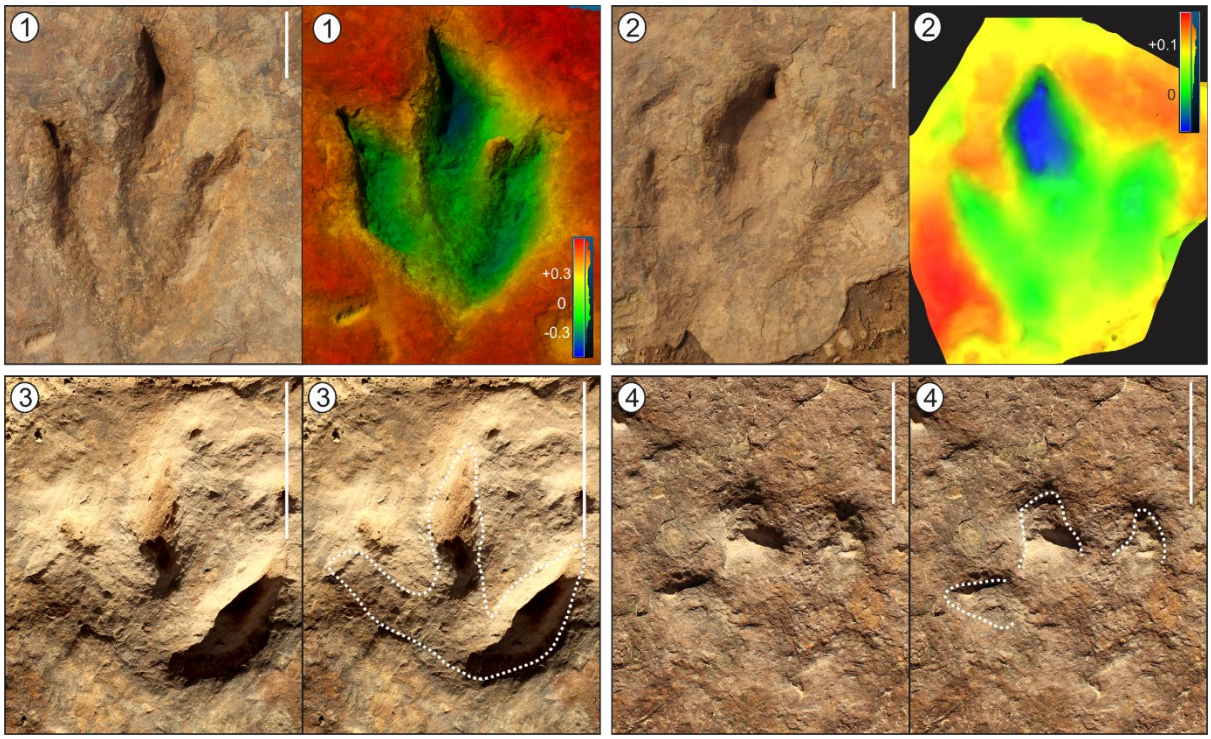

Figure 4.17: Tridactyl tracks at the Roma Site 1 with their interpretive outlines or false depth maps (with a relative depth scale). Scale bar is 10 cm long.

4.1.7.1 Ichnology

The site preserves four tridactyl tracks of which two form a single step (tracks 1 and 2; Fig. 4.17). The tracks have a range in preservation grade from 0.5 to 2 and have no apparent preferred orientation (Appendix Table A.1). Track 1 and track 2, which represent a pace of 1.3 m, have a length and width of 39 and 32 cm and 38 and 32 cm, respectively (mean TL/TW of 1.2), a digit III projection of 35.5 % and a Dp/TS of 0.45 (Appendix Table A.1). Track 1 is the only track to preserve additional morphological detail in form of claw marks associated with all digits (Fig. 4.17). The "heel" region of track 2 is obscured being is preserved on the edge of the outcropping sandstone.

Using traditional PCA, morphological variation can be accounted for by 2 PCs (where PC1 accounts for 87% of variation). This clearly separates tracks 1 and 2 from track 3 (Appendix Fig. A.1). Principal Component 1 is influenced by all linear measurements, excluding ratios, indicating that tracks 1 and 2 have greater dimensions than track 3. Principal Component 2 is primarily affected by Dp/Ts. Because of the limited dataset, landmarks could not be used to describe the morphological variation of the Roma Site 1 tracks.

Tracks 1 and 2 may be assigned to the ichnogenus *Eubrontes,* which is defined as a bipedal tridactyl track with a TL > 25 cm, TL/TW of approximately 1.4, total divarication between 25 and 40^{o} and relatively short digit III with digits II and IV being subequal in length (Olsen *et al*., 1998). Tracks 3 and 4 have too little morphological information to ascribe them to an ichnogenus (Fig. 4.17). When utilising landmark-based PCA to compare tracks 1 and 3 to the comparative ichnogenera database defined in section 3.5, they did lie within any defined morphospace (Fig. 4.18).

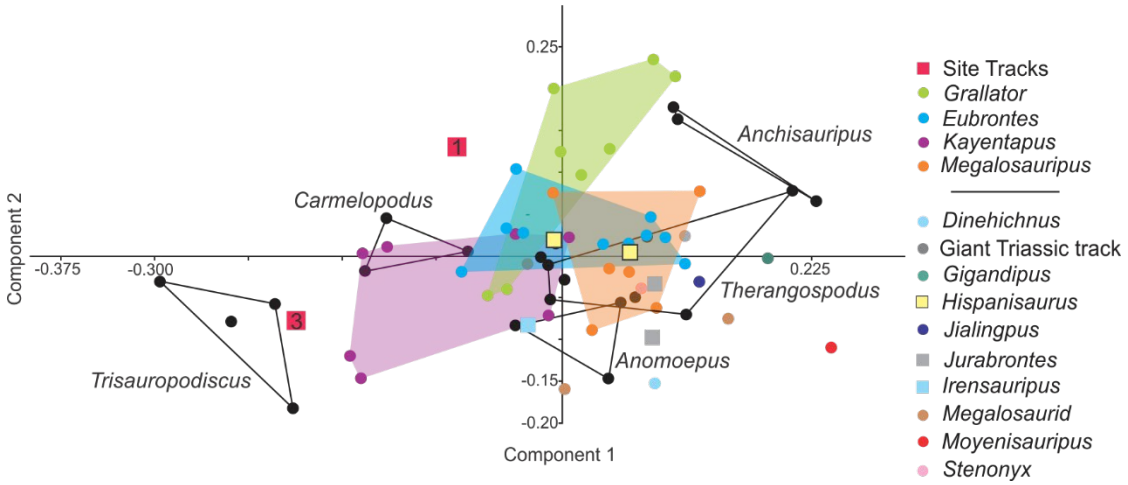

Figure 4.18: PCA morphological comparison between select tridactyl tracks at Roma Site 1 and the comparative ichnogenera database defined in section 3.5.

4.1.8 Roma Site2: Lephoto ichnosite

Multiple uEF tracksites in the Lephoto area were first reported on by Ambrose (2003); Roma Site 3 at Lephoto however is a new site described by Abrahams *et al*. (2017). The tracksite exclusively preserves tridactyl tracks (within five trackways and in isolation) that can be classified into two distinct morphotypes attributable to theropod and ornithischian trackmakers, respectively. The very fine- to fine-grained track-bearing sandstone preserves ripple marks, desiccation cracks, pitted textures and invertebrate bioturbation structures. Herein, we examine select tracks from three trackways ascribed to a single morphotype with a theropod affinity (Abrahams *et al.,* 2017; Appendix Fig. A.3). For a single trackway, only three better preserved tracks are considered (our tacks 8, 9 and 10; Appendix Fig. A.3; Appendix Table A.1); along the trackway morphological preservation grades decrease with some tracks preserved as only partial impressions.

4.1.8.1 Ichnology

Traditional principal component analysis separates larger tracks (from two trackways; tracks 1–4 and tracks 5–7) from the smaller tracks (a single trackway; tracks 8–10) at Lephoto (Appendix Fig. A.1). Excluding tracks 4 and 10, tracks from each trackway plot near to one another. Relative to tracks 1,2 and 3, track 4 is slightly less mesaxonic (Dp/TS of 0.51 vs 0.59–0.6) and digit III projection accounts for less of the TL (35% vs 43). Relative to tracks 8 and 9, track 10 is more elongate (TL/TW of 2.06 vs 1.2–

1.41) and more mesaxonic (Dp/TS of 0.88 vs 0.58–0.64). Nearly all the morphological variation at Lephoto can be accounted for by the first three PCs (67%, ~23% and ~10%, respectively). The ratios and linear measurements form distinct groups with strong associations (Appendix Fig. A.1). Principal Component 1 is almost equally strongly influenced by all the linear measurements, while PC2 variation can primarily be attributed to DP/TS and Dp/TL (Appendix Fig. A.1). The trends observed in the traditional PCA are mirrored to a degree in the landmark-based PCA; significant variation can be seen associated with all landmarks (excluding hypices), which would relate to all track dimensions (Appendix Fig. A.2).

Tracks for the Lephoto trackways, assessed for landmark-based PCA, plot in the same general morphospace but do not greatly overlap with the known theropod ichnogenera considered (listed in section 3.5). The two trackways comprising larger tracks (TL>14 cm) each have a single track in the *Grallator-Eubrontes* morphospace (tracks 3 and 6) while the third trackway has none. The ichnogenera that primarily plot in the same quadrant as the Lephoto tracks are *Grallator* and *Eubrontes* (Fig. 4.19). Given the similar morphology of the tracks, their comparable measured parameters (Appendix Table A.1) and that tracks along a trackway are registered by a single trackmaker, tracks 1, 2, 4, 5 and 7 may lie within the *Grallator-Eubrontes* plexus. The elongate (mean TL/TW of 1.42±0.24) and mesaxonic (mean Dp/TS of 0.63±0.1) morphology of the Lephoto tracks, with their pronounced medial digits, asymmetrical, sub-equal in lengths digits II and IV (mean LII:LIII of 0.87±0.1) and tulip-shaped posteriors are consistent with GAE-plexus tracks.

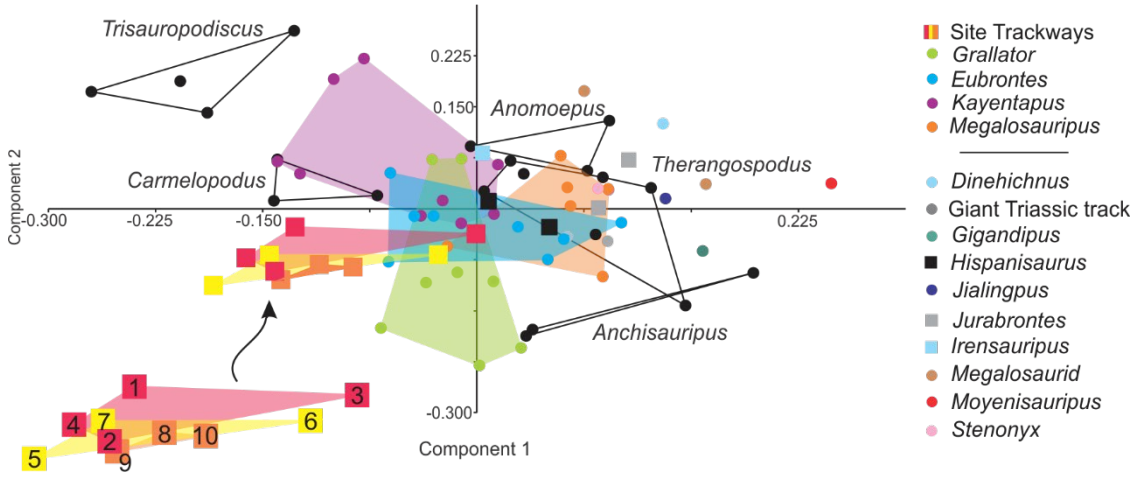

Figure 4.19: PCA morphological comparison between tridactyl tracks at Roma Site 2: Lephoto and the comparative ichnogenera database defined in section 3.5.

4.1.8.2 U-Pb Geochronology

Two samples were collected form the Lephoto ichnosite for U-Pb LA-ICPMS dating: a pedogenic carbonate nodule conglomerate sample (~1.2 m below the track-bearing sandstone) and a track-bearing sandstone sample (LEP_c and LEP_s, respectively). The yield of zircon crystals from the

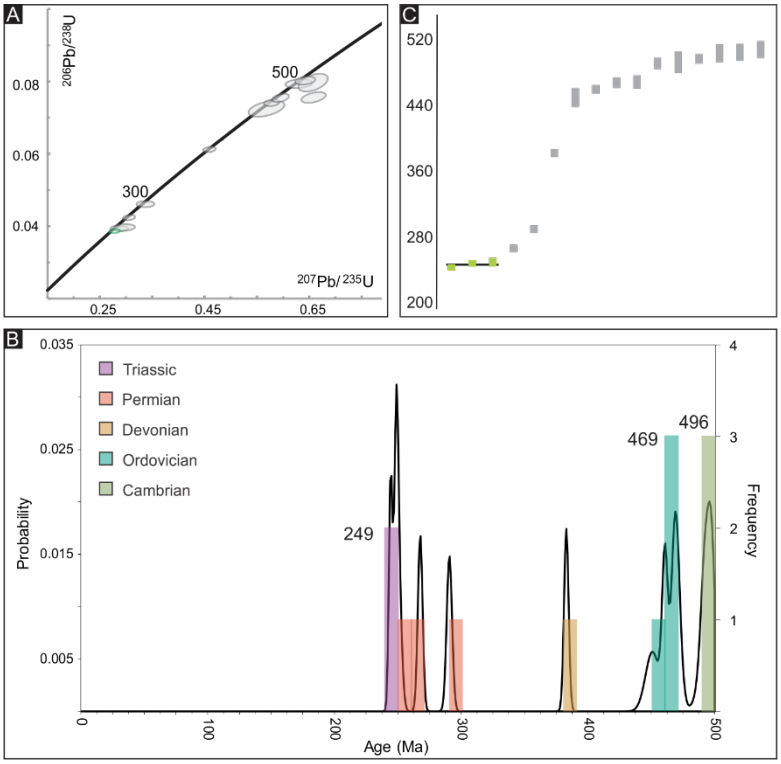

Figure 4.20: Concordant $^{206}P/^{238}U$ date distributions. A) Concordia plot showing the young dates (youngest date highlighted in green); B) Probability density plot for zircon crystals < 500 Ma; C) Weighted mean distribution of young zircons (YC2σ[2+] MDA in green).

conglomerate have a range in length between 16 and 173 µm (mean length of 97 µm; Appendix Fig. B.1). The crystal morphologies vary but most crystals are sub-rounded. Oscillatory and banded zoning are the predominant internal structures observed but minor metamorphic textures are noted (Appendix Fig. B.1). Multiple grains have thick, brightly luminescent metamorphic rims.

Ninety-three of the 113 ablated zircon crystals are concordant (Appendix Table B.1). Of the concordant zircons, 4 have Th/U ratios < 0.1, while the remaining zircons have Th/U ratios spanning from 0.11 to 1.98. The concordant $^{206}Pb/^{238}U$ dates range between 244±3 and 2712±24 Ma with 2% Mesozoic era dates, 27% Paleozoic era dates and 71% Precambrian dates (Fig. 4.20A, B; Appendix Table B.1). Maximum depositional ages were determined for the 6 metrics outlined in section 3.6.3 (Table 4.2). The MDAs vary significantly from the Middle Triassic (244±3 Ma) to the Cambrian (515.6±5.3 Ma; Fig. 4.20). Given that this sample was collected from the uEF, even the youngest MDA (YSG of 244±3 Ma) is significantly older than the Early Jurassic true depositional age expected for this stratigraphic unit.

Zircons retrieved from the sandstone sample are, on average, smaller than the conglomerate sample (mean length of 81 µm). Although small, rounded zircons are present, the zircons are primarily narrow, elongate and sub-rounded (Appendix Fig. B.1). Banded and oscillatory zoning are commonly observed. Minor amounts of inherited cores and inclusions are noted in this sample (Appendix Fig. B.1).

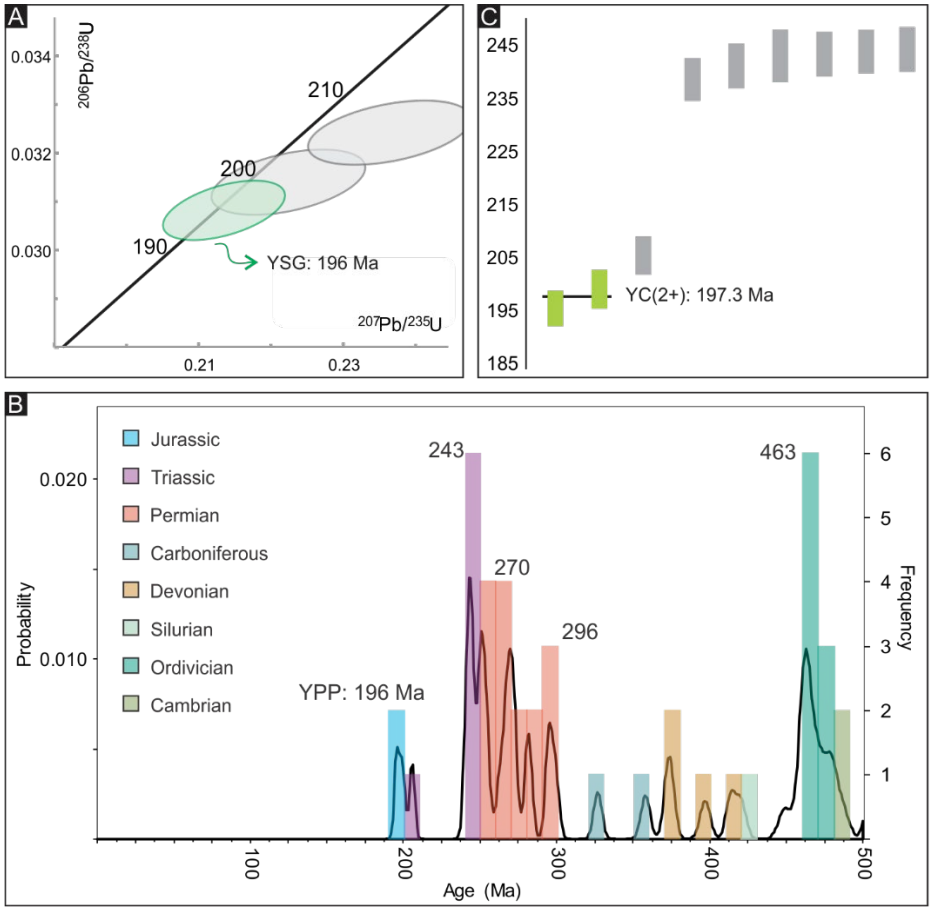

Figure 4.21: Concordant $^{206}P/^{238}U$ date distributions. A) Concordia plot showing the young dates (youngest date highlighted in green); B) Probability density plot for zircon crystals < 500 Ma; C) Weighted mean distribution of young zircons (YC2σ[2+] MDA in green).

Of the 103 ablated zircons, 85 are concordant (Appendix Table B.1). The concordant dates range from 196±3 to 3079±39 Ma and have a 11% Mesozoic, 55% Paleozoic, 34% Precambrian distribution (Fig. 4.21A, B). A single grain ($^{206}Pb/^{238}U$ date of 588±9) has a Th/U<0.1 (Appendix Table B.1). The MDAs calculated from the 6 metrics vary between 196±3.1 and 243±1.5 Ma (Fig. 4.21; Table 4.2). Three of the MDAs have tightly constrained Sinemurian ages (196±3.1 to 197.3±2.3 Ma) and are interpreted to be the MDA of the ichnosite which is consistent with the interpreted age for the uEF.

4.1.9 Roma site 3: Matobo ichnosite

The Matobo tracksite, consisting of multiple tridactyl steps and trackways, was first described by Ambrose (2003) and later revised, with additional new data, by Sciscio *et al*. (2017b). This uEF tracksite is preserved on a very fine- to fine-grained sandstone that is ripple marked. The track impression depths vary significantly (Sciscio *et al*. 2017b, their fig. 3).

4.1.9.1 Ichnology

Traditional PCA shows a clear separation, along the x-axis, between tracks 5, 6, 9 and 10 and the other Matobo tracks (Appendix Figs. A.1, A.3). These tracks belong to two steps (5–6 and 9–10) and they are distinctly larger (TL>40) than the other tracks at Matobo. In addition to plotting separately from the

other tracks, these steps also plot discretely from one another with 9–10 more positively on the x-axis (Appendix Fig. A.1).

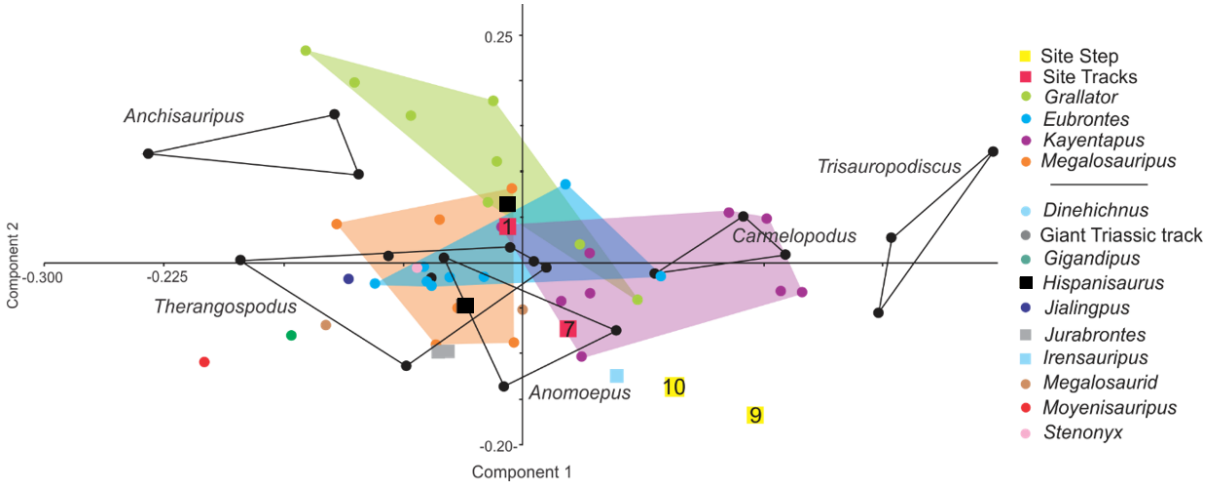

Figure 4.22: PCA morphological comparison between select tridactyl tracks at Roma Site 3: Matobo and the comparative ichnogenera database defined in section 3.5.

The first three PCs, determined from traditional PCA, account for most of the morphological variation at the site (69%, 22% and 7%, respectively). Principal Component 1 is mainly controlled by size (TL, TW ad TS) and PC2 by Dp/TL (Appendix Fig. A.1). Landmark-based PCA variations is predominantly controlled by landmarks 1, 5 and 6 (Appendix Fig. A.2). These landmarks related to the TW, TS and TL. Therefore, the landmark PCA findings are congruent with the traditional PCA findings.

Landmark-based PCA was also used to compare the tracks at Matobo with known ichnogenera (Fig. 4.22). Tracks 1 and 7 plot in the *Eubrontes* and *Kayentapus* morphospace but tracks 9 and 10 do not plot in any of the defined morphospaces. In the traditional PCA, tracks 9 and 10 also plotted distinctly away from the other tracks at Matobo (Appendix Fig. A.1). Tracks 9 and 10 have been assigned to a newly erected ichnospecies *Kayentapus ambrokolohali* by Sciscio *et al.* (2017b). This may be why they do not plot into the existing *Kayentapus* morphospace, though they do plot relatively close to it. Sciscio *et al*. (2017) assigned the remaining tracks at Matobo, including tracks 1 and 7, to the GAE-plexus. Given the morphologies, measured parameters and landmark-based PCA, the tracks documented at Matobo are considered to be K-GAE-like.

4.1.9.2 U-Pb Geochronology

A sample was collected from the track-bearing surface for U-Pb LA-ICPMS dating (MAT). Zircon crystals retrieved from the sandstone range in length from 26 to 130 µm (Appendix Fig. B.1). The zircons

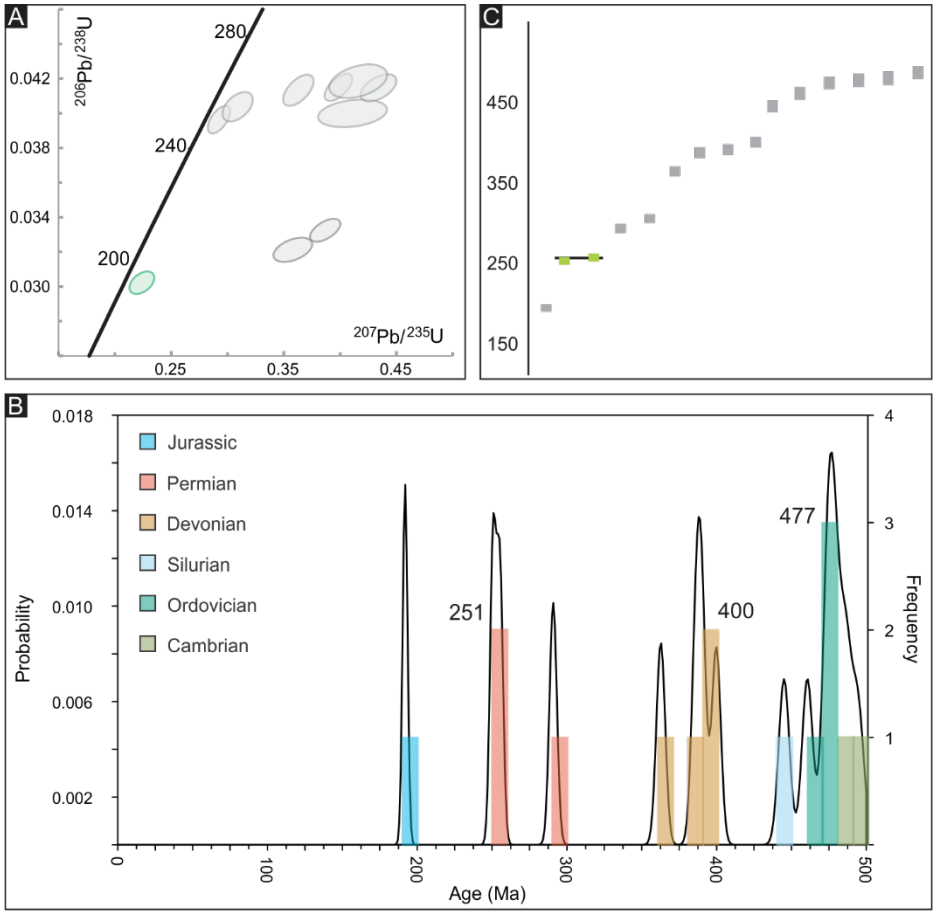

Figure 4.23: Concordant $^{206}P/^{238}U$ date distributions. A) Concordia plot showing the young dates (youngest date highlighted in green); B) Probability density plot for zircon crystals < 500 Ma; C) Weighted mean distribution of young zircons (YC2σ[2+] MDA in green).

possess an array of morphologies, with most crystals classified as sub-euhedral to sub-rounded. Oscillatory zoning is the predominant internal structure observed but some zircon crystals have intricate, zoned internal features (Appendix Fig. B.1). Bright metamorphic rims, inherited cores and inclusions are preserved within some zircon crystals. Bright luminescence of the entire exposed 2D plane is observed for numerous elongate, sub-rounded crystals (Appendix Fig. B.1).

Seventy-one of the 99 ablated zircon crystals are concordant (Appendix Table B.1). Seventy of the zircons have a Th/U ratio > 0.1 indicative of a magmatic origin (0.15<Th/U<1.47). The concordant $^{206}Pb/^{238}U$ dates range between 192±3 and 1880±25 Ma (Fig. 4.23A, B; Appendix Table B.1). The dates are primarily Precambrian (69%), with a single Early Jurassic date for the Mesozoic Era. Maximum depositional ages could be obtained for all 6 of the metrics outlined in section 3.6.3 (Table 4.2). The MDAs range drastically from 192±3 Ma (Early Jurassic) to 514.1±4 Ma (Cambrian; Fig. 4.23). Although a Late Permian age (YPP of 251 Ma and YC2σ[2+] of 253 Ma) is recurrent within the metrics, a YSG MDA of 192±3 Ma is the best MDA estimate for the uEF Matobo ichnosite.

4.1.10 Roma Site 4: Tlapana ichnosite

The Tlapana ichnosite was discovered and briefly reported on by Ambrose (2003; Fig. 3.1). It is located within the uEF, a few meters below Roma Site 3 (Sciscio *et al*., 2017b). The track-bearing medium-grained sandstones form laterally continuous, tabular beds. The discontinuous palaeosurface preserves ripple marks, desiccation cracks and bioturbation. The twenty-four tracks recorded at the site range in preservation quality from 0 to 3 (Fig. 4.22; Appendix Fig. A.3; Appendix Table A.1). There is no apparent trend associated with the degree of track preservation. The tracks occur sporadically across the surface or in isolated clusters of no more than five tracks. Neither a preferred orientation of the tracks nor trackways were observed.

4.1.10.1 Ichnology

The poorest quality tracks at Tlapana (preservation grade 0) are preserved as shallow "holes" with no distinct morphology (Fig. 4.24; Appendix Fig. A.3). The remaining tracks that are morphologically distinguishable are tridactyl (Fig. 4.24, tracks 7,8 and 15; Appendix Fig. A.3). The Tlapana tracks range in length from 17 to 37 cm and have an average TL/TW ratio of 1.3 (Appendix Table A.1). Most of the tracks are elongate with digit III being longer than digits II and IV (average Dp/TL % of 41). The tracks have a range in Dp/Ts from 0.22 to 0.93 (weak to strong mesaxony; Fig. 5.22; Appendix Fig. A.3; Appendix Table A.1). Tracks are preserved as shallow hyporeliefs or natural casts (e.g., tracks 5, 8; Fig. 4.24; Appendix Fig. A3). Digital pad impressions and claw marks are preserved in some tracks (e.g., 1, 3, 5, 7; Fig. 4.24; Appendix Fig. A.3).

The first three PCs, from traditional PCA, account for the bulk of the morphological variation at Tlapana (67%, 25% and 8%, respectively). All measurements appear to have an association, with TL/TW, Dp/TS and Dp/TS, and TL and TW, having the strongest associations (Appendix Fig. A.1). The tracks are clearly distinguished by size. Principal Component 1 is most strongly controlled by TL and Dp while PC2 is strongly controlled by TW (and TS; Appendix Fig. A.1). Variation observed in landmark-based PCA is disparate from traditional PCA; variation is predominantly associated with the hypex landmarks (Appendix Fig. A.2). Hypex positions have no influence on- and are not influenced by the linear measurements.

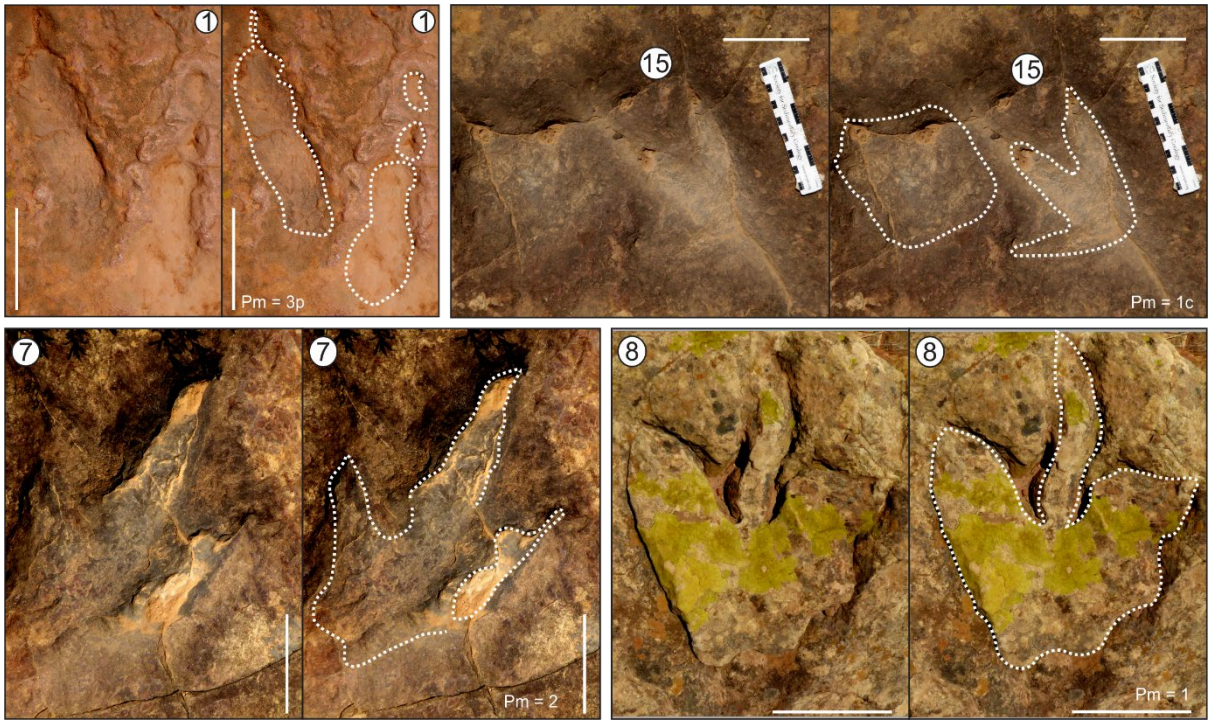

Figure 4.24: Tridactyl tracks at Roma Site 4: Tlapana with their interpretive outlines. Scale bar is 10 cm long. Abbreviations: Pm – morphological preservation grade.

The tridactyl tracks at Tlapana preserve minor morphological detail and/or are incomplete. These tracks cannot be confidently assigned to a specific ichnogenus. The elongate nature of the tracks (TL/TW>1), the narrow digits tapering to V-shaped tips and intermediate mesaxony suggest that these tracks have a theropod affinity (Fig. 4.24; Appendix Fig. A.3; Appendix Table A.1). The track dimensions and overall morphologies (for preservation grades 1 and above) are within the parameters of the *Grallator–Anchisauripus–Eubrontes* plexus (Section 2.3).

Landmark-based principal component analysis was used to evaluate the morphology of the Roma Site 4 at Tlapana tracks in comparison to known theropod ichnogenera listed in section 3.5 (Fig. 4.25). Individual tracks lie within *Grallator, Eubrontes* and *Kayentapus* morphospace (excluding outlier tracks 2 and 6). Track 6 has an unusually long digit III projection accounting for 48% of the total TL (Appendix Table A.1). Given the morphologies, measured parameters, landmark-based PCA and preservation grade, the tracks documented at Matobo are considered to be K-GAE-like.

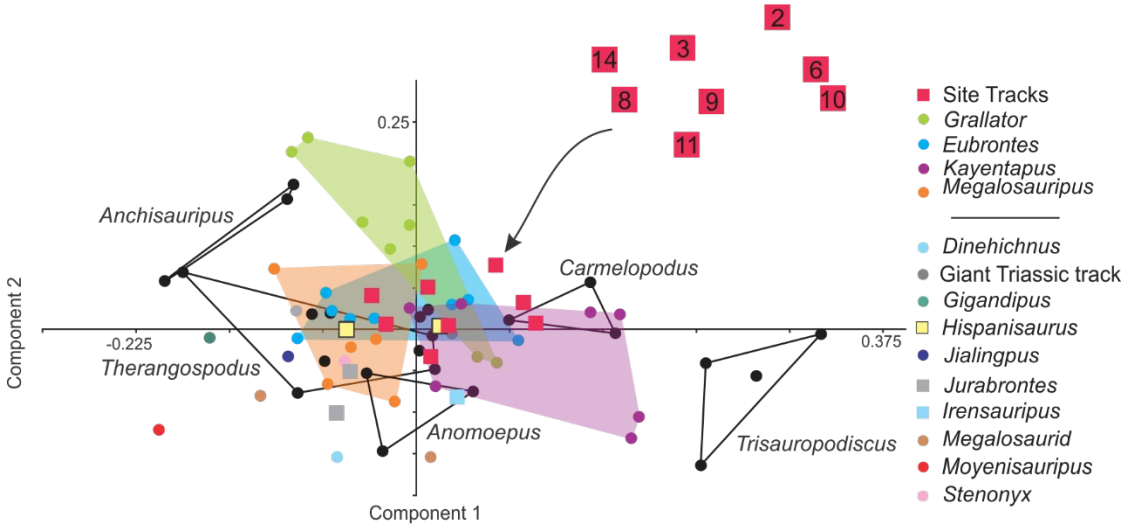

Figure 4.25: PCA morphological comparison between select tridactyl tracks at Roma Site 4 at Tlapana and the comparative ichnogenera database defined in section 3.5.

4.1.10.2 U-Pb Geochronology

The zircon crystals yielded from the Tlapana ichnite-bearing sandstone range in length from 25 to 201 µm (mean crystal length of 99 µm; TLA). The zircon morphologies are primarily elongate and sub-rounded or short and sub-rounded (Appendix Fig. B.1). Oscillatory and banded zoning are common internal structures. Bright luminescence of nearly the entire crystal is observed for both dominant morphologies (Appendix Fig. B.1). Inherited cores and a few inclusions are observed within some zircons.

Of the 105 ablated crystals, 93 have concordant dates (Appendix Table B.1). Nine of the concordant zircons have Th/U ratios < 0.1 (0.02<Th/U<0.1) suggesting a metamorphic influence on the crystals; these zircons are exclusively Precambrian in age (Appendix Table B.1). The concordant $^{206}Pb/^{238}U$ dates range from 205±3 to 3475±41 Ma, with most dates attributed to the Paleozoic Era (69%; Fig. 4.26A, B). The MDAs determined from the 6 metrics outlined in section 3.6.3 vary from 205 Ma (YSG) to 264.5 Ma (Concordia age; Fig. 4.26; Table 4.2). Given that the sample is from the uEF, a Rhaetian YSG MDA is most probable. It should be noted that a younger, Jurassic date (200± Ma) is present in the sample but is only 87% concordant. Although it deviates 3% from the discordance filter, its presence may bolster the 205 Ma MDA interpretation.

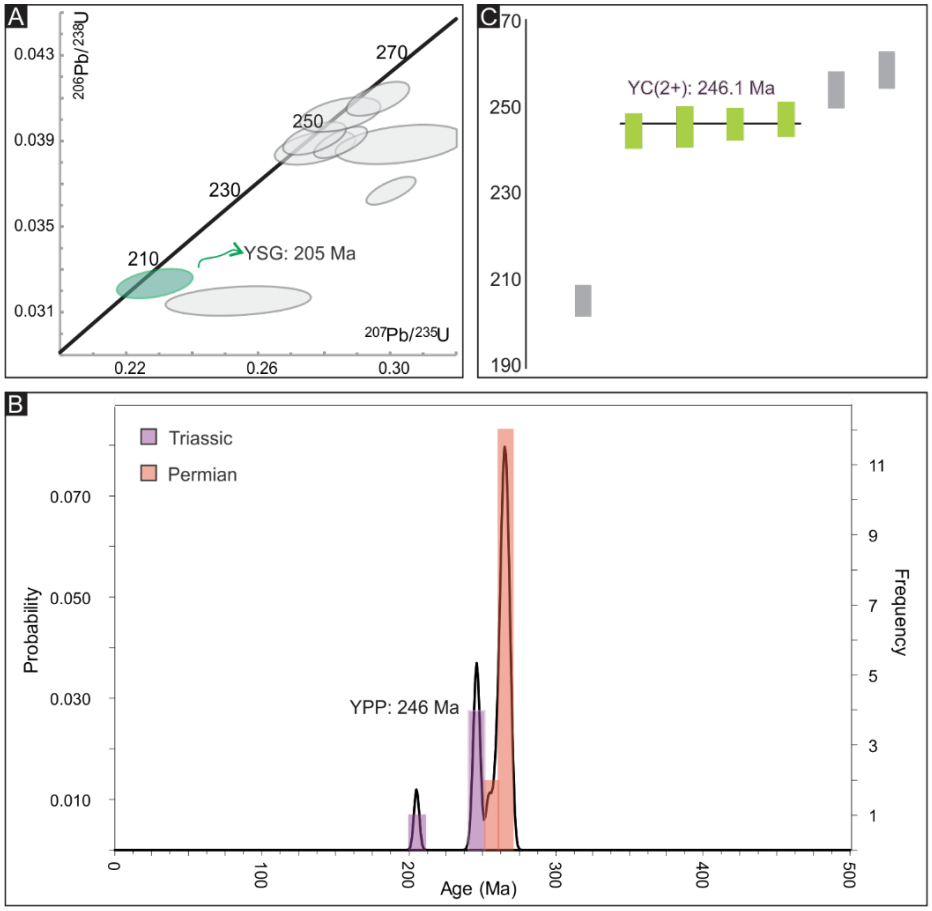

Figure 4.26: Concordant $^{206}P/^{238}U$ date distributions. A) Concordia plot showing the young dates (youngest date highlighted in green); B) Probability density plot for zircon crystals < 500 Ma; C) Weighted mean distribution of young zircons (YC2σ[2+] MDA in green).

4.1.11 Upper Moyeni ichnosite

The Upper Moyeni tracksite is a new ichnosite though it was discovered by locals several decades ago. The site has been briefly outlined by Haupt (2018), who focused on its geological context, and an in depth ichnotaxonomic review has been performed by Abrahams *et al*. (*2020*). The Upper Moyeni tracksite is a 130 m long, 2–2.5 m wide ichnosite preserved on a fine- to medium-grained uEF sandstone that locals use as an informal road. Over fifty tridactyl tracks are preserved at the tracksite (Appendix Fig. A.3). The tracks are impressed to varying depths with a minor component of tracks still preserved with their natural cast infilling. Digital pad and claw mark impressions are preserved with some tracks e.g., 5, 6, 9, 25, 32. Some tracks have extra-morphological features such as expulsions rims and mud collapse features (e.g., tracks 16–19; Appendix Fig. A.3).

4.1.11.1 Ichnology

Ninety-nine percent of the morphological variation, determined from traditional PCA, can be accounted for by the first three PCs (49%, 30% and 20%, respectively). The PCA distinguishes the Upper Moyeni tracks into two groups, based on all measurements. Principal Component 1 is primarily influenced by TL, TW and TS; while PC2 is strongly controlled by Dp/TL (Appendix Fig. A.1). Principal

Components 1–3 from landmark-based PCA are congruent with the traditional PCA – all landmarks show significant variation (Appendix Fig. A.2). Landmark 3 relating to TL and Dp is the largest contributor to PC1 variation, landmark 1 shows a lot of anterior variation of digit II for PC2 and would reflect differences in TS and LIV, and landmark 5 shows lateral shifts in the distal digit IV (reflecting differences in TS and TW) strongly influences PC3.

Landmark-based PCA was also used to compare the Upper Moyeni tracks to known ichnogenera (Fig. 4.27). Most of the tracks plot within *Eubrontes* (and *Eubrontes-Grallator*) morphospace and tracks 34 and 22 plot outside of known morphospace, close to the *Megalosauripus* and *Kayentapus* fields, respectively. These findings are in agreement with the findings of Abrahams *et al.* (2020) who assigned the tracks to *Eubrontes.*

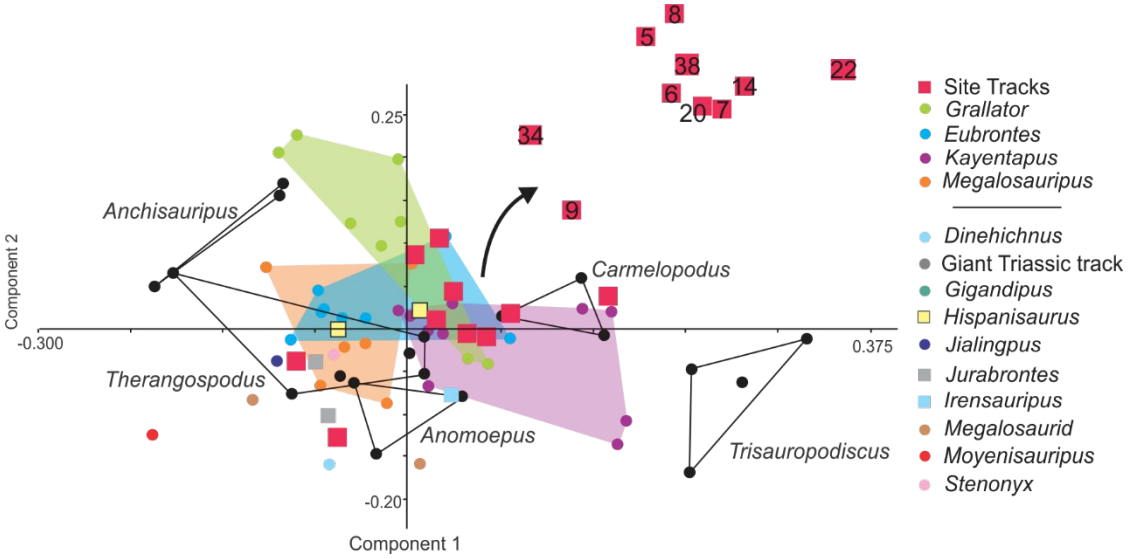

Figure 4.27: PCA morphological comparison between select tridactyl tracks at Upper Moyeni and the comparative ichnogenera database defined in section 3.5.

4.1.11.2 U-Pb Geochronology

Two samples were collected near the Upper Moyeni ichnosite: a sample from the track-bearing sandstone and a Clarens Formation sample associated with plant debris from the Clarens Formation – Drakensberg Group contact (~130 m above the track-bearing surface; see Haupt, 2018; UMO and UMC, respectively). The zircon crystals extracted from the ichnosurface sandstone have a range in length from 41 to 168 µm (average length of 93 µm) and are primarily sub-rounded (Appendix Fig. B.1). The internal structures are dominated by oscillatory zone, but banded zoning and complex domain features are also observed (Appendix Fig. B.1). Inherited cores and inclusions are preserved in some zircons. Many of the sub-rounded grains have bright luminescence.

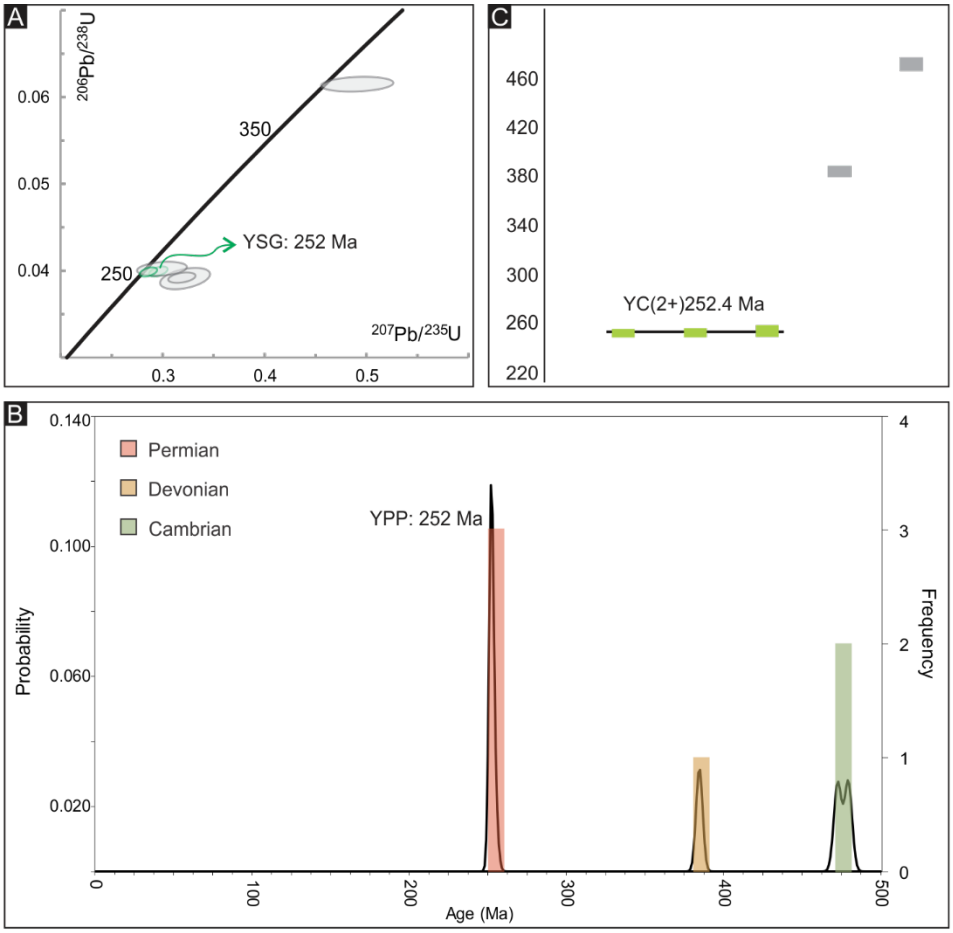

Figure 4.28: Concordant $^{206}P/^{238}U$ date distributions. A) Concordia plot showing the young dates (youngest date highlighted in green); B) Probability density plot for zircon crystals < 500 Ma; C) Weighted mean distribution of young zircons (YC2σ[2+] MDA in green).

The majority of picked zircons were lost during polishing of the mount or were too narrow to ablate. Therefore, only 23 crystals were successfully ablated (Appendix Table B.1). Of these measurements, only 17 are concordant. The concordant $^{206}Pb/^{238}U$ dates range between 252±3 and 1127±39 Ma, with 37% of the dates classified as Paleozoic and 63 % of the dates classified as Precambrian (Fig. 4.28A, B; Appendix Table B.1). All metrics described in section 3.6.3 were used to calculate MDAs (Table 4.2). The calculated MDAs range considerably from 252±3 to 504.7±4.6 Ma (Fig. 4.28). The metrics, excluding the Concordia age, suggest a Late Permian age for the UMO sample (252±3 to 252.4±1.8 Ma). Given the uEF stratigraphic position of the sample, a Late Permian true depositional age for the ichnosite is not plausible. We assign the MDA 252.4 as the interpreted MDA of the palaeosurface with the caveat that the site is likely significantly younger, probably Early Jurassic in age.

The zircon crystals extracted from the plant debris bearing sandstone unit range in length from 65 to 271 µm (mean length of 144 µm) and are predominantly elongate and sub-rounded to rounded (Appendix Fig. B.1). Oscillatory zoning is prevalent throughout the sample and inclusions and inherited cores are common.

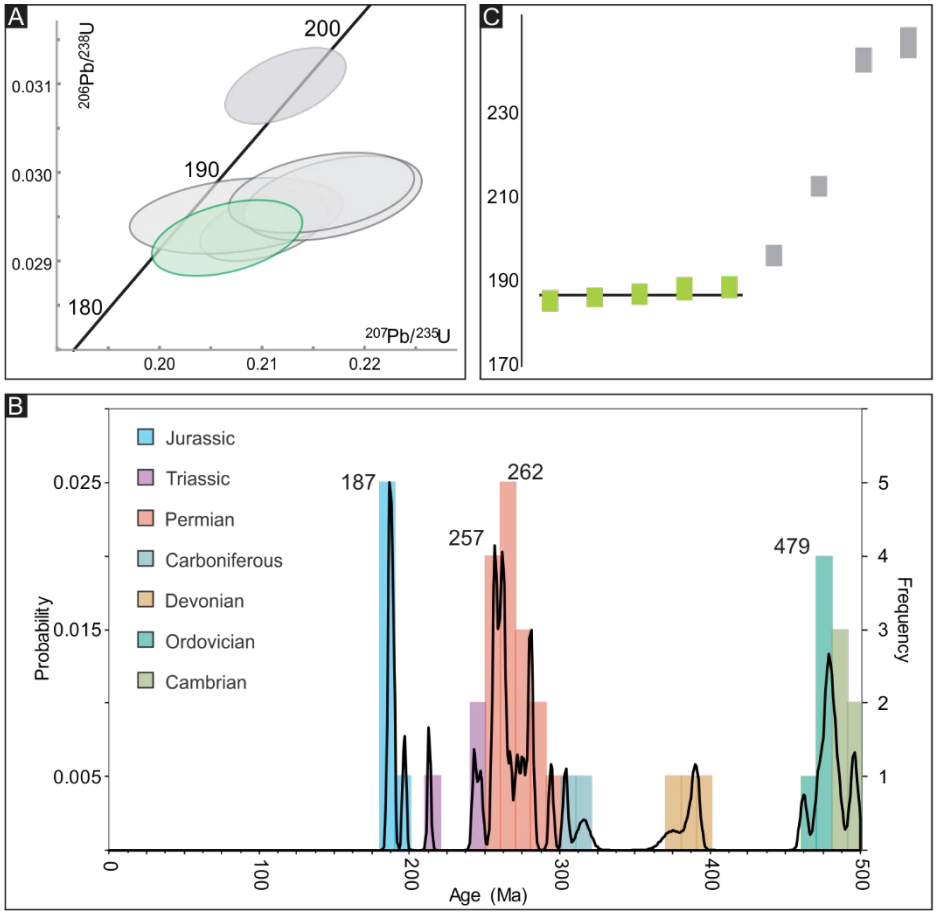

Figure 4.29: Concordant $^{206}P/^{238}U$ date distributions. A) Concordia plot showing the young dates (youngest date highlighted in green); B) Probability density plot for zircon crystals < 500 Ma; C) Weighted mean distribution of young zircons (YC2σ[2+] MDA in green).

Of the 86 ablated zircon crystals, 80 are concordant and only one crystal has a metamorphic signature Th/U ratio < 0.1 (Th/U of 0.07; Appendix Table B.1). The concordant $^{206}Pb/^{238}U$ dates range from 186±2 to 2057±17 Ma with date distributions as follows: 11% Mesozoic, 59% Paleozoic and 30% Precambrian (Appendix Table B.1). Five metrics outlined in the methods were used to calculate MDAs (Table 4.2). The MDAs have almost no variation and all ages overlap within 2s error (186 to 187.5 Ma; Fig. 4.29). Given that this sample is located at the Clarens Formation – Drakensberg Group contact, all calculated MDAs are plausible.

4.1.12 Phahameng ichnosite

Ellenberger (1970) was the first to mention tracks from the lower and middle Clarens at Phahameng (zones B/3 and B4). He described tridactyl and numerous pentadactyl tracks from the ichnosite. In this study, only two tridactyl tracks, forming a single step, were located on a fine-grained lower Clarens Formation sandstone at Phahameng (Appendix Fig. A.3). These tridactyl tracks and the sedimentology of their host rock have been briefly documented by Haupt (2018).

4.1.12.1 Ichnology

Ratio dimensions of the two tridactyl tracks at Phahameng are quite consistent: TL/TW of 1.35, Dp/TS between 0.47 and 0.5 and Dp/TL between 33 and 35% (Appendix Table A.1). Given the limited dataset, traditional and landmark PCA could not be performed on these two tracks.

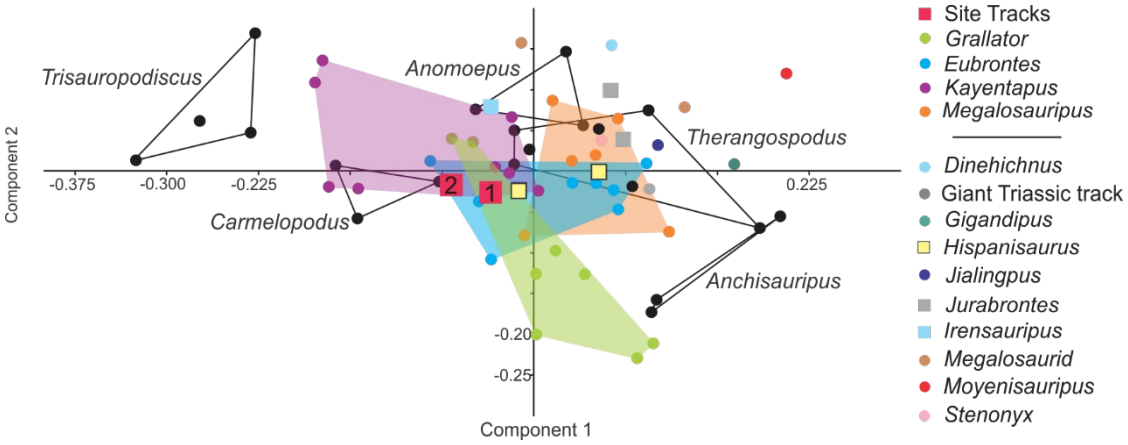

Figure 4.30: PCA morphological comparison between tridactyl tracks at Phahameng and he comparative ichnogenera database defined in section 3.5.

Landmark-based principal component analysis could be used to evaluate the morphology of the Phahameng tracks in comparison to known theropod ichnogenera listed in section 3.5 (Fig. 4.30). The tracks lie within the *Grallator* and *Eubrontes* morphospace, with track 2 plotting within the *Eubrontes* -*Eubrontes* morphospace, and track 1 plotting in the overlap between *Grallator-Eubrontes-Kayentapus* morphospace. Given that the tracks comprise a single step, and because of their dimensions and overall morphology e.g., robust digits, these tridactyl tracks are assigned to the *Eubrontes* ichnogenus, confirming Haupt's (2018) assertion. It is worth nothing that these tracks are likely from the same stratigraphic horizon in the middle Clarens Formation at Phahameng, from where Ellenberger (1970) identified *Platysauropus robustus,* which he attributed to large, three-toed bipeds (Ellenberger, 1975, p. 423). *Platysauropus robustus* is similar to *Ichnites euskelosauroides*, a large tridactyl track from southern Africa named by Huene in 1932 (also see von Huene, 1941; Ellenberger and Ellenberger, 1958, p. 66; Ellenberger, 1970), and later synonymized with *Eubrontes* by Haubold (1971). *Platysauropus robustus* is slightly more elongate (TL/TW), has a higher Dp/TS (0.65) and stronger "heel" asymmetry than the Phahameng tracks considered herein.

4.2 Summary of the U-Pb dating results

The maximum depositional ages (MDAs) obtained from U-Pb LA-ICPMS dating of detrital zircons of the key ichnosites studied in this thesis are consistent with the existing understanding of the age of the upper Stormberg Group (section 2.1.3). More specifically, the lEF samples predominantly have Late Triassic YC2σ[2+] MDAs (Fig. 4.31). The fine-grained sandstone from Ha Falatsa is the only lEF sample which has a Late Permian YC2σ[2+] MDA. However, HAF_f has a YSG MDA of 220 Ma (Norian)

and the second Ha Falatsa sample (HAF_c) has a robust Late Triassic MDA (Table 4.2). Therefore, a Late Triassic MDA can be interpreted for all lEF ichnosites considered.

The uEF samples form two distinct YC2σ[2+] clusters: an Early Jurassic cluster and an Early Triassic-Late Permian cluster (Fig. 4.31). The Early Triassic sample TLA has a Late Triassic YSG MDA of 205 Ma (Table 4.2) and the Anisian sample LEPc is located stratigraphically 1 m below the Early Jurassic sample LEPs. The Late Permian sample MAT has a Sinemurian YSG MDA of 192 Ma (Table 4.2) and the Changhsingian sample UMO is geographically close to and located ~65 m above the Hettangian LMO site. Given that the older uEF can be interpreted as Late Triassic–Early Jurassic from their other MDA metrics or associated samples, we conclude that the uEF ichnosites are Early Jurassic in age. The Clarens Formation overlies the uEF and underlies the radioisotopically dated Pliensbachian-Toarcian Drakensberg Group; therefore, an Early Jurassic age (Sinemurian – Pliensbachian) is expected.

In summary, the lEF is interpreted as Late Triassic and the uEF and Clarens Formation are interpreted as Early Jurassic. The U-Pb dating results obtained during this thesis form part of a larger collaborative project aimed at generating the first chronostratigraphic framework of the upper Stormberg Group. Select geochronological data presented in this thesis contribute to the larger study i.e., many of the detrital zircon samples analysed for this PhD proved unsuccessful for determining MDA (e.g., uEF TLA Late Triassic MDA and uEF UMO Permian MDA, Fig. 4.31) and are consequently excluded from the upper Stormberg review paper (Bordy *et al.,* 2020b). Because the first review paper from this larger project has just been published, this thesis does not repeat here all the aspects of the geochronological dataset gathered during this study. Bordy *et al.* (2020) detail a more robust geochronological dataset which includes select samples presented in this PhD and additional, independent geochronological data obtained from various international laboratories (e.g., TRAIL, BGS). For these as well as details on the palaeontological, ichnological, lithostratigraphic, magnetostratigraphic and chronostratigraphic aspects of the upper Stormberg Group, the reader is kindly referred to the above mentioned review paper: Bordy, E.M., **Abrahams, M**., Sharman, G.R., Viglietti, P.A., Benson, R.B.J., McPhee, B.W., Barrett, P.M., Sciscio, L., Condon, D., Mundil, R., Rademan, Z, Jinnah, Z., Clark, J.M., Suarez, C.A., Chapelle, K.E.J., Choiniere, J.N. 2020. A chronostratigraphic framework for the upper Stormberg Group: implications for the Triassic Jurassic boundary in southern Africa. Earth Science Reviews, 203: https://doi.org/10.1016/j.earscirev.2020.103120

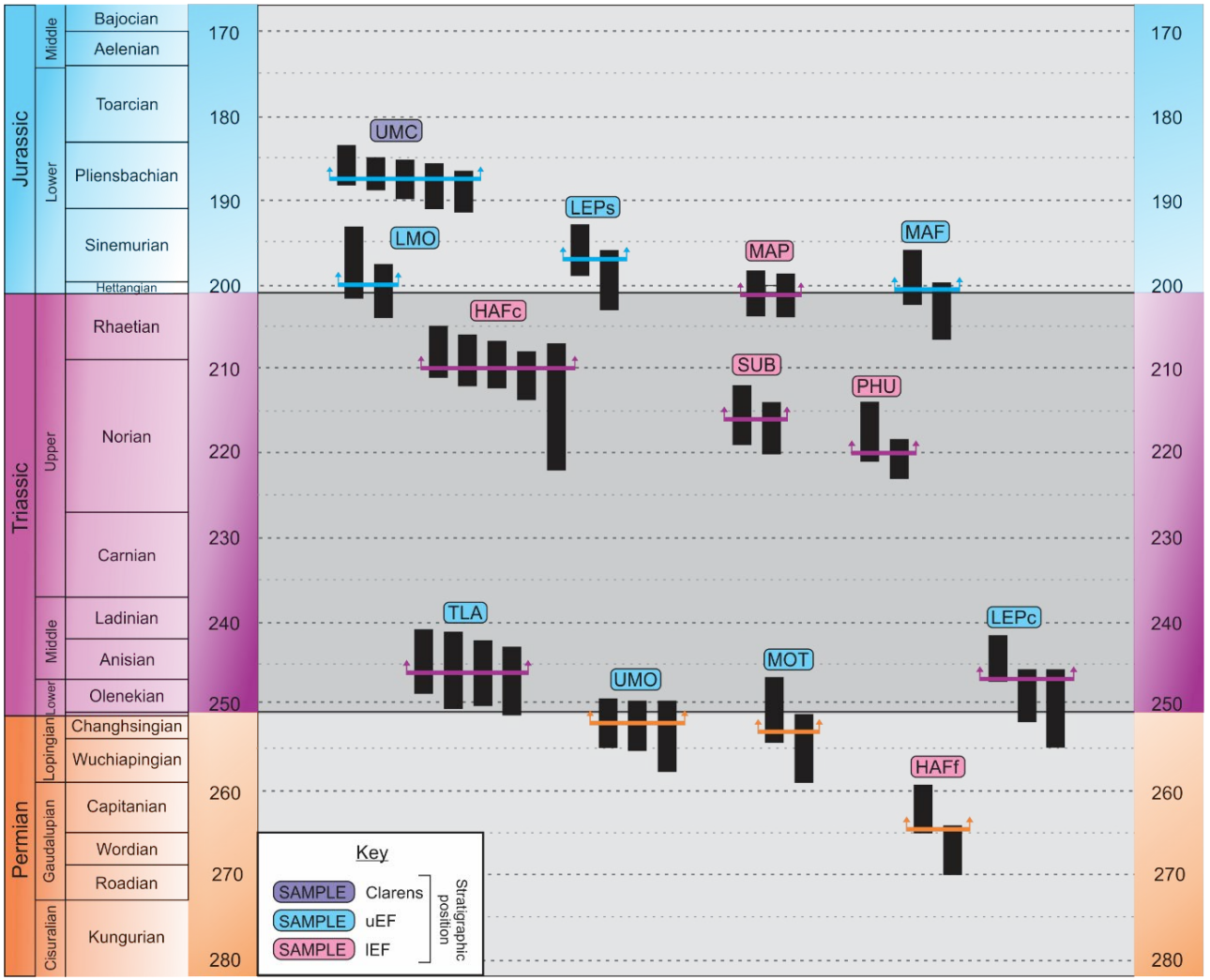

Figure 4.31: Individual zircon dates (with 2σ error) that comprise the YC2σ[2+] maximum depositional ages (marked with a line) for samples analysed in this study from the Elliot and Clarens formations.

5 The Early Jurassic Tsikoane ichnosite

Hidden for one hundred years: a diverse theropod ichnoassemblage and tracks preserved in cross-section from the historic Early Jurassic Tsikoane ichnosite (Clarens Formation, northern Lesotho)

Miengah Abrahams[1], Emese M Bordy[1] and Fabien Knoll[2]

1 Department of Geological Sciences, University of Cape Town, Cape Town, South Africa

2 ARAID- Fundación Conjunto Paleontológico de Teruel-Dinópolis, Teruel, Spain

Hidden for one hundred years: a diverse theropod ichnoassemblage and tracks in cross-section from the historic Early Jurassic Tsikoane ichnosite (Clarens Formation, northern Lesotho)

The upper Stormberg Group of Lesotho has an abundant and diverse ichnological record that dates to the Early Jurassic. Herein, we re-evaluate a known ichnosite in the lowermost Clarens Formation (Karoo Supergroup) at Tsikoane in northern Lesotho. The site was reported to preserve tridactyl tracks as natural casts in the ceiling of overhangs and true track impressions on a fallen sandstone block. At least three track-bearing palaeosurfaces, associated with horizontally laminated sandstones and desiccated green mudstones, can be traced over a distance of 250 m. Associated with one of the track-bearing palaeosurfaces, discrete, U-shaped, cross-sectional structures are interpreted as a series of natural casts, surface tracks, true tracks and undertracks. Although the Tsikoane tracks were historically assigned to a single ichnogenus, later synonymized with *Grallator*, our findings show a higher diversity of tridactyl ichnites, with tracks that have *Kayentapus*-like and *Eubrontes*-like features in addition to previously recognized *Grallator*-like features. These new findings, within their high-resolution sedimentological context, improve the understanding of theropod palaeodiversity and palaeoecology in southern Africa during a crucial period in dinosaur history marked by increases in both abundance and diversity.

Keywords: Sinemurian – Pliensbachian; Karoo Supergroup; *Kayentapus; Eubrontes; Grallator*

Highlights:

- Lower Jurassic ichnosite exposing tridactyl true tracks and natural casts assigned to *Grallator, Eubrontes* and *Kayentapus*
- Natural casts of a high anatomical fidelity are preserved in the ceilings of overhangs; true tracks are impressed into a fallen block that has been relocated for the first time since 1908

- The first documented tracks preserved in cross-section for the Clarens Formation with the true track, undertracks and natural cast infillings observable

5.1 Introduction

The Lower Jurassic Stormberg Group (Karoo Supergroup) hosts a plethora of dinosaur tracksites in southern Africa (e.g., Dieterlen 1885; von Huene 1932; Dornan 1908; Ellenberger and Ellenberger 1958; Ellenberger *et al*., 1970; Ellenberger 1970, 1972; Raath and Yates 2005; Ambrose 2006; Sciscio *et al*., 2016, 2017a; Abrahams *et al*., 2017; Rampersadh *et al*., 2018; Bordy *et al*., 2020a). These ichnosites are dominated by tracks attributed to carnivorous trackmakers, which strongly contrasts with the herbivorous-dominated skeletal record of the region (e.g., Raath 1977; Yates 2005; Bristowe and Raath 2004; Knoll and Battail 2001; Knoll, 2002a, 2002b, 2010, Yates and Barrett 2010; Yates *et al*., 2010; McPhee *et al*., 2015a, 2015b; Sciscio *et al*., 2017a; Bordy *et al*., 2020b). Thus, the tracksites are crucial for providing insights into Early Jurassic theropod palaeoecology during a post-extinction recovery period defined by dinosaur abundance and diversity increases (Baron *et al*., 2017).

Vertebrate tracks are three-dimensional (3D) products resulting from the interaction between a trackmaker and the substrate over which the animal moves (Falkingham 2014). These products can be preserved as either true tracks, natural casts or undertracks (also known as transmitted prints or ghost prints; Lockley 1991). The 3D nature of tracks means that they can be observed in cross-section, which gives an added perspective to the common preservation mode visible in planar view (e.g., Ellenberger 1970; Loope 1986; Romano and Whyte 2003; Ambrose 2006; Milàn and Loope 2007; Xing *et al*., 2013; Lockley *et al*., 2015; Romano and Citton 2017; Díaz-Martínez *et al*., 2018). True tracks are the products of direct contact between the trackmakers and the substrate, referred here as the tracking surface (Fornós *et al*., 2002). They have the highest potential of capturing morphological details such as skin impressions, digital pad impressions and claw marks (Gatesy 2001; Sciscio *et al*., 2016; cf. Marchetti 2019). The natural infilling of the true track creates an epirelief replica of the track. Trackmakers may penetrate well beneath the tracking surface, interacting and having direct contact

with underlying sediments, registering deep true tracks (Bromley 2001). Consequently, the substrate that the trackmaker interacts with is neither a single surface nor layer (Gatesy 2003). In response to the weight of the trackmaker on the tracking surface, subadjacent unconsolidated sediment layers can be deformed mostly downwards, and to some degree radially outwards, generating undertracks (Allen 1997; Milàn *et al*., 2004; Avanzini *et al*., 2012). Consequently, undertracks resemble true tracks, but with reduced anatomical detail and distorted dimensions (e.g., Thulborn 1990; Lockley 1998; Henderson 2006; Milàn and Bromley 2006; cf. Marchetti 2019). The depth to which undertracks can be generated is controlled by the substrate competency and the pressure exerted by the trackmaker, which is related to its mass (size), behaviour (e.g., locomotion) and autopod morphology (Lockley 1986; Platt and Hasiotis 2006; Falkingham 2011). Undertracks are commonly identified in heterolithic sediments that are laminated or bedded, because the variable density gradients of the different sediment layers more readily allow the generation of stacked undertracks (e.g., Anketell *et al*., 1970; Thulborn 1990; Milàn and Bromley 2006; Avanzini *et al*., 2012).

Herein, we re-evaluate the historical Tsikoane ichnosite in the lowermost Clarens Formation in northern Lesotho (southern Africa, Fig. 1), which was discovered by Dieterlen in the early 1900s (cf. Ellenberger 1972) and later recorded by Dornan (1908). Dornan's account briefly describes tridactyl impressions preserved as epireliefs on the ceiling of an overhang and hyporeliefs on a fallen block directly below the overhang. Possibly due to the relative inaccessibility of the many cliff faces at the locality, the Tsikoane ichnosite has, subsequently, only been cursorily mentioned by Ellenberger and Ellenberger (1958), Ellenberger *et al*. (1970), Ellenberger (1970, 1972) and Ambrose (2016), without any mention about the fallen sandstone block described Dornan (1908). Although ichnotaxonomic, stratigraphic and sedimentological details about Tsikoane have not been reported in any of the aforementioned publications, Ellenberger (1970, 1972) assigned the Tsikoane tracks to a single ichnogenus *Kainotrisauropus morijiensis*, which was subsequently synonymised with *Grallator* by Olsen and Galton (1984, p. 109).

In addition to describing the geological context of the ichnosite and revising the ichnotaxonomy of the Tsikoane tracks, our study presents the following novel findings:

- Multiple, track-bearing palaeosurfaces that extend laterally for at least 250 m;
- The first report of tracks preserved in cross-section (including true tracks, natural casts and undertracks) from the Clarens Formation; and
- a diverse ichnoassemblage of vertebrate tracks, which are *Grallator*-like*, Eubrontes*-like and *Kayentapus*-like, and may be attributable to various theropod trackmakers.

5.2 Geological context and stratigraphy of the site

The Tsikoane ichnosite (28˚54'4.90''S, 27˚ 59'41.67''E) is located in the Hlotse district, northern Lesotho, directly above the Tsikoane Anglican Church, in the lowermost Clarens Formation (Zone B/4 of Ellenberger 1970; Fig. 1A). The site extends further south-eastwards for at least 250 m where a fallen block preserves hyporelief vertebrate tracks and additional track-bearing overhangs display several dozen epirelief tracks. The Sinemurian–Pliensbachian Clarens Formation (e.g., Knoll 2005; Bordy *et al*., 2020b) is the youngest formation in the Stormberg Group, gradationally overlying the highly fossiliferous red beds of the upper Elliot Formation and underlying the Karoo continental flood basalts of the Drakensberg Group (183 ± 1 Ma, Duncan *et al*., 1997; Marsh *et al*., 1997; Moulin *et al*., 2017; Fig. 5.1B). The Clarens Formation is a prominent cliff-forming stratigraphic unit that comprises cream coloured, fine- to coarse-grained sandstones with localised minor mudstones (e.g., Beukes 1970; Eriksson 1981; Bordy and Head 2018). Common throughout southern Africa, the Clarens Formation has a complex aeolian origin and is dominated by wind-blown palaeo-dunes (e.g., Beukes 1970; Bordy and Catuneanu 2002; Bordy and Head 2018). In the main Karoo Basin, the Formation is subdivided into three zones, of which the lower and upper zones contain deposits of ephemeral rivers, streams and lakes, reflective of fluctuating wetter and drier climatic conditions (Fig. 5.1B - e.g., Beukes 1970; Bordy and Head 2018). In addition to vertebrate trace fossils, bone fossils (e.g., freshwater fishes, crocodylomorphs, ornithischians, basal sauropodomorphs, mammaliaforms) and plant fossils

(e.g., sphenophytes, conifers) are also preserved in the Clarens Formation (e.g., Broom 1911; Haughton 1924; Ellenberger 1970; Tasch 1984; Kitching and Raath 1984; Bordy and Catuneanu 2002; Bamford 2004; Knoll 2005; Bordy 2008; Bordy *et al.,* 2009; Bordy and Eriksson 2015; McPhee *et al*., 2017; Bordy *et al*., 2020b).

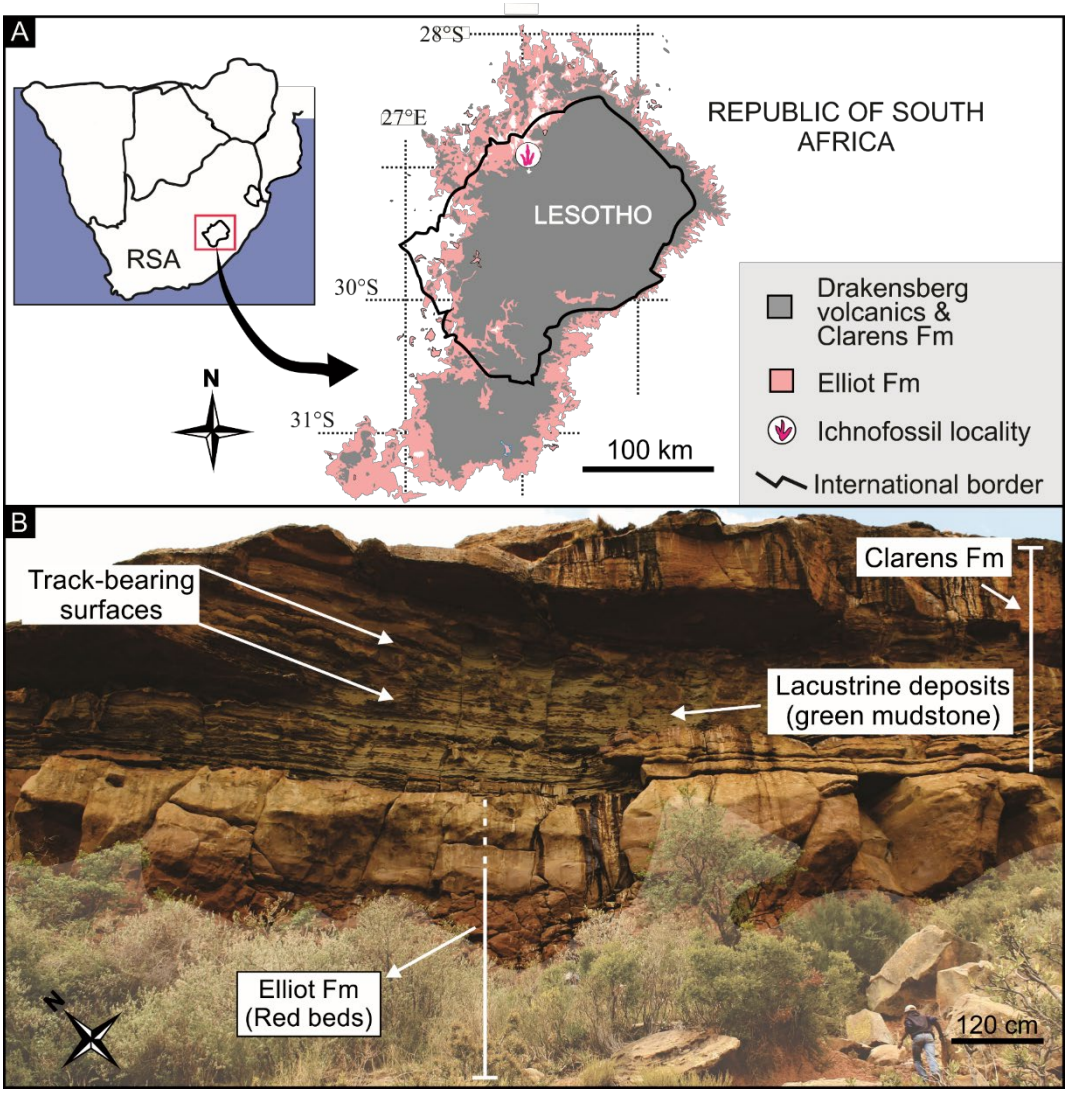

Figure: 5.1. Geological context of the Tsikoane ichnosite. A) Simplified geological map of the study area marking the location of the ichnosite within Lesotho. B) Natural rock exposure at Tsikoane highlighting the gradational contact of the uppermost Elliot and lower Clarens Formations. Abbreviations: RSA – Republic of South Africa; Fm – Formation.

5.3 Materials and methods

The sedimentology of the track-bearing strata at the Tsikoane ichnosite was photographed and described to assess the vertical and lateral variation of the sedimentary facies. The track-bearing surfaces, individual tridactyl ichnites and Tsikoane track cast material collected by Victor Ellenberger

and housed at the Ellenberger Collection at the Université de Montpellier (France) were documented photographically (Canon PowerShot EOS D1200 -Focal length 28 mm, 5184 x 3456 resolution camera). Photogrammetric 3D models of key, accessible ichnites and the cast material were generated using Agisoft Photoscan (standard version 1.1.4) applying the methods described by Mallison and Wings (2014). Utilising these 3D models, false colour depth maps were produced using Cloud Compare software (version 2.6.1). For thirty-two accessible ichnites, the track length (TL), track width (TW) and track span (TS) were measured *in situ* (Fig.5.2; Appendix Table C.1). Additional track parameters, such as digit divarication angles (II^III, III^IV and II^IV) and digit III projection (Dp), were measured from high-resolution photographs using ImageJ software (Schneider *et al*. 2012; Fig. 5.2; Appendix Table C.1). For inaccessible tracks preserved beneath the ceilings of overhangs, absolute linear dimensions could not be measured but the ratio dimensions of fifteen ichnites are considered (Appendix Table C.1). The mesaxony of each track is expressed by the Dp/TS ratio, to quantify the emphasis of the central digit (*sensu* Lockley 2009). Overview photographs, interpretive outlines and track measurements of all tracks considered at Tsikoane are provided in the supplemental material in accordance to Falkingham *et al*. (2018; AppendixAppendix Fig.C.1; AppendixAppendix Table C.1). In addition to conventional statistical plots, landmark-based principal component analysis (PCA) was performed on select tracks from photographs to compare their morphology with known ichnogenera (see supplemental material for a list of the references used in the comparison). Although landmark-based geometric morphometrics is recommended exclusively for tracks with a high anatomical fidelity (*sensu* Gatesy and Falkingham, 2017) or preservation grade (*sensu* Belvedere and Farlow, 2016; Marchetti *et al*., 2019), we have employed these techniques for lower grade tracks as well. Given that tracks with a lower anatomical fidelity are considered, ichnotaxonomic assignment does not purely rely on the landmark-based geometric morphometrics. A TPS file was generated using TpsUtil 1.75 and 6 landmarks were placed for each track in TpsDig software (Fig.5.2). A Procrustes fitting was applied to all the landmark data and the PCA was performed using PAST v3.

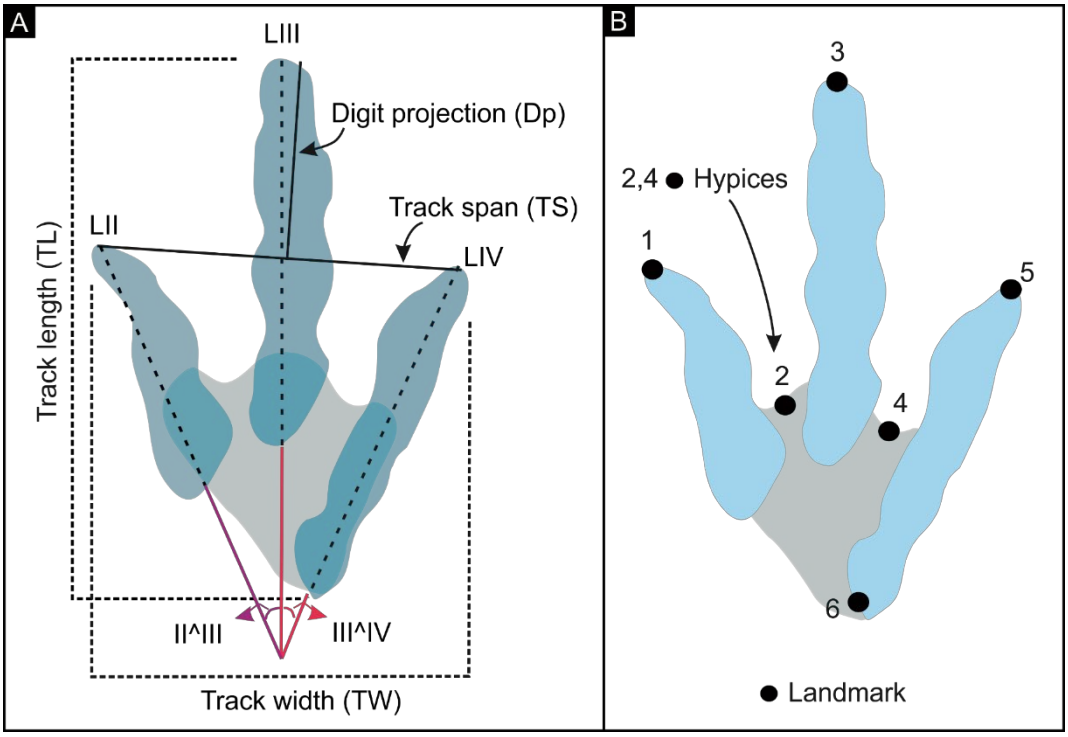

Figure 5.2: Morphometric parameters taken from the tridactyl ichnites. A) Linear measurements and angles taken in the field and using ImageJ. B) Landmark placement for geometric morphometric principal component analysis (PCA).

5.4 Results

5.4.1 Sedimentology

At the Tsikoane ichnosite (*senso stricto*), the upper Stormberg Group is represented by a large-scale upward-coarsening succession comprised of ~ 15 m of upper Elliot Formation (uEF) and ~ 30 m of lowermost Clarens Formation (Figs. 5.1B, 5.3A). The maroon, fine to medium-grained tabular sandstone in the lower part of Fig. 5.3A, and the very fine to fine-grained, silty sandstones in the middle part of Fig. 5.3A are part of uEF. The silty, very fine to fine-grained uEF sandstones preserve two distinct palaeosol-bearing units that are up to ~2 m thick, and contain green and purple mottling, well-preserved, downward-branching and tapering root traces, irregular-shaped, *in situ* carbonate concretions (a few cm in diameter), large- and small-scale desiccation cracks and localised ripple cross-lamination (Figs. 5.3B-F). A single, undiagnostic bone fragment associated with the large-scale desiccation cracks was found *in situ*. The lowermost part of the conformably overlying Clarens Formation (Figs. 5.1B, 5.3A) is the main track-bearing unit at Tsikoane. It comprises laterally continuous, cream-coloured, sheet-like, fine- to medium-grained sandstones that range in thickness

from 0.1 to 1.5 m (Fig. 5.3A). These track-bearing, tabular sandstones are horizontally laminated and interbedded with green mudstone films (drapes) and layers (<0.2 m thick) that preserve desiccation cracks especially in the south-eastern part of the ichnosite (Fig. 5.3G). In the north-western part of the ichnosite, a localised upward-fining unit comprises massive, intraformational, mud-pebble conglomerates at the base that gives way to interbedded green mudstones and grey and cream-brown, horizontally laminated, tabular, fine-grained sandstones (Figs. 5.3A, H). Distinct U-shaped structures disrupt the interbedded part of this well-bedded, upward-fining unit (Fig. 5.3H). The rest of the Clarens Formation at the Tsikoane ichnosite (Figs. 5.1B, 5.3A) is characterised by 1 to 5 m thick, medium- to fine-grained sandstones that are mostly massive and rarely cross-bedded.

Table 5.1. Summary of the sedimentological characteristics at the Tsikoane ichnosite and their brief palaeoenvironmental interpretation.

Formation (Fm)	Key sedimentological characteristics at Tsikoane	Depositional environment	Main references
Lower Clarens Fm	1-5 m-thick sandstones (mostly massive, few cross bedded)	Aeolian dunes in a wet desert system	Beukes, 1970; Bordy and Head, 2018; Bordy et al. 2020
Lowermost Clarens Fm	0.1-1.5 m-thick, tabular sandstones (mostly laminated); thin mudstones with desiccation cracks; track-bearing in parts	Ephemeral lakes in a wet desert system	
Uppermost uEF	Tabular sandstones; thick palaeosols with *in situ* carbonate nodules, roots/rootlets, colour mottling, fossil bones and large-scale desiccation cracks	Vegetated floodplain along the banks of ephemeral streams in a semid-arid fluvio-lacustrine system	Bordy et al. 2004a, 2004 b; Bordy et al. 2020

The above sedimentological characteristics of the uEF and lowermost Clarens Formation at Tsikoane, including their gradational contact forming a large-scale upward-coarsening succession (Fig. 5.3A), are typical in the same stratigraphic interval within the upper Stromberg Group throughout southern Africa, but most of all in the main Karoo Basin (Fig. 5.1; e.g., Bordy and Catuneanu 2001; 2002; Bordy *et al*. 2004a, 2004b; Bordy and Head 2018; Bordy *et al*. 2020). For this reason, a detailed sedimentological interpretation of these units is omitted here, in favour of the following summary table of palaeoenvironmental conditions.

5.4.2Vertebrate ichnology

Forty-seven tridactyl tracks are documented *in situ* at the Tsikoane ichnosite. Most of these tracks occur as hyporeliefs on a fallen sandstone block and epireliefs in three track-bearing palaeosurfaces beneath ceiling overhangs. Additionally, three casts from the Ellenberger Collection at the Université de Montpellier (France; here labelled as tracks 48, 49, 50) and one natural cast (here labelled as track 51) found *ex situ* beneath the track-bearing north-western overhang are also considered (Figs. 5.5B–D). Except for two trackways that are preserved on the fallen sandstone block, all other ichnites described from Tsikoane are isolated tracks (Figs. 5.4A, 5.5A; Appendix Fig. C1). There is no apparent preferred track orientation in the ceiling overhang tracks but the tracks preserved on the fallen sandstone block are predominantly parallel, orientated according to the present-day east–west direction (Figs. 5.4A, 5.5A, Appendix Fig. C.1). The fifty-one Tsikoane tracks described herein are similar in morphology: elongate tracks with gracile digits that taper to V-shaped tips and have an apparent total digit divarication <90˚ (Figs. 5.4, 5.5; Appendix Fig. C1). Although the tracks share these features, they can be grouped into Morphotypes I to V, based on distinct morphological characteristics, i.e., relative digit widths, posterior end ("heel") morphologies, and their measured track parameters. The morphological anatomical fidelity of the tracks varies in accordance with their style of preservation as follows: the epirelief overhang tracks have high anatomical fidelity and commonly preserve distinct digital pad impressions and claw marks (e.g., tracks 36, 37, 39, 40, 43; Fig. 5.5A) in contrast to the shallow true tracks on the fallen block, which rarely preserves these anatomical details (e.g., tracks 37, 40, 43; Appendix Fig. C.1) but overprint the desiccation cracks that are on the tracking surface. Furthermore, some of the true track impressions are preserved with sediment infillings, which are obscuring track detail (e.g., tracks 10, 11, 13, 24; Fig. 5.4; Appendix Fig. C.1).

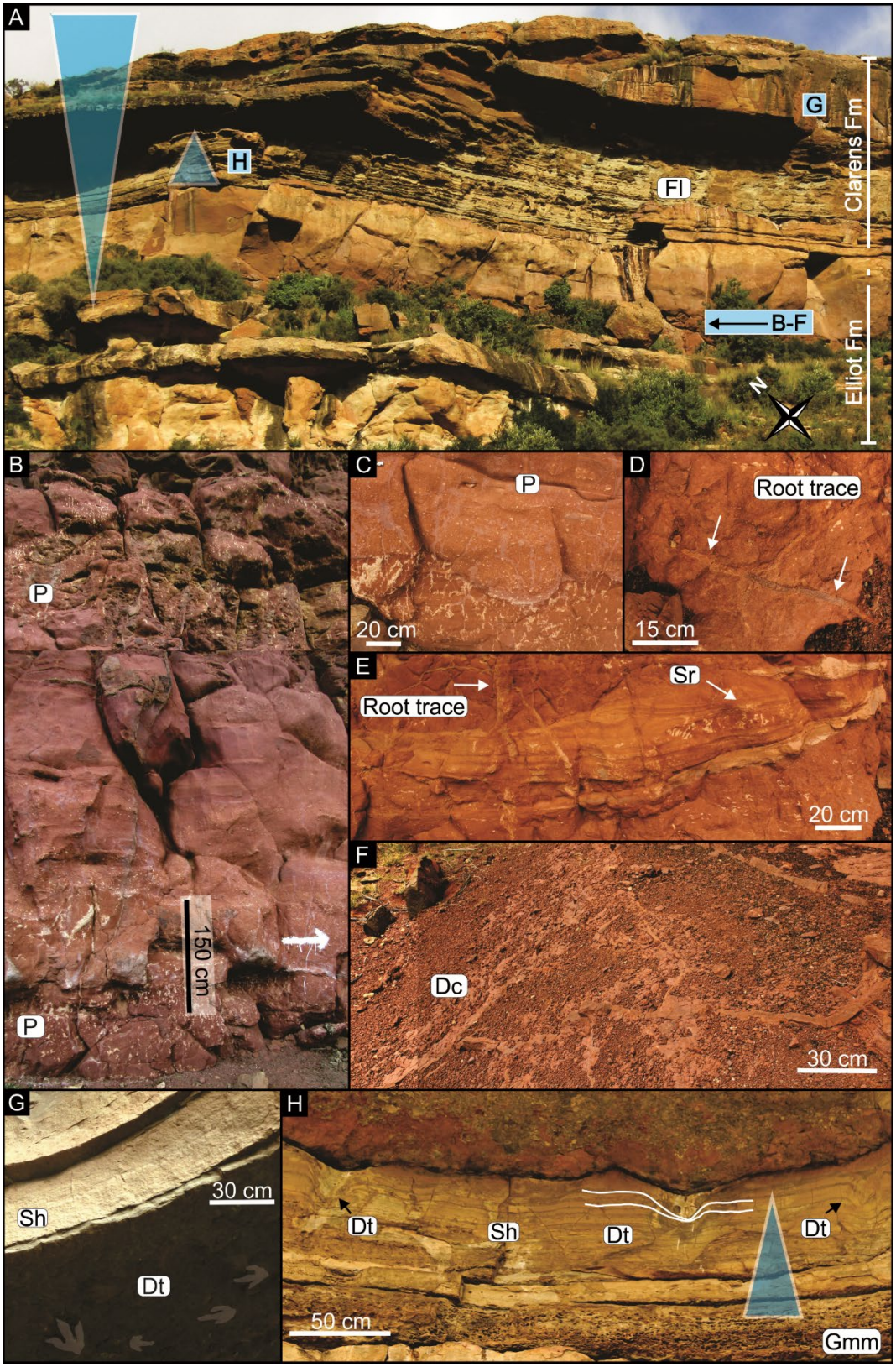

Figure5. 3: Sedimentological aspects of the fluvio-lacustrine upper Elliot Formation and the fluvio-lacustrine lowermost Clarens Formation at Tsikoane. A) Overview of the coarsening upward succession across the formational boundary and localised upward-fining, lacustrine units in the lowermost Clarens Formation. Blue triangles indicate grain size variation and the labels refer to the close-up images shown in the rest of the Figure. B–F) Paleosol-bearing units in the uppermost uEF comprise root traces, irregular calcareous concretions and ripple-cross laminations. H) Large-scale desiccation cracks. G) Track-bearing, horizontally laminated, laterally continuous, tabular sandstones are interbedded with green mudstones. Tridactyl tracks have been digitally highlighted. H) Close-up of the lowermost Clarens Formation showing discrete, U-shaped

structures that disrupt the localised upward-fining, tabular beds comprising sandstones and mudstones. Blue triangle indicates grain size variation. Abbreviations: Fm – Formation, P – Palaeosol-bearing units, Sr – Ripple-cross lamination, Dc – Desiccation cracks, Sh – horizontal laminations, Gmm – Matrix-supported, massive breccia, Dt – Dinoturbation.

It is unclear, though likely, that the fallen block located in this study is identical to the one Dornan (1908) described. His brief description states:

> "... a magnificent series of dinosaurian footprints are to be seen in the same green mud, on the underside of an overhanging cliff. They are all in relief. The huge block which has broken off with impressions in their natural state, lies below. There are more than 50 of these prints all with the same general direction from west to east but crossing and re-crossing each other in the most extraordinary fashion. Large and small are mixed together, but the great bulk of them are small prints. There are two sets of very large prints most conspicuous, evidently belonging to 2 large individuals. The length of these tracks is not less than 15 inches (middle toe)".

The fallen block described herein (Fig. 5.4A) matches the above description, because it is also found directly beneath a track-bearing overhang, contains at least 50 tracks with the largest track being ~41 cm (~16 inches) in length and the tracks on the block are primarily orientated in the present-day east–west direction and occasionally do cross one another.

Tsikoane track morphotypes

Morphotype I

Morphotype I comprises three tracks observed on the fallen block (track 6) and the overhang (tracks 32, 45; Figs. 5.4, 5.5A). These tracks are distinct from other tracks at Tsikoane because they are smaller and more elongate (Figs. 5.4, 5.5A; Appendix Table C.1). Only one TL, 13.6 cm for track 6, could be measured (Appendix Table C.1). Morphotype I is defined as being elongate (average TL/TW of 1.81), having gracile, tapering digits and tulip-shaped posterior ends (Figs. 5.4, 5.5A; Table 5.2). The tracks have variable Dp/Ts (0.48–0.78; mean of 0.64) and Dp/TL (0.27–0.41; mean of 0.34; Table 5.2; Appendix Table C.1). Track 6 has a total digit divarication of 40°. Digital pad impressions (tracks 32 and 45) and claw marks on digit III (tracks 6 and 32) are preserved (Figs. 5.4, 5.5A).

Morphotype II

Morphotype II consists of at least nine tracks, primarily preserved as true tracks (tracks 3, 8, 13, 18, 21, 22, 25, 42, 44; Figs. 5.4, 5.5A; Appendix Fig. C.1). Relative to the other ichnites at Tsikoane, Morphotype II tracks have relatively gracile digits and a wide apparent total digit divarication (average II^IV of 55˚; Table 5.2). The tracks have variable TLs (ranging between 21.3 and 41 cm; Appendix Table C.1), are slightly elongate (mean TL/TW of 1.31; Table 5.2), have an intermediate mesaxony (average Dp/TS of 0.48; Table 5.2), and subequal II^III and III^IV (excluding track 3, II^III and III^IV are within 6˚ of each other). Claw marks are preserved on almost all the tracks, excluding track 18, and digital pad impressions are preserved on digit II of track 42 (Figs. 5.4, 5.5A; Appendix Fig. C.1). The lengths of digit II and III, relative to medial digit III, are subequal (mean LII/LIII of 0.9 and mean LIV/LIII of 1.0; Appendix Table C.1).

Morphotype III

Morphotype III tracks are the most abundant morphotype at Tsikoane, primarily preserved as convex hyporelief, natural casts on the ceilings of overhangs (tracks 5, 33, 35, 36, 37, 38, 43, 46, 47, 49, 50, 51; Fig. 5.5; Appendix Fig. 1; Appendix Table C.1). The tracks are large (TL >25 cm) and slightly elongate, with an average TL/TW of 1.35. The mean Dp/TS of 0.5 and Dp/TL of 0.37 for Morphotype III are comparable to Morphotype II (Table 5.2), but the relatively more robust digits and smaller total digit divarication of Morphotype III tracks (average II^III of 47˚) distinguish them from Morphotype II. Digit II and IV lengths, measured from track 5, are subequal (1:1.1; Appendix Table C.1). The tracks are preserved as either distinct, individual digit impressions or have a merged posterior region (Fig. 5.5; Appendix Fig C.1). Claw marks and digital pad impressions are preserved for all the tracks. Because track 49 is overprinted and obscured by track 48, its measurements are considered as tentative.

Morphotype IV

Morphotype IV is represented by a single track on the fallen block (track 15; Fig. 5.4). Its very robust anterior digits and pronounced, bulbous, tulip-shaped posterior end distinguish it from the other

Tsikoane ichnites. The track is large (TL of 34.9 cm), elongate (TL/TW of 1.46), has higher-intermediate mesaxony (Dp/TS of 0.56) and a total digit divarication of 54˚ (Table 5.2; Appendix Table C.1). Claw traces are preserved on digits III and IV. The track morphology is obscured by some infilling material remaining within the track (Fig. 5.4).

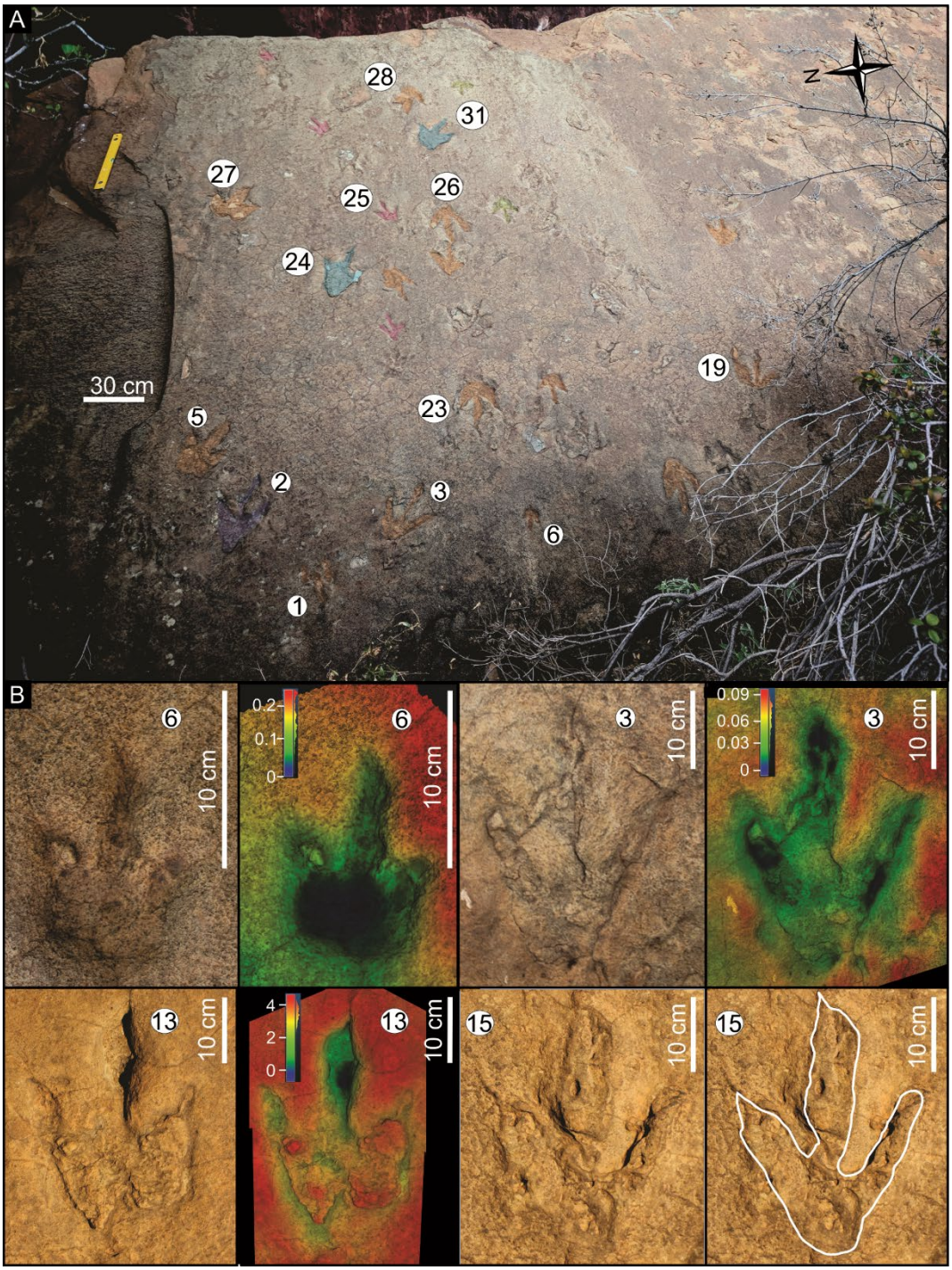

Figure 5.4: True track impressions. A) Overview of the fallen block highlighting potential trackways and measured tracks. B) Individual photographs and false colour depth images (relative scale included) or interpretative outlines of typical Morphotype I (track 6), Morphotype II (track 3 and 13) and morphotype IV (track 15) tracks.

Morphotype V

Morphotype V is represented by a single overhang track (track 34; Fig 5.5A). An elongate, V-shaped tapering proximal feature, resembling a metatarsal impression, distinguishes track 34 from the other Morphotypes at Tsikoane. The digits are merged, with the hypices close to the distal ends of the digits. Digits II and IV appear to be more deeply impressed than digit III with claw marks preserved on two of the three digits.

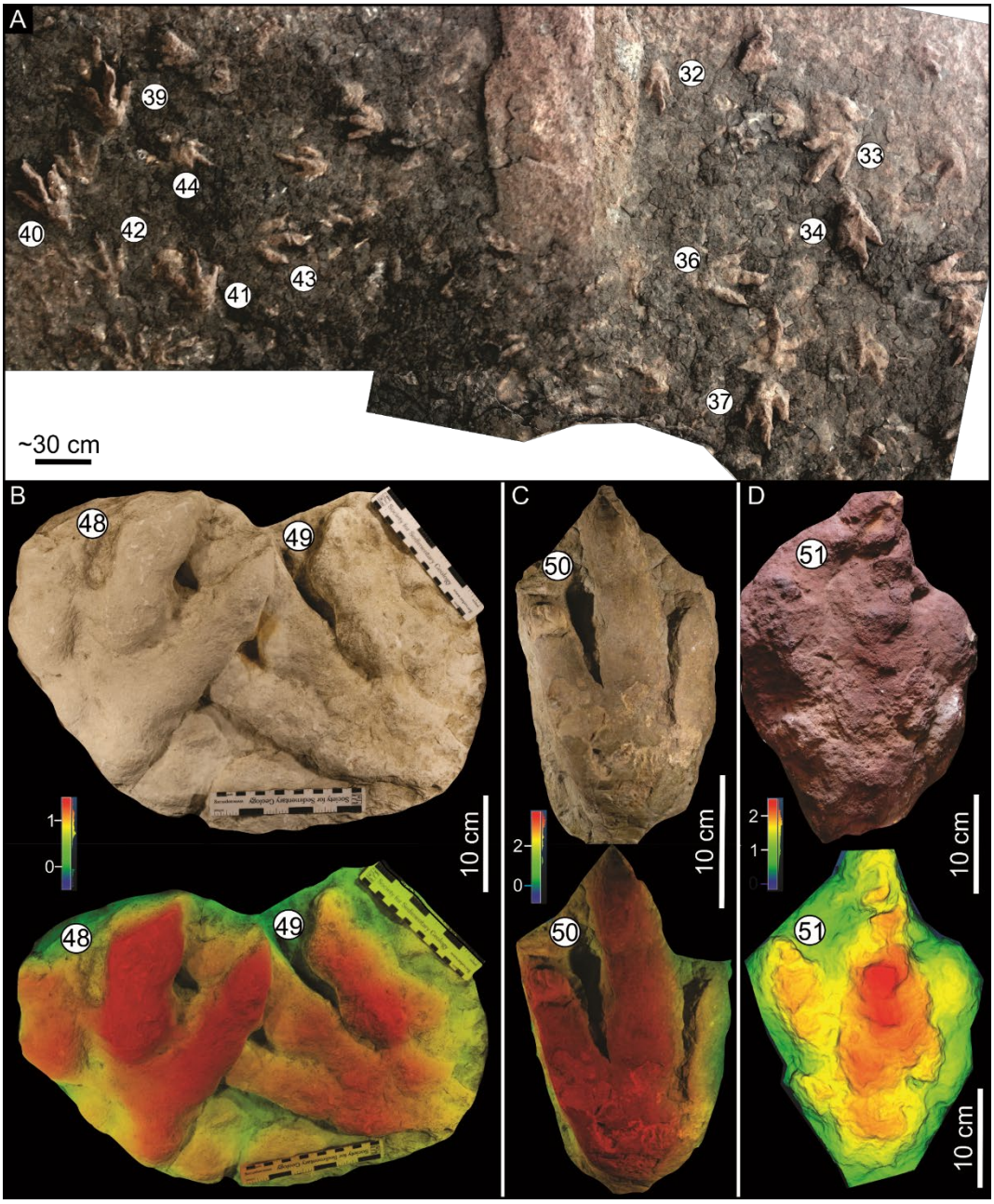

Figure5 .5: Tridactyl tracks preserved as natural casts at the Tsikoane ichnosite. A) Ichnites exposed on the lower bedding plane of a sandstone overhang on the north-western side of the ichnosite. The scale is estimated to be approximately 30 cm; B and B') Tracks 48 and 49 from the Ellenberger Collection cast 270 LES and its false colour depth map (relative scale

included) assigned to Morphotype III. C and C') Track 50 from the Ellenberger Collection unlabelled Tsikoane cast and its false colour depth map (relative scale included) assigned to Morphotype III. D) Natural cast track 51 found ex situ at Tsikoane and its false colour depth map (relative scale included) assigned to Morphotype III.

Cross-sectional, U-shaped structures

In addition to the planar tridactyl tracks, eight cross-sectional, U-shaped structures are also identified in the tabular beds in the lowermost Clarens Formation at Tsikoane (Figs. 5.3H, 5.6). The dimensions of these cross-sectional, U-shaped structures could not be measured directly, because they are exposed in an inaccessible cliff, nonetheless this exposure allows the observation of some key characters (Fig. 5.6). The cross-sectional, U-shaped structures are near vertical, shaft-like bodies that cross-cut the horizontal lamination in the host rocks, distorting them to form 'U's without any mechanical fracturing. The width of the shafts remains reasonably constant with depth, slightly narrowing towards the lower termination of the shafts. The upper terminations of the shafts are U–shaped mounds (bright pink line in Fig. 5.6) that are associated with displacement ridges (dark blue line in Fig. 5.6), and together these result in an irregular bed top surface (Figs. 5.3H, 5.6). The upper parts of the shafts are filled with distinct massive, pale grey sandstone (pink 'natural cast' in Fig. 5.6).

Table 5.2. Summary of the average measured track parameters for Morphotypes I–V at Tsikoane. Morphotype V comprises no measurable tracks, therefore TL and II^IV values are omitted. Abbreviation: N – number of tracks within a given morphotype.

Morphotype	N	TL	TL/TW	Dp/Ts	Dp/TL	II^IV
I	3	13.6	1.81	0.64	0.34	40
Standard Deviation			0.01	0.15	0.07	
II	9	28.6	1.31	0.48	0.37	55
Standard Deviation		8	0.13	0.03	0.04	8
III	11	29.8	1.35	0.50	0.37	47
Standard Deviation		4.39	0.13	0.07	0.06	2
IV	1	34.9	1.46	0.56	0.38	54
Standard Deviation						
V	1		1.58	0.38	0.24	
Standard Deviation						

5.5 Comparative ichnology

5.5.1 Historical ichnology

Tridactyl tracks with morphologies similar to the Tsikoane ichnites are known from other ichnosites in the Clarens Formation of Lesotho such as Qalo and Morija (Dieterlen 1885; Dornan 1908; Ellenberger and Ellenberger 1958; Ellenberger *et al*., 1970; Ellenberger 1970, 1972). Although a detailed description of the Tsikoane ichnosite was not supplied, the Tsikoane tracks have been briefly mentioned in three of the publications by the Ellenberger brothers:

(1) Ellenberger and Ellenberger (1958) mentioned and attributed the Tsikoane tracks, together with those at Qalo and Morija, to bipedal saurischians, maybe theropods;

(2) Ellenberger *et al*. (1970, their Figure 2r) provided one trackway outline from Tsikoane and attributed it to "? Plateosauridé"; and (3) Ellenberger (1970) likened the Tsikoane tracks to those at Morija and assigned them to the ichnotaxa *Kainotrisauropus morijiensis*. It is unclear if the Ellenbergers located the fallen block described by Dornan (1908). It is likely that the Tsikoane tracks ascribed to *Kainotrisauropus morijiensis* are the abundant morphotype III tracks preserved beneath overhangs. The average track ratios and total digit divarications (TL/TW =1.44, Dp/TS=0.55, Dp/TL=0.38 and II^IV = 47˚) from the illustration in Ellenberger *et al*. (1970, their Figure 2r) are comparable to the average Morphotype III dimensions (Table 5.2). Furthermore, the Ellenberger *et al*. (1970) tracks are shown to preserve digital pad impressions and claw marks, which are common features in Morphotype III tracks. As mentioned earlier, in a revision of the southern African vertebrate tracks, Olsen and Galton (1984) synonymised *Kainotrisauropus morijiensis* with *Grallator*.

Figure 5 6 (next page): Interpretive outlines of cross-sectional, U-shaped structures in the lowermost Clarens Formation at Tsikoane. A) Field photograph and B) interpretive outlines of the main features associated with the U-shaped structures. Note the various deformations in the host strata, which are upward-fining, well-bedded, tabular beds (also see Figures 3A, H for context). C) Interpretative outline of a single U-shaped structure (see Discussion for details). Abbreviations: FL – fine laminations.

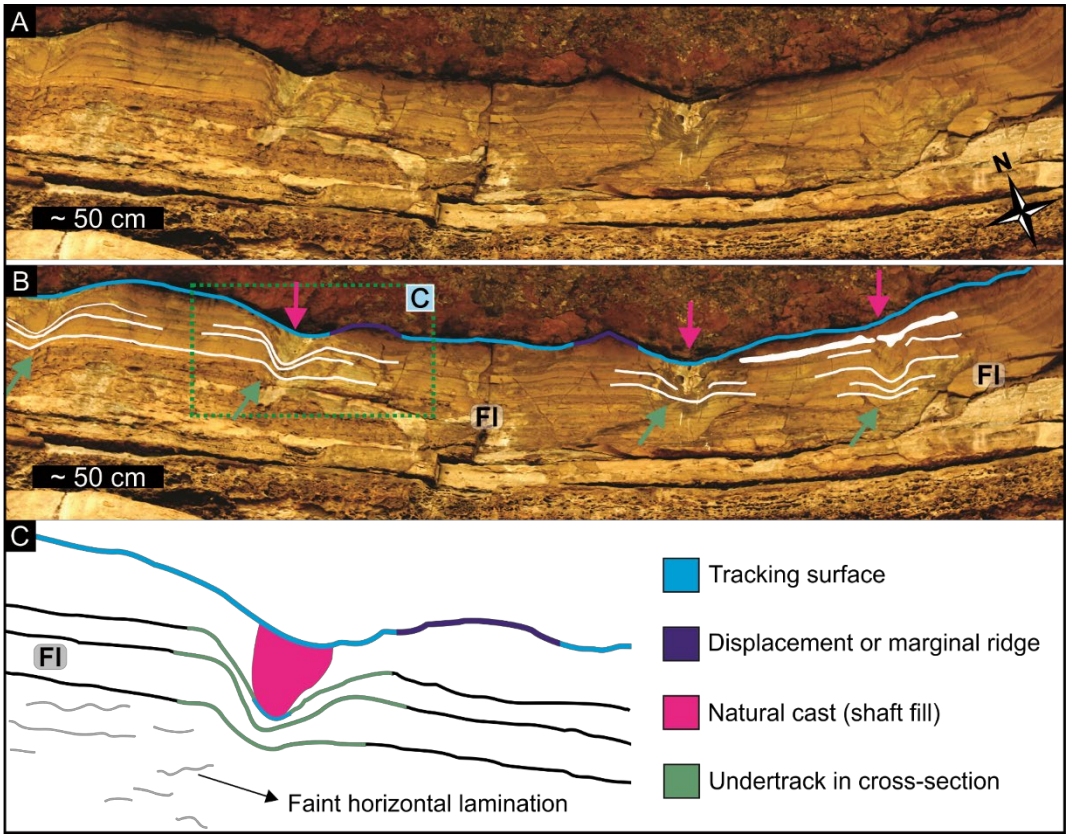

5.5.2 Ichnotaxonomy of the Tsikoane morphotypes

Morphotype I

Morphotype I tracks are elongated (average TL/TW of 1.81) with narrow digits and appear relatively smaller than other tracks at Tsikoane with only a single track, track 6, having a measurable TL of 13.6 cm (Appendix Table C.1). The tracks have intermediate mesaxony (mean Dp/TS of 0.64) and the digit III projection accounts for 34% of the TL (Table 5.2). The lengths of digit II and IV in Track 6 are subequal (1:1.2) and shorter than medial digit III (Appendix Table C.1). The overall morphology and dimensions of Morphotype I tracks are consistent with the ichnogenus *Grallator*, which is defined as a tridactyl track with a TL <15 cm, a high TL/TW ratio >2 and a large digit III anterior projection (Fig. 5.7; Olsen *et al*., 1998). Hyporelief track 6 consistently plots within *Grallator* morphospace when considering ratio dimensions and landmark-based PCA (though the PCA overlaps with *Eubrontes* morphospace, Fig. 5.8), while tracks 32 and 45 plot outside of defined morphospaces or within *Therangospodus* morphospace (Figs. 5.8A, C). The morphology of tracks 32 and 45 are inconsistent with that of *Therangospodus*

pandemicus, which is defined as having fleshy, robust digits and an absence of digital pads (Lockley *et al*., 1998) and has a weaker TL/TW elongation of ~1.3. Tracks 32 and 45 are even more dissimilar to *Therangosposdus oncalensis*, revised to *Igunodontipus oncalensis* by Castanera *et al*. (2013), which has a TL/TW ratio between 1–1.2, a Dp/TS ranging from 0.35 to 0.46, a II^IV between 65˚ and 80˚, and a distinct round to quadrangular posterior pad impression. *Grallator* tracks are known from the Late Triassic (e.g., Gaston *et al*., 2003; Lockley and Gierlinski 2009; Bordy *et al*., 2017), while *Therangospodus* tracks are thought to have appeared in the Late Jurassic. Given the elongation, medial digit projection, gracile features and digital pad impressions of Morphotype I tracks, they are considered to be *Grallator*-like. Although Morphotype I tracks have a smaller elongation and anterior projection relative to *Grallator*, this is commonly observed in *Grallator*-like tracks in southern Africa (Sciscio *et al*., 2016; Abrahams *et al*., 2017; Rampsersadh *et al*., 2018; Abrahams *et al*., 2020).

Morphotype II

Although Morphotype II tracks have variable TLs (from 21.3 to 40 cm; Appendix Table C.1), they consistently have gracile digits, wide total digit divarications (average II^IV of 55˚ with subequal II^III and III^IV) and V-shaped posterior ends (Fig. 5.4; Appendix Fig C.1). Furthermore, the tracks are elongated (mean TL/TW of 1.31) and have an intermediate mesaxony (mean Dp/TS of 0.48; Table 5.2). These features are consistent with *Kayentapus*, which is described as having a TL of 35 cm, a range in Dp/TW between 0.4 and 0.6, with a lily-shaped posterior end (Lockley *et al*., 2011; Fig.5.7) and notably possesses gracile, splayed digits, which distinguish it from contemporaneous ichnogenera like *Eubrontes* (e.g., Welles 1971; Puibelli *et al*., 2005; Lockley 2009; Xing *et al*., 2009; Sciscio *et al*., 2017a). Of the nine Morphotype II tracks, seven plot within *Kayentapus* morphospace with only tracks 18 and 21 consistently plotting as *Kayentapus* (Fig. 5.8). When considering ratio dimensions, tracks that do not plot within *Kayentapus* plot in *Eubrontes* or undefined morphospace (Figs. 5.8A, B). In the landmark-based PCA assessment tracks which do not plot in *Kayentapus* morphospace plot in *Kayentapus-Eubrontes* (tracks 8, 25, 44), *Megalosauripus* (track 22) or undefined morphospaces. In

addition to the morphometrics considered, given the consistently narrow digit widths in Morphotype II, large total digit divarication and lily-shaped posteriors, which are not included in Fig. 8, the tracks are considered to be *Kayentapus*-like. *Kayentapus*, which appears in the Late Triassic, has a global distribution (Lockley *et al*., 2011) and is known from Early Jurassic deposits in southern Africa (Sciscio *et al*., 2017a; Abrahams *et al*., 2020).

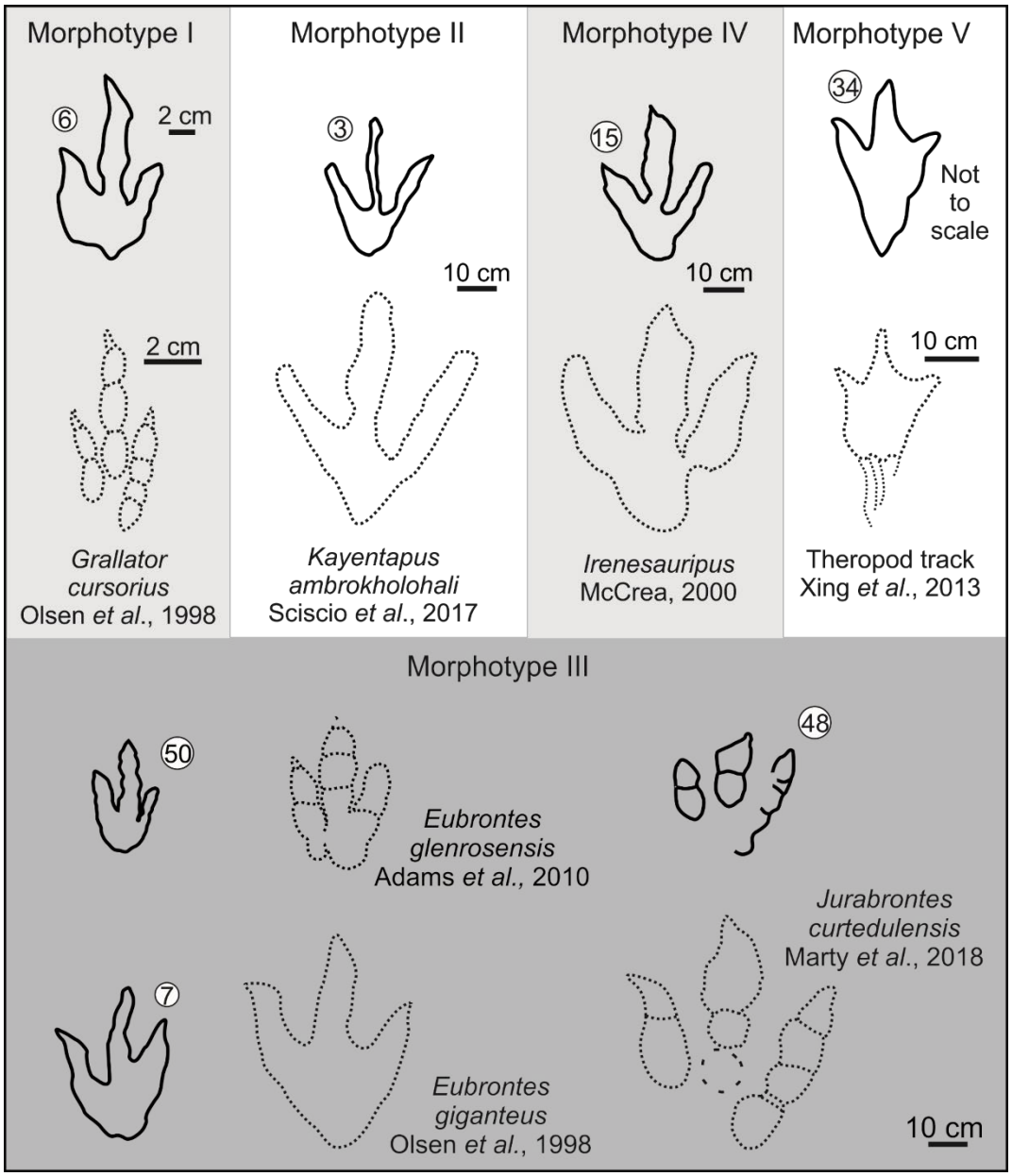

Figure 5.7: Comparative outlines of the ichnite morphotypes observed at Tsikoane and known theropod ichnotaxa.

Morphotype III

Morphotype III tracks are elongated (average TL/TW of 1.35), have an intermediate mesaxony (mean Dp/TS of 0.50; Table 5.2) and robust digits. When a posterior morphology is preserved, it is tulip-shaped. Reliable track measurements could only be obtained from four tracks (tracks 5, 49, 50 and 51; Appendix Table C.1), as all other tracks are preserved on inaccessible, high ceiling overhangs. The measured Morphotype III tracks have an average TL of 29.8 cm and their average TL/TW and Dp/TS ratios (1.35 and 0.50, respectively) are comparable to the Morphotype III overhang tracks (1.31 and 0.48, respectively). The overall morphology and dimensions of Morphotype III tracks appear consistent with the ichnogenus *Eubrontes*, which is defined as having a TL >30 cm, a digit III that projects anteriorly (but not as much as in *Grallator*) and a narrow total digit divarication (Olsen *et al*., 1998; Fig.5. 7). The digits of *Eubrontes* tracks are also relatively robust. However, the large total digit divarication of Morphotype III tracks (average II^IV of 47^{o}) is inconsistent with *Eubrontes*. Of the twelve Morphotype III tracks, nine plot within *Eubrontes* morphospace (Figure 5.8). Tracks 5, 36 and 43 never plot in *Eubrontes* morphospace and plot either in *Kayentapus, Megalosauripus* or undefined morphospace (Fig 5.8C). Tracks 35, 36 and 43 differ from the other Morphotype III tracks as they do not have merged posteriors, which may have affected their measured TLs and the placement of landmark 6. Track 5, a true track, preserves some infilling, which may be obscuring its morphology. Track 37, which plots in the *Grallator* morphospace, is not a gross *Eubrontes* outlier, as *Grallator* and *Eubrontes* are considered to lie on a morphological continuum (Olsen *et al*., 1998). Given these considerations for the outlying tracks, Morphotype III tracks are considered to be *Eubrontes*-like.

Track 48 (which is specimen 270 LES in the Ellenberger Collection) is tentatively assigned to Morphotype III though it possesses characteristics distinct from other tracks in the Morphotype (Fig. 5.5B). Track 48 has a low TL/TW and Dp/TS of 1.14 and 0.23, respectively, and a distinctly long digit IV (28.7 cm compared to its digit III of 17.9 cm and digit II of 14.3 cm, respectively; Appendix Table C.1). These parameters are comparable to the Late Jurassic ichnotaxa *Jurabrontes*, which is defined as large, elongate tracks with small anterior triangle and weak mesaxony and an asymmetrical posterior region

and broad digits (Marty *et al*., 2017; Fig. 5.7). *Jurabrontes* trackway SCR1500-T1 (7 tracks), which comprises the holotype track, has a mean TL/TW of 1.21, mean Dp/TL of 0.38 and mean II^IV of 46˚ with digit lengths IV>III>II. Although track 48 appears to be highly consistent with *Jurabrontes,* given the missing characteristic digital pad arrangement, unknown origin of the track within the ichnosite and the lack of similar tracks found *in situ*, it is not assigned to an ichnogenus.

Morphotype IV

The Morphotype IV track (track 15) has a TL of 34.9 cm (TL/TW of 1.46), Dp/TS of 0.56, Dp/TL of 0.38 and total digit divarication of 54˚ (Fig. 5.4; Table 5.2). It is distinguished from other Tsikoane ichnites by the presence of a distinctly large, bulbous posterior region. Its robust digits and emphasised posterior morphology is reminiscent of the Late Jurassic ichnogenus *Megalosauripus* and Cretaceous ichnogenus *Irenesauripus*. *Megalosauripus* is defined as a large, asymmetrical track (35 cm < TL< 80 cm), with an average TL/TW and II^IV of 1.2 and 70˚, respectively. Furthermore, *Megalosauripus* possesses a sigmoidal digit III and large digit II and IV metatarsal phalangeal pads (Razzolini *et al*., 2017). Morphotype IV is distinct from *Megalosauripus* because its digit III is not sigmoidal, its total divarication is smaller (54˚ vs 70˚) and it is more elongate (TL/TW of 1.46 vs 1.2). *Irenesauripus* is defined as large (~28 – ~41 cm; Sternberg 1932), with well-separated digits (total digit divarication of 70˚; Sternberg 1932) and a digit I that is rarely impressed (McCrea 2000; Fig. 5.7). *Irenesauripus* may preserve digital pad and claw mark impressions (McCrea 2000). Morphotype IV is distinct from *Irenesauripus* because it possesses a tulip rather than lily-shaped posterior and has a significantly smaller total digit divarication. When considering linear dimension ratios and landmark-based PCA assessments, track 15 plots within defined *Eubrontes* morphospace, distinct from *Megalosauripus* and *Irenesauripus* (Figs. 5.8A, C). Given the comparable dimensions of track 15 to Morphotype III, its U-shaped posterior and the morphometric analyses, track 15 is considered to be *Eubrontes*-like.

Figure 5.8 (following page): Statistical analysis of Tsikoane Morphotypes and known ichnogenera. A) Bivariate plot comparing track elongation and the anterior projection triangle of Tsikoane Morphotypes I-V, modified after Castanera et al,. 2016. B) Bivariate biplot comparing the anterior and prosterior projections of Tsikoane Morphotypes I-V, modified after Sciscio et al. 2017a. C) Landmark-based PCA comparing Morphotypes I-V. Biplot schematics illustrate the loadings of the six landmarks considered. Geometric morphometrics utilises tracks of varying anatomical fidelity and needs to be considered in

conjunction, and subsidiary, to the bivariate plots. Morphotype III tracks have highest anatomical fidelity and consistently preserve digital pad impressions and claw mark impressions.

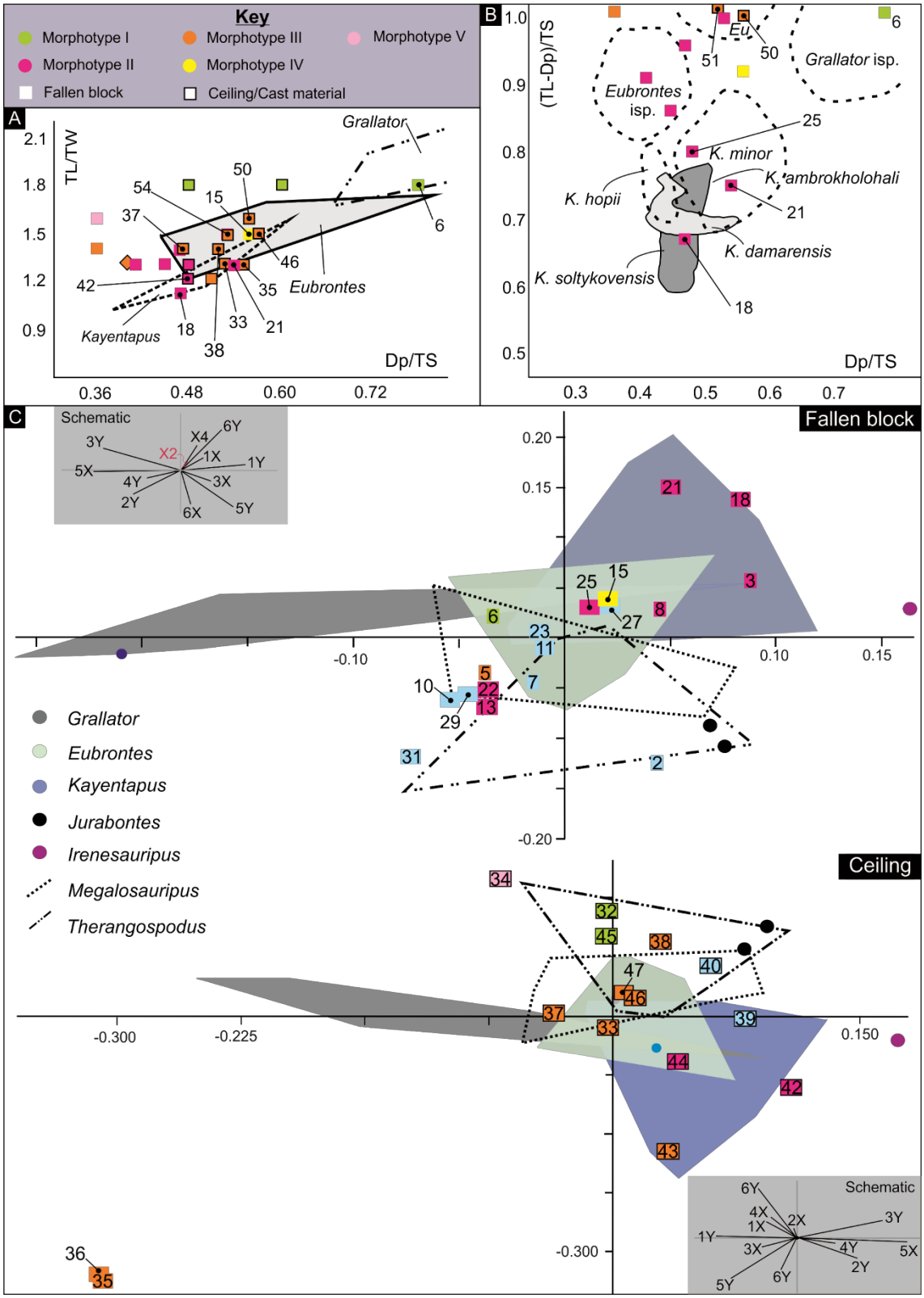

Morphotype V

Morphotype V is represented by a single track with a Dp/Ts of 0.38 and a Dp/TL of 0.24 (Fig. 5.5A; Table 5.2). The digits are merged and indistinct from one another, except near the digit tips, which are V-shaped and occasionally preserve claw marks. Morphotype V is distinguished from other tracks by the presence of an elongate, V-shaped proximal feature, possibly a metatarsal impression (e.g., Gatesy *et al*., 1999; Xing *et al*., 2013; Romano and Citton 2017; Rampersadh *et al*., 2018). Because of the lack of measurable parameters, Morphotype V does not plot in any defined ichnogenus morphospace (Figs. 5.8A, C) and cannot confidently be assigned to any ichnogenus though its morphology is similar to tracks that have been attributed to theropods (e.g., Xing *et al*., 2013; Fig. 5.7) and may be a morphological variation of *Eubrontes.*

5.6 Discussion

5.6.1 Cross-sectional, U-shaped structures

Differentiating between biogenic cross-sectional and non-biogenic, soft-sediment deformation structures (BCSS and SSDS, respectively) is important because in certain stratigraphic units BCSS may be the only evidence of past animal activity. Criteria to distinguish between SSDS and BCSS related to vertebrate tracks have recently been developed (e.g., Manning 2004; Jackson *et al*., 2009; Jackson *et al*., 2010; Melchor 2015). Based on these, BCSS are more discrete and isolated in nature relative to the usually more continuous SSDS, such as load casts and convolute bedding, and tend to have a restricted size distribution. Furthermore, chaotic (isotropic) deformation of associated horizontal layers is expected for SSDS, whereas the deformation associated with BCSS is almost exclusively downward, hence deformation associated with BCSS is anisotropic (Loope 1986; Melchor 2015). The infilling sediment of BCSS may have a different composition to the deformed layers, which is not expected in SSDS. For these reasons, the U-shaped structures at Tsikoane are considered biogenic. The deformation of the underlying layers and the displacement rims associated with the Tsikoane BCSS (Fig 5.6) support their interpretation as vertebrate tracks rather than burrow shafts (e.g., Melchor 2015; Bordy *et al*., 2019). Additionally, field relations show that the south-eastward

correlative of the bedding plane, against which the U-shaped structures terminate (Fig 5.6), is a prominent track-bearing surface exposed in the ceiling of an overhang. This further supports the interpretation of the U-shaped structures as cross-sectional tracks.

Cross-sectional tracks can elucidate properties and the deformation history of the track-bearing substrate (e.g., Allen, 1997; Jackson *et al*., 2009; Jackson *et al*., 2010; Avanzini *et al*., 2012; Melchor 2015; Díaz-Martínez *et al*., 2018). The well-bedded, lowermost Clarens strata at Tsikoane were plastically (i.e., without fracturing) deformed indicating that at the time of track registration the sediment layers were soft to moderately stiff. The absence of desiccation cracks associated with the cross-sectional tracks would suggest that these tracks were most likely made in a portion of the substrate that was wetter for longer periods of time (i.e., the tracks may have formed over slightly deeper lake sediments that could hold moisture for longer) relative to that portion of the track-bearing surface where deformation is absent but desiccation is present (i.e., to the south-east, where likely shallower lake sediments were deposited).

5.6.2 Trackmaker identification

A recent statistical study based on *Kayentapus-Grallator-Anchisauripus-Eubrontes* (k-GAE) from the Newark Basin, North America, suggests that at least three, distinct trackmakers are responsible for the ichnogenera (Farlow 2018). The study proposes that *Kayentapus,* small *Grallator-Anchisauripus,* and large *Anchisauripus-Eubrontes* are attributed to different trackmakers, which are generally assumed to be theropods. However, the identity of the *Eubrontes* trackmaker is disputed with the majority of authors supporting a theropod trackmaker (e.g., Lull 1953; Baird 1957; Olsen 1980; Olsen *et al*., 1998; Lockley 1991; Farlow 2018), and only a small minority giving support to a sauropodomorph trackmaker (e.g., von Huene 1932; Bock 1952; Miller *et al*., 1989; Weems 1992, 2003, 2019).

Though there are some features congruent between *Eubrontes* and theropod autopodia, very few authors provide evidence for attributing *Eubrontes* to a theropod other than the tracks being elongate, asymmetric tridactyl impressions that commonly preserve claw marks. Additional support for a theropod trackmaker includes the length of medial digit (> digits II and IV), the degree of digit III's

anterior projection, and the relatively short length of the claw marks of *Eubrontes* impressions (Farlow 2018). Furthermore, the relative digit length ratios (III/IV, III/II) of GAE from the Newark Supergroup were considered comparable to known theropod body fossil ratios (Olsen *et al*., 1998) but recent re-evaluation of the material suggests a degree of ambiguity for the digit III/IV ratio (Farlow 2018). Some authors (e.g., Lucas *et al*., 2006) consider the Early Jurassic, gracile *Kayentapus*, which is unanimously attributed to a theropod (e.g., Weems 2006; Lockley *et al*., 2011; Farlow 2018), to be a synonymous ichnotaxa of *Eubrontes*. Consequently, *Eubrontes* may be attributed to a theropod. Both Olsen *et al*., (1998) and Farlow (2018) noted an overall similarity of *Eubrontes* with prosauropod and ornithischian feet, highlighting the convergence of footprint morphologies. The bipedal, tridactyl nature of *Eubrontes* leans towards a theropod trackmaker but does not exclude sauropodomorphs. Basal sauropodomorphs, like *Plateosaurus* and *Massospondylus*, were habitual bipeds (e.g., Weems 2003, 2019; Reisz *et al*., 2005; Bonnan and Senter 2007; Mallison 2010a, 2010b, 2011; Yates *et al*., 2010; Chapelle *et al*., 2019) and could plausibly be functionally tridactyl, at least during walking locomotory styles (e.g., Cooper 1981; Weems 2003; Mallison 2010b). Furthermore, authors argue that the robust nature of *Eubrontes* digits is support for a sauropodomorph trackmaker. However, when considering the soft tissue surrounding the digits, *Eubrontes* digit widths are within the range for theropods (Farlow 2018).

Although the identity of the *Eubrontes* trackmaker is not consensual, with the current arguments (see Farlow 2018 and Weems 2019 for details), we support a theropod trackmaker interpretation. Therefore, the *Grallator*-like, *Eubrontes*-like and *Kayentapus*-like tracks at the Tsikoane ichnosite represent a high theropod activity that occurred within an ephemeral lake environment in the Early Jurassic of southern Africa. Similar ichnological and facies assemblages are common globally in fluvial to lacustrine settings and have been defined as the *Grallator* ichnofacies (Lockley *et al*., 1994; Lucas and Hunt 2007).

Globally, there are numerous ichnosites that, like Tsikoane, are dramatically skewed towards interpreted carnivorous, theropod trackmakers relative to herbivorous, sauropod and ornithischian

trackmakers (e.g., Farlow 1987; Petti *et al*., 2008; Lockley and Gielrinski, 2009; Belvedere *et al*., 2010; Moreno *et al*., 2012; Lang *et al*., 2013; Lockley *et al*., 2013; Pérez-Lorente, 2015; D'Orazi Porchetti *et al*., 2016; Abrahams *et al*., 2017; Sciscio *et al*., 2017b; Rampersadh *et al*., 2018; Xing *et al*., 2020). This sample-biased carnivore–herbivore ratio is inconsistent with modern, terrestrial ecosystems, which is assumed to be applicable for dinosaur communities too (Moreno *et al*., 2012; Hatton *et al*., 2015). This discrepancy could reflect higher carnivore activity levels (Leonardi 1989; Farlow 2001) or the dominance of arid – semi-arid climatic conditions resulting in predators staking out waterbodies that attract prey (i.e., palaeoclimatic and palaeoenvironmental constraints). These wetter stream or lacustrine environments that were potentially preferentially exploited by predators are also characterised by sediments that have a higher track preservation potential (Behrensmeyer *et al*., 1992). An alternative ecological argument for the high density of *Eubrontes* tracks offered by those authors who support a prosauropod trackmaker interpretation suggests that the locally high abundance of *Eubrontes* is linked to the potential gregarious behaviour of these ancient herbivores, which could have been similar to herding in modern of grazers and some browsers. However, *Eubrontes* tracks are often randomly orientated and do not commonly preserve parallel trackways which would be expected in a herd.

While the track record at Tsikoane and other ichnosites of the upper Stormberg Group in southern Africa illustrates a diverse theropod record (e.g., Dieterlen 1885; Ellenberger 1970; Raath and Yates 2005; Ambrose 2006; Smith *et al*., 2009; Sciscio *et al*., 2016; Abrahams *et al*., 2017; Sciscio *et al*., 2017a; Rampersadh *et al*., 2018; Abrahams *et al*., in review), osteological remains of theropods, primarily fragmentary cranial material, are known for only two potential trackmakers: *Dracovenator regenti* (Yates 2005) and *Megapnosaurus rhodesiensis* (previously *Syntarsus rhodesiensis* and *Coelophysis rhodesiensis*; Kitching and Raath 1984; Smith and Kitching 1997; Munyikwa and Raath 1999; Bristowe and Raath 2004) and are limited to the upper Elliot and Clarens Formations and their counterparts outside of the main Karoo basin (see Bordy *et al*., 2020b for a review). This contrast in the abundance and diversity between the ichnological and osteological records in the upper

Stormberg Group suggests that the Early Jurassic theropod diversity was much higher in southern Gondwana.

5.7 Conclusion

The tridactyl tracks at the Tsikoane ichnosite are preserved on three palaeosurfaces that are exposed on lower bedding planes in overhangs, on a fallen sandstone block and in cross-sectional views. These ichnites are preserved as natural casts, true tracks and undertracks, with all three preservation styles observable in the tracks in cross-section. The Tsikoane tracks preserved in cross-section are the first of their kind to be described from southern Africa and are associated with ephemeral lacustrine deposits in the lowermost Clarens Formation. Although they present no anatomical detail, the associated deeply penetrating deformation structures suggest that the substrate beneath the surface had a high moisture content at the time of track emplacement. The natural casts and true tracks found in the ceiling of the overhangs and on the fallen sandstone block show a range of anatomical fidelity, with the natural casts abundantly preserving morphological details such as claw impressions and digital pad impressions. To preserve this level of autopod detail, these tracks had to be emplaced in a firmer substrate relative to the cross-sectional tracks. Historical ichnotaxonomic assignment, namely *Kainotrisauropus morijiensis*, subsequently synonymized with *Grallator*, only refers to the tracks (Morphotype III in this study) commonly observed on the ceiling of the overhangs. Our evaluation of the tridactyl ichnites at Tsikoane reveals a total of five ichnite Morphotypes, which are considered to be similar to *Grallator*-like*, Eubrontes*-like and *Kayentapus*-like, representing at least as many theropod species. This ichnoassemblage contrasts with the upper Stormberg Group skeletal record that is represented by only two theropod taxa. Therefore, this study confirms the existence of diverse theropod fauna during Early Jurassic times in southern Africa.

Acknowledgements

We acknowledge Robert A. Muir for locating the fallen block during one of the many field visits to Tsikoane, curator Suzanne Jiquel for access to the Ellenberger Collection at the Université de Montpellier (France), Riyaad Mukaddam for taking photographs of the Ellenberger Collection and Akhil Rampersadh and Howard Head for field assistance. We also thank Emmanuel Fara and Matteo Belvedere for their constructive comments on an

earlier version of this manuscript. We also thank reviewers Peter L Falkingham and Ignacio Díaz-Martínez as reviewers, and Gareth Dyke as chief editor for meaningfully contributing with their insightful comments to the overall quality of this study. Opinions expressed and conclusions reached are those of the authors and are not necessarily to be attributed to the CoE in Palaeosciences or NRF or anybody else.

Disclosure statement

The authors receive no financial benefit from this research.

Funding

The research component of this project was supported from the following research grants obtained by EB as principal investigator: DST-NRF Centre of Excellence in Palaeosciences [CoE PAL 2015]; National Research Foundation (NRF) of South Africa Competitive Programme for Rated Researches (CPRR) and African Origins Programme (AOP) [93544, 113394, 98825]; FK is supported by the research project CGL2017-89123-P funded by ERDF/Spanish Ministry of Science and Innovation-State Research Agency. He is a member of the reference research group E04_20R FOCONTUR, co-founded by the Government of Aragon and the ERDFF; During the study MA was a recipient of postgraduate funding from the DST-NRF Centre of Excellence in Palaeosciences (CoE in Palaeosciences).

Appendix materials

Appendix data for the Tsikoane project are available on Figshare: 10.6084/m9.figshare.12417263 The data include Appendix Table 5.1 and text Tables 5.1–5.2 in a single MS Excel file, photogrammetric models (including their component photographs), the high-resolution version of the in-text figures (TIF) and Appendix Figure C.1 (TIF).

References:

Abrahams M, Bordy EM, Sciscio L, Knoll F. 2017. Scampering, trotting, walking tridactyl bipedal dinosaurs in southern Africa: ichnological account of a Lower Jurassic palaeosurface (upper Elliot Formation, Roma Valley) in Lesotho. *Historical Biol.* 29(7):958–975. doi:10.1080/08912963.2016.1267164.

Abrahams M, Sciscio L, Reid M, Haupt T, Bordy EM. 2020. Large tridactyl dinosaur tracks from the Early Jurassic of southern Gondwana – uppermost Elliot Formation, Upper Moyeni, Lesotho. *Ann Soc Geol Pol.* 89. doi:10.14241/asgp.2020.07.

Adams TL, Stragnac C, Polcyn MJ, Jacobs LL. 2010. High resolution three dimensional laser-scanning of the type specimen of *Eubrontes (?) glenrosensis* Shuler, 1935, from the Comanchean (Lower Cretaceous) of Texas: implications for digital archiving and preservation. *Palaeontol Electron*. 13(3):1–11.

Allen JR. 1997. Subfossil vertebrate tracks and indenter mechanics. *J Geol Soc*. 146(4):600–602. doi:10.1144/gsjgs.146.4.0600.

Ambrose D. 2003. A note on fossil trackways at Roma. Roma: House 9 Publications; p. iv+ 14. Lesotho Miscellaneous Documents No. 4

Ambrose D. 2016. A note on Paul Ellenberger and a checklist of Lesotho Fossil Footprint sites. Roma: House 9 publications; p. 50. Lesotho miscellaneous Documents No. 42.

Anketell JM, Cegla J, Dzulynski S. 1970. On the deformational structures in systems with reversed density gradients. *Ann De La Soicètè Geol De Pol*. 40:3–30.

Avanzini M, Piñuela L, García-Ramos JC. 2012. Late Jurassic footprints reveal walking kinematics of theropod dinosaurs. *Lethaia*. 45(2):238–252. doi:10.1111/j.1502-3931.2011.00276.x.

Baird D. 1957. Triassic footprint faunules from Milford, New Jersey. *Bull of the Mus of Comparative Zool.* 117:449–520.

Bamford MK. 2004. Diversity of the Woody Vegetation of Gondwanan southern Africa. *Gondwana Res.* 7(1):153–164. doi:10.1016/S1342-937X(05)70314-2.

Baron MG, Norman DB, Barret PM. 2017. A new hypothesis of dinosaur relationships and early dinosaur evolution. *Nature*. 543(7646):501–513. doi:10.1038/nature21700.

Behrensmeyer AK, Damuth JD, DiMichele WA, Potts R, H-D S, Wing SL. 1992. Terrestrial ecosystems through time: evolutionary palaeoecology of terrestrial plants and animals. The university of Chicago Press; Chicago, p. 588.

Belvedere M, Farlow JO. 2016. A numerical scale for quantifying the quality of preservation of vertebrate tracks. In: Falkingham PL, Marty D, Richter A, editors. Dinosaur tracks: the next steps. Bloomington (Indiana): Indiana University Press; p. 93–98.

Belvedere M, Mietto P, Ishigaki S. 2010. A Late Jurassic diverse ichnocoenosis from the siliciclastic Iouridene Formation (Central High Atlas, Morocco). *Geol Q*. 54(3):367–380.

Beukes NJ 1970. Stratigraphy and sedimentology of the Cave Sandstone stage, Karoo System. In: Proceedings 2nd IUGS Symposium on Gondwana Stratigraphy and Palaeontology, Pretoria, CSIR. p. 321–341.

Bock W. 1952. Triassic reptilian tracks and trends of locomotive evolution. *J Pal*. 26:395–453.

Bonnan MF, Senter P. 2007. Were the basal sauropodomorphs dinosaurs *Plateosaurus* and *Massospondylus* habitual quadrupeds? *Spec Pap Pal*. 77:139–155.

Bordy EM. 2008. Enigmatic trace fossils from the Lower Jurassic Clarens Formation, southern Africa. *Palaeontol Electron.* 11. 11.3.1.16A. p. 16.

Bordy EM, Abrahams M, Sciscio L. 2017. The Subeng vertebrate tracks: stratigraphy, sedimentology and a digital archive of a historic Upper Triassic palaeosurface (lower Elliot Formation), Leribe, Lesotho (southern Africa). *Boll Soc Paleontol Ital.* 56(2):181–198.

Bordy EM, Abrahams M, Sharman GR, Viglietti PA, Benson RBJ, McPhee BW, Barret PM, Sciscio L, Condon D, Mundil R, et al. 2020. A chronostratigraphic framework for the upper Stormberg Group: implications for the Triassic-Jurassic boundary in southern Africa. *Earth-Sci Rev.* 203:103120. doi:10.1016/j.earscirev.2020.103120.

Bordy EM, Brumby AJ, Catuneanu O, Eriksson PG. 2009. Possible trace fossils of putative termite origin in the Lower Jurassic (Karoo Supergroup) of southern Africa. *S Afr J Sci*. 105:356–362.

Bordy EM, Catuneanu O. 2001. Sedimentology of the Upper Karoo fluvial strata in the Tuli Basin, South Africa. Journal of African Earth Sciences. 33: 605– 629 3-4 doi:10.1016/S0899-5362(01)00090-2

Bordy EM, Catuneanu O. 2002. Sedimentology of the Beaufort-Molteno Karoo fluvial strata in the Tuli Basin, South Africa. *S Afr J Geol*. 105(1):51–66. doi:10.2113/1050051.

Bordy EM, Eriksson P. 2015. Lithostratigraphy of the Elliot Formation (Karoo Supergroup), South Africa. *S Afr J Geol*. 118(3):311–316. doi:10.2113/gssajg.118.3.311.

Bordy EM, Hancox PJ, Rubidge BS. 2004a. Fluvial style variations in the Late Triassic – Early Jurassic Elliot Formation, main Karoo Basin, South Africa. *J Afr Earth Sci.* 38: 383–400

Bordy EM, Hancox PJ, Rubidge BS. 2004b. Basin development during the deposition of the Elliot Formation (Late Triassic - Early Jurassic), Karoo Supergroup, South Africa. *S Afr J Geol,* 107: 395–410 3 107 doi:10.2113/107.3.397

Bordy EM, Hancox PJ, Rubidge BS. 2004. Basin development during the deposition of the Elliot Formation (Late Triassic – early Jurassic), Karoo Supergroup, South Africa. *S Afr J Geol.* 107(3):397–412. doi:10.2113/107.3.397.

Bordy EM, Head HV. 2018. Lithostratigraphy of the Clarens Formation (Stormberg Group, Karoo, Supergroup), South Africa. *S Afr J Geol.* 121 (1):119–130. doi:10.25131/sajg.121.0009.

Bordy EM, Sztanó O, Rampersadh A, Almond J, Choiniere JN. 2019. Vertebrate scratch traces from the middle Triassic Burgersdorp formation of the main Karoo Basin, South Africa: sedimentological and ichnological assessment. *J Afr Earth Sci.* 160:103594. doi:10.1016/j.jafrearsci.2019.103594.

Bristowe A, Raath M. 2004. A juvenile ceolphysoid skull from the Early Jurassic of Zimbabwe and the synonymy of *Coelophysis* and *Syntarsus*. *Palaeontol Afr.* 40:31–41.

Bromley RG. 2001. Tetrapod tracks deeply set in unsuitable substrates: recent musk oxen in fluid earth (East Greenland) and Pleistocene caprines in aeolian sands (Mallorca). *Bull Geol Soc Den*. 48:209–215.

Broom R. 1911. On the dinosaurs of the Stormberg South Africa.

Castanera D, Pascual C, Razzolini NL, Vila B, Barco JL, Canudo JI. 2013. Discriminating between medium-sized tridactyl trackmakers: tracking ornithopod tracks in the base of the Cretaceous (Berriasian, Spain). PlosOne. 8(11):e81830. doi:10.1371/journal.pone.0081830.

Castanera D, Piñuela L, García-Ramos JC. 2016. Grallator theropod tracks from the Late Jurassic of Asturias (Spain): ichnotaxonomic implications. *Span J Pal.* 31(2):283–296.

Chapelle KEJ, Benson RB, Stiegler J, Otero A, Zhao Q, Choiniere JN. 2019. A quantitative method for inferring locomotory shifts in amniotes during ontogeny, its application to dinosaurs and its bearing on the evolution of posture. *Palaeontol.* 63(2):229–242. doi:10.1111/pala.12451.

Cooper MR. 1981. The prosauropod dinosaur *Massospondylus carinatus* Owen from Zimbabwe: its biology, mode of life and phylogenetic significance. Occasional papers Nat Mus and Monum Rhod Series B. 6: 689–840.

D'Orazi Porchetti S, Bernadi M, Cinquegranelli A, dos Santos VF, Marty D, Petti FM, Sa Caetano P, Wagensommer A. 2016. A review of the dinosaur track record from Jurassic and Cretaceous shallow marine carbonate depositional environments. In: Falkingham PL, Marty D, Richter A, editors. Dinosaur tracks- the next steps, Bloomington (Indiana): Indiana University Press; p.380–392

Díaz-Martínez I, Console G, Carlos A, de Valais S, Salgado L. 2018. Vertebrate tracks from the Paso Córdoba fossiliferous site (Anacleto and Allen formations, Upper Cretaceous), Northern Patagonia, Argentina: preservational, environmental and palaeobiological implications. *Cretac Res*. 83:207–220. doi:10.1016/j.cretres.2017.07.008.

Dieterlen H. 1885. Nonyana ea Makhuarane. Leselinyana la Lesotho. 18 (13): 2–3.

Dornan SS. 1908. Notes on the geology of Basutoland. *Geol Mag* (UK). 5(2):57–63. doi:10.1017/S0016756800112877.

Duncan RA, Hooper PR, Rehacek J, Marsh JS, Duncan AR. 1997. The timing and duration of the Karoo igneous event, southern Gondwana. *J of Geophys Res.* 102(B8):18127–18138. doi:10.1029/97JB00972.

Ellenberger F, Ellenberger P. 1958. Principaux types de pistes de Vertébrés dans les couches du Stormberg au Basutoland (Afrique du Sud) (Note préliminaire). [Main types of vertebrate footprints in the Stormberg beds of Basutoland (South Africa). (Preliminary note)]. Compte rendu somm des
séances de la Soc Géol Fr. p. 65–67.

Ellenberger F, Ellenberger P, Ginsburg L. 1970. Les Dinosaures du Trias et du Lias en France et en Afrique du Sud, d'après les pistes qu'ils ont laissèes. [The Triassic and Lias dinosaurs in France and South Africa, according to the tracks they left]. Bull Geol Soc Fr. 7(1):151–159. doi:10.2113/gssgfbull.S7-XII.
1.151.

Ellenberger P 1970. Les niveaux paleontologiquesde premiere appartition des mammiferes primordiaux en Afrique du Sud et leur ichnologie: establissement de zones stratigraphiques detaillees dans le Stormberg du Lesotho (Afrique du Sud)(Trias superieur a Jurassique) [The fossil-bearing strata
associated with the earliest appearance of mammals in South Africa and their ichnology: establishment of detailed stratigraphic zones in the Stormberg of Lesotho (South Africa)(Upper Triassic to Jurassic)]. In:
Haughton SH, editors. Second Gondwanaland Symposium on Gondwana Stratigraphy and Palaeontology: proceedings and papers;Council for Scientific & Industrial Research, Pretoria; p. 343–370.

Ellenberger P. 1972. Contribution à la classification des Pistes de Vertébrés du Trias : Les types du Stormberg d 'Afrique du Sud (I)[Contribution to the classification of Triassic vertebrate trackways: types found in the Stormberg Series of South Africa (I)]. Paleovertebrata. Memoire Extraordinaire. 1972
(Montpellier): p.152.

Eriksson PG. 1981. A palaeoenvironmental analysis of the Clarens Formation in the Natal Drakensberg. *Trans Geol Soc S Afr*. 87:224–237.

Falkingham PL. 2014. Interpreting ecology and behaviour from the vertebrate fossil track record. *J Zoology.* 292(4):222–228. doi:10.1111/jzo.12110.

Falkingham PL, Bates KT, Avanzini M, Bennett M, Bordy EM, Breithaupt BH, Castanera D, Citton P, Díaz-Martínez I, Farlow JO, et al. 2018. A standard protocol for documenting modern and fossil ichnological data. *Palaeontology*. 61(4):469–480. doi:10.1111/pala.12373.

Falkingham PL, Bates KT, Margetts L, Manning PL. 2011. The 'Goldilocks' effect: preservation bias in vertebrate track assemblages. *J R Soc Interface*. 8 (61):1142–1154. doi:10.1098/rsif.2010.0634.

Farlow JO. 1987. A guide to lower cretaceous dinosaur footprints and tracksites of the Paluxy River, Somevell County, Texas. Field trip Guidebook, South Central Section. Waco (Texas): Geological Society of America, Baylor University; p. 50.

Farlow JO. 2001. Acrocanthosaurus and the maker of Comanchean large theropod footprints. In: Tanke DH, Carpenter K, Skrepnick MW, editors. Mesozoic Vertebrate life: new research inspired by the Paleontology of Phillip J. Currie. Bloomington: Indiana University Press; p. 408–427.

Farlow JO. 2018. Noah's ravens: interpreting the makers of tridactyl dinosaur footprints. Life of the Past. Bloomington (Indiana): Indiana University Press; p. 644.

Fornós JJ, Bromley RG, Clemmensen LB, Rodríguez-Perea A. 2002. Tracks and trackways of m*yotragus balearicus bate* (artiodactyla, caprinae) in Pleistocene aeolianites from Mallorca (Balearic Islands, Western Mediterranean). *Palaeogeogr Palaeoclimotol Palaeoecol*. 180(4):277–313. doi:10.1016/S0031-
0182(01)00431-X.

Gaston R, Lockley MG, Lucas S, Hunt A. 2003. Grallator-dominated fossil footprint assemblages and associated enigmatic footprints from the Chinle Group (Upper Triassic), Gateway Area, Colorado. *Ichnos*. 10(2–4):153–163. doi:10.1080/10420940390256258.

Gatesy SM. 2001. Skin impressions of Triassic theropods as records of foot movement. *Bull Mus Comparative Zool.* 156:137–149.

Gatesy SM. 2003. Direct and Indirect track features: what sediment did a dinosaur touch? *Ichnos.* 10(2–4):91–98. doi:10.1080/10420940390255484.

Gatesy SM, Falkingham PL. 2017. Neither bones nor feet: track morphological variation and 'preservation quality'. *J Vertebr Pal.* 37(3):e1314298. doi:10.1080/02724634.2017.1314298.

Gatesy SM, Middleton KM, J enkinsFA, Shubin NH. 1999. Three-dimensional preservation of foot movements in Triassic theropod dinosaurs. *Nature.* 399 (6732):141–144. doi:10.1038/20167.

Hatton IA, McCann KS, Fryxell T, Davies J, Smerlack M, Sinclair ARE, Loreau M. 2015. The predator-prey power law: biomass scaling across terrestrial and aquatic biomes. *Science.* 369(6252):aac6284. doi:10.1126/science.aac6284.

Haughton SH. 1924. The Fauna and stratigraphy of the Stormberg Series. *Ann S Afr Mus.* 8:1–517.

Henderson DM. 2006. Simulated Weathering of dinosaur tracks and the implications for their characterization. *Canadian J Earth Sci*. 43(6):691–704. doi:10.1139/e06-024.

Hunt AP, Lucas SG. 2007. Late Triassic tetrapod tracks of western North America. In: Lucas SG, Spielman JA, editors. Triassic Of the American West (Vol. 40). New Mexico: New Mexico Museum of Natural History and Science Bulletin; p. 215–230.

Jackson SJ, Whyte MA, Romano M. 2009. Laboratory-controlled simulations of dinosaur footprints in sand: a key to understanding vertebrate track formation and preservation. *Palaios.* 24(4):222–238. doi:10.2110/palo.2007.p07-070r.

Jackson SJ, Whyte MA, Romano M. 2010. Range of experimental dinosaur (*hypsilophodon foxii*) footprints due to variation in sand consistency: how wet was the Track? *Ichnos.* 17(3):197–214. doi:10.1080/10420940.2010.510026.

Kitching JW, Raath MA. 1984. Fossils from the Elliot and Clarens Formations (Karoo Sequence) of the northeastern Cape, Orange Free State and Lesotho, and a suggested biozonation based on tetrapods. *Palaeontol Afr*. 25:111–125.

Knoll F. 2002a. Nearly complete skull of *Lesothosaurus* (Dinosauria: ornithischia) from the Upper Elliot Formation (Lower Jurassic: Hettangian) of Lesotho. *J Vertebr Pal.* 22(2):238–243. doi:10.1671/0272-4634(2002)022[0238:NCSOLD]2.0.CO;2.

Knoll F. 2002b. New skull of *Lesothosaurus* (Dinosauria: ornithischia) from the Upper Elliot Formation (Lower Jurassic) of southern Africa. *Geobios.* 35 (5):595–603. doi:10.1016/S0016-6995(02)00072-4.

Knoll F. 2005. The tetrapod of the Upper Elliot and Clarens formations in the main Karoo Basin (South Africa and Lesotho). *Bull Soc Geol Fr*. 1(1):81–91. doi:10.2113/176.1.81.

Knoll F. 2010. A primitive sauropodomorph from the upper Elliot Formation of Lesotho. *Geol Mag*. 147(6):814–829. doi:10.1017/S001675681000018X.

Knoll F, Battail B. 2001. New ornithischian remains from the Upper Elliot Formation (Lower Jurassic) of Lesotho and stratigraphical distribution of southern African fabrosaurids. *Geobios*. 34(4):415–421. doi:10.1016/S0016-6995(01)80005-X.

Läng E, Boudad L, Maio L, Samankoussa E, Tabouelle J, Tong H, Cavin L. 2013.Unbalanced food web in a Late Cretaceous dinosaur assemblage. *Palaeogreogr Palaeoclimatol Palaeoecol*. 381–382:26–32. doi:10.1016/j.palaeo.2013.04.011.

Leonardi G. 1989. Inventory and statistics of the South American dinosaurian ichnofauna and its paleobiological interpretation. In: Gillette DD, Lockley MG, editors. Dinosaur tracks and traces. Cambridge (UK): Cambridge University Press; p. 165–178.

Lockley MG. 1991. Tracking dinosaurs: a new look at an ancient world. New York: Cambridge University Press.

Lockley MG, Hunt AP, Meyer C. 1994. Vertebrate tracks and the ichnofacies concept: implications for the paleoecology and palichnostratigraphy. In: Donovan S, editor. The paleobiology of trace fossils. London: Wiley; p. 241–268.

Lockley MG. 2009. New perspectives on morphological variation morphological variation in tridactyl footprints: clues to widespread convergence in developmental dynamics. *Geol Q*. 53:415–432.

Lockley MG, Gierlinksi GD, Lucas SG. 2011. *Kayentapus* revisited: notes on the type material and the importance of this theropod ichnogenus. In: Sullivan RM, Lucas SG, Spielmann JA, editors. Fossil Record 3 (Vol. 62). Albuquerque: New Mexico Museum of Natural History and Science Bulletin; p. 33–336.

Lockley MG, Gierlinski GD. 2009. A *Grallator*-dominated tracksite from the Chinle Group (Late Triassic), Moab, Utah. *Geol Q*. 53:433–440.

Lockley MG, Li R, Li R, Matsukawa M, Harris JD, Xing L. 2013. A review of the tetrapod record in China, with special reference to type ichnospecies: implications for ichnotaxonomy and paleobiology. *Acta Geol Sinica*. 87(1):1–20. doi:10.1111/1755-6724.12026.

Lockley MG, McCrea RT, Buckley LG. 2015. A review of dinosaur track occurrences from the Morrison Formation in the type area around Dinosaur Ridge. *Palaeogeogr Plaeoclimatol Palaeoecol.* 433:10–19. doi:10.1016/j.palaeo.2015.05.018.

Lockley MG, Meyer CA, Moratalla JJ. 1998. *Therangospodus*: trackway evidence for the widespread distribution of a Late Jurassic Theropod with well-padded feet. *Gaia*. 15:339–353.

Loope DB. 1986. Recognizing and utilizing vertebrate tracks in cross section; Cenozoic hoofprints from Nebraska. *Palaios.* 1(2):141–151. doi:10.2307/ 3514507.

Lucas SG, Klein H, Lockley MG, Spielmann JA, Gierlinski GD, Hunt AP, Tanner LH. 2006. Triassic-Jurassic stratigraphic distribution of the theropod footprint ichnogenus Eubrontes. *N M Mus Nat Hist Sci Bull.* 37:86–93.

Lull RS. 1953. Triassic life of the Connecticut valley. Connecticut state geological and natural history survey bulletin. 81, p. 331.

Mallison, H. 2011. Plateosaurus in 3D: how CAD models and kinetic-dynamic modelling bring an extinct animal to life. In: Klein N, Remes K, Gee CT, Sander PM, editors. Biology of sauropod dinosaurs: understanding the life of giants. Bloomington (Indiana): Indiana University Press; p. 219–236

Mallison H, Wings O. 2014. Photogrammetry in paleontology – a practical guide. *J Pal Tech.* 12:1e31

Mallsion H. 2010a. The digital *Plateosaurus* I: body mass, mass distribution and posture assessed using CAD and CAE on a digitally mounted skeleton. *Palaeontol Electron.* 13:1–26.

Mallsion H. 2010b. The digital *Plateosaurus* II: an assessment of the range of motion of the limbs and vertebral column and of previous reconstructions using a digital skeletal mount. *Acta Pal Polonica.* 55(3):433–458. doi:10.4202/app.2009.0075.

Manning PL. 2004. A new approach to the analysis and interpretation of tracks: examples from the dinosauria. In: McIlroy D, editor. The application of ichnology to palaeoenvironmental and stratigraphic analysis. London: Geological Society, Special Publications; p. 93–123.

Marchetti L. 2019. Can undertracks show higher morphologic quality than surface tracks? Remarks on large amphibian tracks from the Early Permian of France. *J Iber Geol.* 45(2):353–363. doi:10.1007/s41513-018-0080-4.

Marchetti L, Belvedere M, Voigt S, Klein H, Castanera D, Díaz-Martínez I, Marty D, Xing L, Feola S, Melchor RN, et al. 2019. Defining the morphological quality of fossil footprints. Problems and principles of preservation in tetrapod ichnology with examples from the Paleozoic to the present. *Earth- Sci Rev.* 193:109–145. doi:10.1016/j.earscirev.2019.04.008.

Marsh JS, Hooper PR, Rehacek JJ, Duncan RA, Duncan AR. 1997. Stratigraphy and age of Karoo basalts of Lesotho and implications for correlations within the Karoo igneous province. Large Igneous Provinces. *Spec Publ Geol Soc S Afr*. 100:27–67.

Marty D, Belvedere M, Razzolini NL, Lockley MG, Paratte G, Cattin M, Lovis C, Meyer CA. 2017. The tracks of giant theropods (*Jurabrontes curtedulensis* ichnogen. & ichnosp. nov.) from the Late Jurassic of NW Switzerland: palaeoecological & palaeogeographical implications. *Historical Biol*. 30 (7):928–956. doi:10.1080/08912963.2017.1324438.

McCrea RT 2000. Vertebrate palaeoichnology of the Lower Cretaceous (lower Albian) Gates Formation of Alberta [dissertation]. Saskatoon: University of Saskatchewan.

McPhee BW, Bonnan MF, Yates AM, Neveling J, Choiniere JN. 2015. A new basal sauropod from the pre-Toarcian Jurassic of South Africa: evidence of niche-partitioning at the sauropodomorph-sauropod boundary? *Sci Rep.* 5 (1):13224. doi:10.1038/srep13224.

McPhee BW., Bonnan MF, Yates AM, Neveling J, Choiniere JN. 2015b. A new basal sauropod from the pre-Toarcian Jurassic of South Africa: evidence of niche-partitioning at the sauropodomorph–sauropod boundary? *Scientific Rep.* 5: 13224.

Mcphee BW, Bordy EM, Sciscio L, Choiniere JN. 2017. The sauropodomorph (Dinosauria) biostratigraphy of the Elliot Formation of southern Africa: tracking the evolution of Sauropodomorpha across the Triassic-Jurassic boundary. *Acta Pal Polonica*. 62:441–465.

Melchor RN. 2015. Application of vertebrate trace fossils to palaeoenvironmental analysis. *Palaeogeogr Palaeoclimatol Palaeoecol*. 439:79–96. doi:10.1016/j. palaeo.2015.03.028.

Milàn J, Bromley RG. 2006. True tracks, undertracks and eroded tracks experimental work with tetrapod tracks in laboratory and field. *Palaeogeogr Palaeoclimatol Palaeoecol.* 231(3–4):253–264. doi:10.1016/j.palaeo.2004.12.022.

Milàn J, Clemmensen LB, Bonde N. 2004. Vertical sections through dinosaur tracks (Late Triassic lake deposits, East Greenland): undertracks and other subsurface deformation structures revealed. *Lethaia.* 37(3):285–296. doi:10.1080/00241160410002036.

Milàn J, Loope DB. 2007. Preservation and erosion of theropod tracks in eolian deposits: examples from the Middle Jurassic Entrada Sandstone, Utah, USA. *J Geol.* 115(3):375–386. doi:10.1086/512758.

Miller WE, Britt BB, Stadtman KL. 1989. Tridactyl trackways from the Moenave Formation of southwestern Utah. In: Gillette DD, Lockley MG, editors. Dinosaur tracks and traces. Cambridge: Cambridge University Press; p. 209–215.

Moreno K, de Valais S, Blanco N, Tomlinson AJ, Jacay J, Calvo JO. 2012. Large theropod dinosaur footprint associations in western Gondwana: behavioural and palaeogeographic implications. *Acta Pal Polonica*. 57(1):73–83. doi:10.4202/app.2010.0119.

Moulin M, Fluteau F, Courtillot V, Marsh J, Delpech G, Quidelleur X, Gèrard M. 2017. Eruptive history of the Karoo lava flows and their impact on early Jurassic environmental change. *J Geophy Res.* 122(2):738–772. doi:10.1002/ 2016JB013354.

Munyikwa D, Raath MA. 1999. Further material of the ceratosaurian dinosaur *Syntarsus* from the Elliot Formation (Early Jurassic) of South Africa. *Palaeontol Afr*. 35:55–59.

Olsen PE. 1980. Fossil great lakes of the Newark Supergroup. In: Manspeizer W, editor. Field studies of New Jersey geology and guide to field trips, 52nd annual meeting, New York state geological association. Newark: Newark College of Arts and Sciences; p. 352–398.

Olsen PE, Galton PM. 1984. A review of the reptile and amphibian assemblages from the Stormberg Group of southern Africa with special emphasis on the footprints of the age of the Stormberg. *Palaeontol Afr.* 25:87–110.

Olsen PE, Smith JB, McDonald NG. 1998. Type material of the type species of the classic theropod footprint genera *Eubrontes, Anchisauripus*, and *Grallator* (early jurassic, hartford and deerfield basins, Connecticut and Massachusetts, U.S.A.). *J Vertebr Pal*. 18(3):586–601. doi:10.1080/02724634.1998.10011086.

Pérez-Lorente F. 2015. Dinosaur Footprints and Trackways of La Rioja. Bloomington: Indiana University Press; p. 363.

Petti FM, Conti MA, D'Orazi Porchetti S, Morsilli M, Nicosia U, Gianolla P. 2008. A theropod dominated ichnocoensis from Late Hauterivian-Early Barremian of Borgo Celano (Gargano promontory, Apulia, Southern Italy). *Ivista Ital Paleontol Stratigr*. 114:3–17.

Piubelli D, Avanzini M, Mietto P. 2005. The Early Jurassic ichnogenus Kayentapus at Lavini di Marco ichnosite (NE Italy); global distribution and palaeogeographic implications. *Boll Soc Geol Ital*. 124:259–267.

Platt BF, Hasiotis ST. 2006. Newly discovered sauropod dinosaur tracks with skin and foot-pad impressions from the Upper Jurassic Morrison Formation, Bighorn Basin, Wyoming, USA. *Palaios*. 21(3):249–261. doi:10.2110/ palo.2004.p04-69.

Raath MA 1977. The anatomy of the Triassic theropod *Syntarsus rhodesiensis* (Saurischia: Podokesauridae) and a consideration of its biology [dissertation]. Grahamstown: Rhodes University.

Raath MA, Yates AM. 2005. Preliminary report of large theropod dinosaur trackway in Clarens Formation sandstone (Early Jurassic) in the Paul Roux district, northeastern Free State, South Africa. *Palaeontol Afr.* 41:101–104.

Rampersadh A, Bordy EM, Sciscio L, Abrahams M. 2018. Dinosaur behavior in an Early Jurassic palaeoecosystem – uppermost Elliot Formation, Ha Nohana, Lesotho. *Ann Soc Geol Pol.* 88:163–179.

Razzolini NL, Belvedere M, Marty D, Paratte G, Lovis C, Cattin M, Meyer CA. 2017. *Megalosauripus transjuranicus* ichnosp. nov. A new Late Jurassic theropod ichnotaxon from NW Switzerland and implications for tridactyl dinosaur ichnology and ichnotaxomy. *Plos one.* 12, e0180289

Reisz RR, Scott D, Sues HD, Evans C, Raath MA. 2005. Embryos of an Early Jurassic prosauropod dinosaur and their evolutionary significance. *Science.* 309(5735):761–764. doi:10.1126/science.1114942.

Romano M, Citton P. 2017. Crouching theropod at the seaside. Matching footprints with metatarsal impressions and theropod autopods: a morphometric approach. *Geol Mag.* 154(5):946–962. doi:10.1017/S0016756816000546.

Schneider CA, Rasband WS, Eliceiri KW. 2012. NIH Image to ImageJ: 25 years of image analysis. *Nat Methods*. 9(7):671–675. doi:10.1038/nmeth.2089.

Sciscio L, Bordy EM, Abrahams M, Knoll F, McPhee BW. 2017a. The first megatheropod tracks from the Lower Jurassic upper Elliot Formation, Karoo Basin, Lesotho. *Plos one*. 12(10):e0185941. doi:10.1371/journal.pone.0185941.

Sciscio L, Bordy EM, Reid M, Abrahams M. 2016. Sedimentology and ichnology of the Mafube dinosaur track site (Lower Jurassic, eastern Free State, South Africa): a report on footprint preservation and palaeoenvironment. *PeerJ.* 4: e2285. doi:10.7717/peerj.2285.

Sciscio L, Knoll F, Bordy EM, de Kock M, Redelstoff R. 2017b. Digital reconstruction of the mandible of an adult *Lesothosaurus diagnosticus* with insight into the tooth replacement process and diet. *PeerJ*. 5:e3054. doi:10.7717/ peerj.3054.

Smith RM, Kitching J. 1997. Sedimentology and vertebrate taphonomy of the Tritylodon Acme Zone: a reworked palaeosol in the Lower Jurassic Elliot Formation, Karoo Supergroup, South Africa. *Palaeogeography, Palaeoclimatology, Palaeoecology.* 131(1 1-2): 29–50 doi:10.1016/S0031-0182(96)00143-5

Smith RMH, Marsicano CA, Wilson JA. 2009. Sedimentology and Paleoecology of a diverse Early Jurassic Tetrapod tracksite in Lesotho, southern Africa. Palaios. 24(10):672–684. doi:10.2110/palo.2008.p08-115.

Sternberg CM. 1932. Dinosaur tracks from Peace River, British Columbia. *Annu Rep Natl Mus Canada* 1930. 59–85.

Tasch P. 1984. Biostratigraphy and palaeontology of some conchostracan-bearing beds in southern Africa. *Palaeontol Afr*. 25:61–85.

Thulborn T. 1990. Dinosaur Tracks. London: Chapman and Hall.

von Huene F. 1932. Die fossile Reptil-Ordnung Saurischia, ihre Entwicklung und Geschichte. Monogr. Geol. Paläont. 4: i–viii. 1-361.

Weems RE 1992. A re-revaluation of the taxonomy of Newark Supergroup saurischian dinosaur tracks, using extensive statistical data from a recently exposed tracksite near Culpeper, Virginia. In: Sweet PC, editor. Proceedings of the 26th forum on the Geology of Industrial Minerals, 113–127; Charlottesville, Virginia: Publication 119, Virginia Division of Mineral Resources.

Weems RE. 2003. *Plateosaurus* foot structure suggests a single trackmaker for Eubrontes and Gigandipus footprints. In: Letourneau PM, Olsen PE, editors. The Great Valleys of Pangea in Eastern North America, volume 2: sedimentology, Stratigraphy and Paleontology. New York: Columbia Press University; p. 293–313.

Weems RE. 2006. The manus print of *Kayentapus* minor: its bearing on the biomechanics and ichnotaxonomy of early Mesozoic saurischian dinosaurs. In: Harris JD, Lucas SG, Spielman JA, Lockley MG, Milner ARC, Kirkland JJ, editors. The Triassic-Jurassic Terrestrial Transition. Albuquerque: New Mexico Museum of Natural History and Science Bulletin 37; p. 369–378.

Weems RE. 2019. Evidence for Bipedal Prosauropods as the Likely *Eubrontes* Track-Makers. *Ichnos.* 26(3):187–215. doi:10.1080/10420940.2018.1532902.

Welles SP. 1971. Dinosaur footprints from the Kayenta Formation of northern Arizona. *Plateau.* 44:27–38.

Xing L, Dai H, Wei G, Lockley MG, Klein H, Scott Persons W, Wang M, Jing S, Hu H. 2020. The Early Jurassic *Kayentapus* dominated tracks from Chongqing, China. *Historical Biol.* 1–7. doi:10.1080/08912963.2020.1769093

Xing L, Harris JD, Toru S, Masato F, Dong Z. 2009. Discovery of dinosaur footprints from the lower Jurassic Lufeng Formation of Yunnan Province, China and new observations on *Changpeipus*. *Geol Bull China*. 28:16–28.

Xing L, Lockley MG, Zhang J, Milner ARC, Klein H, Li D, Persons WS iv, Ebi J. 2013. A new Early Cretaceous dinosaur track assemblage and the first definite non-avian theropod swim trackway from China. *Chin Sci Bull.* 58 (19):2370–2378. doi:10.1007/s11434-013-5802-6.

Yates A. 2005. A new theropod dinosaur from the Early Jurassic of South Africa and its implications for early evolution of theropods. *Palaeontol Afr*. 41:105–122.

Yates AM, Barret PM. 2010. *Massospondylus carinatus* Owen 1854 (Dinosauria: sauropodomorpha) from the Lower Jurassic of South Africa: proposed conservation of the usage by designation of a neotype. *Palaeontol Afr*. 45:7–10.

Yates AM, Bonnan F, Neveling J, Chinsamy A, Blackbeard MG. 2010. A new transitional sauropodomorph dinosaur from the Early Jurassic of South Africa and the evolution of sauropod feeding and quadrupedalism. *Proc R Soc B*. 277(1682):787–794. doi:10.1098/rspb.2009.1440.

6 Exploratory statistics

Landmark-based geometric morphometrics was performed on the southern African tracks considered in this study as an additional method to refine their ichnotaxonomic assignment. It was found that tracks that placed within known ichnotaxa morphospace, predominantly plotted as either *Grallator*, *Eubrontes* or *Kayentapus* when considering PC1 and PC2 (e.g., Figs. 4.12, 4.25). Many of the tracks plot outside of known morphospace boundaries, which may be due to variation in morphological preservation grade, substrate conditions, etc. During the ichnotaxonomic assignments, it had to be considered that the known ichnogenera morphospaces had been created using higher anatomical fidelity tracks from the literature (e.g., holotypes, lectotypes), while the tracks of this dataset have a range in preservation quality (0–3, Appendix Table A.1). Furthermore, tracks included in this morphological assessment are not limited to true tracks as natural casts are also considered (e.g., Upper Moyeni tracks 35, 36; Appendix Fig. A.3). One should bear in mind that track morphology is the product of complex, interacting processes between a trackmaker and the substrate and may therefore show significant variability (Falkingham, 2014; section 2.2). Given these considerations —preservation quality, preservation type and track morphology controls— the studied southern African tridactyl tracks that do not plot within known ichnotaxa morphospace fields may still belong to the inchnogenera in the K-GAE plexus. The conclusion from this attempt at landmark-based ichnotaxonomy, is that it cannot be used independently from visual assessments and traditional measurements. However, it must be acknowledged that tracks with a morphological preservation grade lower than the recommended 3 (Farlow and Belvedere, 2016 and Marchetti *et al.,* 2019) were used for the land-mark analysis. On higher anatomical fidelity tracks it may prove more useful, especially because the preservation of morphological detail allows for additional landmarks to be placed consistently.

A morphological study utilizing such complex objects is also likely to be riddled with problems that may create “statistical noise”. The following considerations regarding the treatment of the database can attempt to mitigate, but cannot eradicate, these negative signals:

1. Subjective track outlines: Defining the boundaries of a track by outlining it in the field or from a collected digital and physical specimen is subjective. Standardizing the track outlining method has been proposed repeatedly (e.g., Thulborn, 1990; Falkingham, 2016; Belvedere *et al*., 2018; Lallensack, 2019). To reduce outlining subjectivity in this study, track outlines and measurements were performed by a single operator (MA).

2. Lack of trackway data: Trackways are the product of a single trackmaker, and under ideal conditions (i.e., uniform substrate, steady locomotion), the component tracks can be assumed to be a fairly consistent reflection of the true feet. This assumption allows the validation of the track

measurements within a given trackway. The current database predominantly comprises individual tracks, and within-trackway validation of the track measurements cannot be done to remove this uncertainty. However, tracks that have a low anatomical fidelity and possibly do not reflect the autopod morphology have been excluded/or are treated tentatively in this database. For example, some tracks at the Mafube ichnosite have been omitted because there is a strong substrate control on morphology and the tracks are preserved as indistinct "holes" (Sciscio *et al*., 2016).

3. Influence of preservation quality on the quantity of measurable track parameters: Pristinetracks with a high anatomical fidelity allow for the measurement of the maximum number of morphological parameters. While incorporating only high preservation quality tracks allows one to have a robust dataset in terms of the number of measured parameters, it vastly reduces the number of tracks included in the dataset. Conversely, incorporating lower quality tracks increases the number of individual measured parameters. For some statistical representation in this study, only the best tracks (i.e., those that include all measured parameters) are considered to test or remove artifact trends that may be attributed to poorer quality tracks.

The methods used for the various means of statistical exploration are described within each chapter 6 subsection and was performed by myself or the UCT statistical science consultancy (STA-CON) with my assistance. Tracks of this database are viewed through two lenses aimed at commenting on how these southern African tracks vary in time and across the K-GAE spectrum (Olsen *et al*., 1998; Lockley, 2009). The database is subdivided in the following ways, respectively:

1. Tracks are broadly classified by their stratigraphic position: lEF (Late Triassic), uEF (Early Jurassic) and Clarens Formation (or CLAR, Early Jurassic).

2. Tracks are classified by their size class based loosely on the TLs of *Grallator*, *Anchisauripus* and *Eubrontes* defined by Olsen *et al*. (1998): small (TL<15 cm), medium (15< TL <25 cm), large (25< TL <40 cm) and huge (TL >40 cm). Classically, GAE spectrum tracks have primarily been assigned based on their TL (e.g., *Grallator*-like tracks have a TL < 15 cm). However, we acknowledge that smaller tracks may have a morphology or measurements that resemble classically larger ichnotaxa such as *Eubrontes* e.g. Lephoto ichnosite (Appendix Fig. A.1; Appendix Table A.1) and *Minisauripus* (Lockley, 2009).

6.1 Bivariate analyses

6.1.1 Pairwise scatterplots: ungrouped data

Pairwise scatter plots compare the absolute values of two measured parameters and is employed here to illustrate any relationships the variables measured in this study may have e.g., positive (or negative), linear (or exponential) correlation or random. All track data were included (Appendix Table A.1).

There are pervasive positive trends between all linear measurements (Fig. 6.1A): a moderate-strong positive linear relationship between TL and TW; strong positive trend between TW and TS; moderate-poor positive relationship between Dp and TL, TW and TS; positive trends, to different degrees, between all digit lengths; and all digit lengths have positive relationships with TL, TW (TS) and Dp (although the Dp trend is a lot more complex and has variability). The TW and TS relationship is near perfect i.e., 1:1 and it can be concluded that for this dataset TW and TS do not vary significantly and may be considered equivalent measurements. This is not unexpected given how the parameters are measured (Fig. 3.2). Strong correlations between TW and TS were observed in some of the traditional PCAs performed on individual tracksites e.g., Phuthiatsana (Appendix Fig. A.1). The positive relationship between Dp and TL shows an interesting inflection along its gradient suggesting that at a certain TL, the Dp increases at a reduced proportion compared to smaller TLs. Although all digit lengths have a positive relationship, the trend for LII and LIV is the most constrained, proposing that these digits have stronger, positive, linear relationship. This would be expected for GAE tracks which are defined as having subequal length digits II and IV.

Unlike the linear measurements, interdigit angles have a lot of scatter, though interdigit angles II^III and III^IV appear to have a linear relationship. (Fig. 6.1A). When compared to the linear measurements, no true relationship can be discerned though there is an intermediate positive relationship between total digit divarication and TW. This would be expected given how the track parameters are measured (Fig. 3.2). A high degree of interdigital angle variation is commonly observed in the track record (Moratalla *et al*., 1988; Belvedere, 2008; Lallensack *et al*., 2016; Wings *et al.*, 2016). In nature, this variation can be attributed to differences in substrate conditions (Lockley, 2009) and in practice, variability may additionally arise from a difficulty in measuring the angles consistently i.e., it easy to define a midline axis for straight digits but it is subjective for curved digits (Thulborn, 1990). Because of the significant scatter in our data, digit divarication is omitted from most of the analysis presented herein. Furthermore, Moratalla *et al*. (1988) and Lockley (2009) highlighted that interdigital angles are secondary contributors to track morphology that are not particularly informative.

When considering track parameter ratios, several interesting relationships can be observed (Fig. 6.1A). The numerical expression of the degree to which a track is elongate, i.e., the TL/TW ratio, has an exponential negative relationship with the interdigit angles i.e., more elongate tracks have narrower

total digit divarication. This would be expected given how the measurements are taken (Fig. 3.2); if digits II and IV are more splay relative to digit III, the TS and TW would be greater. The Dp/TS and TL/TW ratios are moderately-poorly positively correlated; given that TS = TW this relationship illustrates the positive relationship between Dp and TL.

6.1.2 Correlation matrices

Correlation matrices were generated to statistically quantify the apparent relationships shown in the pairwise scatter plots (Figs. 6.1A, B; Appendix Table A.3). Missing track data was excluded from the matrix (Appendix Table A.1). The non-parametric correlation statistic Spearman rs was applied because the data does not follow a normal distribution (Appendix Table A.4). The correlation matrix indicates that all the linear measurements considered are statistically correlated. Interdigit angles have a significantly weaker probability of being correlated with TL, TW, TS and Dp (Fig. 6.1B; Appendix Table A.3). Interdigit angles are uncorrelated with digit lengths. These matrices are consistent with the apparent relationships observed in the pairwise scatter plots (Figs. 6.1; Appendix Table A.3).

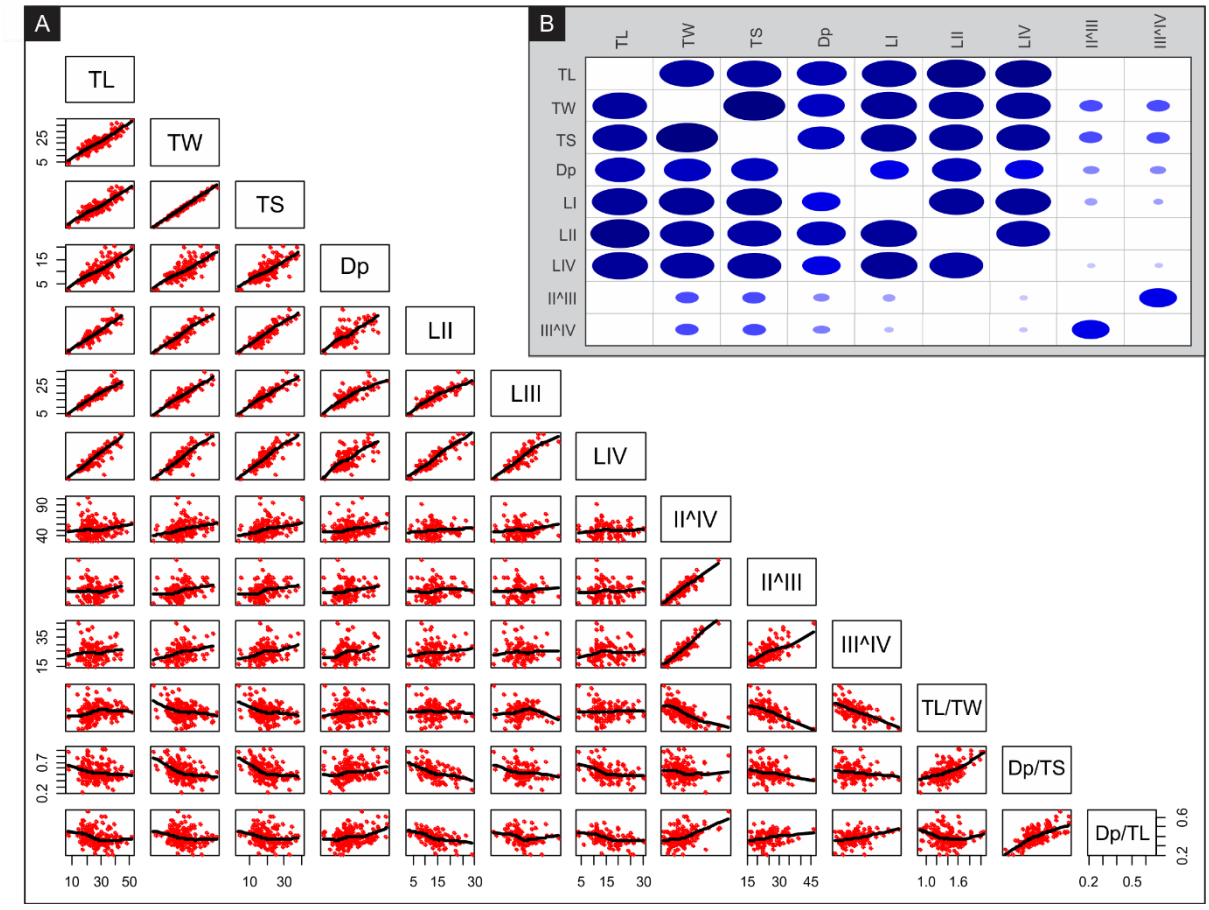

Figure 6.1: Relationships between bivariate analyses: A) Pairwise scatter plots (STA-CON), B) Correlations between parameters with correlation values in the lower triangle of the matrix and two-tailed probabilities that the parameters are uncorrelated in the upper triangle; larger diameters correspond to higher correlation values and lower probabilities (p(uncorr)).

To sum it up, in absolute terms, as TL increases all linear measurements (TW, TS, Dp and Digit Lengths) increase. Interdigit divarication angles (II^IV, II^III, III^IV) do not have a significant relationship with the linear measured parameters; given how the parameters are measured, it is expected that II^IV have a linear correlation with TW and TS. Interdigit angles II^III and III^IV have a possible, weak linear relationship. Considered ratios (TL/TW, Dp/TS and Dp/TL), for the most part, do not have clear relationships with the individual measured parameters. Trends among ratios are observed, e.g., TL/TW vs Dp/TS and Dp/TS vs Dp/TL, suggesting that as tracks become more elongate their mesaxony increases and as mesaxony increases digit III projections accounts for more of the TL.

6.1.3 Pairwise scatterplots: grouped data

Pairwise scatter plots incorporating all data were generated to compare tracks into the stratigraphic and size groupings outlined at the beginning of this chapter (Fig. 6.2; Appendix Table A.1). The groupings are employed herein to check if trends observed in the ungrouped pairwise scatterplots (Fig. 6.1) are also observed within groups. Similar observations to the ungrouped data can be made for the grouped data (Fig. 6.1A). Within each stratigraphic subdivision, TL and TW have a positive relationship (Fig. 6.2). However, the uEF has a lower TW for a given TL when compared to the lEF and CLAR (Fig. 6.2A). Track elongation (i.e., TL/TW) and mesaxony (i.e., Dp/TS) have comparable, positive trends within each stratigraphic unit. The Dp relative to TL has a negative trend with TL for each stratigraphic grouping; this trend is most strongly observed in the CLAR (Fig. 6.2A). Comparing Dp/TW and (TL-Dp)/TW proved successful for Weems (1992) to distinguish between ichnotaxa. This comparison does not allow one to differentiate between the different stratigraphic subdivisions. When considering linear measurements, the uEF has the largest range in values while the lEF is the most constrained.

Given that size classes are based on measured TL, scatter plots considering TL as an axis clearly separates groups (Fig. 6.2B). As with the stratigraphic subdivision, size class groups show a positive relationship between TL and TW. Size groupings cannot be distinguished from one another when considering TL/TW and Dp/TS (Fig. 6.2B). Within in all size groupings, Dp/TL decreases; this decrease has a limited change for tracks within the huge class.

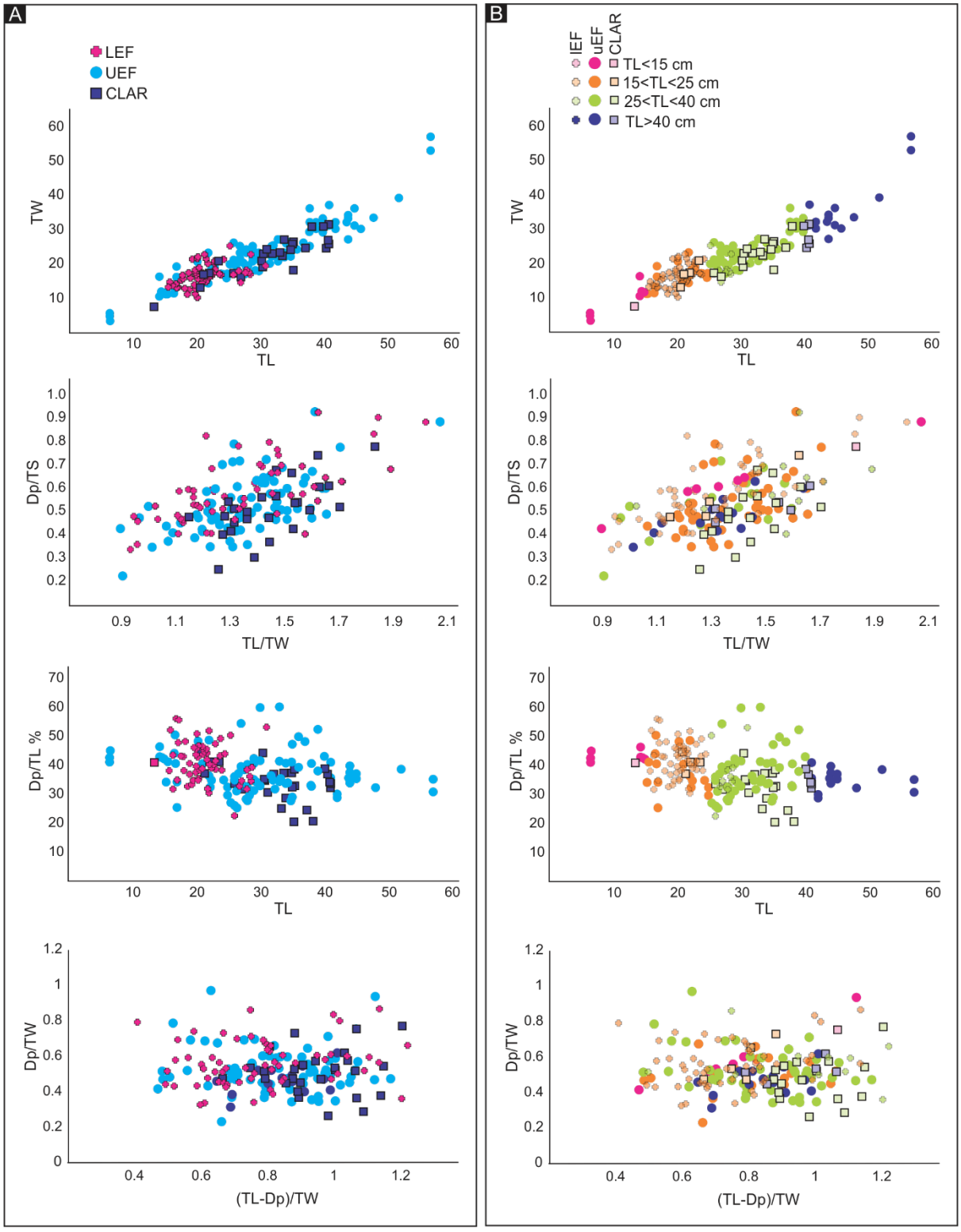

Figure 6.2: Pairwise scatter plots for stratigraphic subdivisions (A) and size class groupings (B) defined in Chapter 6.

6.2 Frequency distributions

Absolute frequency distribution plots were generated using all linear measurements (Appendix Table A.1). Normalised track parameters were considered to visualize and compare the distribution and peaks of the data within stratigraphic or size class groupings (Figs. 6.3, 6.4, respectively). All measurements were log transformed and the mean of each measured parameter was subtracted from the parameter's individual measurements for scaling. Histograms were plotted using PAST v3 with bin sizes automatically calculated and optimized for each parameter.

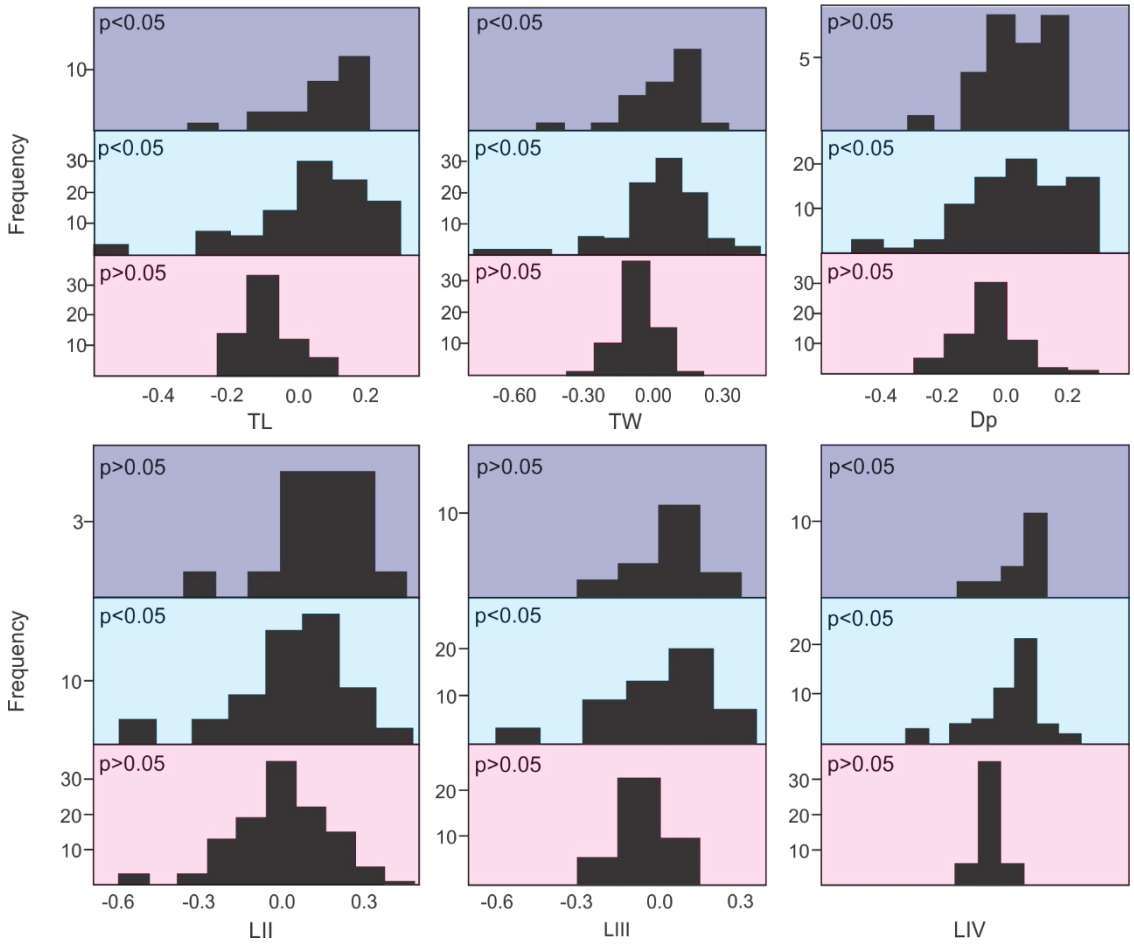

Figure 6.3: Frequency distributions of linear track measurements for lEF (pink), uEF (light blue) and CLAR (dark blue) stratigraphic position groupings. A Shapiro-Wilk probability of normality is included for each distribution (p>0.05 follows a normal distribution; detailed normality test data in Appendix Table A.5).

Tracks from the lEF are characterized by having relatively shorter TL, TW, Dp and digit lengths than tracks from the uEF and CLAR (Fig. 6.3). Excluding LII, the data for lEF is tightly constrained with minimal tailing. Tracks of the uEF show a large spread in data for all measured parameters (Fig. 6.3). Peaks for each parameter are relatively greater than those of lEF and often coincide with CLAR peaks. Frequency distributions cannot distinguish uEF tracks from the other considered stratigraphic positions (Fig. 6.3). The Clarens Formation data has less spread than the uEF, but some parameters

have a lot of tailings (e.g., TL, TW, LII). The peaks of CLAR data are distinct from the lEF, with CLAR tracks having relatively longer TL, TW, Dp and digit lengths. The lEF tracks follow a normal distribution for all measured parameters.

Conclusion: The lEF and CLAR appear distinguishable from one another when considering parameter peaks. Relative to the CLAR, the lEF has distinctly smaller linear measurements i.e., lEF peaks plot primarily negative while CLAR peaks are positive. Kolmogorov-Smirnov tests yield a $p<0.05$ for all parameters considered when comparing the lEF and Clarens Formation indicating that their populations do not have equal distributions. Track parameters from the uEF encompass those of the lEF and CLAR and are indistinguishable from the other stratigraphic units when examining frequency distributions.

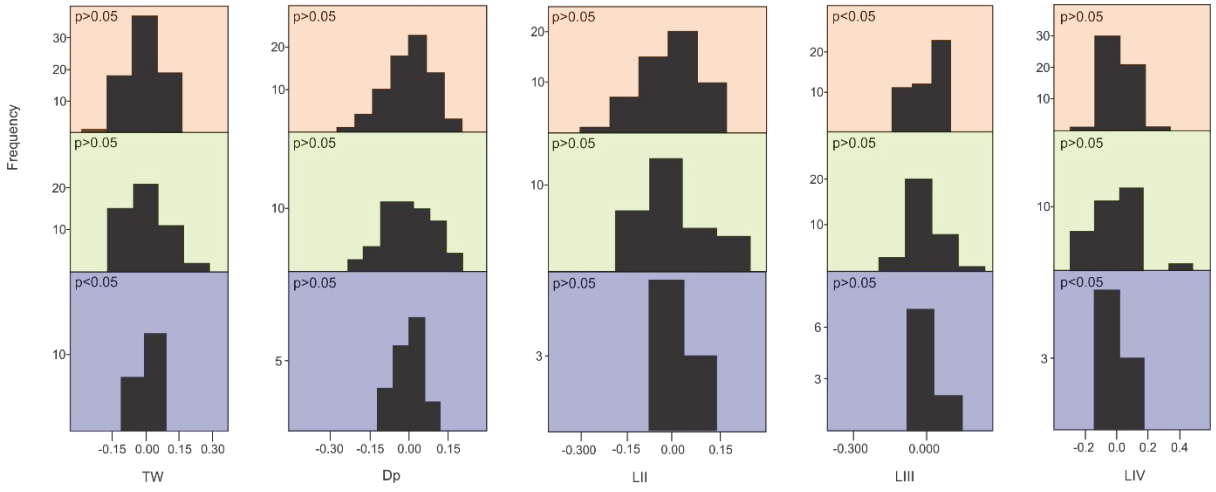

Figure 6.4: Frequency distributions of linear track measurements for "medium" (orange), "large" (green) and "huge" (dark blue) track length class grouping. A Shapiro-Wilk probability of normality is included for each distribution (p>0.05 follows a normal distribution; detailed normality test data in Appendix Table A.6).

Tracks classified as "small" in the track length class grouping were omitted from the frequency distribution analyses because the group comprises too few data points (Fig. 6.4). Track length was not considered as a parameter due to the groupings being based on the TL. When considering TW, Dp and digit lengths, the various TL groupings appear to indistinguishable (Fig. 6.4). Relative to one another, the peaks of each parameter coincide. The distribution patterns of the data are variable. Kolmogorov-Smirnov tests for the medium and large size class groupings, selected because of their bigger sample sizes, yield a $p<0.05$ for all parameters considered indicating that the populations do not have equal distributions. The "huge" track dataset comprises few tracks (max twenty-four tracks) and presents as very homogenous. Given the small sample size, its distribution cannot meaningfully be compared with the "medium" and "large tracks" which consists of a maximum of ~eighty tracks each.

Conclusion: Tracks between different TL groupings cannot be distinguished from one another when examining their linear scaled parameters.

6.3 Box and whiskers plots

Box and Whiskers plots were generated by STA-CON. The plots included herein incorporate all measured data. Like the frequency distributions, the box plots are useful for examining the distribution of data. However, unlike the frequency distributions, the box and whisker plots consider absolute values. The box encompasses 50% of the data, with the median value dividing the box in half i.e., 25% of the data is represented below and above the median within the box. The height of the box is an indication of the degree of variability of the data i.e., thin boxes still contain 50% of the data but there is little variability in the measured parameter.

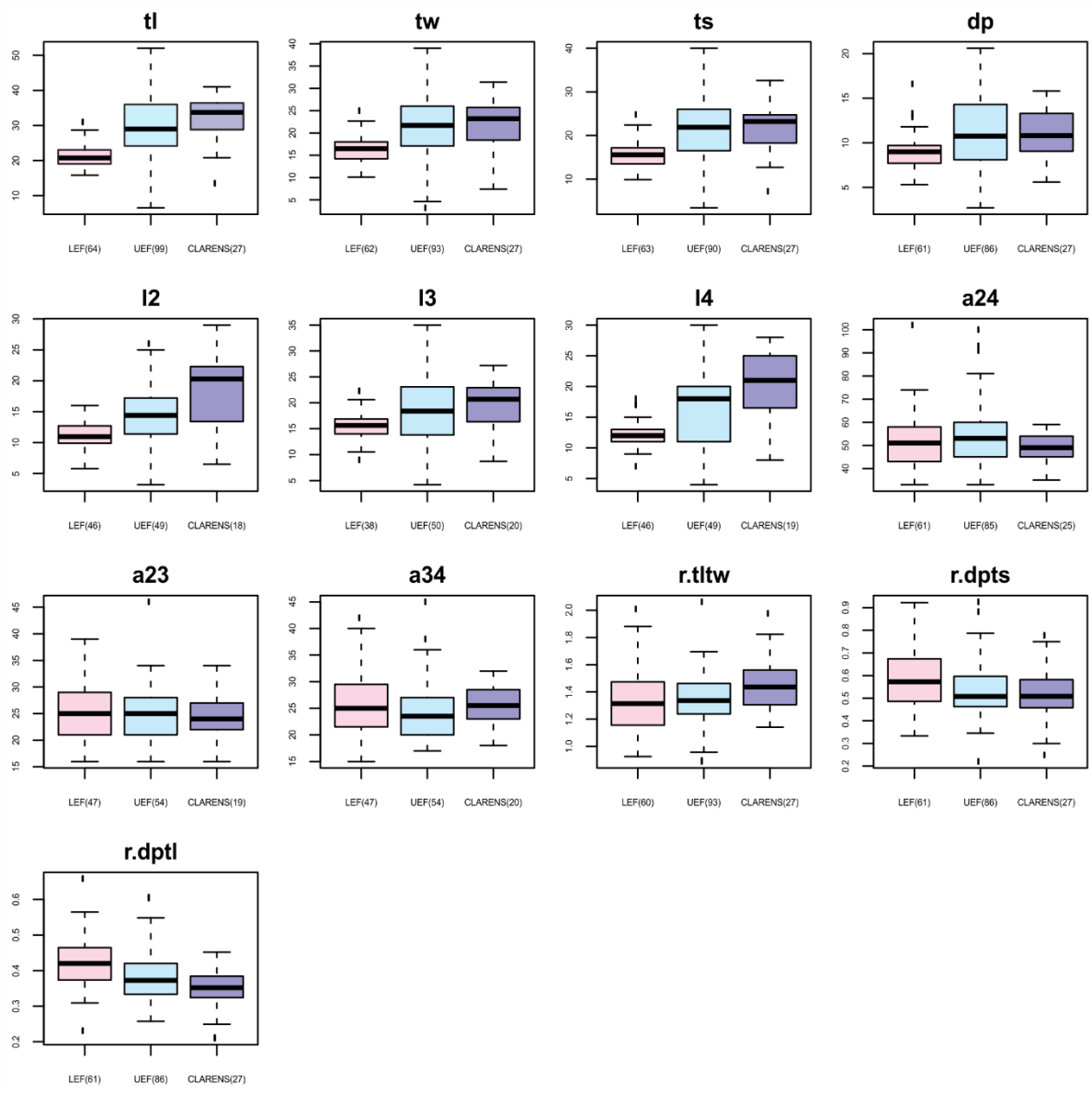

Figure 6.5: Box and Whiskers plots of measured track parameters within each stratigraphic unit (lEF, uEF, CLAR), highlighting the median, quartiles, maximum, minimum and distribution of data for each variable. All data included (number of tracks considered shown in figure). STA-CON.

Across stratigraphy, i.e., from lEF to CLAR, there is an apparent increase in TL, TW, TS, Dp and digit lengths (Fig. 6.5; Table 6.1). This is evidenced byboth the box and median positions. For the TW, TS and Dp there is a slight increase in median values between uEF and CLAR, but the boxes overlap, with uEF having the higher upper 1st quartile value. When the entire spread of data is considered, i.e., whiskers included, a similar trend cannot be observed as the uEF encompasses and exceeds the absolute value measurements of the lEF and CLAR (as mentioned previously, there is significant overlap of the data; Fig. 6.5). The boxes of the lEF and CLAR do overlap but do so to a lesser degree than the uEF and lEF or uEF and CLAR. The lEF boxes for the linear measurements are the most constrained i.e., there is little variability in data, the boxes are not strongly skewed. The uEF boxes for the linear measurements show are thick indicating that the uEF has the largest spread in data (Fig. 6.5). The data is often skewed e.g., LIV skewed right (third quartile has a large range in data). Measurements of the angles show significant overlap between each stratigraphic position box and whiskers; there is no apparent trend for the box and median positions (Fig. 6.5). The interdigit angle data is highly variable. Unlike for the linear measurements, the lEF shows high variability for the interdigit angles.

Interesting trends appear when one considers the ratios of linear measurements for tracks from the various stratigraphic positions. The TL/TW ratio shows an apparent increase from the lEF to CLAR - medians(quartiles) of 1.31 (1.16; 1.47), 1.34 (1.24; 1.46) and 1.44 (13.1; 1.56) respectively (Fig. 6.5, Table 6.1). Given that TL and TW both appear to increase across stratigraphy, an increase in TL/TW suggests that an increase in TL exceeds the increase in TW i.e., the two do not increase proportionally. A decrease in Dp/TS across stratigraphy is observed - medians (quartiles) of 0.57 (0.49, 0.67), 0.51 (0.46, 0.6) and 0.51 (0.46, 0.58), respectively (Fig. 6.5; Table 6.1). Both Dp and TS have an apparent increase in length through time; to observe a decrease in Dp/TS either Dp is becoming relatively shorter or TS is becoming relatively wider (or a combination of the two phenomena). An apparent decrease for DP/TL can be seen through time - medians (quartiles) of 0.42 (0.37; 0.46), 0.37 (0.33; 0.42) and 0.35 (0.32; 0.38) respectively. Both Dp and TL box plots indicate an increase between stratigraphic groups. Track length and stratigraphic position may have a relationship e.g., larger tracks in CLAR then lEF. With increasing TL, a decrease in the gradient (representing the increase in Dp) was observed in Fig. 6.1A. This artefact may be represented in the decrease in Dp/TS observed between stratigraphic groups.

Table 6.1: Summary data represented in box and whisker plots for stratigraphic position groupings data. All tracks from which parameters could be measured are included. STA-CON.

	lEF	uEF	CLAR
TL_meansd	21.30 (3.56)	29.59 (9.65)	32.06 (7.14)
TW_meansd	16.44 (3.24)	21.98 (7.33)	22.29 (5.53)
TS_meansd	15.73 (3.12)	21.69 (7.72)	21.93 (5.61)
Dp_meansd	8.99 (1.95)	11.18 (4.15)	10.94 (2.62)
LII_meansd	11.12 (2.43)	14.52 (5.48)	18.23 (5.53)
LIII_meansd	15.52 (3.14)	18.38 (6.82)	19.71 (4.82)
LIV_meansd	12.37 (2.23)	16.55 (6.32)	20.21 (5.85)
TL/TW_meansd	1.34 (0.25)	1.35 (0.18)	1.46 (0.19)
Dp/TS_meansd	0.59 (0.13)	0.53 (0.12)	0.52 (0.13)
Dp/TL_meansd	0.42 (0.07)	0.39 (0.07)	0.35 (0.06)
TL_medianq	20.75 (19.00,23.00)	29.00 (24.15,36.00)	33.70 (28.75,36.35)
TW_medianq	16.50 (14.25,17.98)	21.70 (17.10,26.00)	23.20 (18.40,25.75)
TS_medianq	15.60 (13.50,17.15)	21.90 (16.65,25.75)	23.20 (18.25,24.75)
Dp_medianq	9.00 (7.70,9.70)	10.75 (8.12,14.23)	10.80 (9.05,13.30)
LII_medianq	10.95 (9.93,12.67)	14.40 (11.40,17.20)	20.30 (13.62,22.05)
LIII_medianq	15.65 (14.10,16.88)	18.40 (13.85,23.00)	20.70 (16.38,22.75)
LIV_medianq	12.00 (11.00,13.00)	18.00 (11.00,20.00)	21.00 (16.50,25.00)
TL/TW_medianq	1.31 (1.16,1.47)	1.34 (1.24,1.46)	1.44 (1.31,1.56)
Dp/TS_medianq	0.57 (0.49,0.67)	0.51 (0.46,0.60)	0.51 (0.46,0.58)
Dp/TL_medianq	0.42 (0.37,0.46)	0.37 (0.33,0.42)	0.35 (0.32,0.38)
TL_n	64	99	27
TW_n	62	93	27
TS_n	63	90	27
Dp_n	61	86	27
LII_n	46	49	18
LIII_n	38	50	20
LIV_n	46	49	19
TL/TW_n	60	93	27
Dp/TS_n	61	86	27
Dp/TL_n	61	86	27

Three statistical tests (Anova, Anova on logged values and Kruskal Wallis) were performed to test the statistical relevance of the trends observed for the ratios. The means and medians of the individual ratios (Table 6.1) were considered. A $P < 0.001$ was determined by all metrics for DP/TL, thus rejecting the null hypothesis that the samples are from populations of equal means or medians i.e., the Dp/TL of each grouping is statistically distinct (Table 6.2).

Table 6.2: Statistics summary for stratigraphic position groupings means. STA-CON.

	TL/TW				Dp/Ts				DP/TL			
		lEF	uEF	CLAR		lEF	uEF	CLAR		lEF	uEF	CLAR
Anova	0.02983				0.01556				4.09E-05			
Anova (on logged values)	0.02220				0.01692				2.68E-05			
Kruskal Wallis (non-parametric)	0.02561				0.02736				6.32E-05			
Mean		1.34	1.35	1.46		0.585	0.530	0.520		0.423	0.385	0.348
Standard deviation		0.248	0.184	0.190		0.135	0.118	0.128		0.0748	0.0739	0.0635
Number of tracks		60	93	27		61	86	27		61	86	27

The trends observed across stratigraphy may be obscured by the inclusion of lower quality tracks (Fig. 6.5). However, when solely considering tracks from which complete measurements were taken, similar observations are made (Appendix Table A.7).

Conclusion: The Dp/TL ratios of the lEF, uEF and Clarens Formation are from populations which have different means or medians. The stratigraphic groups appear to have distinct digit projections relative to their track lengths.

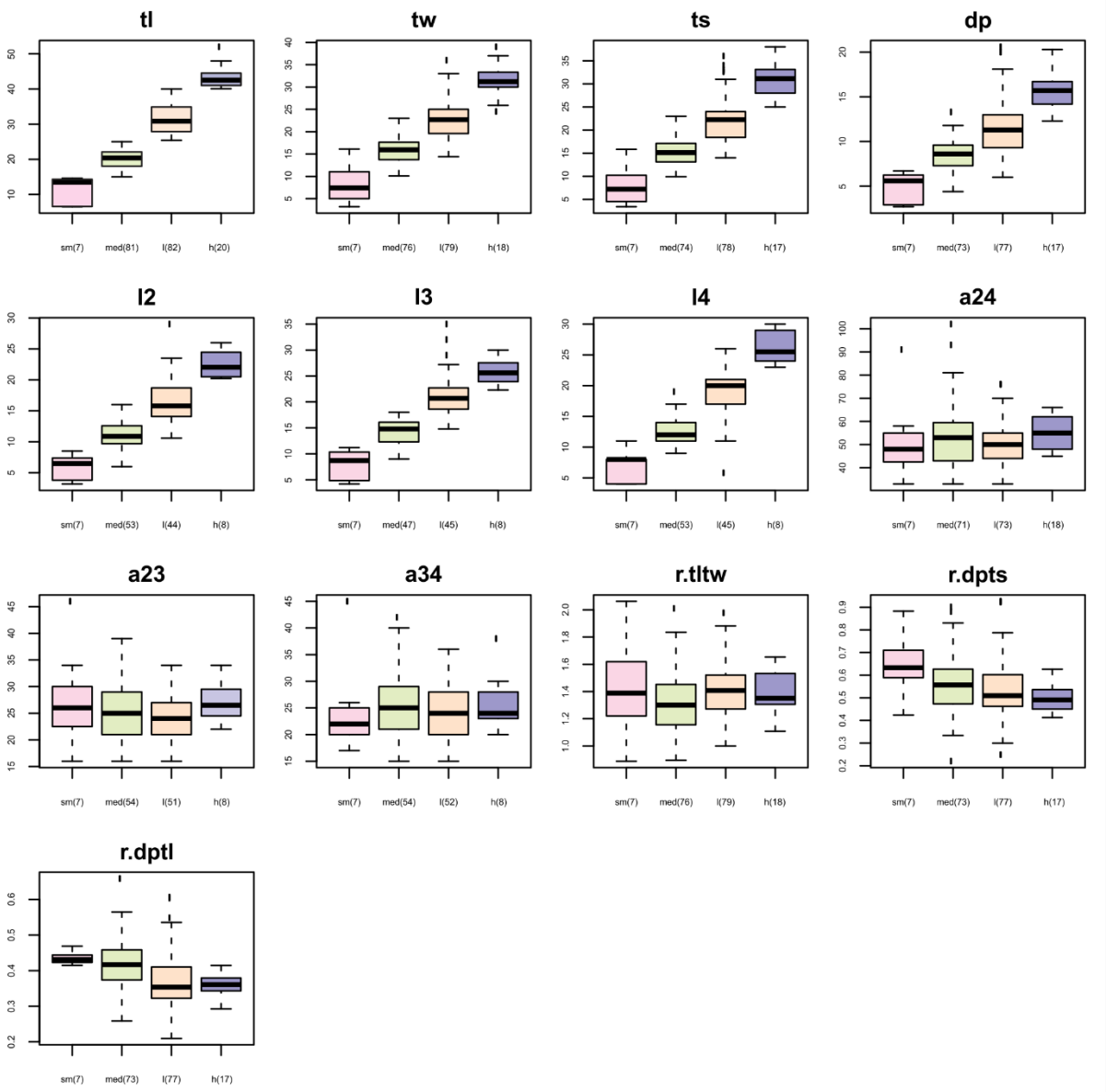

Figure 6.6: Box and Whiskers plots of measured track parameters within each size class grouping, highlighting the median, quartiles, maximum, minimum and distribution of data for each variable. All track data included. STA-CON.

Across size class i.e., from small to huge, there is apparent increase in TL, TW TS, Dp and digit lengths. There is some overlap between groups (particularly their whiskers rather than the boxes) but the small and huge classes are distinct from one another (Fig. 6.6). The box for the "small" group shows the

most variability for all linear measurements (excluding LIV) and the data is predominantly skewed to the right. The "medium" class has the least box variability and the data is rarely significantly skewed. Measurements of the angles show significant overlap between each track length class's box and whiskers; there is no apparent trend for the box and median positions (Fig. 6.6). The interdigit angle data is highly variable.

Table 6.3: Summary data for size class groupings data. All tracks from which parameters could be measured are included. STA-CON.

	small	medium	large	huge
TL_meansd	10.90 (4.10)	20.22 (2.70)	31.44 (4.14)	43.27 (2.96)
TW_meansd	8.40 (4.58)	15.98 (3.12)	22.71 (4.29)	31.36 (3.83)
TS_meansd	7.97 (4.42)	15.31 (3.14)	22.11 (4.56)	31.16 (3.85)
Dp_meansd	4.76 (1.83)	8.45 (1.63)	11.57 (3.10)	15.52 (1.94)
LII_meansd	5.80 (2.18)	10.97 (2.27)	16.89 (3.84)	22.52 (2.29)
LIII_meansd	7.79 (3.07)	14.26 (2.28)	21.22 (4.00)	25.80 (2.53)
LIV_meansd	6.71 (2.75)	12.43 (2.34)	18.68 (4.28)	26.25 (2.76)
TL/TW_meansd	1.43 (0.40)	1.31 (0.22)	1.40 (0.19)	1.40 (0.14)
Dp/TS_meansd	0.65 (0.15)	0.57 (0.13)	0.53 (0.13)	0.50 (0.06)
Dp/TL_meansd	0.44 (0.02)	0.42 (0.07)	0.37 (0.08)	0.36 (0.03)
TL_medianq	13.50 (6.55,14.30)	20.40 (18.00,22.10)	30.85 (27.92,34.90)	42.50 (41.00,44.25)
TW_medianq	7.40 (5.00,11.05)	15.95 (13.83,17.52)	22.70 (19.60,25.00)	31.20 (30.00,33.22)
TS_medianq	7.20 (4.50,10.20)	15.10 (13.10,17.10)	22.25 (18.55,24.00)	31.10 (28.00,33.10)
Dp_medianq	5.60 (2.90,6.25)	8.60 (7.30,9.60)	11.30 (9.30,13.00)	15.70 (14.20,16.70)
LII_medianq	6.50 (3.80,7.40)	10.90 (9.70,12.60)	15.80 (14.10,18.45)	22.05 (20.55,24.17)
LIII_medianq	8.70 (4.85,10.35)	14.80 (12.30,16.10)	20.70 (18.60,22.70)	25.60 (24.25,27.33)
LIV_medianq	8.00 (4.00,8.00)	12.00 (11.00,14.00)	20.00 (17.00,21.00)	25.50 (24.00,28.50)
TL/TW_medianq	1.39 (1.22,1.62)	1.30 (1.16,1.45)	1.41 (1.27,1.52)	1.35 (1.31,1.51)
Dp/TS_medianq	0.63 (0.59,0.71)	0.56 (0.47,0.63)	0.51 (0.46,0.60)	0.49 (0.45,0.54)
Dp/TL_medianq	0.43 (0.42,0.44)	0.42 (0.37,0.46)	0.35 (0.32,0.41)	0.36 (0.34,0.38)
TL_n	7	81	82	20
TW_n	7	76	79	18
TS_n	7	74	78	17
Dp_n	7	73	77	17
LII_n	7	53	44	8
LIII_n	7	47	45	8
LIV_n	7	53	45	8
TL/TW_n	7	76	79	18
Dp/TS_n	7	73	77	17
Dp/TL_n	7	73	77	17

Unlike the stratigraphic position grouping, the ratio trends are less clear (Fig. 6.6; Table 6.3). Track elongation (i.e., TL/TW) between size classes is variable and has no dominant trend. There is an apparent decrease in Dp/TS across classes with the following medians (quartiles), respectively - 0.63 (0.59; 0.71), 0.56 (0.47; 0.63), 0.51 (0.46; 0.6) and 0.49 (0.45; 0.54). Dp/TL seems to decrease from "small" to "huge" tracks – medians(quartiles) as follows 0.43 (0.42; 0.44), 0.42 (0.37; 0.46), 0.35 (0.32; 0.41) and 0.36 (0.34; 0.38), respectively. The "small" and "huge" boxes are constrained (0.42–0.44 and

0.34–0.38, respectively), showing minimal Dp/TL spread in the Tl<15 cm and TL>40 cm size groupings (Fig. 6.6; Table 6.3).

Three statistical tests (Anova, Anova on logged values and Kruskal Wallis) were performed to test the statistical relevance of the trends observed for the ratios (Table 6.4). The means and medians of the individual ratios were considered (Table 6.3).

A P<0.001 was determined by all metrics for DP/TL, suggesting that of all the ratios, thus rejecting the null hypothesis that the samples are from populations of equal means or medians i.e., the Dp/TL of each grouping is statistically distinct (Table 6.4). The trends observed between size class groupings may be obscured by the inclusion of lower quality tracks (Fig. 6.6). However, when solely considering tracks from which complete measurements were taken, similar observations are made (Appendix Table A.8).

Conclusion: Tracks from bigger track length classes have shorter Dp relative to their TL than smaller tracks.

Table 6.4: Statistics summary for size groupings means. STA-CON.

	TL/TW					Dp/TS					Dp/TL				
		small	medium	large	huge		small	medium	large	huge		small	medium	large	huge
Anova	0.02145					0.02664					5.29E-05				
Anova (on logged values)	0.01353					0.04769					1.88E-05				
Kruskal Wallis (non-parametric)	0.01640					0.02657					2.60E-05				
Mean		1.43	1.31	1.40	1.40		0.648	0.566	0.532	0.502		0.436	0.420	0.370	0.359
Standard deviation		0.396	0.219	0.186	0.144		0.147	0.130	0.129	0.063		0.0197	0.0696	0.0830	0.0337
Number of tracks		7	76	79	18		7	73	77	17		7	73	77	17

6.4 Reviewing the lenses: time and size class

The exploratory statistics performed thus far can lead one to review the lenses from which the data is viewed - e.g., stratigraphic position groupings and TL "size" groupings. The stratigraphic subdivision of the data acted as a proxy to compare tracks through time. It was found that the uEF and Clarens Formation track data often coincided, although some differences between the two groupings are apparent (Figs. 6.2, 6.3, 6.5). Given that both the uEF and CLAR Formation are interpreted as Early Jurassic deposits and that track data from the uEF is primarily from the upper half of the Formation and that the CLAR data is exclusively from the lower Clarens Formation, an alternative chronological subdivision may be considered to compare morphologies: Late Triassic tracks (lEF) vs Early Jurassic tracks (uEF and CLAR). Mann-Whitney test of equal medians was performed on all track data in the Late Triassic and Early Jurassic subdivisions (Table 6.5). All measurements, excluding TL/TW were statistically distinct between the Early Jurassic and Late Triassic data (p<0.05; Table 6.5). The Dp/TS ratio is not as convincingly distinct as the TL, TW, DP, and Dp/TL which are significantly smaller than p = 0.05. The TL/TW ratio of 0.06 marginally misses the threshold probability; perhaps with a larger dataset the elongation of Early Jurassic and Late Triassic tracks would have distinct medians.

Table 6.5: Mann-Whitney test for equal medians of Late Triassic and Early Jurassic tracks.

		Mann whitney (equal medians)	
		Late Triassic	Early Jurassic
TL	N	64	126
	p	**1.47E-12**	
TW	N	60	120
	p	**7.60E-10**	
TL/TW	N	60	117
	p	0.06	
Dp	N	61	113
	p	**9.17E-05**	
Dp/TS	N	61	111
	p	0.008	
Dp/TL %	N	58	110
	p	**1.00E-04**	

When the data are examined by size classes, their stratigraphic position and consequently their "relative age" is disregarded. A recurrent trend observed through numerous data representations is that across stratigraphy/or time there is an apparent increase in TL (and related linear track measurements; Figs. 6.1, 6.5). Given this relationship between stratigraphy and TL, it is worth considering the "time" element when viewing the data from size class lenses. Consequently, we amend our current size groupings which are independent of stratigraphic position to a comparison of single size groupings across stratigraphy i.e., how do tracks of a single size class vary through time? (Fig. 6.7).

"Small" tracks (TL<15 cm) have been grouped with "medium" tracks (15<TL<25 cm) because they consist of so few specimens (Appendix Table A.1). Pairwise scatter plots show that tracks with a TL<25 cm from different stratigraphic positions are indistinguishable from one another (Fig. 6.7A). Medium tracks from the Clarens Formation appear to have a distinctly lower TL/TW ratio but there is not a consistent decrease in track elongation from the lEF to CLAR (CLAR has no overlap with lEF and minimal overlap with uEF; Fig. 6.7A). The mesaxony (Dp/TS) and and relative digit projection (Dp/TL) seem to illustrate a decreasing trend through time for the medium track size. This follows the Dp/TS trend observed across stratigraphy independent of track size (Fig. 6.5). The Early Jurassic Dp/TL overlap significantly, but do not coincide with DP/TL measurements of the lEF (Fig. 6.7). The Dp/TS and Dp/TL trends do not appear prolonged as there is a rather a discrete decrease between Late Triassic and Early Jurassic tracks. The Mann-Whitney test for equal medians for medium-sized tracks have a p>0.05, indicating that the medium track population across stratigraphy have equal medians (Table 6.6). An important consideration to bear in mind, is that only 3 tracks comprise the CLAR dataset for this size grouping.

Pairwise scatter plots for “large” tracks do not separate tracks from different stratigraphic horizons (Fig. 6.7B). However, tracks from the lEF form a more constrained grouping and have smaller TL than those of the uEF and CLAR. Track elongation ratios (TL/TW) for this size class are variable with no visible trend (Fig. 6.7B). The mesaxony (Dp/TS) illustrates a discrete decrease from lEF to uEF (and CLAR). The Dp/TS of uEF and CLAR values are comparable and their measurements overlap with those of the lEF. This suggests that large tracks from the Early Jurassic have distinctly a lower Dp/Ts than those of the Late Triassic (Fig. 6.7B). A similar observation is noted for Dp/TL i.e., tracks of the uEF and CLAR have discretely lower Dp/TS relative to the lEF. The lEF Dp/TS of large tracks show a range in values while the uEF and CLAR are more constrained (Fig. 6.7B). Mann-Whitney test for equal medians suggests that the TL/TW of uEF is statistically distinct from the lEF. The uEF Dp/TS for large tracks is also statistically distinct from the lEF (Table 6.6). The Dp/TS of Clarens Formation tracks marginally miss being statistically distinct from the lEF tracks (p of 0.0596; Table 6.6). This warrants further investigations; perhaps with a larger dataset large tracks form the lEF and Clarens Formation would have unequal medians. A Dp/TS and Dp/TL decrease is apparent for both “large” and “medium” tracks: large tracks show a sudden decrease in Dp/TS while “medium” tracks show a gradational decrease and both “large” and “medium” tracks show a sudden in decrease in Dp/TL in the uEF (Fig. 6.7A, B).

Table 6.6: Summary of Mann-Whiney testing for equal medians for size classes through time.

	TL<25 cm				25 cm< TL <35 cm				TL >40 cm			
TL/TW		lEF	lEF	CLAR		lEF	uEF	CLAR		lEF	uEF	CLAR
	lEF		0.2248	0.7434	lEF		0.04845	0.1317	lEF			
	uEF	0.2248		0.2289	uEF	0.04845		0.2941	uEF			0.2205
	CLAR	0.7434	0.2289		CLAR	0.1317	0.2941		CLAR		0.2205	
Dp/TS		lEF	uEF	CLAR		lEF	uEF	CLAR		lEF	uEF	CLAR
	lEF		0.7109	0.2649	lEF		0.02041	0.0596	lEF			
	uEF	0.7109		0.3338	uEF	0.02041		0.9774	uEF			0.2445
	CLAR	0.2649	0.3338		CLAR	0.05956	0.9774		CLAR		0.2445	
Dp/TL %		lEF	uEF	CLAR		lEF	uEF	CLAR		lEF	uEF	CLAR
	uEF		0.2522	0.5164	lEF		0.1656	0.1312	lEF			
	lEF	0.2522		0.8225	uEF	0.1656		0.6909	uEF			0.6408
	CLAR	0.5164	0.8225		CLAR	0.1312	0.6909		CLAR		0.6408	

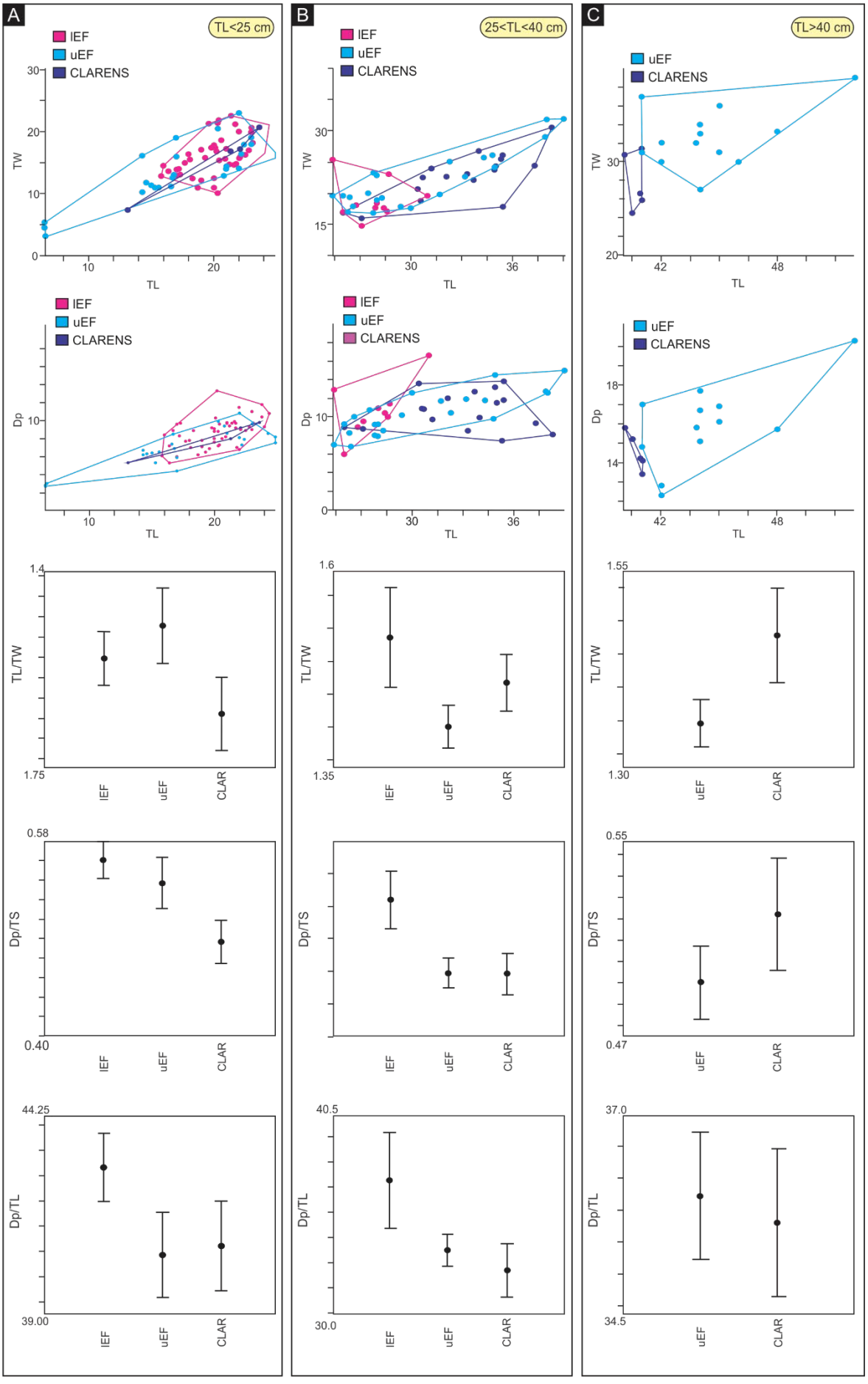
A
TL<25 cm
IEF
uEF
CLARENS
TW
TL
Dp
TL/TW
Dp/TS
Dp/TL
B
25<TL<40 cm
C
TL>40 cm

Figure 6.7 (previous page): Comparison of tracks within a single size through time. A) "small" and "medium" tracks, B) "large" tracks, C) "huge" tracks.

"Huge" tracks, TL>40 cm, have only been found in the uEF and CLAR. Pairwise scatterplots are able to separate "huge" tracks of the uEF and CLAR: CLAR tracks have a lower TL than uEF (Fig. 6.7). It should be noted that the CLAR grouping only consists of 5 tracks. Track elongation (TL/TW) and mesaxony (Dp/TS) seem to show an increase from uEF to CLAR " huge" tracks (Fig. 6.7C). An increase in TL/TW from the uEF to CLAR is also observed in the "large" size grouping (Fig. 6.24B). The Dp/TL for "huge" tracks in the two stratigraphic horizons overlap entirely, which is similar to the trend observed in the "large" size grouping. Mann-Whitney test shows that none of the ratio trends observed in the plots are statistically relevant (Table 6.6).

Conclusion: Tracks from various size classes primarily do not show significant trends through time. However, Dp/TS for "large" tracks shows a distinct decrease in medians from the Late Triassic to Early Jurassic. An apparent decrease is also noted for "medium" tracks and may be statistically relevant if a larger data set was considered. "Large" tracks would have been assigned to *Eubrontes* or *Kayentapus*. This reduction in Dp/TS would have interesting implications for the trackmakers, suggesting that the theropod autopodia possibly became more mesaxonic with time. Further investigation, especially in medium size tracks which appear to show a similar trend, is needed.

6.5 Multivariate statistics: Principal component analysis

Principal component analysis using measurements and landmarks was performed to differentiate tracks from different stratigraphic positions. Measurement-based PCA exclusively considered tracks from which all parameters (excluding angles) were measured. This was done on the raw measurements and log-transformed, mean subtracted measurements (Figs. 6.8A and B, respectively). Morphological variation based on raw measurements can be accounted for by two PCs (PC1 accounts for 87% of variation; Fig. 6.8A; Appendix Fig. A.4). Principal Component 1 is strongly affected by absolute size: TL, followed by TW, TS and Dp contribute the most to positive variation. The ratios Dp/TL and Dp/TS contribute significantly to the negative variation in PC1. Variation in PC2 can primarily be attributed to TL/TW ratio. For PC2, Dp, TW and TS are strongly correlated (Fig. 6.8A; Appendix Fig. A.4). Principal component analysis using the log transformed data can account for all morphological variation in two PCs (PC1 accounts for 97% of variation; Fig. 6.8B, Appendix Fig. A.4). Track length is the main contributor to PC1 variation. Principal Component 2 is mainly affected by TL/TW. For PC2, TW, TS and Dp are strongly correlated (Fig. 6.8B; Appendix Fig. A.4).

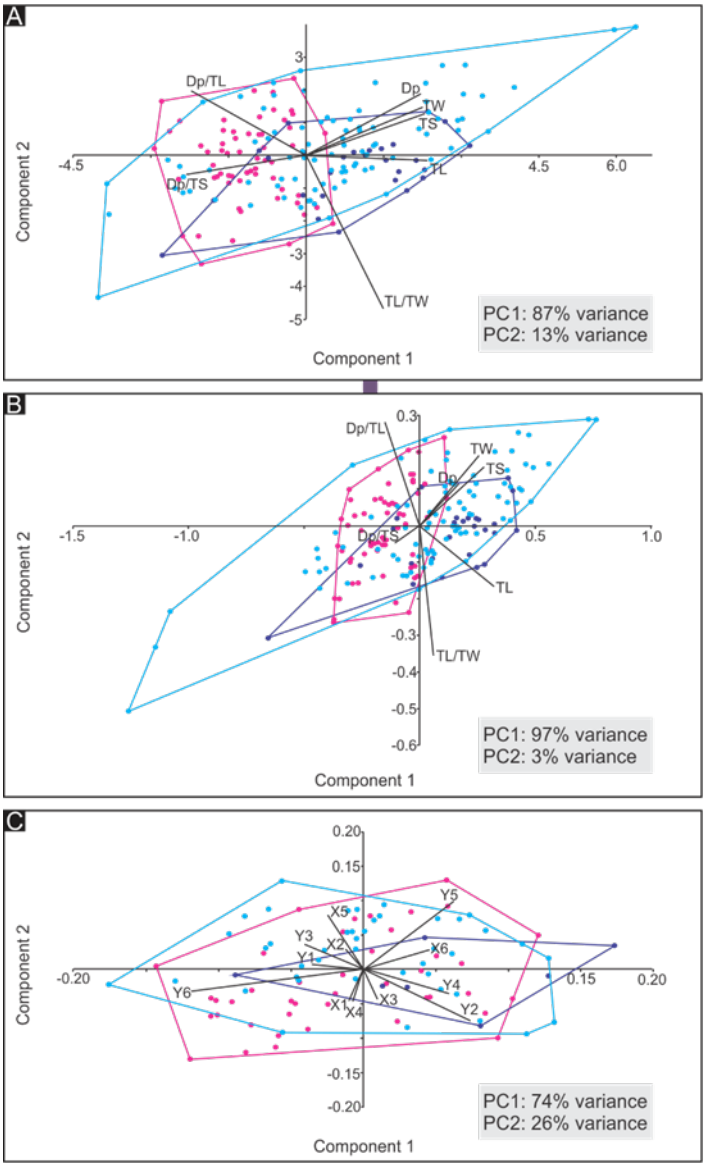

Figure 6.8: Principal component analysis comparing tracks with complete measurements from the IEF, uEF and CLAR. A) PCA using measurements with a correlation matrix applied, B) PCA using log-transformed, mean subtracted data with a variance-covariance matrix applied, C) PCA using Procrustes fitted landmarks with a variance - covariance matrix applied).

Principal component analysis from landmarks can account for morphological variation in two PCs (PC1 accounts for 74% of the variation; Fig. 6.8C; Appendix Fig. A.4). Principal Component 1 is most strongly affected by landmark 6, the proximal digit IV landmark. Landmark 5, associated with the distal placement of digit IV, is the main contributor to PC2 variation.

Conclusion: Principal component analysis, applied to various forms of data, is unable to differentiate tracks from various stratigraphic horizons. As seen in earlier analysis, the uEF has the most morphological variation.

Principal component analysis exclusively using tracks with complete data was used to distinguish tracks from different size classes. Small tracks were merged into the medium track group. The PCA

was performed on two sets of data: the absolute values of parameters and measurements normalized relative to the TL (Fig. 6.9A and B, respectively). Using raw measurements, PCA can account for morphological variation with only two PCs (with PC1 accounting for 98% of the morphological variation Fig. 6.9A, Appendix Fig. A.5). Principal Component 1 is strongly affected by size, and there is a clear separation of groupings (as seen previously, this is expected; size class-groupings are based on measured TL). Principal Component 2 is primarily affected by Dp/TL and Dp. The large size class has the most variation within PC2. Digit lengths II and III are strongly correlated (Fig. 6.9A). Principal Component Analysis performed on normalized data yield distinctly different results than when using raw measurements. Morphological variation between size classes can be accounted for with two PCs (with PC accounting for 78% of the variation; Fig. 6.9B; Appendix Fig. A.5). Principal Component 1 is mainly affected by TW and Dp while PC2 is chiefly influenced by LIII. Unlike the PCA using raw measurement, PCA using normalised data does not clearly differentiate between size groupings i.e., there is overlap between size classes (Fig. 6.9B). The medium and large groupings can somewhat be distinguished from one another along the PC1 axis; medium tracks plot towards more positive PC1 and large tracks trend toward more negative PC1 (Fig. 6.9B).

Conclusion: When size groupings are normalized relative to their TLs, there is minimal difference in morphology between tracks from different size classes.

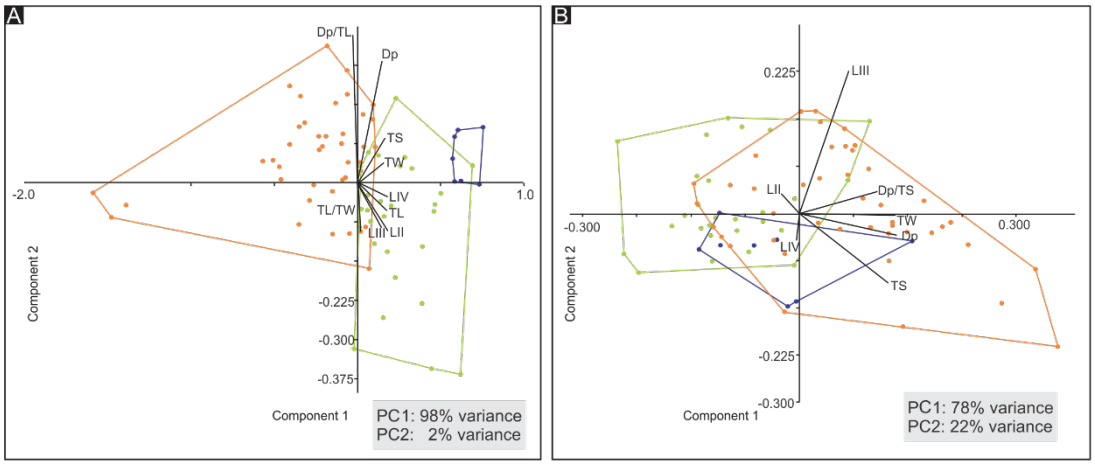

Figure 6.9: Principal component analysis comparing tracks from different size groupings. A) PCA using raw measurements with a correlation matrix applied, B) PCA using data normalized relative to TL with a variance-covariance matrix applied.

6.6 Cluster analysis

Cluster analysis was performed using PAST v3. The hierarchical clustering was performed using the classical clustering function, with a Paired-group (UGMA) algorithm and Euclidean similarity index. Only tracks with complete linear measurements (TL, TW, TS, and Dp) were included in the cluster analysis (Appendix Table A.1). Individual parameters were log transformed with the mean for each parameter subtracted from individual measurements. It is important to note that the Euclidian

method weighs larger measurements more than smaller measurements but normalizing the data is aimed at circumventing that. The cluster analysis classification technique is employed herein to complement earlier ordination techniques. From the automated groupings it forms, one can see which measured parameters are the stronger influences.

The track data was split into two random groupings to see whether the same variables would have the strongest effect on the clustering. The groupings are termed “unpublished” and “published” data. “Published” data refers to ichnosites which have been revised in publications dating from 2009 – present while “unpublished” data refers to ichnosites that have not been revised since 2003 (Table 4.1).

For the “unpublished” track data, the clustering analysis identified three main groups and a single significant outlier (Fig. 6.10). Characteristics of the groupings are as follows:

Group 1 (orange): The “Group 1” cluster comprises 10 tracks, which primarily have a TL > 35 cm. The Dp/Ts of individual tracks is > 0.5 (a weak mesaxony but relatively stronger than in some other groupings) and have a high (relative to the other groups) Dp/TL% (> 40 %). T*he main variable that makes “Group 1” distinguishable from the other groupings is a larger track length.*

Group 2 (blue-green): “Group 2” can further be subdivided in 4 subgroups (Fig. 6.10). Subgroup 2A is the smallest subgroup and consists of three tracks. The tracks are characterized by a TL<25 cm, 1.5<TL/TW<2 and a Dp/TS>0.5. Relative to other subgroupings, 2A comprises the most elongate tracks. Subgroup 2B encompasses eleven tracks with a TL<25 cm, 1<TL/TW<1.5 and Dp/TS of approximately 0.5. Tracks of subgroup 2C (n = 10) have a TL<25 CM, 1<TL/TW<1.5, Dp/Ts>0.5 and a Dp/TL%>40. Subgroup 2D comprises six tracks with TL<35 cm, 1<TL/TW<1.5 and Dp/TS>0.5. *The main variable that is responsible for “Group 2” being distinguishable from the other groupings is a larger Dp/TS i.e., tracks are more strongly mesaxonic.*

Group 3 (pink): “Group 3” includes three subgroups (Fig. 6.10). Subgroup 3A consists of seven tracks, with a TL<25 cm, 1<TL/TW<1.5, average Dp/TS of 0.5 and Dp/TL% > 40. 3B tracks (n=7) are characterised by TL<35 cm, 1<TL/TW<1.5, Dp/TS of approximately 0.5 and a Dp/TL%<40. Subgroup 3C comprises four tracks, which primarily have TL/TW= 1 and Dp/TS<0.4. *The main variable that attributes to “Group 3” being distinguishable from the other groupings is a relatively smaller Dp/TS i.e., tracks of “Group 3” have the weakest mesaxony.*

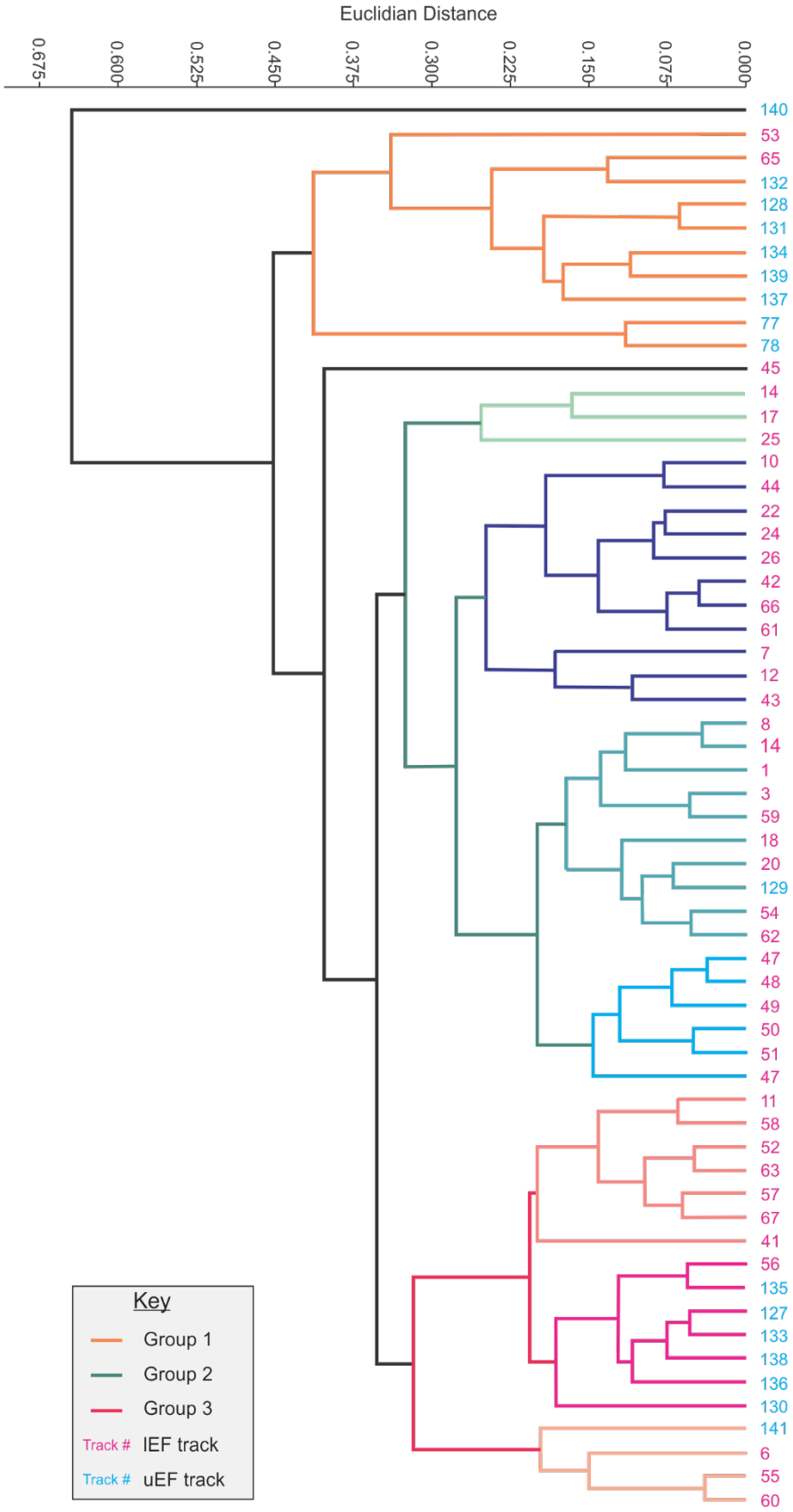

Figure 6.10: Classical clustering of unpublished track data (Appendix Table A. 1, numbering refers to database track numbering). Only data with complete linear measurements are included in the clustering.

The outlier track (Track 140; Appendix Table A.1) is an uEF track from the Tlapana ichnosite. It has a TL of 17 cm, TL/TW of 0.9, Dp/TS of 0.22 and DP/TL% of 26. Relative to the other tracks, track 140 is the only track that is not at least as long as it is wide, and it has the weakest mesaxony.

Conclusion: The cluster analysis suggests that groupings are not controlled by stratigraphic positions i.e., groups consists of lEF and uEF samples. TL is a parameter that clearly distinguishes groupings e.g., Group 1. Groups 1 and 2 are more mesaxonic than Group 3, however Group 1 has a larger mean TL than Group 2.

For the "published" track data, the clustering analysis identified three main groups and five outliers (Fig. 6.11). Characteristics of the groupings are as follows:

Group 1 (orange): The "Group 1" cluster can be subdivided in to three subgroups (Fig. 6.11). Subgroup 1A comprises seven tracks, with a TL<35 cm, a 1.5<TL/TW<2 (although one track has a TL/TW<1.5), Dp/TS>0.6 and Dp/TL %<40. The 2B cluster consists of tracks (n= 11) with a TL predominantly < 35 cm, variable TL/TW, a Dp/TS > 0.5 (excluding on track) and a Dp/TL% primarily < 40%. Subgroup 2C includes ten tracks with most TL<45 cm, 1<TL/TW< 1.5, Dp/TS ranging between 0.4 and 0.6 and DP/TL% principally < 40%. *The main variable that distinguishes "Group 1" from the other groupings is a relatively smaller Dp/TL%.*

Group 2 (purple): "Group 2" is made up of two subgroups (Fig. 6.11). 2A comprises eleven tracks which predominantly have a TL<35cm, 1<TL/TW<1.5, Dp/TS primarily of 0.4 and Dp/TL% < 40%. Subgroup 2B (n=25) tracks are characterized by TL<25 cm, mainly 1<TL/TW<1.5, Dp/TS<0.5 and DP/TL% < 40%. *The main variable that attributes to "Group 2" being distinguishable from the other groupings is a relatively smaller Dp/Ts i.e., "Group 2" tracks have the weakest mesaxony.*

Group 3 (blue): "Group 3" consists of twelve tracks (Fig. 6.11). The tracks are chiefly < 25 cm, have a 1 < TL/TW < 1.5, Dp/TS > 0.6 and a Dp/TL% predominantly > 40%. *The main variable that attributes to "Group 3" being distinguishable from the other groupings is a relatively high Dp/TL% (> 40%).*

Classical clustering of the "published" data suggests that stratigraphy is not a strong factor for distinguishing the tracks. All groupings of the published data are linked to factors including the Dp. The strongest Dp component that separates Groups 1 and 3 are related to track length.

Conclusion: Classical cluster analysis applied to the datasets suggests that size (TL) is a strong parameter to separate tracks and that stratigraphic position is a minor one. Second to TL, the digit projection plays an important role in subdividing these tridactyl tracks.

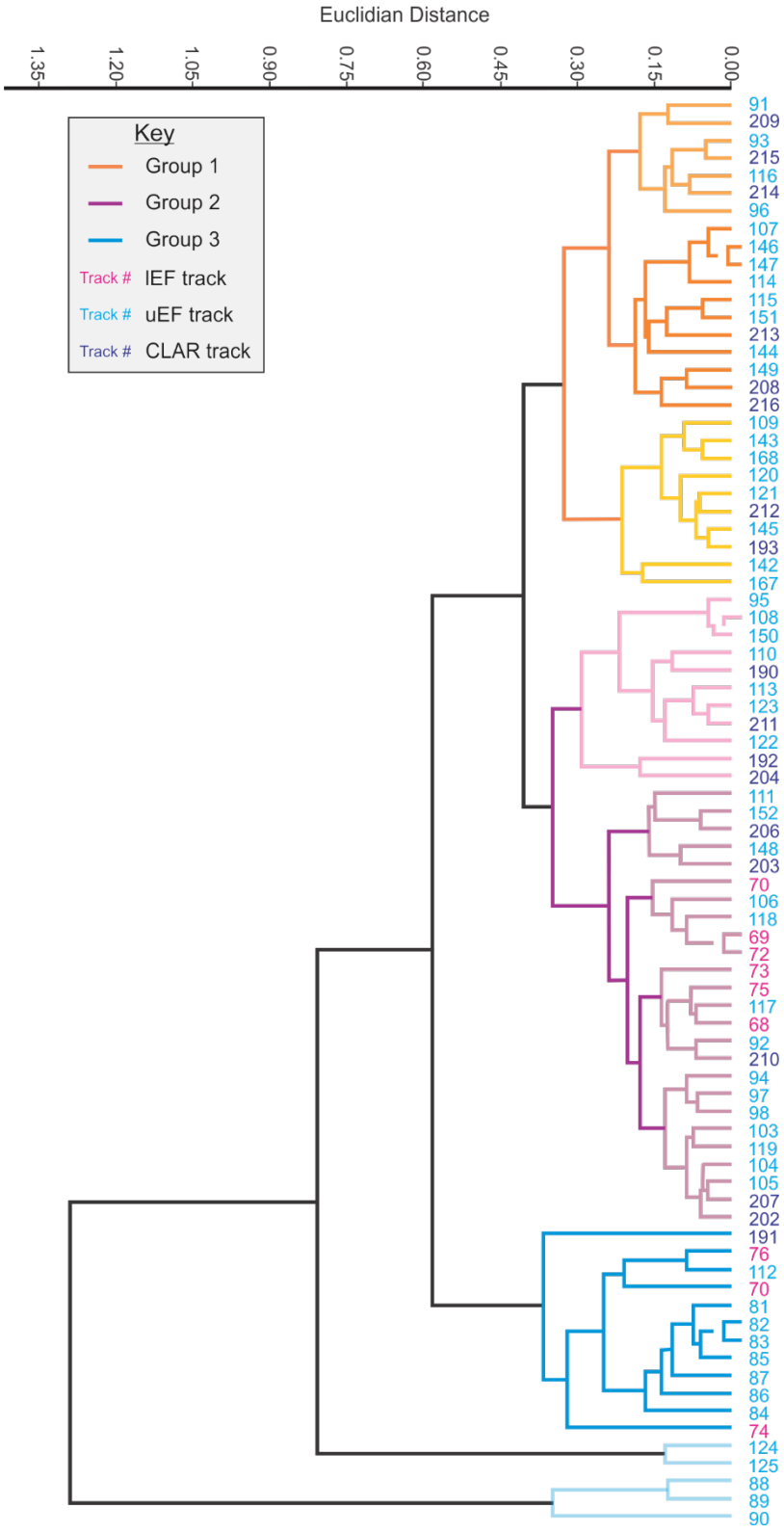

Figure 6.11: Classical clustering of published track data (Appendix Table A.1, numbering corresponds to database track numbering). Only data with complete linear measurements are included in the clustering.

6.7 Discriminant analyses

Discriminant analyses was performed on our original two subgroupings - "stratigraphic position" and "track length class" – to see the degree to which the analysis could correctly assign tracks to their

groups using their individual measurements. Discriminant analyses was performed using PAST v3. For each grouping, two sets of slightly different datasets were included in the analyses: all measurements excluding digit lengths and angles, and all measurements excluding angles (Table 6.7). Digit lengths and total digit divarication is excluded because a) incorporating digit length significantly reduces the number of tracks included in the analyses and b) digit divarication is highly variable due t measurement style and its influence by trackmaker-substrate interactions Exclusively, tracks with all parameters measured were included.

Table 6.7: Summary of the discriminant analysis confusion matrix. Data is not jackknifed.

Excluding digit lengths and angles					
	LEF	UEF	CLARENS	TOTAL	% correctly identified
LEF	51	4	5	60	
UEF	22	37	26	85	**59,88**
CLARENS	5	7	15	27	
TOTAL	78	48	46	172	
Including digit lengths, excluding angles					
	LEF	UEF	CLARENS	TOTAL	% correctly identified
LEF	23	9	0	32	
UEF	13	22	7	42	**60,87**
CLARENS	0	7	11	18	
TOTAL	36	38	18	92	
Excluding digit lengths and angles					
	SMALL	MEDIUM	LARGE	MEGA	TOTAL	% correctly identified
SMALL	6	0	0	0	6	
MEDIUM	4	66	2	0	72	
LARGE	0	1	45	3	49	**93.06**
MEGA	0	0	0	17	17	
TOTAL	10	67	47	20	144	
Including digit lengths, excluding angles					
	SMALL	MEDIUM	LARGE	MEGA	TOTAL	% correctly identified
SMALL	6	0	0	0	6	
MEDIUM	3	33	2	0	38	
LARGE	0	0	27	0	27	**93.67**
MEGA	0	0	0	8	8	
TOTAL	9	33	29	8	79	
Excluding digit lengths and angles					
	Late Triassic	Early Jurassic		TOTAL	% correctly identified
Late Triassic	54	7		61	
Early Jurassic	29	85		114	**79,43**
TOTAL	83	92		175	
Excluding digit lengths and angles					
	Late Triassic	Early Jurassic		TOTAL	% correctly identified
Late Triassic	24	8		32	
Early Jurassic	15	44		59	**74,73**
TOTAL	39	52		91	

Discriminant analyses correctly identified the stratigraphic position of ~ 60 % of the tracks without the inclusion of digit length measurements (Table 6.7; Appendix Table A.9). The addition of digit length measurements only slightly improved the percentage of correctly identified tracks (~61; Table 6.7; Appendix Table A.10). Clarens Formation tracks are often misidentified as uEF tracks; this could be because the uEF has the most variation in parameters and often coincides with CLAR dimensions. As mentioned, the CLAR tracks are from the basal most horizons of the unit. When the stratigraphy is divided into Late Triassic and Early Jurassic the discriminant analysis is more successful in correctly identifying the time period for each track (79% without digit lengths, 75% with digit lengths; Table 6.7)

Discriminant analyses correctly identified the size class of ~93% of the tracks without including the digit length variables (Table 6.7; Appendix Table A.11). The addition of digit length measurements only slightly improved the percentage of correctly identified tracks (~94%, Table 6.7; Appendix Table A.12). Five "medium" tracks (discrimination excluding digit lengths) were incorrectly identified as "small"; these tracks have small TL (16–17.3 cm) and relatively high Dp/TS (>0.6).

The large disparity in correctly identifying the "stratigraphic position" and "size class" groupings was expected. The stratigraphic placement of tracks is independent from their measured parameters, unlike the "size class" grouping. One may have expected better identification of the stratigraphic unit a track is from given the correlation between size and stratigraphy (Figs. 6.2, 6.5). However, while the lEF and CLAR are distinct and are not misinterpreted for one another, the uEF spans a range of dimensions overlapping with both the lEF and CLAR.

6.8 Synthesis of exploratory statistics

Various methods of data representation have been applied to the southern African tridactyl tracks in this study to evaluate morphological differences of the tracks in different stratigraphic horizons and size length classes. The following key observations can be made:

1. The parameters that prmarily influence cluster analysis groupings are TL and Dp (Figs. 6.10, 6.11).
2. Tracks from the lEF and CLAR can be distinguished from one another, to varying degrees, using scatter plots, box and whisker plots and normailsed frequency distributions. Considering absolute values, lEF and CLAR have very little overlap in TL and TW forming two near-distinct groupings (Figs. 6.2, 6.5, 6.7). Normalised frequency distributions show that lEF tracks have smaller TL, TW and digit III and IV lengths relative to tracks from the CLAR (Fig. 6.3). This is supported by Kolmogorov-Smirnov tests comparing the populations of the lEF and CLAR which indicate that they do not have equal distributions. Track data from the uEF spans that of the lower Elliot and Clarens formations (Figs. 6.2, 6.3, 6.5, 6.7).

3. amending the groupings from lEF, uEF and CLAR to Late Triassic and Early Jurassic, improves the distinction between tracks e.g., discriminant analyses can correctly identify a higher proportion of tracks as Late Triassic vs Early Jurassic than lEF vs uEF vs CLAR (79.43% vs 59.88%, respectively; Table 6.7).
4. When exclusively considering linear measurements, normalised track parameters from different size classes are almost indistinct from one another (Figs. 6.4, 6.9B).
5. Track length increases from the lEF to uEF and Clarens Formation. Tracks with TL>35 cm are common in the Early Jurassic strata with TL>50 cm Solely observed in Early Jurassic strata. This may be an artefact of sampling bias, with the lEF (Late Triassic) being under-represented relative to the uEF and Clarens Formation (Early Jurassic).
6. Similar ratio trends are observed for the stratigraphy and TL groupings – an apparent decrease in TL/TW, Dp/TS and DP/TL (with the decrease in Dp/TL having distinct medians shown by Mann-Whitney tests; Figs. 6.5, 6.6). However, as mentioned in point 5, there is a strong relationship between TL and stratigraphic position i.e., tracks from the uEF and CLAR reach maximum TLs greater than those of the lEF (Fig. 6.5). Therefore, the trends observed across stratigraphy may simply be the trends we see across size groupings. However, although not statistically robust, an apparent decrease in Dp/TS and Dp/TL is observable for tracks within size groupings across stratigraphy (i.e., TL<25 cm and 25<TL<40 cm; Fig. 6.7). This suggests that a decrease in Dp/TL from the lEF to CLAR may be an evolutionary pattern than purely a link to TL within the dataset.

7 Discussion

7.1 Assessing the upper Stormberg Group track database

7.1.1 Preservation grade

Footprint morphology is the basis of vertebrate ichnology (Marchetti *et al*., 2019; Section 4.1). A trackmaker's anatomical characters are observable in tracks with high morphological preservation grades between 2 and 3 (Belvedere and Farlow, 2016; Marchetti *et al*., 2019; Table 2.2). The tracks from the upper Stormberg Group considered in this study encompass the entire range of morphological preservation grades from 0 to 3, with only a small proportion of the tracks having a high morphological preservation grade of 3 (Appendix Fig. A.3; Appendix Table A.1). Tracks with a preservation grade of 3 are exclusively advised to be used for landmark-based shape analyses (Belvedere and Farlow, 2016; Marchetti *et al.,* 2019; Table 2.2). For example, the Phuthiatsana trackway (tracks 1 to 6) which have a high morphological grade of 3 plot firmly within the *Grallator* morphospace during landmark-based analyses (Fig. 4.9). However, for the Lower Moyeni trackway, some high morphological grade tracks such as tracks 4, 6 and 15 plot outside of known morphospaces, while the remaining tracks along the trackway plot in *Kayentapus-Grallator-Eubrontes* morphospaces (Fig. 4.13). Due to the limited number of grade 3 tracks in this database, select tracks with distinct morphologies and lower morphological grades were included for landmark assessment. This inclusion of lower grade tracks has varying success for ichnotaxonomic refinement e.g., Maphutseng track 7 (morphological grade of 2) plots outside of defined ichnotaxonomic morphospaces, while Tlapana tracks 3 and 9 (morphological grades of 2) plot within K-GAE morphospace (Figs. 4.6 and 4.23, respectively).

Fossilized tracks often have an incomplete or ambiguous morphology which may be due to the initial foot impression being incomplete or modified subsequently by, for example, overprinting footprints (e.g., Phuthiatsana tracks 9 and 10, Upper Moyeni tracks 11 and 12; Appendix Fig. A.3), bioturbation (e.g., Lephoto track 6; Appendix Fig. A.3) or diagenetic processes. Generally, incomplete tracks are not very useful for morphometric evaluation e.g., Tlapana track 1, Phuthiatsana track 20, 21, Maphutseng track 9 (Appendix Fig. A.3, Appendix Table A.1), because they provide limited measurements. Furthermore, incomplete tracks cannot confidently be assigned to an ichnotaxon i.e., in this study, incomplete tracks were disregarded from landmark-based ichnotaxonomic assignment. Incomplete tracks considered in this study have varying morphological grades e.g., Phuthiatsana track 20 preserves two digit impressions, one of which is incomplete vs Tlapana track 1 which preserves two complete digit impressions with digital pads and claw marks (Appendix Fig. A.3). Some track parameters and the trackmaker's identity may be deduced from the latter track; therefore, measurements from incomplete tracks are considered in the analyses performed in this study. Tracks

with a morphological preservation grade of 0, like Phuthiatsana track 20, are inadequate for morphological analyses (Appendix Fig. A.3).

Statistical methods were applied to the upper Stormberg Group tridactyl track database, irrespective of individual track's anatomical fidelity, to observe trends within stratigraphic or size class groupings. To mitigate artefact-trends produced by the inclusion of lower morphological grade tracks, some statistical methods were only applied to the best tracks i.e., tracks with a defined morphology from which all track parameters could be measured (e.g., Appendix Tables A.5, A.6). This was done to assess the validity and refine trends observed when considering the entire Stromberg Group tridactyl track database (Figs. 6.5, 6.6; Tables 6.1, 6.3; Appendix Tables A.5, A.6).

7.1.2 Preservation style

As mentioned in section 2.2, fossil tracks can be preserved as true tracks (e.g., Phuthiatsana tracks 1–6; Fig. 4.8), natural casts (replicas of true tracks at the time of infilling; e.g., Tlapana track 8, Fig. 4.24) and undertracks, with the latter forming in response to the pressure exerted by the autopodia on the underlying unconsolidated sediment layers (Figs. 5.7). All three preservation styles are present at the upper Stormberg Group ichnosites in this study (Appendix Fig. A.3). Some of the tracks included in the database preserve their complete natural cast infilling and capture varying degrees of anatomical detail - e.g., Mafube track 5 preserves claw marks, while Upper Moyeni track 35 shows very little other than three digits (Appendix Fig. A.3). Because general dimensions and tridactyl morphologies are observable in these filled tracks, their measurements are still considered in the analyses. Many true tracks in the upper Stormberg Group database preserve partial natural cast infillings - e.g., Phuthiatsana track 8 (Appendix Fig. A.3), while others preserve extra-morphological features such as desiccation cracks (e.g., Maphusteng track 31, Subeng track 8, Mafube track 1; Appendix Fig. A.3) and bioturbation (e.g., Lephoto track 6; Appendix Fig. A.3) within the tracks. True tracks usually have the highest likelihood of preserving anatomical details such as claw marks and digital pad impressions (e.g., Maphutseng track 2, Appendix Fig. A.3), and in rare cases some true tracks preserve finer details like skin impressions (e.g., Currie *et al*., 1991; Gatesy, 2001; Milan, 2006; Kim *et al*., 2019). While skin impressions were not observed in any of the tracks considered in this study, they are known from the upper Stormberg Group (Dornan, 1908; Rampersadh and Bordy, 2019). Except for rare cases (e.g., Marchetti, 2019), undertracks are less detailed than true tracks (Nadon, 2001). Furthermore, undertrack linear dimensions are also subjected to an overall enlargement due to the radial transfer of pressure from the pes load. Moreover, undertracks have higher interdigital angles with broader and rounder digit morphologies (Avanzini *et al*., 2012). Consequently, the morphology and measured dimensions of undertracks need to be treated with caution. The lack of anatomical detail preserved in undertracks may have interesting implications for ichnotaxonomy; conventionally, tracks preserving

morphological detail are more confidently assigned to ichnotaxa but in the case of - e.g., *Therangospodus pandemicus* (Lockley *et al.*, 1998; Milan and Bromley, 2006) and *Kayentapus ambrokholohali (*Sciscio *et al.,* 2017)*,* the lack of additional morphological features such as digital pad impressions are used to define the ichnotaxon and ichnospecies, respectively. Although they lack morphological details such as pad impressions, the authors argue that the tracks preserve distinct morphologies sufficient to erect new ichnogenera and ichnospecies. In southern Africa, *K. ambrokholohali* is distinct from other *Kayentapus* isp e.g., at Tsikoane and Upper Moyeni (also see Fig. 4.22). Some of the isolated tracks considered in this study have round, robust digit morphologies, and it is ambiguous whether they are undertracks, erosional tracks or true track that can be attributed to ornithischian trackmakers (e.g., Phuthiatsana track 11; Appendix Fig. A.3). These tracks often lack additional anatomical features such as digital pad impressions and claw marks which may be consistent with undertracks but these are also the features destroyed early on by erosion. To mitigate the effects of warped undertrack dimensions in this study, ratio trends were considered in this study (e.g., TL/TW, Dp/TS and Dp/TL) to better understand morphological differences within the database. Additionally, the size of the database should reduce noise signals from possible undertracks, which are a minor component of the database.

7.1.3 Potential size bias

Track size and track depth play important roles in preservation potential; relative to larger/deeper impressions, shallower impressions are more susceptible to degradation (Gatesy, 2001; Henderson, 2006; Wiseman and de Groote, 2018). In a given substrate, smaller trackmakers are, relatively, more likely to leave lightly pressed impressions. However, the load (weight) a trackmaker exerts on a substrate is nota function of its size but also, for example, the morphology of its pes (and/or manus, Falkingham *et al*., 2011). Ichnological assemblages recorded at a tracksite will be biased towards the larger animals that the substrate can support. Therefore, it is likely that lower trackmaker diversities skewed towards larger body sizes may be inferred from the preserved fossil tracks. These size biases have been observed in the track record, and ichnosites where exclusively large tracks with a TL > 50 cm are preserved are assumed to represent substrate conditions where only animals above a certain threshold were able to generate distinct tracks (Falkingham *et al.,* 2011). These biases may be reduced if the substrate is exposed for an extended period allowing its mechanical properties to change. None of the tracksites described in this upper Stormberg Group study exclusively preserve tracks with a TL > 50 cm. Where larger tracks are preserved (e.g., Matobo, Tsikoane, Upper Moyeni), smaller tracks are also observed - e.g., 13.5 cm TL at Tsikoane, 15 cm TL at Upper Moyeni (Appendix Table A.1). Small tracks (TL < 15 cm) are not common at the tracksites considered in this study; most small tracks are

observed from a single site, the uEF Lephoto ichnosite, and were produced by three individuals (Appendix Fig. A.3; Appendix Table A.1; Abrahams *et al.,* 2017)

7.1.4 Distribution of tracks within the upper Stormberg Group

In the statistical analyses of the upper Stormberg Group track dataset, the tracks are viewed through two lenses: stratigraphic position (Late Triassic vs Early Jurassic) and size (irrespective of stratigraphic position). A flaw in the dataset is that the distribution of the collected track data is not consistent throughout the lEF, uEF and Clarens Formation. Most of the 216 tracks in the upper Stormberg Group database are from the uEF (50%) with only 15% of the tracks from the Clarens Formation (Appendix Table A.1). This imbalance may arise from a combination preservational biases (see section 7.1.5) and sampling biases (additional Clarens Formation sites are known from the literature but are not included in this study, e.g., Rampersadh and Bordy, 2019). Furthermore, the uEF has the highest proportion of tracks with a morphological preservation grade of 2 or more (67% vs the approximately 50% for both the lEF and CLAR; Appendix Table A.1). Consequently, the uEF has the highest percentage of measurable parameters such as TL, TS and Dp, which were shown to be paramount for morphological descriptions (94, 86, 82%, respectively; Figs. 6.3, 6.10, 6.11). This means that the best data, in terms of completeness of track parameters and usefulness for ichnotaxonomic assignment, are in the Lower Jurassic (particularly the uEF). This bias in the track data, which has been unaccounted for, may affect the interpretations made in section 4.4. Additional distribution inconsistencies are also noted within the stratigraphic horizons: the bulk of the uEF ichnosites are from the middle–upper sections of this stratigraphic unit, while the CLAR ichnosites are exclusively from the lowermost Clarens Formation. Therefore, there is limited track data the from the lower uEF and an absence of track data from middle–upper Clarens Formation. To circumvent the issues related to the stratigraphic distribution of track (in terms of number of tracks and stratigraphic position), additional sites in the lEF and CLAR need to be located or data from extensive track documentation by Ellenberger (1970, 1972) needs to be included into the database. Data included from Ellenberger (1970, 1972) would rely heavily on interpretative drawing thus introducing additional biases and complexities into the track observations interpretations. The Clarens Formation track data may also be bulked up by including data from basal Clarens Formation ichnosites Ha Talimo, Matsieng and Morija tentatively described by Rampersadh and Bordy (2019).

7.1.5 Palaeoenvironment

Track registration and preservation requires specific substrate conditions and rapid burial to prevent erosional reworking of the track-bearing sediments (section 2.2). Consequently, tracks are commonly preserved in environments where sediment accumulation occurs rapidly and periodically. During periods of non-deposition, the tracking surface is exposed allowing for tracks to be registered.

Dinosaur tracks in the upper Stormberg Group are frequently associated with sedimentary structures indicative of shallow-water conditions and subaerial exposure e.g., associated with ripple marked and desiccated surfaces (e.g., Lower Moyeni, Phuthiatsana, Lephoto, Subeng). Some palaeosurfaces e.g., Lephoto, Lower Moyeni, Mafube, preserve microbial mat textures which are thought to aid preservation through biostabilisation (Carvalho *et al.*, 2013).

The lEF, uEF and Clarens Formation were deposited under aridifying climatic conditions (section 2.1; Bordy *et al*., 2020b). The Elliot Formation reflects fluviolacustrine deposits while the Clarens Formation reflects wet to dry desert conditions. The lEF was deposited in mainly meandering fluvial systems during humid to semi-arid climatic conditions, while the uEF from in ephemeral water courses (stream, rivers) and lakes that were flash-flooding prone as is typical under semi-arid climatic conditions (Bordy *et al.,* 2004b; Bordy *et al*., 2020b). Unlike the lEF, the uEF deposits experienced extended periods of exposure evidenced by the common pedogenic alteration features (e.g., palaeosols, in situ pedogenic carbonates, root traces, desiccation cracks; Bordy *et al.,* 2004b; Bordy *et al*., 2020b). The seasonal flooding and exposure events of the uEF may have created more favourable conditions to register and preserve tracks than in the lEF. Furthermore, the uEF rock record, which encompasses 10 Ma of deposition relative to the 20 Ma of the lEF, has a higher resolution (Bordy *et al*., 2020). Additionally, the dramatic thinning of the Elliot Formation from south to north is more pronounced and variable for the lEF, which may suggest that parts of the lEF in the north are missing, affecting sampling (Bordy *et al.,* 2004a; Bordy and Eriksson, 2015; Bordy *et al*., 2020b). The Clarens Formation is subdivided into three zones, with the basal and upper zones having been interpreted as deposits of wetter aeolian systems with lakes (Beukes, 1970; Bordy and Head, 2018), which are more suitable for track registration and preservation. The Clarens Formation ichnosites reported in this study are exclusively from the lower Clarens Formation (zones B4 and B5 of Ellenberger, 1970), but Ellenberger (1970) did note some tracks from the middle Clarens Formation (zone B6), which he assigned to *Grallator molapoi* and *Kaintrisauropus morijiensis.* Given these environmental considerations, our skewed uEF dataset may not reflect a bias in sampling but rather a bias in preservation controlled by large-scale palaeoenvironmental conditions.

7.1.6 Are all the studied tridactyl tracks part of the K-GAE?

This study considered tridactyl tracks with a theropod affinity. This, in part, relied on an early, field-based qualitative assessment of the tracks: theropod tracks are classically gracile, elongate and have digits that taper to V-shaped tips. However, all tracks incorporated into this upper Stormberg Group tridactyl track database do not wholly meet these criteria - e.g., Ha Falatsa track 5, Maphutseng track 35 (Appendix Fig. A.3) and some have qualities reminiscent of ornithopod tracks e.g., Phuthiatsana track 13 (Appendix Fig. A.3). Distinguishing ornithopod and theropod tracks of a lower morphological

preservation quality is difficult (Moratalla *et al.,* 1988; Henderson, 2006b; Lallensack *et al*., 2016, Razzolini *et al.,* 2017). Henderson (2006b) has shown that erosion can alter theropod tracks to appear more ornithopod-like: during erosion, narrow and angular features such as claw marks and interdigital ridges are removed and sharp corners such as digit tips are rounded. The erosion model of Henderson (2006b) suggests that despite these morphological alterations, tracks retain their basic shape and dimensions (surface linear measurements vary by a few percentage). Consequently, theropod tracks should still be distinguishable from ornithopod tracks when considering various linear measurements. Therefore, tracks in this study that may preserve ornithpod features, can arguably still be considered theropod tracks i.e., Maphutseng track 35 and Phuthiatsana track 13 are not wider than they are long as is characteristic of ornithopod tracks (Appendix Table A.1). Because these rounded tracks are isolated tracks, it is difficult to discern whether their morphology is the result of erosion, substrate conditions, trackmaker behaviour or true reflection of the trackamker's autopod morphology.

Geometric morphometrics was employed to compare tracks with known ichnogenera. Many of the tracks in this study did not lie within the K-GAE morphospaces when using landmark-based PCA techniques but were still considered to be K-GAE based on visual assessments, e.g., tapering, V-shaped digit tips, and measured track parameters. The relatively large volume of the database should mitigate artefact signals from tracks that may not belong to the K-GAE spectrum.

7.1.7 Controls on track morphology

Track morphology is controlled by the trackmaker's autopod morphology (e.g., the track of a functionally tridactyl theropod will differ significantly from a pentadactyl sauropodomorph), its locomotory style (e.g., at higher speeds digit tips are more deeply impressed than at lower speeds) and the conditions of the substrate it interacts with (e.g., in semi-fluid, saturated mediums a trackmaker may "sink" allowing additional anatomical parts to interact with the substrate; section 2.2; Falkingham, 2014). Although substrate and locomotion independently affect track morphology, the two factors may also interact. For example, a trackmaker may adjust its locomotory style in response to variations in substrate consistency (Wilson et al., 2009) or larger trackmakers (TL > 25 cm) may move their feet backwards, slipping, generating sigmoidal striations prior to lifting their foot in softer substrates (Avanzini et al., 2012)..

7.1.7.1 Trackmaker

It is difficult to confidently ascribe a specific trackmaker to a track. In order to do so, tracks with a high morphological preservation grade that reflect the trackmakers anatomy are required, as well as numerous body fossils that record the autopod morphology of the trackmaker. It is assumed that tracks described herein are attributed to theropods. However, theropod body fossils are scarce in the Stormberg Group, which has yielded a few specimens of only two theropods: *Dracovenator* and

Megapnosaurus (previously *Syntarsus rhodesiensis*). A rigorous statistical study on K-GAE from the Newark Supergroup suggests that at least two distinct trackmakers produced GAE tracks and a third trackmaker produced *Kayentapus* (Farlow, 2018). The lack of osteological remains and poor morphological preservation grade of some of the studied tracks prevents confident linking of the tracks to a specific trackmaker taxa or attributing morphological variations to differences in trackmakers. Additional complications arise from the trackmaker dispute for *Eubrontes* (section 2.4).

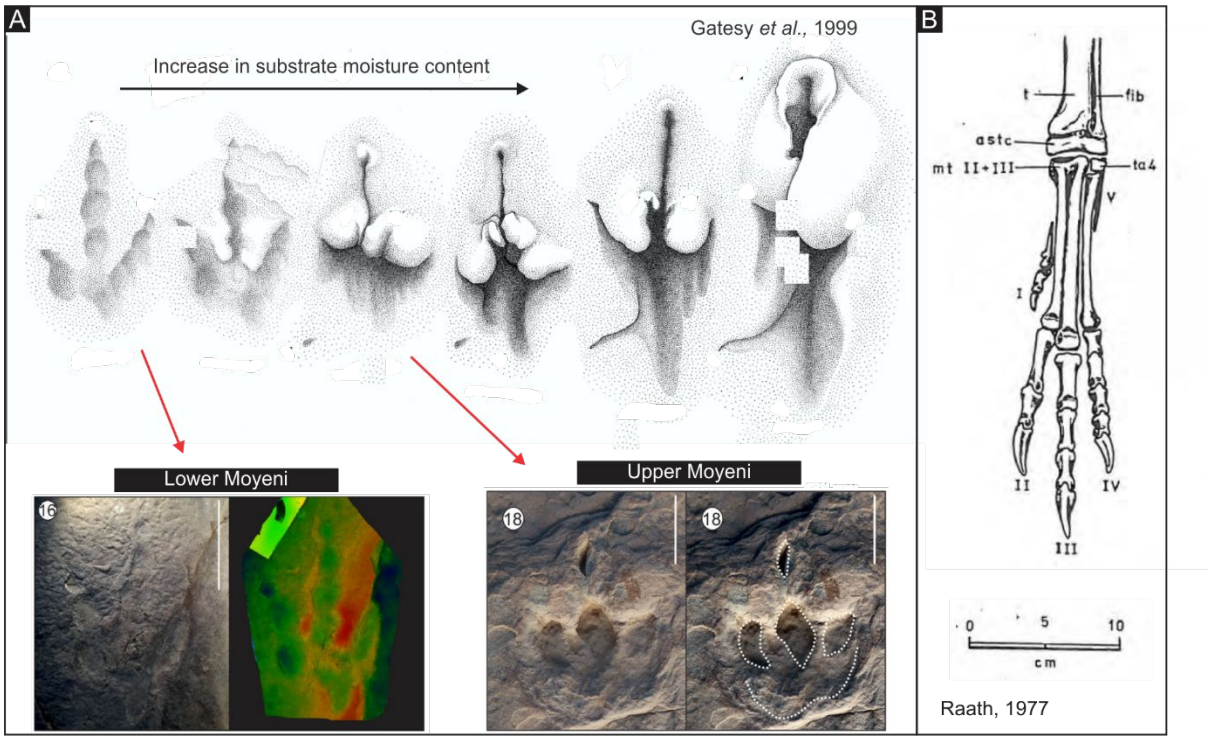

Figure 7.1: Track and pes morphologies. A) Morphological variation for a track specimen in different substrate conditions; B) Megapnosaurus rhodensiensis pes hplotype reconstruction.

7.1.7.2 Locomotion

In geological terms, footprint registration is instantaneous and may appear to be the product of a single movement. However, tracks represent a sequence of movements that can be divided into three phases: touch down, weight-bearing and kick-off (Avanzini, 1998; section 2.2). During each phase, different parts of the pes are functionally dominant (Fig. 2.3). For example, a deep digit III impression can be observed in the colour depth maps of some tracks (e.g., Lephoto tracks 1–6; Appendix Fig. A.3), which may reflect the kick-off phase. In some studies, the deepest penetration is observed in digit II (Avanzini, 1998); this is also observed in the Stormberg track dataset (e.g., Lower Moyeni tracks 6 and 16; Appendix Fig. A.3). For all digits, the distal tip is commonly the most deeply impressed (Gatesy, 2001). During the step cycle, there is an inward rotation of digit III, which is especially apparent in claw mark impressions (e.g., Tlapana track 6; Appendix Fig. A.3).

Theropods shared a common locomotory design and maintained conservative aspects to their locomotion throughout their evolution (Farlow *et al*., 2000). Most theropods were digitigrade bipeds with functionally tridactyl feet and fully adducted hindlimbs. Theropod track impressions typically preserve a digit III that is anteriorly projected with asymmetrical digit II and IV impressions noted in the "heel" region of the track. This asymmetry exists because the digit II and III metatarsophalangeal pads are constantly raised off the ground while the entire digit IV is impressed (Ellenberger, 1972; Farlow *et al.,* 2000). This asymmetrical character is also observed for basal ornithischian tracks - e.g., *Anomoepus* (Olsen and Rainforth, 2003), suggesting this may be a general feature for early dinosaurs. For theropods, the digit III midline corresponds to the walking axis of the trackmaker (Ellenberger, 1972) and the trackways are generally narrow, indicating that they walked with their feet near to the midline of their body. Theropods were striders as opposed to hoppers and general preferred a walking gait over a running gait (average of $\boldsymbol{\lambda}$/h = 1.3, Thulborn, 1984). Trackway evidence for running theropods is limited and typically restricted to small and medium sized trackmakers (e.g., Thulborn, 1990; Perez-Lorente, 2015; Abrahams *et al.*, 2017). In rare cases, tracks with whole metatarsus impressions (Thulborn and Wade, 1984; Pérez-Lorente, 2015) and quadrupedal trackways (Wright, 1996) have been attributed to theropods. A large proportion of dinosaur swim traces have also been attributed to theropod trackmakers (Milner and Lockley, 2016). The same, general locomotory trends, i.e., narrow trackways, walking gaits are observed in the southern African theropod tracks throughout the studied stratigraphic interval, from ,the Late Triassic to the Early Jurassic (Ellenberger, 1972). The isolated nature of the bulk of tracks in this study, among others, prevents the systematic assessment of the effect of locomotion on the track morphology. Trackways are present at the Lower Moyeni, Lephoto, Upper Moyeni, Tsikoane, Maphutseng, and Phuthiatsana ichnosites, but track morphology and gait appear to be consistent along these trackways (with the exception of the Lower Moyeni trackway as documented in Wilson *et al*., 2009).

7.1.7.3 Substrate

The grain size and moisture content of the tracking surface, at the time of track registration, are shown to be important factors affecting track registration and preservation (section 2.2, Fig. 7.1A). Furthermore, it has been highlighted that exposure time, prior to track burial, may play an important role in track preservation (Paik *et al.,* 2001; Milan, 2006). Various upper Stormberg Group tracks preserve desiccation cracks (Mafube track 1; Maphutseng track 31, Phuthiatsana tracks 1–6), overprinting (Tsikoane tracks 48, 49; Upper Moyeni tracks 11, 12), and invertebrate activity within the track (e.g., Lephoto track 6) indicative of track exposure (Appendix Fig. A.3). The effects of the exposure on the preservation grade has not been considered, though it is noted that the Mafube track and Phuthiatsana tracks 1–6 have high morphological grades (Appendix Table A.1).

Limited high-resolution sedimentological work was performed at each ichnosite to understand the substrate conditions (e.g., porosity) of the track-bearing sedimentary rocks. All tracking surfaces preserve ripple marks or desiccation cracks (or both), respectively indicating the presence of gentle currents and drying under subaerial conditions. Grain size variations, from very fine-grained to medium-grained sand, are noted at the different tracksites. Pitted textures, interpreted to be products of microbial activity, are sporadically preserved on the palaeosurfaces of some of the ichnosites considered in this study - e.g., Mafube (Sciscio *et al*., 2016), Lower Moyeni (Smith *et al*., 2009) and Lephoto (Abrahams *et al*., 2017). Microbial biofilms are known to aid track preservation as the mats stabilize substrates (increase sediment cohesion) and induce early cementation (e.g., Dai *et al.,* 2015; Sciscio *et al*., 2016). Furthermore, the nature of the mat (i.e., composition and thickness, in addition to the underlying sediments) introduces additional substrate complexities, which affect track registration and morphology if it predates the bioturbation (Marty *et al*., 2009; Carvalho *et al*., 2013; Dai *et al*., 2015). The timing of the microbial mats in the upper Stormberg Group vary - e.g., at Lower Moyeni and Lephoto the tracks do not preserve any pitted textures and seem to post-date the biofilm, while at Mafube, pitted textures are pervasive in some tracks. The effects these microorganisms had on the upper Stormberg Group tracks requires further investigation.

Although high resolution sedimentological assessments of the track-bearing rocks were not performed, significant differences in substrate conditions are observed in association with track morphology. Deep tracks are observed at Matobo and Upper Moyeni, which may reflect relatively wetter substrate conditions. In water-saturated substrates, trackmakers impress deeper into the substrate and interact with underlying sediments (see Chapter 5). This may allow additional anatomical features such as their raised digit I and metatarsals to interact with the substrate (Gatesy *et al.,* 1999; Rampersadh *et al.,* 2018). Tetradactyl tracks are not observed in this study, but metatarsal impressions are noted at Mafube and Tsikoane (tracks 2 and 34, respectively; Fig.5.5; Appendix Fig. A.3). Variations in substrate conditions from water-logged to firm are noted by Sciscio *et al.* (2016) at Mafube, though the metatarsal impression is associated with a clearly defined track and may be a resting trace rather than the product of substrate conditions. At Upper Moyeni, the deep tracks are associated with mud-collapse features (tracks 16–19, Appendix Fig. A.3). In semi-fluid to fluid substrates, surface sediments may collapse into the true tracks as the trackmaker removes its autopod during the step cycle, distorting and obscuring the track morphology (Fig. 6.1B; Milan, 2006; Milan and Bromley, 2006; Heurta *et al.,* 2012). Even if the tracks have ideal preservation conditions, the tracks will have minimal anatomical fidelity and can only be tentatively assigned to an ichnotaxon. In the case of the Upper Moyeni tracks, three digits could be discerned for three of the tracks and claw marks were evident on some of the medial digits. Expulsion rims, indicative of wet substrates and

formed when cohesive sediments are displaced due to the pressure exerted by the autopod, are observed at Upper Moyeni (e.g., track 6; Appendix Fig. A.3). Although not associated with the tridactyl tracks, expulsion rims associated with slipping traces are observed for some tetradactyl tracks on "section 1" at Phuthiatsana (Sciscio *et al.,* in review; Appendix Fig. A.3).

Considerations were made to mitigate the effects of substrate conditions on tracks. For example, tracks with poor morphological grade that occur in the pitted textured, saturated substrate at Mafube are omitted from this database (Sciscio *et al.,* 2016). Contrarily, the Upper Moyeni tracks which preserve extramorphological features were included in the database because the tracks with expulsion rims have clear morphologies and those with sediment-collapse features still have some measurable parameters. Although not linked to moisture content, Wilson *et al*. (2009) showed that the trackmaker of the Lower Moyeni trackway adjusted its locomotory style in response to the palaeosurface slope conditions. Consequently, only the first 8 tracks of the extensive trackway which terminates in a ripple marked surface, were considered in this study.

Although the importance of understanding the substrate conditions during track generation is well-established (for reviews, see Razzolini *et al.*, 2014; Sciscio *et al.*, 2016), in this study substrate conditions are only inferred from macro-observations - e.g., relative to Upper Moyeni where mud collapse and expulsion rim features are observed, the conditions at Maphutseng were "drier" based on the presence of digital pad and claw mark impressions and absence of soft sediment deformation features. To better understand the substrate conditions, thin sections of host rocks could have been studied to evaluate grain size and porosity in more detail (e.g., Razzolini *et al.*, 2014), but this level of investigation was beyond the scope of this project.

In summary, the upper Stormberg Group tridactyl tracks have variable morphological preservation grades, and while most tracks included in the database have theropod affinities, some may preserve ornithopod-like features. Footprint morphology is complex to account for: a) although field observations can shed light on the substrate controls on track morphology, detailed, high-resolution micro-morphological investigation is needed because small difference in substrate consistencies can affect track morphology, b) the effects of locomotory style on the upper Stormberg tracks is predominantly unknown because the tracks are primarily shallow and isolated, c) while trace and body fossil records ideally complement one another, the scarcity of theropod body fossils in the Stormberg Group limits the high fidelity identification of the potential trackmakers. However, a the functionally tridactyl pes reconstruction of *Megapnosaurus rhodisiensis* (previously *Syntarsus rhodensirensis*) in Raath (1977; Fig. 7.1B) is consistent with *Grallator:* TL< 15 cm, TL/TW of 2.1 and a Dp/TS of 0.76 and

1.18 (including and excluding the claw marks for TS, respectively). Furthermore, II^III<III^IV and LII:LIV is 1:1.

7.2 Theropod body size trends across the TJB

There is a direct link between TL and the body size of the trackmaker; hip heights (*h*) and body lengths (BL) can be estimated from TL (e.g., *h*= 4.5TL or h=3.06$TL^{1.14}$; BL= 4*h*(TL) or BL = 2*h* +3.5(TL); Thulborn, 1990). Therefore, the increase in TL observed across the upper Stormberg Group may reflect an increase in overall theropod body size from the Late Triassic to the Early Jurassic (Figs. 6.2, 6.5). Body size is an important biological parameter because of its correlation with metabolism, life history, speciation and evolutionary rates (Sereno, 1997). It is well established that dinosaur body sizes had a general increasing trend throughout the Mesozoic (e.g., Benson *et al*., 2014; McPhee *et al*., 2018; Fig. 7.2), though whether significant increases occurred at the TJB is contested (e.g., Olsen *et al.,* 2002; Griffin and Nesbitt, 2019). Benson *et al*. (2014) noted five sets of pivotal Late Triassic – Early Jurassic evolutionary shifts from small dinosaurian masses of approximately 10–35 kgs to large body masses in derived sauropodomorphs (>1 000 kgs), armored ornithischians and theropods. Comparing the body sizes of theropods like *Tyrannosaurus rex* and sauropods to modern carnivores and herbivores, respectively show similar outsizing disparities; therefore, there may be a link between sauropod gigantism and theropod gigantism (Sander and Clauss, 2008).

The ETE and TJB mark pivotal periods in dinosaur evolution and radiation. Unfortunately, an incomplete fossil record obscures the early evolution of large body sizes of theropod dinosaurs (Griffin, 2019). An abrupt, dramatic increase of 20% in maximum TL for theropod tracks after the ETE is noted in eastern North America, 10 000 years after the TJB(Olsen et al., 2002; Fig. 7.2A). This 20% increase in track size led these authors to hypothesise that the significant increase was a possible character release in surviving theropods following an "ecological release". Alternatively, although less favoured by the authors, they suggest that these larger predators may have migrated from different, unknown localities. Lucas *et al.* (2006) and Lucas and Tanner (2007a, b) contested the "ecological release" view, highlighting that "*Eubrontes"*-sized tracks, as defined by Olsen *et al*. (1998), are preserved in Triassic deposits elsewhere in the world. Triassic tracks, with lengths of 25–27 cm have a global distribution and are observed in western North America (Hunt and Lucas 2007), Europe (Bernadi *et al*., 2013), and Morocco (Langnaoui *et al*., 2012) and a very large 45 cm track has been described in Sweden in deposits that have been dated as Rhaetian using micro and macroflora (Niedzwiedzki, 2011). Based on these Triassic "*Eubrontes*"-sized tracks, Lucas *et al.* (2006) rejected the hypothesis by Olsen *et al.* (2002) that there was a sudden increase in theropod body size across the TJB. Instead, they advocated for a gradual increase in theropod track sizes across the TJB nullifying the "ecological

release" proposal (Fig. 7.2B). Olsen (2010) maintains that the "ecological release" hypothesis is valid, highlighting that it is based on a specific ichnospecies *Eubrontes giganteus* (Olsen *et al*., 1998). Tracks considered in the arguments of Lucas *et al*. (2006) and Lucas and Tanner (2007) are not classified as *Eubrontes giganteus* for the most part. Therefore, they do not nullify the hypothesis by Olsen *et al.* (2002) proposal. To base a global macroevolutionary process on a single ichnospecies in a small region (as per Olsen, 2010) would require further substation. Given that Lucas *et al*. (2006) consider a broader track database, we support their interpretation of body size increase across the TJB. Furthermore, it has been shown that the severity of the ETE on continental ecosystems was relatively low, at least on a global scale (Lucas and Tanner, 2015). Instead of a single, sudden extinction near the TJB, multiple extinctions more likely occurred in phases throughout the Norian (Late Triassic) to Hettangian (Early Jurassic; Lucas and Tanner, 2015).

Tracks with TL>25 cm and *Eubrontes*-like morphologies, are observed in Triassic deposits of the upper Stormberg Group. In this upper Stormberg Group study, TLs between 26–31 cm are observed at the Late Triassic Phuthiatsana ichnosite (Appendix Table A.1). Additional large southern African tracks, with a TL of 35 cm and TW between 25 and 26 cm, from Lower Qeme (Lesotho), which is most likely an uppermost Molteno Formation ichnosite, were described by Ellenberger (1972). Multiple attempts were made to relocate this site during this study but were unsuccessful. However, a well-preserved cast of the Qeme track was studied at the Morija Museum and Archives in Lesotho. Ellenberger (1972) assigned this track to *Qemetrisauropus princeps*, which was later synonymized with *Grallator* (Olsen and Galton, 1984). The digits of *Qemetrisauropus princeps* are stout and curved and preserve small claw marks. The robust nature of the digits, a TL/TW of ~1.4 and Dp/TW of 0.6 is more comparable with *Eubrontes* than *Grallator*.

The early evolution of theropod body size has historically been less well-understood than later in the Mesozoic when gigantic body sizes evolved. Early studies suggested that theropods remained small bodied (1–2 m) during the Triassic with larger bodied theropods becoming more common in the post-Triassic (e.g., Olsen *et al*., 2002; Brusatte *et al.,* 2010). However, osteological remains of large sized theropods are known from the Norian – *Liliensternus* with an estimated length of 5 m from Germany and *Gojirosaurus* with an estimated length of 5.5 m from USA (Welles, 1984; Rowe and Gauthier, 1990; Carpenter, 1997).

Recent ancestral body size reconstructions indicate that theropods evolved larger body sizes prior to the ETE but these larger bodied dinosaurs remained relatively rare until the Jurassic (Griffin and Nesbitt, 2019). These larger reconstructed theropod body sizes in the Late Triassic are consistent with body size estimates projected from the largest Triassic theropod tracks Olsen *et al.* (2002) considered.

However, Griffin and Nesbitt (2019) recently reviewed the bone morphology of the largest Triassic theropod skeletal remains and concluded that the Late Triassic body fossil record is dominated by specimens of young individuals with morphological and histological characters typical of immature ontogenetic stages. More specifically, although the largest Triassic theropod, *Gojisaurus*, is approximately 79% the size of the largest Early Jurassic theropod, the Late Triassic specimen was still in a rapid growth stage at the time of death. Therefore, the maximum body size estimates for Late Triassic theropods is underestimated for the osteological record, and if their entire growth is considered then "Jurassic"-sized theropods were already present in the Late Triassic (Griffin and Nesbitt, 2019).

Both the osteological and ichnological records indicate that larger theropods were present in Late Triassic ecosystems. Consequently, the shift in abundance of larger tracks during the Earliest Jurassic (e.g., Raath and Yates, 2005; Cook *et al*., 2009; Demathieu *et al.*, 2014; Sciscio *et al*., 2017b) cannot simply be attributed to the rapid evolution of large sized theropods in response to a mass extinction. The bias in the body and trace fossil record, i.e., the absence of the largest Triassic theropods, may be explained by high mortality rates i.e., mature, large theropods were rare and had a low likelihood of having their tracks and bones preserved (Griffin and Nesbitt, 2019). Though this is unlikely, as the bias should have persisted into the earliest Jurassic. The "jump" in body size across the TJB suggested by Olsen *et al*. (2002) is further contradicted by body size reconstructions by Irmis (2011), which illustrate large

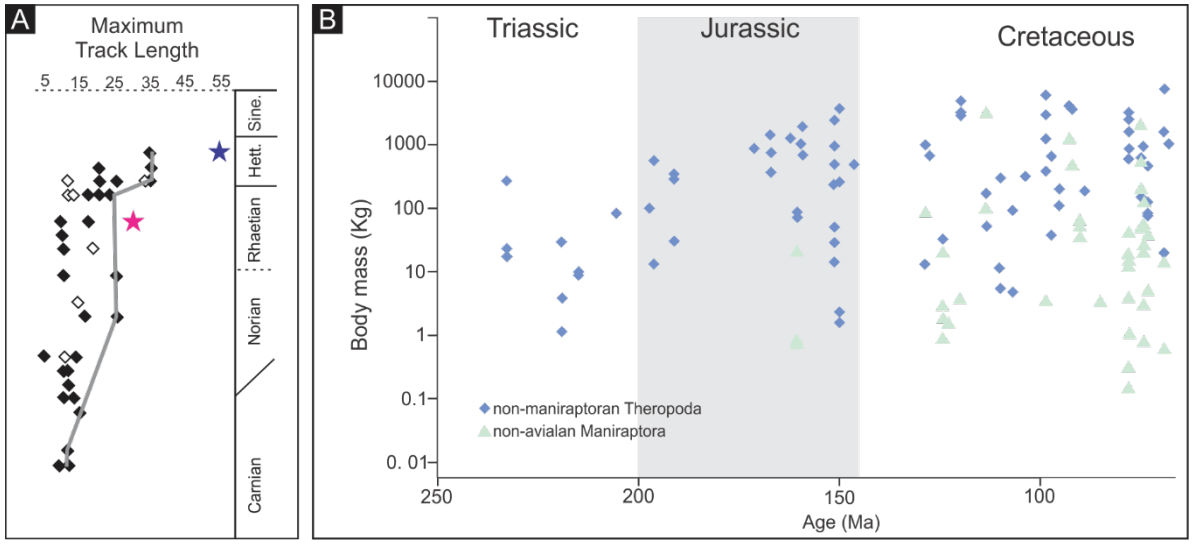

Figure 7.2: Global track and body size trends during the Late Triassic – Early Jurassic. A) Maximum TL for eastern North American GAE-plexus tracks (from Olsen et al., 2002) and the upper Stormberg tracks considered (marked by stars). B) Body size trends (Benson et al., 2014).

Theropods with femur lengths > 500 mm predating the TJB, and suggest a consistent, steady increase in dinosaur body size through the Late Triassic and Early Jurassic. While a maximum and mean body

size increase across the TJB is apparent, the magnitude of the increase is no greater than body size increases observed during the Late Triassic. The studies by Irmis (2011) and Griffin and Nesbitt (2019) are limited in sample size and do not explicitly invalidate the localized body size increase noted for the Newark Supergroup observed by Olsen *et al*. (2002). In the dataset considered for this study, tracks greater than 30 cm are almost exclusive to the Early Jurassic deposits (uEF and Clarens Formation; Appendix Table A.3). However, it should be considered that the abundance of larger (30–40 cm) tracks in the Early Jurassic may simply reflect an increase in the abundance of large theropods after the ETE and not an evolutionary trend (Brusatte *et al.,* 2008; Griffin and Nesbitt, 2019). Furthermore, the lEF is under-represented relative to the uEF, and an absence of larger tracks may be a sampling bias. To-date, theropod body fossils in the Stormberg Group are very rare and are relatively more abundant in the Lower Jurassic than in the Upper Triassic. Upper Triassic theropod remains are limited to isolated teeth (e.g., Ray and Chinsamy, 2002), while Lower Jurassic remains are primarily fragmentary or partial cranial material (e.g., Kitching and Raath, 1984; Smith and Kitching, 1997; Yates, 2005). Thus, theropod body fossils, due to their scarcity in the Stormberg Group, are not suitable for robust conclusions on theropod body size trends in southern Africa, and until new discoveries are made, they add little to the global body size trends across the TJB. The southern African tridactyl track record with theropod affinity is consistent with global observations, suggesting the presence of larger theropods in the Late Triassic and an increase in their abundance in the Early Jurassic.

As mentioned, the current dataset is limited, particularly with respect to samples from the lEF and Clarens Formation. It is possible to improve the sample size of this dataset by including observations from Ellenberger (1970, 1972, 1974) and his collection of cast materials housed at the Morija Museum and Archives, Lesotho and Université de Montpellier, France. Ellenberger (1970, 1972) performed detailed, descriptive documentation of tracks in Lesotho. His observations indicate that he too noted an increase in theropod track length across the Stormberg Group (Fig. 7.3). Considering Ellenberger's largest illustrated tridactyl tracks, there is an apparent maximum TL increase of ~ 15±3 cm from his 'lower Stormberg' (which includes the lEF and Molteno Formation) to the 'upper Stormberg (uEF–Clarens Formation). The large 'lower Stormberg' tracks 16, 17 and 25 (outlined in pink in Fig. 7.3) have TLs of 38, 35 and 32 cm, respectively, when measured directly from illustrations. Ellenberger (1972) quoted a TL of 35 cm for track 25, so an error of ±3 cm is assumed for all these measured TLs. The large TLs of tracks 16 and 17 are questionable given their illustrated morphologies. Track 16 is shown with an extended, tapering V-shaped heel which may be a metatarsal impression and track 17 has a dashed, instead of solid, outline suggesting there was a greater level of interpretive outlining. Therefore, the TLs of tracks 16 and 17 may be over estimations. Consequently, track 25's TL of 35 cm is interpreted to be the largest reliable TL for the 'lower Stormberg'. This TL is larger than the longest

track in the current database (i.e., maximum TL of 31 cm in track 21 from Phuthiatsana; Appendix Table A.1). The largest illustrated 'upper Stormberg' tracks of Ellenberger are from zones B/4 and B/5, which correspond to the uppermost uEF and basal Clarens Formation, respectively. Tracks 103, 105A, 105B, 124A and 126 have TLs of 36 (39), 32(35), 43(46), 39(42) and 50(53) cm, respectively. Additional maximum TLs between 36 and 40 cm from lower Clarens Formation ichnosites at Ha Talimo, Morija, Matsieng (Lesotho) are also noted by Rampersadh and Bordy (2019). These larger TLs are comparable with our observations where TLs of ~40 cm are more common in the uEF and Clarens Formation (e.g., tracks 8, 10, 23, 27, 31 from Tsikoane). Our observations surpass these TLs, with TL >50 cm recorded at Matobo and Upper Moyeni. The current upper Stormberg Group dataset and Ellenberger's dataset indicate the presence of TL >25 cm in the Late Triassic. The abundance of Tl>25 cm, maximum TL and mean TL increases across the TJB.

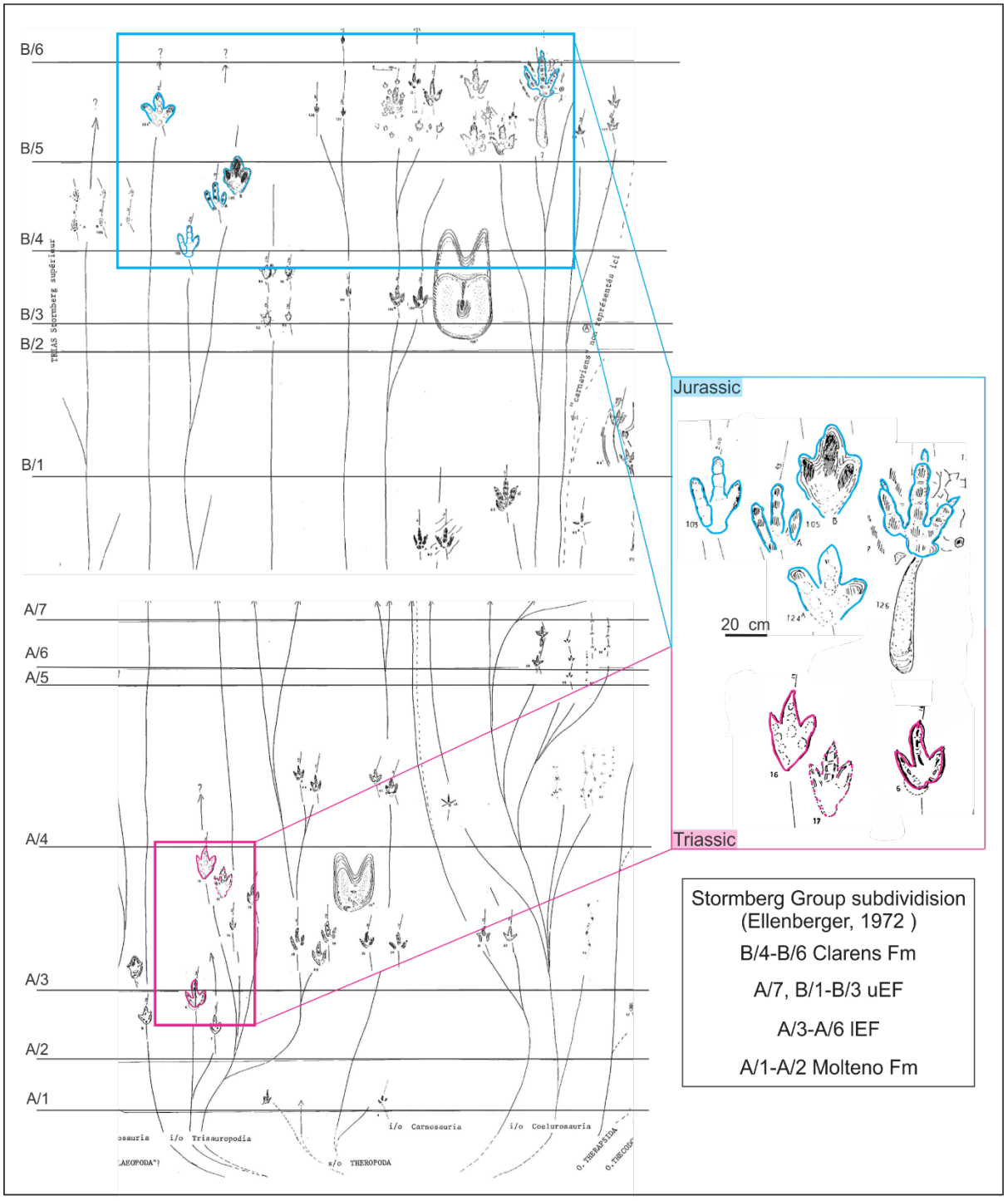

Figure 7.3: Trends in TL for theropod attributed tracks from the Molteno, Elliot and Clarens Formation with the largest tracks from the Triassic and Jurassic highlighted in pink and blue, respectively (modified after Ellenberger, 1972; pages 167–168).

7.3 The GAE morphological continuum

Most theropods (including terrestrial birds) and ornithopods have a functionally tridactyl pes where the medial digit is most prominent with subordinate lateral digits II and IV often having subequal digit lengths. The pes tracks of theropod dinosaurs have the simple morphology described above, but in some cases preserve the fourth digit (digit I or hallux; Xing *et al*., 2018; Rampersadh *et al*., 2018). Theropod tracks are globally common in the Late Triassic – Early Jurassic and are often assigned to the ichnogenera *Grallator*, *Anchisauripus* and *Eubrontes* (e.g., Thulborn, 1998; Gand *et al*., 2005; Rainforth, 2005; Cook *et al*., 2009; Demathieu *et al.*, 2014; Sciscio *et al*., 2016). With an increase in TL from *Grallator* to *Eubrontes*, tracks from the Newark Supergroup, USA, become relative wider, coupled with increasing digit width, and the medial digit projection relative to digits II and IV decreases (i.e., a positive correlation between track elongation and mesaxony; Olsen, 1980; Fig. 7.4; see section 2.3). The southern African tracks show similar trends: an apparent decrease in the mesaxony and a statistically relevant reduction in Dp relative to the TL as TL increases. It is worth noting that the TL/TW and Dp/Ts ratios of smaller and larger tracks from the upper Stormberg Group are not statistically distinct (Fig. 6.6). The TL/TW related to size findings of the upper Stormberg Group tracks is dissimilar from the observations of Lallensack *et al.* (2019), which indicate a correlation of the ratio with increasing TL for theropod tracks with a global distribution. We evaluated GAE comparative datasets, outlined in section 3.5, from the USA, Europe and Asia (Fig. 3.3.; see section 3.5 and reference list reference material) and the box and whiskers distributions of TL/TW by sizes also show a decrease in the median value but also show a strong overlap for TL/TW ratios within each grouping (Fig. 7.4). The Dp/TL decrease observed in the upper Stormberg dataset is more strongly attributed to an increase in TL than a decrease in Dp (Fig. 6.1). In fact, normalized Dp through time appears to only slightly increase (Fig. 6.3) and normalised Dp for different size groups shows no trend (Fig. 6.4). Similarly, Lallensack *et al.* (2019) did not observe a significant trend for Dp across the Late Triassic–Early Jurassic when considering globally distributed theropod and ornithischian tracks.

Lockley (2009) quotes the following TL/TW and Dp/TS ratios for the holotype *Grallator-Anchisauripus-Eubrontes* material: 2.64 (1.22), 1.9 (0.68) and 1.7 (0.58), respectively (Fig. 7.4). Compared to this data, the grallatoroid TL sized tracks in the upper Stormberg Group are less elongate and mesaxonic with a mean TL/TW of 1.4±0.37 and Dp/TS of 0.65±0.14, respectively. In the upper Stormberg, tridactyl tracks with TL between 15 and 25 cm, comparable to *Anchisauripus* TLs, are also less elongate than the North American holotype but to a smaller degree than the grallatoroid tracks (mean TL/TW of 1.31 and Dp/TS of 0.57). However, *Eubrontes* sized tracks in the upper Stormberg have more comparable dimensions to the North American holotypes, with a mean TL/TW of 0.53 and 0.5, and a mean Dp/TS of 0.53 and 0.53, for “large” and “huge” tracks, respectively (Fig. 6.6; Table 6.3). Similar observations are made

when only tracks with complete datasets are considered (Appendix Table A.8). These differences in the GAE spectrum may be why the southern African tracks were not discernable using Weems (1992) methods (Fig. 6.2)

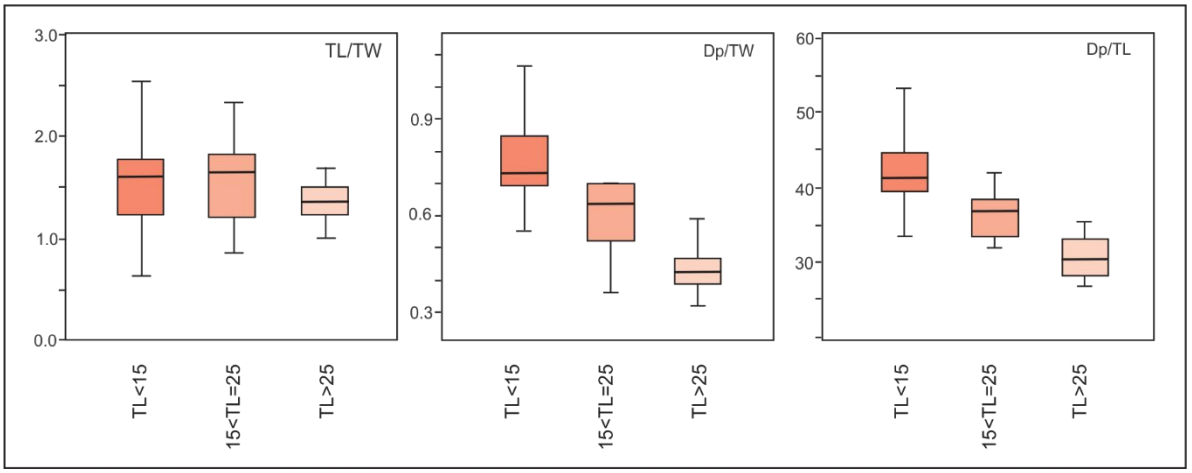

Figure 7.4: Global comparison of track ratio trends (TL/TW, Dp/TW and Dp/TL) through time (see reference list for source data).

The trends observed in the GAE plexus are observable globally universally for many Dinosauria through geological time. For example, in case of ornithopods, the Jurassic tracks (e.g., *Anomoepus*) are more gracile and mesaxonic relative to Cretaceous ornithopod tracks (Kim *et al.,* 2009; Lockley, 2009). During the Jurassic, there is no deviation from the allometric pattern observed for tridactyl track morphology - i.e., a reduction in track elongation and mesaxony as TL increases (Lockley, 2009). However, deviations from this trend are observed in the Cretaceous. Gracile *Grallator* and robust *Eubrontes* tracks co-occur with small and medium sized tridactyl tracks that have morphologies convergent with *Eubrontes* in the Cretaceous (Lockley, 2009). *Minisauripus*, a Cretaceous ichnogenus, is a small track (TL of 3 cm has been reported) that have TL/TW comparable with *Eubrontes* and weak mesaxony (Lockely *et al.,* 2008; Lockley, 2009). The *Minisauripus* trackmakers were themselves small; therefore, one can infer that the track widening and digit III shortening "trend" observed for the GAE plexus, miniaturised and applied to small Cretaceous dinosaurs. Given that the "trend" can operate independently of size, it suggests that not all morphological changes in the foot have a functional explanation (Lockley, 2009).

Track lengths have a direct relationship with limb length. As tracks become wider (with corresponding increases in TLs), limbs get longer. This relationship is observable in modern birds. It is worth noting that the relationship between the limb and foot is distinct from digital relationships within the foot (Lockley *et al.,* 2008; Lockley, 2009). Lockley (1999) has proposed that the widening of the pes, relative to the emphasis of digit III, is related to broadening trends observed in all the other organs. In narrow, gracile feet the elongation of the foot is focused towards the sagittal plane and is reduced in the lateral

digits II and IV, while in broader feet the elongation is focused on the parasagittal digits or the whole foot i.e., there is a loss of emphasis on the central digit III (Lockley, 2009). Reduced digit III projections would allow for a more equal distribution of weight stresses across the foot (this is observed in large sauropods, Lallensack *et al.,* 2019). The trend of broadening the foot and reducing mesaxony, as theropod body size increases, is likely related to an increase in relative length of the hindlimb and shortening and widening of the body (Thulborn, 1990; Bakker and Bir, 2004).

There are limited studies focusing on theropod pes functionality, which can be attributed to the scarcity of pedal osteological remains. Therefore, contextualising these track trends with functionality is difficult. Lallensack *et al.* (2019) highlights that digit III projection, which is arguably one of the most important parameter for theropod tracks, may be a proxy for cursorial ability, because cursors reduce central digit length with respect to track length to minimise surface traction. Claw mark lengths were not considered in this study but may warrant further investigation as Lallensack *et al.* (2019) found that claw mark impressions length decreased with an increase in TL, which may indicate increased specialization of theropod feet for locomotion.

8 Conclusion

The Stormberg Group in the main Karoo Basin encompasses the end-Triassic Mass Extinction event and encapsulates the early history of the origin and diversification of Dinosauria. Additionally, it preserves a rich assemblage of Dinosaurian osteological remains, primarily sauropodomorphs, and ichnofossils, primarily attributed to theropods. Consequently, the Stormberg Group offers the opportunity to examine and understand faunal changes across a period of major faunal devastation and recovery. This study presents the first absolute radiometric dates for the most prominent upper Stormberg Group ichnosites along with quantitative morphological trends for tridactyl tracks with a theropod affinity across the Triassic–Jurassic Boundary.

To date, the age of the Stormberg Group has largely focused on biostratigraphy and magnetostratigraphy. A Carnian age for the Molteno Formation and a Norian–Sinemurian age for the Elliot Formation were primarily interpreted from fossil evidence (e.g., Anderson and Anderson, 1983, 1984; Kitching and Raath, 1984; Lucas and Hancox, 2001; Knoll 2004, 2005; Labandeira *et al*., 2018). The Norian–Sinemurian age for the Elliot Formation is supported by a recent magnetostratigraphic study, which suggested a 219–213Ma for the lEF and a 195–190 Ma for the uEF (Sciscio *et al.,* 2017a). The upper limit of the Stormberg Group is tightly constrained by an absolute isotopic date of 183 Ma for the conformably overlying flood basalts of the Drakensberg Group (Duncan *et al.,* 1997). The maximum depositional ages interpreted in this study for the upper Stormberg Group are consistent with previous findings: predominantly Late Triassic (from 220 Ma) MDAs are interpreted for the lEF and Early Jurassic (from 201 Ma) MDAs are interpreted for the upper Elliot and Clarens Formations.

Over 200 tridactyl tracks with theropod affinity from the upper Stormberg Group were considered in this study to discern morphological trends: a) across the TJB and b) within the *Grallator-Anchisauripus-Eubrontes* plexus, which is largely defined by track length. The following observations were made for this southern African tridactyl track record:

From the Late Triassic to Early Jurassic, there is an increase in track length, an apparent decrease in Dp/TS and a statistically distinct decrease in Dp/TL. These differences are most easily seen when comparing tracks from the lEF to the Clarens Formation, which tend to show distinct groupings with the lEF track dimensions being relatively smaller than those of the Clarens Formation. The uEF data is variable and spans that of the lEF and Clarens Formation, resulting in it being indistinguishable within the upper Stormberg Group. An apparent decrease in Dp/TS and a statistically relevant decrease in Dp/TL is also noted across different size class groupings (i.e., GAE plexus) from TL< 15 cm to TL>40 cm, independent of their stratigraphic position. The parallel between Dp/TS and Dp/TL trends across time and across the GAE plexus, brings into question whether the trends reflect changes across the TJB or are simply an artefact of the Lower Jurassic strata more commonly preserving larger track lengths.

However, when comparing track data from different size classes across the TJB similar observations are made: a decrease Dp/TS and Dp/TL is noted for both TL<25 cm and 25<TL<40 cm size groupings. This suggests that the decrease in these ratios across the TJB may be a true morphological change with time affecting both small and large theropods.

Tracks on the GAE spectrum from southern Africa differ to their North American counterparts. With an increase in size (TL), the North American tracks display a clear decrease in elongation (TL/TW). This trend is not distinctly observed for the southern African tracks because the TL/TW ratio data is widespread within size class groupings and overlaps significantly between the size classes. The lack of a clear elongation trend may be due to the southern African *Grallator* and *Anchisauripus* having smaller TL/TW (and Dp/TS) ratios relative to the North American tracks, while the *Eubrontes* dimensions are more comparable to global observations. Reduced TL/TW ratios for smaller TLs in southern Africa results in a more plateau-like distribution, rather than a clear decrease, when compared to *Eubrontes* tracks.

The refinement of the chronostratigraphic framework of the key ichnosites in the upper Stormberg Group presented within this thesis advances the understanding of approximate rates of faunal changes within the Karoo Supergroup and aids with global comparison of similarly aged, fossiliferous units globally. Furthermore, the upper Stormberg Group tracks have proven to be useful proxies to tease out trends in theropod autopod changes with time, across the TJB, which is especially useful in strata, like the Stormberg Group, where osteological remains of theropods are scarce.

END

9 Reference list

Abdala, F., Damiani, R., Yates, A., Neveling, J. 2007. A non-mamaliaform cynodont from the Upper Triassic of South Africa: a therapsid Lazarus taxon? *Paleontologia Africana*, 42:17–23.

Abrahams, M. 2015. The stratigraphic value of the Pronksberg bentonite in the upper Elliot Formation (Early Jurassic) Eastern Cape, South Africa. BSc(Honours) thesis (unpublished), University of Cape Town, 50p.

Abrahams, M., Bordy, E.M., Sciscio, L., Knoll, F. 2017. Scampering, trotting, walking tridactyl bipedal dinosaurs in southern Africa: ichnological account of a Lower Jurassic palaeosurface (upper Elliot Formation, Roma Valley) in Lesotho. *Historical Biology*, 29: 958–975.

Alexander, RMcN. 1976. Estimates of speeds of dinosaurs. *Nature*. 261:129–130.

Ambrose, D. 2003. A note on fossil trackways at Roma, Lesotho. Lesotho miscellaneous documents No 4, House 9 publications Roma, 14p.

Anderson, H.M., Anderson, J.M. 1970. A preliminary review of the biostratigraphy of the uppermost Permian, Triassic and lowermost Jurassic of Gondwanaland. *Palaeontologia Africana*, 13: 1–22.

Anderson, J.M., Anderson, H.M. 1983. Palaeoflora of southern Africa Molteno Formation (Triassic), A.A Balkema, Rotterdam, The Netherlands, 1, P. 227

Anderson, J.M., Anderson, H.M. 1984. The fossil content of the Upper Triassic Molteno Formation, South Africa. *Palaeontogia Africana*, 25: 39–59.

Anderson, J.M., Anderson, H.M., Cruickshank A.R.I. 1998. Late Triassic ecosystems of the Molteno/Lower Elliot biome of Southern Africa. *Palaeontology,* 41: 387–421.

Avanzini, M. 1998. Anatomy of a footprint: Bioturbation as a key to understanding dinosaur walk dynamics. *Ichnos*, 6: 129–139.

Avanzini, M., Piñeula, L., Garcia-Ramos, J.C. 2012. Late Jurassic footprints reveal walking kinematics of theropod dinosaurs. *Lethaia,* 45: 238–252.

Avnimelech, M.A. 1966. Dinosaur tracks in the Judean Hills. Proceedings of the Israel Academy of Sciences and Humanities, Section of Sciences, 1:1–19.

Baez, A.M., Marsicano, C.A. 2001. A heterodontosaurid ornithischian dinosaur from the Upper Triassic of Patagonia. *Ameghiniana*, 38: 271 – 279.

Baird, D. 1957. Triassic footprint faunules from Milford, New Jersey. *Bulletin of the Museum of comparative zoology, Harvard University,* 117: 449–520.

Baird, D. 1980. A prosauropod dinosaur trackway from the Navajo sandstone (Lower Jurassic) of Arizona. *In*: Jacobs, L.L. (*Ed*): Aspects of Vertebrate History, 219–230, Museum of Northern Arizona Press, Flagstaff.

Bakker, R.T., Bir, G. 2004. Dinosaur crime science investigations: theropod behavior at Como Bluff, Wyoming and the evolution of birdness. In: Currie, P.J., Koppelhaus, E.B., Shuga, M.A., Wright, J.L. (*Eds*): Feathered dragons – Studies on the transition from the Dinosaurs to Birds, 301–342, Indiana University Press, Indiana.

Bakker, R.T., Galton, P.M. 1974. Dinosaur monophyly and a new class of vertebrates. *Nature*, 248: 168–172.

Barco J.L. Canudo, J.I., Ruiz-Omenaca J.I. 2006. New Data on *Therangospodus oncalensis* from the Berriasian Fuentesalvo Tracksite (Villar del Río, Soria, Spain): An Example of Gregarious Behaviour in Theropod Dinosaurs. *Ichnos*, 13: 237–248.

Baron, M.G., 2019. *Pisanosaurus mertii* and the Triassic ornithischian crisis: could phylogeny offer a solution? *Historical Biology*, 31: 967–981. https://doi.org/10.1080/08912963.2017.1410705

Baron, M.G., Norman, C.B., Barret, P.M. 2017. A new hypothesis of dinosaur relationships and early dinosaur evolution. *Nature*, 543: 501–513.

Bates, K.T., Rarity, F., Manning, P.L., Hodgetts, D., Vila, B., Oms, O., Galobart, A., Gawthorpe, R.L. 2008. High-resolution LiDAR and photogrammetric survey of the Fumanya dinosaur tracksites (Catalonia): implications for the conservation and interpretation of geological heritage sites. *Journal of the Geological Society,* 165: 115–127.

Bates, K.T., Falkingham, P.L., Hidgetts, D., Farlow, J.O., Breithaupt, B.H., O'Brien, M., Matthews, N., Sellers, W.I., Manning P.L. 2009. Digital imaging and public engagement in palaeontology. *Geology Today*, 25: 134–139.

Belvedere, M. 2008. Ichnological researches on the Upper Jurassic dinosaur tracks in the Iouaridene area (Demnat, Central High-Atlas, Morocco). PhD thesis (unpublished), Universita Degli Studi Di Padova, 121p.

Belvedere, M., Bennet, M.R., Marty, D., Budka, M., Reynolds, S.C., Bakirov, R. 2018. Stat-tracks and mediotypes: powerful tools for modern ichnology based on 3D models. *PeerJ* 6:e4247; DOI 10.7717/peerj.4247.

Belvedere, M., Farlow, J.O. 2016. A Numerical Scale for Quantifying the Quality of Preservation of Vertebrate Tracks. *In*: Falkingham, P.L., Marty, D., Richter, A. (*Eds*): Dinosaur tracks: the next steps, 93–98, Indiana University Press, Bloomington and Indianopolis.

Belvedere, M., Jalil, N., Breda, A., Gattolin, G., Bourget, H., Khaldoune, F., Dyke G.J. 2013. Vertebrate footprints from the Kem Kem beds (Morocco): A novel ichnological approach to faunal reconstruction. *Palaeogeography, Palaeoclimatology, Palaeoecology*, 383–384: 52–58.

Benson, R.B.J., Campione, N.E., Carrano, M.T., Mannion, P.G., Sullivan, C., Upchurch, P., Evans, D.C. 2014. Rates of dinosaur bdy mass evolution indicate 170 million years of sustained ecological innovation on the avian stem lineage. *Plos bio,* 12: e1001853. doi:10.1371/journal.pbio.1001853.

Benton, M.J. 1983. Dinosaur success in the Triassic; a noncompetitive ecological model. *The quarterly Review of Biology*, 58: 29–55.

Benton, M.J. 2004. Origin and relationships of Dinosauria. In: Weishampel, D.B., Dodson, P., Osmolska, H. (*Eds*): The Dinosauria, 7–19, University of California Press, Berkely.

Bernardi, M., Gianolla, P., Petti, F.M., Mietto, P., Benton, M.J. 2018. Dinosaur diversification linked with the Carnian Pluvial Episode. *Nature Communications*, 9:1499 DOI: 10.1038/s41467-018-03996-1

Bernadi, M, Petti, F.M., Porchetti, S.D., Avanzini, M. 2013. Large tridactyl footprints associated with a diverse ichnofauna from the Carnian of Southern Alps. *New Mexico Museum of Natural History and Science Bulletin*, 61: 48–54.

Beukes, N.J. 1970. Stratigraphy and sedimentology of the Cave Sandstone stage, Karoo System. In: *Proceedings 2nd IUGS Symposium on Gondwana Stratigraphy and Palaeontology*, Pretoria, CSIR, 321–341.

Blewett, S.C., Phillips, D., Matchan, E.L. 2019. Provenance of Cape Supergroup sediments and timing of Cape Fold Belt orogenesis: Constraints from high-precision $^{40}Ar/^{39}Ar$ dating of muscovite. *Gondwana Research,* 70: 201–221.

Bock, W. 1952. Triassic reptilian tracks and trends of locomotive evolution. *Journal of Paleontology,* 26: 395– 433.

Bonnan, M.F., Senter, P. 2007. Were the basal sauropodomorphs dinosaurs *Plateosaurus* and *Massospondylus* habitual quadrupeds? *Special papers in Palaeontology*, 77: 139–155.

Bordy, E.M. 2008. Enigmatic trace fossils from the Lower Jurassic Clarens Formation, southern Africa. *Palaeontologia Electronica.* 11/3, 16A. 16p.

Bordy, E.M., Abrahams, M. 2016. Geochemistry of the Pronksberg bentonite of the upper Elliot Formation (Early Jurassic), Eastern Cape, South Africa. *In*: Linol, B., de Wit, M.J. (*Eds*): Origin and evolution of the Cape Mountains and Karoo Basin, 119–127, Springer International Switzerland.

Bordy, E.M., Abrahams, M., Sciscio, L. 2017. The Subeng vertebrate tracks: stratigraphy, sedimentology and a digital archive of a historic Upper Triassic palaeosurface (lower Elliot Formation), Leribe, Lesotho (southern Africa). *Bollettino della Societa Paleontologica Italiana*, 56: 181–198. doi:10.4435/BSPI.2017.12

Bordy, E.M., Abrahams, M., Sharman, G.R., Viglietti, P.A., Benson, R.B.J., McPhee, B.W., Barrett, P.M., Sciscio, L., Condon, D., Mundil, R., Rademan, Z, Jinnah, Z., Clark, J.M., Suarez, C.A., Chapelle, K.E.J., Choiniere, J.N. 2020b. A chronostratigraphic framework for the upper Stormberg Group: implications for the Triassic Jurassic boundary in southern Africa. Earth Science Reviews, doi.org/10.1014/j.earscirev.2020.103120.

Bordy, E.M., Brumby, A.J., Catuneanu, O., Eriksson, P.G. 2009. Possible trace fossils pf putative termite origin in the Lower Jurassic (Karoo Supergroup) of southern Africa. *South African Journal of Science*, 105: 356–362.

Bordy, E.M., Catuneanu, O. 2001. Sedimentology of the upper Karoo fluvial strata in the Tuli Basin, South Africa. *African Earth Sciences*, 33: 605–629.

Bordy, E.M., Hancox, P.J., Rubidge, B.S. 2004a. Basin development during the deposition of the Elliot Formation (Late Triassic – Early Jurassic), Karoo Supergroup, South Africa. *South African Journal of Geology*, 107: 397–412.

Bordy, E.M., Hancox, P.J. and Rubidge, B.S. 2004b. Fluvial style variations in the Late Triassic-Early Jurassic Elliot formation, main Karoo Basin, South Africa. *Journal of African Earth Sciences*, 38: 383–400.

Bordy, E.M., Hancox, P.J., Rubidge, B.S. 2004c. Provenance Study of the Late Triassic – Early Jurassic Elliot Formation, main Karoo Basin, South Africa. South African. *South African Journal of Geology*, 107: 587–602.

Bordy, E.M., Hancox, P.J., Rubidge, B.S. 2005. The contact of the Molteno and Elliot formations through the main Karoo Basin, South Africa: A second-order sequence boundary. *South African Journal of Geology*, 108: 351–364.

Bordy, E.M, Head, H.V. 2018. Lithostratigraphy of the Clarens Formation (Stormberg Group, Karoo Supergroup), South Africa. *Geological Society of South Africa*, 121: 119–130.

Bordy, E.M., Rampersadh, A., Abrahams, M., Lockley, M.G., Head, H.V. 2020a. Tracking the Pliensbachian–Toarcian Karoo firewalkers: Trackways of quadruped and biped dinosaurs and mammaliaforms. *Plos one*, 15:e0226847.

Botha, B.J.V., Theron, J.C. 1967. New evidence for the early commencement of Stormberg volcanism. *Tydskrif Natuurwet*, 6: 496–573.

Bowring, S.A., Schoene, B., Crowley, J.L., Ramezani, J., Condon D.J. 2006. High-precision U-Pb zircon geochronology and the stratigraphic record: progress and promise. *Paleontological Society Papers.* 11: 23–43.

Bristowe, A., Raath, M.A. 2004. A juvenile coelophysoid skull from the Early Jurassic of Zimbabwe, and the synonymy of *Coelophysis* and *Syntarsus*. *Palaeontologia Africana*, 40: 31–41.

Brusatte, S.L., Benton, M.J., Ruta, M., Lloyd, G.T. 2008. The first 50 Myr of dinosaur evolution: macroevolutionary pattern and morphological disparity. *Biology letters,* 4: 711–736. doi:10.1098/rsbl.2008.0441

Brusatte, S.L., Nesbitt, C.J., Irmis, R.B., Butler, R.J., Benton, M.J., Norrel, M.A. 2010. The origin and early radiation of dinosaurs. *Earth Science Reviews*, 101: 68–100. https://doi.org/10.1016/j.earscirev.2010.04.001

Brusatte, S.L., Niedzwiedzki, G., Butler, R.J. 2011. Footprints pull origin and diversification of dinosaur stem lineage deep int Early Triassic. *Proceedings of the Royal Society*, 278: 1107–1113.

Buckland F., 1875. Log-book of a Fisherman and Zoologist. Chapman and Hall, London.

Burret, C., Zaw, K., Meffre, S., Lai, C.K., Khositanont, S., Chaodumrong, P., Udchachon, M., Enkins, S., Halpin, J. 2014. The configuration of greater Gondwana – Evidence from LA-ICPMS, U-Pb geochronology of detrital zircons from the Palaeozoic and Mesozoic of Southeast Asia and China. *Gondwana Research,* 26: 31–51.

Butler, R.J., Smith, R.M.H., Norman, D.B. 2007. A primitive ornithischian dinosaur from the Late Triassic of South Africa, and the early evolution and diversification of Ornithischia. *Proceedings of the Royal Society London*, 274: 2041–2046.

Cadle, A.B., Cairncross, B., Christie, A.D.M., Roberts, D.L. 1993. The Karoo Basin of South Africa: type basin for the coal-bearing deposits of southern Africa. *International Journal of Coal Geology*, 23: 117–157.

Cairncross, B. 2001. An overview of the Permian (Karoo) coal deposits of southern Africa. *Journal of African Earth Science*, 33: 529–562.

Cairncross, B., Anderson, J.M., Anderson, H.M. 1995. Palaeoecology of the Triassic Molteno Formation, Karoo Basin, South Africa – sedimentological and palaeontological evidence. *South African Journal of Geology*, 98: 452–478.

Carpenter, K. 1997. A giant coelophysoid (*Ceratosauria*) theropod from the Upper Triassic of New Mexico, USA. *Neues Jahrbuch fur Geologie und Palaontologie Abhandlungen*, 205: 189–208.

Carvalho, I.S., Borghi, L., Leonardi, G. 2013. Preservation of dinosaur tracks induced by microbial mats in the Sousa Basin (Lower Cretaceous), Brazil. *Cretaceous Research*, 1–10. http://dx.doi.org/10.1016/j.cretres.2013.04.004

Castanera, D., Pascual, J.I., Canudo, N., Hernandez., Barco, J.L. 2012. Ethological variations in gauge in sauropod trackways from the Berriasian of Spain. *Lethaia*, 45: 476–489.

Castanera, D., Colmenar, J., Saque, V., Canudo, J.I. 2015. Geometric morphometric analysis applied to theropod tracks from the Lower Cretaceous (Berriasian) of Spain. *Palaeontology*, 58: 183–200.

Castanera, D., Piñuela, L. and Garcia-Ramos, J.C. 2016. *Grallator* theropod tracks from the Late Jurassic of Asturias (Spain): ichnotaxonomic implications. *Spanish Journal of Palaeontology,* 31: 283–296.

Catuneanu, O. 2004. Basement control on flexural profiles and the distribution of foreland facies: the Dwyka Group of the Karoo Basin, South Africa. *Geology,* 32: 517–520.

Catuneanu, O., Hancox, P.J., Rubidge, B.S. 1998. Reciprocal flexural behaviour and contrasting stratigraphies: a new basin development model for the Karoo retroarc foreland system. South Africa. *Basin Research*, 10: 417–439.

Catuneanu, O., Wopfner, H., Eriksson, P.G., Cairncross, B., Rubidge, B.S., Smith, R.M.H., Hancox, P.J. 2005. The Karoo basins of south-central Africa. *Journal of African Earth Sciences*, 43(1): 211–253.

Cawood, P.A., Nemchin, A.A. 2000. Provenance record of a rift basin: U/Pb ages of detrital zircons from the Perth Basin, Western Australia. *Sedimentary Geology*, 134: 209–234.

Chapelle, K.E.J., Barret, P.M., Botha, J., Choiniere, J.N. 2019a. *Ngwevua intloko*: a new early sauropodomorph dinosaur from the Lower Jurassic Elliot Formation of South Africa and comments on cranial ontogeny in *Massospondylus carinatus. PeerJ*, 7:e7240.

Chapelle, K.E., Benson, R.B., Stiegler, J., Otero, A., Zhao, Q., Choiniere, J.N. 2019b. A quantitative method for inferring locomotory shifts in amniotes during ontogeny, its application to dinosaurs and its bearing on the evolution of posture. *Palaeontology*. https://doi.org/10.1111/pala.12451

Charig, A.J. 1984. Competition between therapsids and archosaurs during the Triassic Period: a review and synthesis of current theories. *In:* Ferguson, M.W.J. (*Ed):* The structure, development and evolution of reptiles. Symposia of the Zoological Society of London, 52: 597–628, London.

Cole, D.I. 1992. Evolution and development of the Karoo Basin. *In*: De Wit, M.J., Ransome, I.G.D. (*Eds*). Inversion Tectonics of the Cape Fold Belt, Karoo and Cretaceous Basins of Southern Africa, Balkema, 97–99, Rotterdam, Netherlands.

Cook, A.G., Saini, N., Hocknull, S.A. 2009. Dinosaur footprints from the lower Jurassic of Mount Morgan, Queensland. *Memoirs of the Queensland Museum – Nature*, 55: 13 –146.

Cooper, M.R. 1981. The prosauropod dinosaur *Massospondylus carinatus* Owen from Zimbabwe: Its biology, mode of life and phylogenetic significance. *Occasional Papers of the National Museums and Monuments, Rhodesia*, 6: 690–840.

Coutts, D.S., Matthews, W.A. and Hubbard, S.M. 2019. Assessment of widely used methods to derive depositional ages from detrital zircon populations. *Geoscience Frontiers,* https://doi.org/10.1016/j.gsf.2018.11.002

Currie, P.J. 1989. Dinosaur footprints of western Canada. *In*: Gillette, D.D., Lockley. M.G. (*Eds)*: Dinosaur tracks and traces, 293–300, Cambridge University Press, Cambridge, UK.

Currie, P.J., Nadon, G.C., Lockley, M.G. 1991. Dinosaur footprints with skin impressions from the Cretaceous of Alberta and Colorado. *Canadian Journal of Earth Science*, 25: 102–115.

Dai, H., Xing, L., Marty, D., Zhang, J., Persons IV, W.S., Hu, H., Wang, F. 2015. Microbially-induced sedimentary wrinkle structures and possible dinosaur impact of microbial mats for the enhances preservation of dinosaur tracks from the Lower Cretaceous Jiaguan Formation near Qijiang (Chongqing, China). *Cretaceous Research*, 53: 98–109.

Day, J.J., Norman, D.B., Gale, A.S., Upchurch, P., Powell, H.P. 2004. A middle Jurassic dinosaur trackway site from Oxfordshire, UK. *Palaeontology*, 47:319–348.

Demathieu, G.R. 1970. Les empreintes des pas de vertebres du Trias de la bordure nord-est du Massif Central. *Paleontology*. C.N.R.S. 1–211.

Demathieu, G., Gand, G., Sciau, J., Freytet, P. 2014. Les Traces de pas de Dinosaures et autres Archosaures du lias inferieur des Grands Causses, Sud de la France. *Palaeovertebrata, Montpellier*, 31: 1 – 143.

de Valais S., Melchor R.N. 2008. Ichnotaxonomy of bird-like footprints: an example from the Late Triassic-Early Jurassic of Northwest Argentina. *Journal of Vertebrate Paleontology*, 28 :14–159.

Diamini, R. 2004. Temnospondyls from the Beaufort Group (Karoo Basin) of South Africa and their biostratigraphy. *Gondwana Research*, 7: 165–173.

Dickinson, W.R., Gehrels, G.E. 2009. Use of U-Pb ages of detrital zircons to infer maximum depositional ages of strata: A test against a Colorado Plateau Mesozoic database. *Earth and Planetary Science Letters*, 288: 115–125.

D'Orazi Porchetti, S., Bernadi, M., Cinquegranelli, A., dos Santos, V.F., Marty, D., Petti, F.M., Sa Caetano, P., Wagensommer, A. 2016. A review of the dinosaur track record from Jurassic and Cretaceous shallow marine carbonate depositional environments. *In*: Falkingham, P. Marty, D., Richet, A. (*Eds*): Dinosaur tracks- the next steps, 380–392, Indiana University Press, Bloomington and Indianapolis.

Dornan S.S. 1908. Notes on the geology of Basutoland. *Geological Magazine* (UK), 5: 57–63.

Duncan, R.A., Hooper, P.R., Rehacek, J., Marsh, J.S., Duncan, A.R. 1997. The timing and duration of the Karoo igneous event, southern Gondwana. *Journal of Geophysical Research: Solid Earth*, 102:18127–18138.

Ellenberger P. 1955. Note preliminaire sur les pistes et les restes osseuex de vertebres du Basutoland (Afrique du Sud). *Comptes Rendus des Seances de l 'Academie des Sciences (FR*), 240: 889–891.

Ellenberger, P. 1970. Les niveaux paléontologiques de première apparition des mammifères primordiaux en Afrique du Sud et leur ichnologie. Establissement de zones stratigraphique détaillées dans le Stormberg du Lesotho (Afrique du Sud) (Trias superior a Jurassique). *Proceedings and Papers of thesecond Gondwana Symposium*. 343–370.

Ellenberger, P. 1972. Contribution à la classification des Pistes de Vértebrés du Trias: les Stormberg d'Afrique du Sud (I). *Paleovertebrata, Memoire Extraordinaire 1972, Montpellier*. 152p.

Ellenberger, P. 1974. Contribution a la classification des pistes de Vértebrés du Trias; les types du Stormberg d'Afrique du Sud, (2). *Palaeovertebrata, Memoire Extraordinaire 1974, Montpellier*. 170p.

Ellenberger, F., Ellenberger, P. 1956. Quelques precisions sur la Serie du Stormberg au Basutoland (Afrique du Sud). (Some details on the Stormberg Series in Basutoland, South Africa). *Comptes Rendus des Seances de l 'Acadamie des Sciences (FR)*, 242: 799–801.

Ellenberger, F., Ellenberger, P. 1958. Principaux types de pistes de Vertébrés dans les couches du Stormberg au Basutoland (Afrique du Sud) (Note préliminaire). C*ompte rendu sommaire des séances de la Société Géologique de France*, 65–67.

Ellenberger, F., P. Ellenberger, P. 1960. Sur une nouvelle dalle à pistes de Vertébrés, découverte au Basutoland (Afrique du Sud). *Compte Rendus de la Société Géologique de France* 1960: 236–238.

Ellenberger, F., Ellenberger, P., Fabre, J., Mendrez, Ch. 1963. Deux nouvelles dalles à pistes de Vertébrés fossiles découvertes au Basutoland (Afrique du Sud). *Compte Rendus de la Société Géologique de France*, 315–317.

Ellis, R.G., Gatesy, S.M. 2013. A biplanar X-ray method for three-dimensional analysis of track formation. *Palaeontologia Electronica:* PalaeoElectronica.Org/Content/2013/371-X-Ray-Track-Analysis.

Eriksson, P.G. 1981. A palaeoenvironmental analysis of the Clarens Formation in the Natal Drakensberg. *Transactions Geological Society of South Africa*, 84: 7–17.

Falk, A.R., Martin, L.D., Hasiotis, S.T. 2011. A morphologic criterion to distinguish bird tracks. *Journal of Ornithology.* DOI 10.1007/s10336-011-0645-x

Falkingham, P.L. 2014 Interpreting ecology and behaviour from the vertebrate fossil track. *Journal of Zoology,* 292: 222–228.

Falkingham, P.L. 2016. Applying objective methods to subjective track outlines. *In*: Falkingham, P.L., Marty, D., Richter, A. (*Eds*): Dinosaur tracks- the next steps, 73–80, Indiana press university, Indiana.

Falkingham, P.L., Bates, K.T., Margetts, L., Manning, P.L. 2011. The 'Goldilocks' effect: preservation bias in vertebrate track assemblages. *Journal of Royal Society Interface,* 8: 1142–1154.

Falkingham, P.L., Bates, K.T., Avanzini, M., Bennett, M., Bordy, E.M., Breithaupt, B.H., Castanera, D., Citton, P., Díaz-Martínez, I., Farlow, J.O., Fiorillo, A. R., Gatesy, S.M., Getty, P., Hatala, K.G., Hornung, J.J., Hyatt, J.A., Klein, H., Lallensack, J.N., Martin, A.J., Marty, D., Matthews, N.A., Meyer, C.A., Milàn, J., Minter, N.J., Razzolini, N.L., Romilio, A., Salisbury, S.W., Sciscio, L., Tanaka, I., Wiseman, A.L.A., Xing, L.D., Belvedere, M. 2018. A standard protocol for documenting modern and fossil ichnological data. *Palaeontology,* 61: 469–480. doi: 10.1111/pala.12373

Farlow, J.O. 1981. Estimates of dinosaur speeds from a new tracking site in Texas. *Nature*, 294: 747–748.

Farlow, J.O., Gatesy, S.M., Holtz, T.R. jnr, Hutchinson, J.R., Robinson, J.M. 2000. Theropod locomotion. *American Zoologist*, 40: 640–663.

Farlow, J.O. 2018. Noah's Ravens- Interpreting the makers of tridactyl dinosaur footprints. Life of the Past. Indiana University Press.

Farlow, J.O., Gatesy, S.M., Holtz Jr, T.R., Hutchinson, J.R., Robinson J.M. 2000. Theropod locomotion. *American Zoology,* 40: 640–663.

Fornós, J.J., Bromley, R.G., Clemmensen, L.B., Rodriguez-Perea, A. 2002. Tracks and trackways of *Myotragus balearicus Bate* (Artiodactyla, Caprinae) in Pleistocene aeolianites from Mallorca (Balearic Islands, Western Mediterranean). *Palaeogeography, Palaeoclimatology, Palaeoecology,* 180: 277–313.

Furin, S. Preto, N., Rigo, M., Roghi, G., Gianolla, P., Crowley, J.L., Bowring, S.A. 2006. High- precision U-Pb zircon age from the Triassic of Italy: implications for the Triassic time scale and the Carnian origin of calcareous nannoplankton and dinosaurs. *Geology*, 34: 1009–1012.

Gallagher, W., Hanczaryk, P.A. 2006. The Western Paterson Quarry: An Early Jurassic dinosaur track site in the Newark Basin of New Jersey. *The Triassic-Jurassic Terrestrial Transition. New Mexico Museum of Natural History and Science Bulleti*n, 37: 238–240.

Gand, G., Demathieu, G., Grancier, M., Sciau, J. 2005. Dinosauroid footprints of French Upper Triassic. Discrimaiton, interpretation and comparison. *Bulletin De la Societe Geologique De France*, 176: 69–79. DOI 10.2113/176.1.69

Gatesy, S.M. 2001. Skin impressions of Triassic theropods as records of foot movement. *Bulletin of the Museum of comparative Zoology*, 156: 137–149.

Gatesy S.M., Falkingham, P.L. 2017. Neither bones nor feet: Track morphological variation and 'preservation quality'. *Journal of Vertebrate Paleontology*, 37(3): e1314298.

Gatesy, S.M., Middleton, K.M., Jenkins, F.A., Shubin N.H. 1999. Three-dimensional preservation of foot movements in Triassic theropod dinosaurs. *Nature*, 399: 141–144.

Gehrels, G. 2012. Detrital Zircon U-Pb Geochronology: Current methods and new opportunities. *In*: Busby, C., Azor, A (*Eds*): Tectonics of Sedimentary Basins: Recent Advances, 47–62, Wiley-Blackwell Publishing.

Gauthier, J.A. 1986. Saurischian monophyly and the origin of birds. *Memoirs of the California Academy of Sciences*, 8: 1–55.

Geel, C., deWit, M., Booth, P., Schultz, H-M., Horsfield, B. 2015. Plaeoenvironment, diagenesis and characteristics of Permian black shales in the Lower Karoo Supergroup flanking the Cape Fold Belt near Jansenville, Eastern Cape, South Africa: implications for the shale gas potential of the Karoo Basin. *South African Journal of Geology*, 118: 249–274.

Geel, C., Schulz, H-M., Booth, P., deWit, M., Horsfield B. 2013. Shale gas characteristics of Permian Black Shales in South Africa: Results from recent drilling in the Ecca Group (Eastern Cape). *Energy Procedia*, 40: 256–265.

Getty, P.R. 2012. Were Early Jurassic dinosaurs gregarious? Re-examining the evidence from dinosaur footprint reservation in Holyoke, Massachusetts. In: Getty, P.R. Judge, A., Csoka, J., Bush, A.M. Guidebook for Fieldtrips in Connecticut and Massachusetts: Northeast Section Geological Society of America Meeting 2012 State Geological and Natural History Survey of Connecticut, Guidebook Number 9 DOI: 10.13140/2.1.4998.7208

Getty, P.R., Aucoin, C., Fox, N., Judge, A., Hardy, L., Bush, A.M. 2017. Perennial lakes as an environmental control on theropod movement in the Jurassic of the Hartford Basin. *Geosciences*, 7: doi:10.3390/geosciences7010013

Gerlinski, G., Niedzwiedski, G. 2005. New saurischian dinosaur footprints from the Lower Jurassic of Poland. *Geological Quarterly*, 49: 99–104.

Griffin, C.T. 2019. Large neotheropods from the Upper Triassic of North America and the early evolution of large theropod body sizes. *Journal of Paleontology*, 93: 1010-1030.

Griffin, C.T., Nesbitt, S. J. 2019. Does the maximum body size of theropods increase across the Triassic-Jurassic boundary? Integrating ontogeny, phylogeny and body size. *The Anatomical Record*. DOI: 10.1002/ar.24130

Hammer, Ø., Harper, D.A.T., Ryan, P.D. 2001. PAST: paleontological statistics software package for education and data analysis. *Palaeontologia Electronica*, 4: 1–9.

Hancox, P.J., Rubidge, B.S. 2001. Breakthroughs in the biodiversity, biogeography, biostratigraphy and basin analysis of the Beaufort Group. *Africa Earth Science*, 33: 563–577.

Hansma, J., Tohver, E., Jourdan, F., Schrank, C., Adams, D. 2015. The timing and deformation of the Cape Orogeny: New $^{40}Ar/^{39}Ar$ age constraints on deformation and cooling of the Cape Fold Belt, South Africa. *Gondwana Research*, doi: 10.1016/j.gr.2015.02.005

Hanson, E.K., Moore, J.M., Bordy, E.M., Marsh, J.S., Howarth, G., Robey, J.V.A. 2009. Cretaceous erosion in central South Africa: Evidence from upper-crustal xenoliths in kimberlite diatremes. *South African Journal of Geology*, 112: 125–140.

Haubold, H. 1971. In O. Kuhn (*ed*), Handbuch der Paläoherpetologie [Encyclopedia of paleoherpetology]. Part 18. Ichnia Amphibiorum et Reptiliorum Fossilium. *Gistav Fischer Verlag, Stuttgart* ,1–124.

Haupt, T. 2018. Palaeoenvironmental change from the Hettangian to Toarcian in Moyeni (Quthing District), southwestern Lesotho. Master Thesis (unpublished), University of Cape Town, Cape Town 119p.

Hay, R.L., Leakey, M.D. 1982. The fossil footprints of Laetoli. *Scientific American*, 246: 50–55.

Heckroodt, R. 1991. Clay and clay minerals in South Africa. *Journal of South African Institute of Mineral and Metallurgy*, 91: 343–363.

Henderson, D. 2003. Tracks, trackways, and hip heights of bipedal dinosaurs – testing hip height predictions with computer models. *Ichnos*, 10: 99–114. DOI: 10.1080/10420940390257914

Henderson, D.M. 2006a. Burly gaits: centers of mass, stability, and the trackways of sauropod dinosaurs. *Journal of Vertebrate Paleontology*, 26: 907–921.

Henderson, D.M. 2006b. Simulated weathering of dinosaur tracks and the implications for their characterization. *Canadian Journal of Earth Science*, 43: 691–704.

Hietpas, J., Samson, S., Moecher, D., Chakraborty, S. 2011. Enhancing tectonic and provenance information from detrital zircon studies: assessing terrane-scale sampling and grain-scale characterization. *Journal of the Geological Society, London,* 168: 309–318.

Hitchcock, E. 1836. Ornithichnology: Description of the Footmarks of birds (Ornithichnites) on new Red Sandstone in Massachusetts. *American Journal of Science*. Series 1 (29), 307–340.

Hitchcock, E. 1856. Description of a new and remarkable species of fossil footmark, from the sandstone of Turner's Falls, in the Connecticut Valley. *American Journal of Science*. Series 2 (21), 97–100.

Hitchcock, E. 1858. Ichnology of New England. A Report on the sandstone of the Connecticut Valley, especially its fossil footmarks, *Made to the Commonwealth of Massachusetts*, 199p, Boston: William White.

Hopson, J.A. 1984. Late Triassic traversodont cynodonts from Nova Scotia and southern Africa. *Plaeontologia Africana*, 25: 181–201.

Huerta, P., Fernández-Baldor, F.T., Farlow, J.O., Montero, D. 2012. Exceptional preservation process of 3D dinosaur footprint casts in Costalomo (Lower Cretaceous, Cameros Basin, Spain). *Terra Nova,* 24: 136–141.

Huh, M., Paik, I.S., Lockley, M.G., Hwang, K.G., Kim, B.S., Kwak, S.E. 2006. Well-preserved theropod tracks from the Upper Cretaceous of Hwasun County, southwestern South Korea, and their paleobiological implications. *Cretaceous Research*, 27: 123–138.

Hunt, A.P., Lucas, S.G. 2007. Late Triassic tetrapod tacks of western North America. *New Mexico Museum of Natural History and Science Bulletin*, 40: 215–230.

Hunt., A.P., Lucas, S.G. 2007. Tetrapod ichnofacies: A new paradigm. *Ichnos*, 14: 59–68.

Irmis, R.B. 2011. Evaluating hypothesis for early diversification of dinosaurs. *Earth and Environmental Science Transactions of the Royal Society of Edinburgh*. 101: 397–426. doi:10.1017/S1755691011020068

Irmis, R.B., Parker, W.G., Nesbitt, S.J. and Liu, J., 2007. Early ornithischian dinosaurs: the Triassic record. *Historical Biology,* 19:3–22.

Isbell, J.L., Cole, D.I., Catuneanu, O. 2008. Carboniferous-Permian glaciation in the main Karoo Basin, South Africa: Stratigraphy, depositional controls and glacial dynamics). *In*: Fielding, C.R., Frank, T.D.,

Isbell, J.L. (*Eds*): Resolving the Late Palaeozoic Ice Age in Time and Space: Boulder, CO, 71–82, Geological Society of America Special Paper.

Jackson, S.E., Pearson, N.J., Griffin, W.L, Belousova E.A. 2004. The application of laser ablation-inductively coupled plasma-mass spectrometry to in situ U–Pb zircon geochronology. *Chemical Geology,* 211: 47–69.

Jackson, S.J., Whyte, M.A., Romano, M. 2010. Range of experimental dinosaur (*Hypsilophodon foxii*) footprints due to variation in sand consistency: How wet was the track? *Ichnos*, 17: 197–214. https://doi.org/10.1080/10420940.2010.510026

Johnson, M.R. 1971. Provisional geological report on occurrences of bentonite in the Pronksberg (Mountain), Wodehouse District, Cape Province: Report, Geological Survey of South Africa, 1971-0012 (unpubl.).

Johnson, M.R. 1976. Stratigraphy and sedimentology of the Cape and Karoo sequences in the Eastern Cape Province. Ph.D. Thesis (unpublished), Rhodes University, Grahamstown.

Johnson, M.R. 1991. Sandstone petrography, provenance and plate tectonic setting in Gondwana context of the south-eastern Cape-Karoo basin. *South African Journal of Geology*, 94: 137–154.

Johnson, M.R., Van Vuuren, C. J., Visser, J.N.J., Cole, D.I., Wickens, H.D.V., Christie, A.D.M., Roberts, D.L. 1997. The foreland Karoo Basin, South Africa. *African basins. Sedimentary basins of the World*, 3: 269–317.

Johnson, M. R., van Vuuren, J. N. J., Visser, D. I., Cole, H. d. V., Wickens, A. D. M., Christie, Roberts, D. L., Brandl, G. 2006. Sedimentary rocks of the Karoo Supergroup. *In*: Johnson, M. R., Anhaeusser, C. R., Thomas, R. J. (*Eds*): The geology of South Africa, 461–499, Geological Society of South Africa and Council for Geoscience.

Kim, J., Lockley, M.G. 2013. Review of dinosaur tail traces. *Ichnos*, 20: 129–141.

Kim, J.Y., Lockley, M.G., Kim, H.M., Lim, J-D., Kim, K.S. 2009. New dinosaur tracks from Korea, *Ornithopodichnus masanensis* ichnogen. Et ichnosp. Nov. (Jingdong Formation, Lower Cretaceous): implications for polarities in ornithopod foot morphology. *Cretaceous Research*, 30: 1387–1397. doi:10.1016/j.cretres.2009.08.003

Kim, K.S., Lockley, M.G., Lim, J.D., Xing, L. 2019. Exquisitely preserved, high definition skin traces in diminutive theropod tracks from the Cretaceous of Korea. *Scientific Reports*, 9: https://doi.org/10.1038/s41598-019-38633-4

Kitching, J. W., Raath, M. A. 1984. Fossils from the Elliot and Clarens formations (Karoo Sequence) of the north-eastern Cape, Orange Free State and Lesotho, and a suggested biozonation based on tetrapods. *Palaeontologia Africana*, 25:111–125.

Klein, H., Milan, J., Clemmensen, N.F., Mateus, O., Klein, N., Adolfssen, J.S., Estrup, E.J., Wings O. 2015. Archosaur footprints (cf. *Brachychirotherium*) with unusual morphology from the Upper Triassic Flemin Fjord Formation (Norian-Rhaetian) of East Greenland. *In*: Kear B.P., Lindgren J., Hurum J.H., Milan J., Vajda V (*Eds*): Mesozoic biotas of Scandinavia and its Arctic Territories, 434, Geological Society, London Special publications, http://doi.org/10.1144/SP434.1

Knoll, F. 2004. Review of the tetrapod fauna of the “Lower Stormberg Group” of the main Karoo Basin (southern Africa): implication for the age of the Lower Elliot Formation. *Bulletin de la Societe géologiquede France*, 175(1): 73–83.

Knoll, F. 2005. The tetrapod fauna of the Upper Elliot and Clarens formations in the main Karoo Basin (South Africa and Lesotho). *Bulletin de la Société géologique de France*, *176*(1); 81–91.

Kuban, G.J. 1994. An overview of dinosaur tracking. M.A.P.S. Digest, Mid America Paleontology Society, Rock Island, IL.

Labandeira, C.C., Anderson, J.M., Anderson, H.M. 2018. Expansion of arthropod herbivory in Late Triassic South Africa: The Molteno Biota, Aasvoëlberg 411 site and developmental biology of a gall. *In*: Tanner, L.H *(Ed)*: The Late Triassic World, 623-719, Springer, Cham.

Langnaoui, A., Klein, H., Voight, S., Hminna, A., Saber, H., Schneider, J.W., Werneburg, R. 2012. Late Triassic tetrapod-dominated ichnoassmeblages from the Argana basin (Western High Atlas, Morocco). I*chnos*, 19: 238 –253.

Lallensack, J.N. 2019. Automatic generation of objective footprint outlines. *PeerJ*, 7:e7203 http://doi.org/10.7717/peerj.7203.

Lallensack, J.N., Engler, T., Barthel, H.J. 2019. Shape variability in tridactyl dinosaur footprints: the significant of size and function. *Palaeontology,* 1–26. doi: 10.1111/pala.12449

Lallensack, J.N., van Heteren, A.H., Wings O., 2016. Geometric morphometric analysis of intra-trackway variability: a case study on theropod and ornithopod dinosaur trackways from Munchehagen (Lower Cretaceous, Germany). *PeerJ* 4:e2059; DOI 10.7717/peerj.2059.

Langer, M.C. 2014. The origins of dinosauria: Much ado about nothing. *Palaeontology*, 57: 469–478.

Langer, M.C., Ezcurra, M.D., Bittencourt, J.S. and Novas, F.E., 2010. The origin and early evolution of dinosaurs. *Biological Reviews*, *85*:55–110.

Langer, M.C., Ezcurra, M.D., Rauhut, O.W.M., Benton, M.J., Knoll, F., McPhee, B.W., Novas, F.E., Pol, D., Brusatte, S.L. 2017. Untangling the dinosaur family tree. *Nature,* 551, E1 – E3. http://doi.org/10.1038/nature24011

Laporte, L.F., Behrensmeyer, A.K. 1980. Tracks and substrate reworking by terrestrial vertebrates in Quaternary sediments of Kenya. *Journal of sedimentary petrology*, 50: 1337–1346.

Li, D., Azuma, Y., Fujita, M., Lee, Y. and Arakawa, Y. 2006. A preliminary report on two new vertebrate track sites including dinosaurs from the Early Cretaceous Hekou Group, Gansu province China. *Journal of the Paleontological society of Korea*, 22: 29–49.

Lindeque, A.S., de Wit, M.J., Ryberg, T., Weber, M., Chevallier, L. 2011. Deep crustal profile across the Southern Karoo basin and Beattie magnetic anomaly, South Africa: An integrated interpretation with tectonic implications. *South African Journal of Geology,* 114: 265–292.

Lockley, M.G. 1986. The paleobiological and paleoenvironmental importance of dinosaur footprints. *Palaios*, 1: 37–47.

Lockley, M.G. 1998. The vertebrate track record. *Nature*, 396: 429–432.

Lockley, M. 1991. Tracking dinosaurs: a new look at an ancient world. Cambridge University Press, Cambridge, 238p.

Lockley, M.G. 1999. The Eternal trail: a tracker looks at evolution. Erseus Books, Reading. 344p.

Lockley, M.G. 2009. New perspectives on morphological variation in tridactyl footprints: clues to widespread convergence in developmental dynamics. *Geological Quarterly*, 53: 415–432.

Lockley, M.G., Gierlinski, G.D. 2014. Jurassic tetrapod footprint ichnofaunas and ichnofacies of the Western Interior, USA. *Volumina Jurassica*, 7: 133–150. DOI: 10.5604/17313708 .1130134

Lockley, M.G., Gierlinski, G.D., Lucas, S.G. 2011. *Kayentapus* revisited: Notes on the type material and the importance of this theropod footprint ichnogenus. *New Mexico Museum of Natural History and Science Bulletin,* 53: 330–336.

Lockley, G.M., Hunt, A., Paquette, M., Bilbey, S., Hamblin, A. 1998. Dinosaur tracks from the Carmel formation, northeastern Utah: Implications for Middle Jurassic paleoecology. I*chnos*, 5: 255–267.

Lockley, M.G., Kim J.Y., 2013. Review of dinosaur tail traces. *Ichnos*, 20: 129–141.

Lockley, M.G., Kim, J.Y., Kim, K.S., Kim, S.H., Matsukawa, M., Rihui, L., Jianjun, L., Ynamg, S-Y. 2008. *Minisauripus* – the track of a diminutive dinosaur from the Cretaceous of China and South Korea: implications for stratigraphic correlation and theropod foot morphodynamics. *Cretaceous Research,* 29: 115–130. doi:10.1016/j.cretres.2007.04.003

Lockley, M.G., Li, J., Li, R., Matsukwa, M., Harris, J.D., Xing, L. 2013. A review of the tetrapod track record in China, with special reference to type ichnospecies: Implications for ichnotaxonomy and Paleobiology. *Acta Geological Sinica,* 87: 1–20.

Lockley, M., Matsukawa, M., Jianjun, L. 2003. Crouching theropods in taxonomic jungles: ichnological and ichnotaxonomic investigations of footprints with metatarsal and ischial impressions. Ichnos, 10: 169–177.

Lockley, M.G., McCrea, R.T., Buckley, L.G., Lim, J.D., Matthews, N.A., Breithaupt, B.H. Houck, K.J. Gierlinski G.D., Surmik D., Kim S.O., Xing L., Kong D.Y., Cart, K., Martin, J., Hadden, G. 2016. Theropod courtship: large scale physical evidence of display arenas and avian-like scrape ceremony behaviour by Cretaceous dinosaurs. *Scientific Reports*. 6:18952

Lockley, M.G., Meyer, C.A., Moratalla, J.J. 1998. *Therangospodus*: Trackway evidence for the widespread distribution of late Jurassic theropod with well-padded feet. *Gaia*, 15: 339–353.

Lockley, M.G., Young, B.H., Carpenter, K. 1983. Hadrosaur locomotion and herding behavior: evidence from footprints in the Mesaverde Formation, Grand Mesa coal field, Colorado. *Mountain Geology,* 2:5–14.

Lockley, M.G., Hunt, A.P., Meyer, C. 1994. Vertebrate tracks and the ichnofacies concept: implications for the paleoecology and palichnostratigraphy. *In*: Donovan, S. (*Ed*): The paleobiology of trace fossils, 241–268, Wiley, London.

Lucas, S. G., Hancox, P. J. 2001. Tetrapod-based correlation of the nonmarine Upper Triassic of southern Africa. *Albertiana*, 25: 5–9.

Lucas, S.G., Klein, H., Lockley, M.G., Spielmann, J.A., Gierlinski, G.D., Hunt, A.P., Tanner, L.H. 2006. Triassic-Jurassic stratigraphic distribution of the theropod footprint ichnogenus *Eubrontes. In*: Harris, J.D., Lucas, S.G., Spielmann, J.A., Lockley, M.G., Milner, A.R.C., Kirkland, J.I. (*Eds*): The Triassic-Jurassic terrestrial transition, vol. 37, 86–93, New Mexico Museum of Natural History and Science Bulletin, New Mexico.

Lucas, S.G., Tanner, L.H. 2007a. Tetrapod biostratigraphy and biochronology of the Triassic-Jurassic transition on the southern Colorado Plateau, USA. *Palaeogeography, Palaeoclimatology, Palaeoecology*, 244:242–256.

Lucas, S.G., Tanner, L.H. 2007b. The nonmarine Triassic-Jurassic boundary in the Newark Supergroup of eastern North America. Earth Science Reviews, 84: 1–20.

Lucas., S.G., Tanner, L.H. 2015. End-Triassic nonmarine biotic events. *Journal of Palaeogeography*: doi: 10.1016/j.jop.2015.08.010

Lucas, S.G. and Tanner, L.H. 2018. The missing mass extinction at the Triassic-Jurassic boundary. In: Tanner, L.H. (*ed):* The Late Triassic World, 721–785, Springer, Cham.

Lucas, S.G., Tanner, L.H., Donohoo-Hurley, J.W., Kozure, H.W., Heckert, A.B., Weems, R.E. 2011. Position of the Triassic–Jurassic boundary and timing of the end-Triassic extinctions on land: Data from the Moenave Formation on the southern Colorado Plateau, USA. *Palaeogeography, Palaeoclimatology, Palaeoecology*, 302: 194-205.

Ludwig, K.R. 2003. Isoplot/EX version 3.0, A geochronological toolkit for Microsoft Excel: Berkeley Geochronology Center Special Publication.

Lull, R.S. 1904. Fossil footprints of the Jurassic-Triassic of North America. *Memoirs of the Boston Society of Natural History,* 5: 461–557.

Mallsion, H. 2010a. The digital *Plateasaurus* I: body mass, mass distribution and posture assessed using CAD and CAE on a digitally mounted skeleton. *Palaeontologia Electronica*, 13: 1–26.

Mallsion, H. 2010b. The digital assessment of *Plateosaurus* II: an assessment of the range of motion of limbs and vertebral column and of previous reconstructions using a digital skeleton mount. *Acta Palaeontologia Polonica*, 55: 433–458.

Mallison, H. 2011. *Plateosaurus* in 3D: how CAD models and kinetic-dynamic modelling bring an extinct animal to life. *In*: Klein, N., Remes, K., Gee, C.T., Sander, P.M. (*Eds*): Biology of sauropod dinosaurs: understanding the life of giants, 219–236, Bloomington, Indiana Univeristy Press.

Mallison H., Wings O. 2014. Photogrammetry in paleontology – a practical guide. J Pal Tech. 12:1e31

Marchetti, L. 2019. Can undertracks show higher morphological quality than surface tracks? Remarks on large amphibians tracks from the Early Permian of France. *Journal of Iberian Geology,* 45: 353 – 363. https://doi.org/10.1007/s41513-018-0080-4

Marchetti, L., Belvedere, M., Voigt, S., Klein, H., Castanera, D., Díaz-Martínez, I., Marty, D., Xing, L., Feola, S., Melchor, R.N., Farlow, J.O. 2019. Defining the morphological quality of fossil footprints. Problems and principles of preservation in tetrapod ichnology with examples from the Paleozoic to the present. *Earth-Science Reviews*, 193: 109–145. https://doi.org/10.1016/j.earscirev.2019.04.008

Marsicano, C.A., Domnanovich, N.S., Mancuso, A.C. 2007. Dinosaur origins: evidence from the footprint record. *Historical Biology*, 19: 83–91. https://doi.org/10.1080/08912960600866920

Marsicano, C.A., Wilson, J.A., Smith, R.M.H. 2009. A temnospondyl trackway from the Early Mesozoic of western Gondwana and its implications for basal tetrapod locomotion. *Plos one*, 9(8): e103255. doi:10.1371/journal.pone.0103255

Marty, D., Strasser, A., Meyer, C.A. 2009. Formation and taphonomy of human footprints in microbial mats of present day tidal flat environments: Implication for the study of fossil footprints. *Ichnos*, 16: 127–142. https://doi.org/10.1080/10420940802471027

Mattinson, J.M. 2010. Analysis of the relative decay constants of ^{235}U and ^{238}U by multi-step CA-TIMS measurements of closed-system natural zircon samples. *Chemical Geology,* 275: 186–198.

McCarthy, T., Rubidge, B. 2005. The story of Earth and life: a southern African perspective on a 4.6 billion year journey. Struik publishers, Cape Town (South Africa), 333p.

McElwain, J.C., Beerling, D.J., Woodward, F.I. 1999. Fossil plants and global warming at the Triassic–Jurassic boundary. Science, 285:1386–1390.

McPhee, B.W., Bordy, E.M., Sciscio, L., Choiniere, J.N. 2017. The sauropodomorph (Dinosauria) biostratigraphy of the Elliot Formation of southern Africa: tracking the evolution of *Sauropodomorpha* across the Triassic–Jurassic boundary. *Acta Palaeontologica Polonica*, 62: 441–465.

McPhee, B.W., Benson R.N., Both-Brink, J., Bordy, E.M., Choiniere, J.N. 2018. A giant dinosaur from the earliest Jurassic of South Africa and the transition to quadrupedality in early sauropodomorphs. *Current Biology*, 28: 3143–3151.

Miall, A. 1996. The geology of fluvial deposits. Springer Berlin Heidelberg, Berlin, Germany.

Michael, S.Y., Baron, M.G., Norman, D.B., Barrett, P.M. 2019. Dynamic biogeographic models and dinosaur origins. *Earth and Environmental Science Transactions of the Royal Society of Edinburgh*, *109*(1-2): 325–332.

Milan, J. 2006. Variations in the morphology of emu (*Dromaius Novaehollandiae*) tracks reflecting difference in walking pattern and substrate consistency: Ichnotaxonomic implications. *Palaeontology*, 49: 405–420.

Milan, J., Clemmensen, L.B., Bonde, N. 2004. Vertical sections through dinosaur tracks (late Triassic lake deposits, East Greenland): undertracks and subsurface deformation structures revealed. *Lethaia*, 37: 285–296.

Milan, J., Avanzini, M., Clemmensen, L.B., Garcia-Ramos, J.C., Piñuela, L. 2006. Theropod foot movement recorded from Late Triassic, Early Jurassic and Late Jurassic footprints. In: Harris, J.D., Lucas, S.G., Spielmann, J.A., Lockley, M.G., Milner, A.R.C., Kirkland, J.I. (*Eds*): The Triassic – Jurassic Terrestrial Transition, 352–364, New Mexico Museum of Natural History and Science Bulletin 37, New Mexico.

Mílan, J., Bromley, R.G. 2006. True tracks, undertracks and eroded tracks, experimental work with tetrapod tracks in laboratory and field. *Palaeogeography, Palaeoclimatology, Palaeoecology*, 231: 231–264.

Mílan, J., Bromley, R.G. 2007. The impact of sediment consistency on track and undertrack morphology: experiments with Emu tracks in layered cement. *Ichnos*, 15: 19–27. https://doi.org/10.1080/10420940600864712

Mílan, J., Loope, D.B. 2007. Preservation and erosion of theropod tracks in eolian deposits: Examples from the Middle Jurassic Entrada Sandstone, Utah, USA. *The Journal of Geology*, 115: 375–386.

Miller, W., Britt, B., Stadtman, K. 1989. Tridactyl trackways from the Moenave Formation of southwestern Utah. *In*: Gillette, D.D., Lockley, M.G. (*Eds*): Dinosaur tracks and traces, 209–215, Cambridge University Press, New York.

Milner, A.R.C., Harris, J.D., Lockley, M.G., Kirkland, J.I., Matthews, N.A. 2009. Bird-Like anatomy, posture, and behavior revealed by an Early Jurassic theropod dinosaur resting trace. *Plos one* 4(3): e4591. doi:10.1371/journal.pone.0004591

Milner, A.R.C., Lockley, M.G. 2016. Dinosaur swim track assemblages: characteristics, contexts and ichnofacies implications. *In*: Falkingham, P.L., Marty, D., Richter, A. (*Eds*): Dinosaur tracks – the next steps, 152–181, Indiana University Press, Bloomington and Indianapolis.

Moratalla, J.J., Sanz, J.L., Jimenez, S. 1988. Multivariate analysis on Lower Cretaceous dinosaur footprints: Discrimination between ornithopods and theropods. *Geobios*, 21: 395–408.

Moulin, M., Flateau, F., Courtillot, V., Narsh, J., Delpech, G., Quidelleur, X., Gerard, M. 2017. Eruptive history of the Karoo lava flows and their impact on early Jurassic environmental change. Journal of Geophysical research: Solid Earth, 116(B7).

Muir, R.A., Bordy, E.M., Frei, D., Mundil, R. 2019. Recalibrating the Breakup History of SW Gondwana: U-Pb Radioisotopic Constraints from the Southern Cape of South Africa. *In*: AGU Fall Meeting 2019. AGU.

Muir, R.M., Bordy, E.M., Frei, D., Mundil, R. 2020. Recalibrating the breakup history of SW Gondwana: U-Pb radioisotopic age constraints from the southern Cape of South Africa. *Gondwana Research*, https://doi.org/10.1016/j.gr.2020.02.011

Mukkadam, R. 2019. The resurrection of *Kalosauropus isp*. A massospondylid tack from the Lower Jurassic of southern Africa. Honours thesis (unpublished), University of Cape Town, Cape Town. 36p.

Nadon, G.C. 2001. The impact of sedimentology on vertebrate track studies. *In:* Tanke, D.H., Carpenter, K. (*Eds*). Mesozoic Vertebrate Life. Indiana University Press, Indiana, 395–407.

Nasdala, L., Hofmeister, W., Norberg, N., Mattinson, J.M., Corfu, F., Dörr, W., Kamo, S.L., Kennedy, A.K., Kronz, A., Reiners, P.W., Frei, D., Košler, J., Wan, Y., Götze, J., Häger, T., Kröner, A., Valley, J.W. 2008. Zircon M257 – a homogeneous natural reference material for the ion microprobe U-Pb analysis of zircon. *Geostandards and Geoanalytical Research*, 32: 247–265.

Nesbitt, S.J., Norell, M.A. 2006. Extreme convergence in the body plans of an early suchian (Archosauria) and ornithommid dinosaurs (*Theropoda*). *Proceedings of the Royal Society: Biological Sciences*, 273: 1045 – 1048. DOI: 10.1098/rspb.2005.3426

Nesbitt, S. J., Barrett, P. M., Werning, S., Sidor, C. A., Charig, A. J. 2012. The oldest dinosaur? A Middle Triassic dinosauriform from Tanzania. *Biological Letters*, 9: 20120949.

Nesbitt, S. J., Sidor, C.A., Irmis, R.B., Angielczyk, K.D., Smith, R.M.H., Tsuji, L.A. 2010. Ecologically distinct dinosaurian sister group shows early diversification of Ornithodira. *Nature*, 464: 95–98.

Nesbitt. S.J., Smith, N.D., Irmis, R.B., Turner, A.H., Downs, A., Norell, M.A. 2009. A complete skeleton of a Late Triassic saurischian and the early evolution of dinosaurs. *Science*, 326: 1530–1533.

Niedzwiedzki, G. 2011. A Late Triassic dinosaur-dominated ichnofauna from the Tomanova Formation of the Tatra Mountains, Central Europe. A*cta Palaeontologica Polonica*, 56: 291–300.

Olsen, P.E. 1980. Fossil great lakes of the Newark Supergroup in New Jersey. *In*: Manspeizer, W. (*Ed*): Field studies in New Jersey geology and Guide to field trips, 352–398, New York state ecology association, Newark College of arts and sciences, Newark, Rutgers University.

Olsen, P.E. 1995. Paleontology and paleoenvironments of Early Jurassic age strata in the Walter Kidde Dinosaur Park (New Jersey, USA). *In*: Baker, J.E.B. (*Ed*): Field Guide and Proceedings of the Twelfth Annual Meeting of the Geological Association of New Jersey, Geological Association of New Jersey, 156–190, Rider College, Lawrenceville.

Olsen, P.E. 2010. Fossil Great Lakes of the Newark Supergroup – 30 years later.

Olsen, P.E., Baird, D. 1986. The ichnogenus *Atreipus* and its significance for Triassic biostratigraphy. *In*: Padian, K. (*Ed*): The Beginning of the Age of Dinosaurs, Faunal Change Across the Triassic-Jurassic Boundary, 61–87, Cambridge University Press, New York.

Olsen, P.E., Galton, P.M. 1984. A review of the reptile and amphibian assemblages from the Stormberg of southern Africa, with special emphasis on the footprints and age of the Stormberg. *Palaeontologia Africana,* 25: 87–110.

Olsen, P.E., Kent, D.V., Sues, H.D., Koeberl, C., Huber, H., Montanari, A., Rainforth, E.C., Fowell, S.G., Szajna, M.J., Hartline, B.W. 2002. Ascent of dinosaurs linked to an Iridium anomaly at the Triassic – Jurassic Boundary. *Science*. 296: 1305 – 1307. DOI: 10.1126/science.1065522

Olsen, P.E., Kent, D.V., Whiteside, J.H. 2010. Implications of the Newark Supergroup-based astrochronology and geomagnetic polarity time scale (Newark-APTS) for the tempo and mode of the early diversification of Dinosauria. *Earth and Environmental Science Transactions of the Royal Society of Edinburgh*, 101: 201–229.

Olsen, P.E., Rainforth, E. 2003. The Early Jurassic Ornithischian dinosaurian ichnogenus *Anomoepus. In*: LeTourneau, P.M., Olsen, P.E. (*Eds*): The Great Rift Valleys of Pangea in Eastern North America, Volume 2: Sedimentology, Stratigraphy, and Paleontology, 314–367, Columbia University Press.

Olsen, P.E., Smith, J.B., McDonald, N.G. 1998. Type material of the type species of the classic theropod footprint genera *Eubrontes, Anchisauripus*, and *Grallator* (Early Jurassic, Hartford and Deerfield basins, Connecticut and Massachusetts, USA). *Journal of vertebrate Paleontology*, 18: 586–601.

Osi, A., Palfy, J., Makadi, L., Szentesi, Z., Gulyas, P., Rabi, M., Botfalvai, G., Hips, K. 2011. Hettangian (Early Jurassic) dinosaur tracksites from the Mecsek Mountains, Hungary. *Ichnos,* 18: 79–94.

Otero, A., Cuff, A.R., Allen, V., Summer-Rooney, L., Pol, D., Hutchinson, J.R. 2019. Ontogenetic changes in the body plan of the sauropodomorph dinosaur *Mussaurus patagonicus* reveal shifts of locomotor stance during growth. *Scientific reports,* 9: https://doi.org/10.1038/s41598-019-44037-1

Padian, K. 2012. The problem of dinosaur origins: integrating three approaches to the rise of Dinosauria. *Earth and Environmental Science Transactions of the Royal society of Edinburgh*, 103: 423–442.

Padian, K., de Ricqles, A.J., Horner, J.R. 2001. Dinosaurian growth rates and bird origins. *Nature*, 412: 405–408.

Padian, K., Horner, J.R., de Ricqles, A. 2004. Growth in small dinosaurs and pterosaurs: evolution of archosaurian growth strategies. *Journal of Vertebrate Paleontology*, 24: 555–571.

Padian, K., Li, C., Pchelnikova, J. 2010. The trackmaker of *Apatopus* (Late Triassic, North America): implications for the evolution of arcosaur stance and gait. *Palaeontology*, 53: 175–189.

Padian, K., Olsen, P. 1984. The fossil trackway pteraichnus: not pterosaurian but crocodilian. *Journal of Palaeontology,* 58: 178–184.

Paik, I.S., Kim, H.J., Lee, Y.I. 2001. Dinosaur track-bearing deposits in the Cretaceous Jindong Formation, Korea: occurrence, palaeoenvironments and preservation. *Cretaceous Research*, 22: 79–92. doi:10.1006/cres.2000.0241

Paik, I.S., Kim, H.J., Lee, H., Kim, S. 2017. A large and distinct skim impression of the cast of a sauropod dinosaur footprint from Early Cretaceous floodplain deposits, Korea. *Scientific Reports*, 7: 16339 DOI:10.1038/s41598-017-16576-y

Parker, W.G., Irmis, R.B., Nesbitt, S.J., Martz, J.W., Browne, L.S. 2005. The Late Triassic pseudosuchian *Revueltosaurus callenderi* and its implications for the diversity of early ornithischian dinosaurs. *The Royal Society Proceedings Biological Sciences,* 272: 963–969. Doi:10.1098/rspb.2004.3047

Paton C., Woodhead J.D., Hellstrom J.C., Hergt J.M., Greig A., Maas R. 2010. Improved laser ablation U-Pb zircon geochronology through robust downhole fractionation correction. *Geochemistry Geophysics Geosystems,* 11: Q0AA06, doi:10.1029/2009GC002618.

Paton C., Hellstrom J., Paul B., Woodhead J., Hergt J. 2011. Iolite: freeware for the visualisation and processing of mass spectrometric data*. J. Anal. At. Spectrom*. 26: 2508–2518.

Pálfy, J., Demény, A., Haas, J., Carter, E. S., Görög, Á., Halász, D., Oravecz-Schefferg, A., Hetényih, A., Mártonf, E., Orchardi, M. J., Ozsvárta, P., Vetőj, I., Zajzon, N. 2007. Triassic–Jurassic boundary events inferred from integrated stratigraphy of the Csővár section, Hungary. *Palaeogeography, Palaeoclimatology, Palaeoecology,* 244:11–33.

Pérez-Lorente, F.G. 2015. Dinosaur footprints and trackways of La Rioja, University Press, Bloomington, 363p.

Petrus, J.A., Kamber, B.S. 2012. VizualAge: A Novel Approach to Laser Ablation ICP-MS U-Pb Geochronology Data Reduction. *Geostandards and Geoanalytical Research*, 36: 247–270.

Petti, F.M., Avanzini, M., Belvedere, M., De Gasperi, M., Ferretti, P., Girardi, S., Remondino, F., Tomasoni, R. 2008. Digital 3D modelling of dinosaur footprints by photogrammetry and laser scanning techniques: integrated approach at the Coste dell'Anglone tracksite (Lower Jurassic, Southern Alps, Northern Italy). *Studi Trentini di Scienze Naturali, Acta Geologica*, 83: 303–315.

Piubelli, D., Avanzini, M., Mietto, P. 2005. The Early Jurassic ichnogenus *Kayentapus* at Lavino de Marco ichnosite (NE Italy). Global distribution and paleogeographic implications. *Bulletin Geological Society of Italy*, 124: 259–267.

Platt, B.F., Hasiotis, S.T. 2006. Newly discovered sauropod dinosaur tracks with skin and foot-pad impressions from the Upper Jurassic Morrison Formation, Bighorn Basin, Wyoming, U.S.A. *Palaios*, 21: 249–261.

Prevece, R., Gastaldo, R.A., Neveling, J., Reid, S.B., Looy, C.V. 2010. An autochtonous *glossopterid* flora with latest Permian palynomorphs and its depositional setting in the *Dicynodon* Assemblage Zone of the southern Karoo Basin, South Africa. *Palaeography, Palaeoclimatology and Palaeoecology*, 292: 391–408.

Raath, M.A. 1996. Earliest evidence of dinosaurs from central Gondwana. *Memoirs of the Queensland Museum,* 39: 703–709.

Raath, M.A. 1977. The anatomy of the Triassic theropod *Syntarsus rhodesiensis* (*Saurischia: Podokesauridae*) and a consideration of its biology. PhD, Rhodes University, 233p.

Raath, M.A., Kitching, J.W., Shone, R.W., Rossouw, G.J. 1990. Dinosaur tracks in Triassic Molteno sediments: the earliest evidence of dinosaurs in South Africa? *Paleontologia Africana,* 27: 89–95.

Raath, M.A., Yates, A.M. 2005. Preliminary report of a large theropod large theropod dinosaur trackway in Clarens Formation sandstone (Early Jurassic) in the Paul Roux, district, northeastern Free State, South Africa. *Palaeontologia Africana*, 41: 101–104.

Rainforth, E.C. 2005. Ichnotaxonomy of the fossil footprints of the Connecticut Valley (Early Jurassic, Newark Supergroup, Connecticut and Massachusetts), PhD thesis (unpublished), Columbia University, New York, 1301 p.

Rainforth, E.C. 2007. Ichnotaxonomic updates from the Newark Supergroup. In Rainforth, E. (ed.), Contributions to the Paleontology of New Jersey (II), Field Guide and Proceedings. Geological Association of New Jersey, XXIV Annual Conference and Field Trip (October 12-13, 2007), East Stroudsburg University, Pennsylvania, 49–59.

Rainforth E.C., Manzella M. 2007. Estimating speeds of dinosaurs from trackways: a re-evaluation of assumptions. Contributions to the paleontology of New Jersey (II): Field Guide and Proceedings, Geological Association of New Jersey 24th Annual Conference and Field Trip, 41–48.

Rampersadh, A., Bordy, E.M., Sciscio, L., Abrahams, M. 2018. Dinosaur behaviour in an early ecosystem – uppermost Elliot formation, Ha Nohana, Lesotho. *Annales Societatis Geologorum Poloniae*, 88: doi: https://doi.org/10.14241/asgp.2018.010

Rampersadh, A., Bordy, E.M. 2019. Early Jurassic dinosaur ecosystem in southwestern Gondwana: steps towards refining its palaecology. *Hallesches Jahrbuch fur Geowissenschaften*, 46, p49.

Raup, D.M., Sepkoski, J.J. 1982. Mass extinctions in the marine fossil record. *Science*, 2015: 1501–1503.

Razzolini, N.L., Belvedere, M., Marty, D., Paratte, G., Lovis, C., Cattin, M., Meyer, C.A. 2017. *Megalosauripus transjurancisu*s ichnosp. Nov. A new Late Jurassic theropod from NW Switzerland and implications for tridactyl dinosaur ichnology and ichnotaxonomy. *Plos one,* 12:e0180289.

Razzolini, N.L., Vila, B., Castenera, D., Flakingham, P.L., Barco, J.L., Canuda, J.I., Manning, P.L., Galobart, A. 2014. Intra-Trackway Morphological Variations Due to Substrate Consistency: The El Frontal Dinosaur Tracksite (Lower Cretaceous, Spain). *Plos one*, 9: p.e93708.

Reisz, R.R., Scott, D., Sues, H.D., Evans, C., Raath, M.A. 2005. Embryos of an Early Jurassic prosauropod dinosaur and their evolutionary significance. Science, 309: 761–764.

Roberts, E.M., Stevens, N.J., O'Connor, P.M., Dirks, P.H.G.M., Gottfried, M.D., Clyde, W.C., Armstrong, R.A., Kemp, A.I.S., Hemming, S. 2012. Initiation of the western branch 47 of the East African Rift coeval with the eastern branch. *Nature Geoscience,* 5 (4): 289–294.

Romano M., Citton, P. 2017. Crouching theropod at the seaside: Matching footprints with metatarsal impressions and theropod autopods: a morphometric approach. *Geological Magazine*, 154: 946–962.

Romer, A.S. 1966. Vertebrate paleontology. University of Chicago Press, Chicago.

Rowe, T., Gauthier, J. 1990. *Ceratosauria*. *In:* Weishampel, D. B., Dodson, P., Osmolska, H. (*Eds)*: The *Dinosauria*, 151–168, University of California Press, Berkeley.

Rubidge, B.S., Day, M.O., Barbolin, N., Hancox, P.J., Choiniere, J.N., Bamford, M.K., Viglietti, P.A., McPhee, B.W., Jirah, S. 2016. Advances in nonmarine Karoo biostratigraphy: Significance for understanding basin development. *In*: Linol, B., de Wit, M.J (*Eds*): Origin and Evolution of the Cape Mountains and Karoo Basin, 141–149. Springer International Switzerland.

Rubidge, B.S., Erwin, D.H., Ramezani, J., Bowring, S.A., de Klerk, W.J. 2013. High-precision temporal calibration of Late Permian vertebrate biostratigraphy: U-Pb constraints from the Karoo Supergroup, South Africa. *Geology*, DOI. 10.1130 G33622.1.

Rutherford, A.B., Rubidge, B.S., Hancox, P.J. 2015. Sedimentology and palaeontology of the Beaufort Group in the Free State Province supports a reciprocal foreland basin model for the Karoo Supergroup, South Africa. *South African Journal of Geology*, 118: 355–372.

Sander, P.M., Clauss, M. 2008. Sauropod gigantism. *Science*, 322: 200–201 DOI: 10.1126/science.1160904

Sarjeant, W.A.S. 1970. Fossil footprints from the Middle Triassic of Nottingham and the Middle Jurassic of Yorkshire. *American Geology,* 3: 269–282.

Sarjeant, W.A.S. 1989. Ten paleoichnological commandments: A standardized procedure for the description of fossil vertebrate footprints. In: Gillette, D.D., Lockley, M.G. (*Eds*): Dinosaur tracks and Traces, 369–370, Cambridge University Press, Cambridge.

Scheiber-Enslin, S.E., Ebbing, J., Webb, S.J. 2015. New depth maps of the main Karoo Basin, used to explore the Cape isostatic anomaly. *South African Journal of Geology*, 118: 225–248.

Schneider, C.A., Rasband, W.S., Eliceiri K.W. 2012. NIH Image to ImageJ: 25 years of image analysis. *Nature Methods*, 9: 671–675.

Schoene, B. 2014. U-Th-Pb Geochronology. DOI10.1016/B978-0-08-095975-7.00310-7

Schmidt, E.R. 1976. Clay. In: Coetzee, C (ed): Mineral resources of the Republic of South Africa. Fifth edition. Geological Survey of South Africa Pretoria Handbook 7:275–286.

Sciscio, L. 2016. Position of the Triassic-Jurassic boundary in South Africa and Lesotho: A multidisciplinary approach aimed at improving the chronostratigraphy and biostratigraphy of the Elliot Formation, Stormberg Group. PhD thesis (unpublished), University of Cape Town, 310p.

Sciscio, L., Bordy, E.M., Abrahams, M., Knoll, F., McPhee B.W. 2017b. The first megatheropod tracks from the Lower Jurassic upper Elliot Formation, Karoo Basin, Lesotho. *Plos ONE* 12(10): e0185941.

Sciscio, L., Bordy, E.M., Reid, M., Abrahams, M. 2016. Sedimentology and ichnology of the Mafube dinosaur track site (Lower Jurassic, eastern Free State, South Africa): a report on footprint preservation and palaeoenvironment. *Peer J*. p.e2285.

Sciscio, L., de Kock, M., Bordy, E.M., Knoll, F. 2017a. Magnetostratigraphy across the Triassic-Jurassic boundary in the main Karoo Basin. *Gondwana Research*, 51: 177–192.

Scrivner, P.J., Bottjer, D.J. 1986. Neogene avian and mammal tracks from Death Valley National Monument, California: their context, conservation and preservation. *Palaeogeography, Palaeoclimatology, Palaeoecology*, 57: 285–331.

Sereno, P.C. 1997. The origin and evolution of dinosaurs. *Annual Review of Earth Planetary Science,* 25: 435–489.

Sláma, J., Košler, J., Condon, D.J., Crowley, J.L., Gerdes, A., Hanchar, J.M., Horstwood, M.S.A., Morris, G.A., Nasdala, L., Norberg, N., Schaltegger, U., Schoene, B., Tubrett, M.N., Whitehouse, M.J. 2008. Plešovice zircon – a new natural reference material for U-Pb and Hf isotopic microanalysis. *Chemical Geology*, 241: 1–35.

Smith, J., Farlow, J. 1996. Were the track-makers for the dinosaur ichnotaxa *Grallator, Anchisauripus,* and *Eubrontes* really theropods? *In*: LeTourneau, P., Olsen, P. *(Eds)*: Aspects of Triassic-Jurassic rift basin geosciences: Abstracts. State Geological and Natural History Survey of Connecticut Miscellaneous Reports, 1: 46–47.

Smith, R.M.H. 1990. A review of the stratigraphy and sedimentary environments of the Karoo basin of South Africa. *Journal of African Earth Science*, 10: 117–137.

Smith, R. M., Kitching, J. 1997. Sedimentology and vertebrate taphonomy of the Tritylodon acmezone: a reworked palaeosol in the Lower Jurassic Elliot Formation, Karoo Supergroup, South Africa. *Palaeogeography, Palaeoclimatology, Palaeoecology*, 131(1): 29–50.

Smith, R.M.H., Marsicano, C.A. Wilson, J.A. 2009. Sedimentology and paleoecology of a diverse Early Jurassic tetrapod tracksite in Lesotho, southern Africa. *Palaios*, 24: 672–684.

Soergel, W. 1925. Die fahrten de Chirotheira. Jena Fisher 92 pp.

Spencer, C.J., Kirkland, C.L., Taylor, R.J.M. 2016. Strategies towards statistically robust interpretations of *in situ* U-Pb zircon geochronology. *Geoscience Frontiers,* 7: 584–589.

Spencer, C.J., Prave, A.R., Cawood, P.A., Roberts, N.M.W. 2014. Detrital zircon geochronology of the Grenville/Llano foreland and basal Sauk Sequence in west Texas, USA. *Geological Society of America Bulletin*, 126 (7e8), 1117e1128. http://dx.doi.org/10.1130/B30884.1.

Steiger, R.H., Jäger, E. 1977. Subcommission on geochronology: convention on the 804 use of decay constants in geo- and cosmochronology. *Earth and Planetary Science 805 Letters,* 36: 359–362.

Svensen, H., Corfu, F., Polteau, S., Hammer, Ø. and Planke, S., 2012. Rapid magma emplacement in the Karoo large igneous province. *Earth and Planetary Science Letters*, 325: 1–9.

Tagart, E. 1846. On markings in the Hastings sands near Hastings, supposed to be the footprints of Birds. *Quarterly Journal of the Geological Society of London,* 2: 267.

Tankard, A., Welsink, H., Aukes, P., Newton, R., Stettler, E. 2009. Tectonic evolution of the Cape and Karoo basins of South Africa. *Marine and Petroleum Geology*, 26(8): 1379–1412.

Tankard, A., Welsink, H., Aukes, P., Newton R., Stettler, E. 2012. Geodynamic interpretation of the Cape and the Karoo Basins, South Africa. Phanerozoic Passive Margins, Cratonic Basins and Global Tectonics Maps. USA and UK: Elsevier, 869–942.

Thulborn, R.A. 1984. Preferred gaits of bipedal dinosaurs. *Alcheringa*, 8:243–252.

Thulborn. R.A. 1989. The gaits of dinosaurs. *In*: Gillete, D.O., Lockley, M.G. (*Eds*): Dinosaur tracks and traces, 39–50, Cambridge University Press, Cambridge.

Thulborn, T. 1990. Dinosaur tracks. London: Chapman and Hall.

Thulborn, T. 1998. Australia's earliest theropods: footprint evidence in the Ipswich Coal Measures (Upper Triassic) of Queensland. *Gaia*, 1: 301–311.

Thulborn, T. 2017. Behaviour of Dinosaurian Track-Makers in the Winton Formation (Cretaceous, Albian–Cenomanian) at Lark Quarry, Western Queensland, Australia: Running or Swimming? *Ichnos,* 24: 1–18.

Thulborn, R.A., Wade, M. 1984. Dinosaur trackways in the Winton Formation (mid Cretaceous) of Queensland. *Memoirs of Queensland Museum*, 21: 413–517.

Tucker, R.T., Roberts, E.M., Hu Y, Kemp A.I.S., Salisbury I.S. 2013. Detrital zircon age constraints for the Winton Formation, Queensland: Contextualizing Australia's Late Cretaceous dinosaur faunas. *Gondwana Research*, 24: 767–779.

Turner, B.R. 1975. The stratigraphy and sedimentary history of the Molteno Formation in the main Karoo Basin of South Africa and Lesotho. Ph.D. thesis (unpublished), University of the Witwatersrand, Johannesburg, 314p.

Turner, B.R. 1983. Braidplain deposition of the Upper Triassic Molteno Formation in the main Karoo (Gondwana) Basin, South Africa. *Sedimentology*, 30: 77–89.

Turner, B.R. 1990. Continental sediments in south Africa. *Journal of African earth science*, 101: 139–149.

Turner B.R. 1999. Tectonostratigraphical development of the Upper Karoo foreland basin: orogenic unloading versus thermally-induced Gondwana rifting. *Journal of African earth science*, 28: 215–238.

Van Gend, V., Bordy, E.M., Tucker, R., McPhee, B. 2015.Maphutseng fossil heritage: stratigraphic context of the dinosaur trackways and bone bed in the Upper Triassic-Lower Jurassic Elliot Formation (Karoo Supergroup Lesotho).First international Congress on Continental Ichnology (ICCI 2015) Proceeds of abstracts, Faculty of Sciences, Chouaib Doukkali University, April 21-25, El Jadida, Morocco, p. 67.

Visser, J.N.J. 1987. The palaeogeography of part of southwestern Gondwana during the Permo-Carboniferous glaciation. *Palaeogrography, Palaeoclimatology, Palaeoecology*, 61: 205–219.

Visser, J.N.J. 1991. Geography and climatology of the Late Carboniferous to Jurassic Karoo Basin in south-western Gondwana. *Ann. S. afr. Mud*, 99: 415–431.

Visser, J.N.J., Botha B.J.V. 1980. Meander channel, point bar, crevasse splay and aeolian deposits from the Elliot Formation in Barkly Pass, North-Eastern Cape. *Transactions of the Geological Society of South Africa*, 83: 55–62.

Viglietti, P.A., Rubidge, B.S., Smith, R.M.H. 2017. New Late Permian tectonic model for South Africa's Karoo Basin: foreland tectonics and climate change before the end-Permian crisis. *Scientific Reports,* 7:10861. DOI:10.1038/s41598-017-09853-3

Von Huene, F. 1932: Die fossil Reptil-Ordnung Saurischia, ihre Entwicklung und Geschichte. *Monog. Geol. und Pal., Berlin,* 213–214.

Wagensommer, A., Latiano, M., Mocke, H.B., D'Orzai Porchetti, S., Wanke A. 2016. A dinosaur ichocoenosis from the Waterberg Plateau (Etjo Formation, Lower Jurassic), Namibia. *Ichnos*, 23: 312–321.

Warren, A., Jupp, R., Bolton, B. 1986. Earliest tetrapod trackway. *Alcheringa,* 10: 183–186.

Weems, R.E. 1992. A re-evaluation of the taxonomy of Newark Supergroup saurischian dinosaur tracks, using extensive statistical data from a recently exposed tracksite near Culpeper, Virginia. In: Sweet P.C (Ed): Proceedings of the 26th Forum on the Geology of Industrial Minerals, May 14–18, 113–127, Virginia Division of Mineral Resource Publication.

Weems, R.E. 2003. *Plateosaurus* foot structure suggests a single trackmaker for *Eubrontes* and *Gigandipus* footprints. *In*: LeTourneau, P.M., Olsen, P.E. (*Eds*): The great rift valleys of Pangea in eastern North America, volume 2, 293–313, Columbia University Press, New York.

Weems, R.E. 2006. The manus print of *Kayentapus* minor: its bearing on the biomechanics and ichnotaxonomy of early Mesozoic saurischian dinosaurs. *In:* Harris, J.D., Lucas, S.G., Spielmann, J.A., Lockley, M.G., Milner, A.R.C., Kirkland, J.I. (*Eds)*: The Triassic-Jurassic transition, 369–378, New Mexico Museum of Natural Science Bulletin 37, Albuquerque.

Weems, R.E. 2019. Evidence for bipedal Prosauropods as the likely *Eubrontes* track-makers. *Ichnos*, https://doi.org/10.1080/10420940.2018.1532902

Welles, S.P. 1971. Dinosaur footprints from the Kayenta Formation of northern Arizona. *Plateau*, 44: 27–38.

Welles, S. P. 1984. *Dilophosaur*us wetherilli (Dinosauria, Theropoda*)* osteology and comparisons. *Palaeontographica Abteilung A*, 185:85–180.

Wetherill, G.W. 1956. Discordant uranium–lead ages. T*ransactions of the American Geophysical Union,* 37: 320–326.

Wilson, J.A., Marsicano, C.A., Smith, R.M.H. 2009. Dynamic locomotor capabilities revealed by early dinosaur trackmakers from southern Africa. *Plos one*, 4(10): e7331. doi:10.1371/journal.pone.0007331

Wings, O., Lallensack, J.N., Mallison, H. 2016. The Early Cretaceous dinosaur trackways in Münchehagen (Lower Saxony, Germany): 3-D Photogrammetry as basis for geometric morphometric analysis of shape variation and evaluation of material loss during excavation. *In*: Falkingham, P.L., Marty, D., Richter, A. (*Eds*): Dinosaur tracks - the next steps, 56–71, Indiana university press, Bloomington and Indianapolis.

Wiseman, A.L.A. De Groote, I. 2018. A three-dimensional geometric morphometric study of the effects of erosion on the morphologies of modern and prehistoric footprints. *Journal of Archeaological Science* Reports 1, 17: 93–102.

Wright, J.L. 1996. Fossil terrestrial trackways: Function, taphonomy, and palaeoecological significance. Ph.D. thesis, University of Bristol.

Xing, L., Harris, J.D., Toru, S. Masato, F., Dong, Z. 2009. Discovery of dinosaur footprints from the lower Jurassic Lufeng Formation of Yunnan Province, China and new observations on *Changpeipus*. *Geological Bulletin of China*, 28: 16–28.

Xing, L.D., Lockley, M.G., Chen, W., Gierlinski, G.D., Li, J., Persons IV, W.S., Matsukawa, M., Ye, Y., Gingras, M.K., Wang, C. 2013. Two theropod track assemblages from the Jurassic of Chongqing, China, and the Jurassic Stratigraphy of Sichuan Basin. *Vertebrata Palasiatica*, 51:107–130.

Xing, L., Lockley, M.G., Klein, H., Zeng, R., Cai, S., Luo, X., Li, C. 2018. Theropod assemblages and a new ichnotaxon *Gigandipus chiappei* ichnosp. Nov. from the Jiaguan Formation, Lower Cretaceous of Guizhou Province, China. *Geoscience Frontiers*, 1745–1754. https://doi.org/10.1016/j.gsf.2017.12.012

Yates, A.M. 2005. A new theropod dinosaur from the Early Jurassic of South Africa and its implications for the early evolution of theropods. *Palaentologia Africana*, 41: 105–122.

Comparative ichnogenera database (reference material): Landmark-based PCA

The morphology of tracks from the upper Stormberg Group considered in this study were compared to tracks with a global distribution from published literature using a land-mark based PCA approach. Below, are the sources of track photographs used for this comparative analysis. The figures considered and the ichnotaxonomic assignment made by the relevant authors are noted.

Foster, J.R. 2015. Theropod dinosaur ichnogenus *Hispanosauropus* identified from the Morrison Formation (Upper Jurassic, western North America. *Ichnos*, 22:3-4, 183-191, DOI: 10.1080/10420940.2015.1059335

Fig. 3 B, C; Fig. 5B, D, E (*Megalosauripus, Irenesauripus, Carmelopodus*)

Niedzwiedzkli, G., Remin, Z. 2008. Giant theropod dinosaur footprints from the Upper Pliensbachian of the Holy Cross Mountain, Poland. *Pzeglad Geologizny*, 56: 823–825.

Fig. 1B, E (*Megalosauripus*)

Gierlinski, G. 1990. New dinosaur ichnotaxa from the Early Jurassic of the Holy Cross Mountains, Poland. *Palaeogeography, Palaeoclimatology, Plaeoecology*, 85: 137–148. https://doi.org/10.1016/0031-0182(91)90030-U

Fig. 2A, B (*Grallator*)

Gierlinski, G.D., Lagnaoui, A., Klein, H., Saber, H., Oukassou, M., Charriere, A. 2017. Bird-like traks from the Imilchil Formation (Middle Jurassic, Bajocian-Bathonian) of Central High Atlas, Morocco, in comparison with similar Mesozoic tridactylous ichnotaxa. *Bolletino della Societa Paleontological Italiana*, 56: 207–215.

Fig. 2A, B, C, D (*Trisauropodiscus*); Fig. 4B, C (*Anomoepus, Moyenisauropus*); Fig. 6A, B (*Carmelopodus*)

Gierlinksi, G.D., Meducki, P., Janiszewska, Wicik, I., Boczarowski, A. 2009. A preliminary report on dinosaur track assemblages from the Middle Jurassic of the Imilchil area, Morocco. *Geological Quarterly*, 53: 477–482.

Fig. 3B, D, E (*Jialingpus, Carmelopodus, Dinehichnus)*

Gierlinski, G., Pienkowski, G., Niedzwiedzki, G. 2004. Tetrapod track assemblage in the Hettangian of Soltykow Poland and its Paleoenvironmental background. *Ichnos,* 11: 195–213.

Fig. 8A, B (*Kayentapus, Eubrontes*); Fig. 11B, C (*Grallator, Stenonyx*)

Lockley, M.G., Gierlinski, G.D., Lucas, S.G. 2011. *Kayentapus* Revisited: notes on the type material and the importance of this theropod footprint ichnogenus. *In*: Sullivan *et al.* (eds), Fossil record 3. *New Mexico Museum of Natural History and Science Bulletin*, 53: 330–336.

Fig. 3 (1-5) (*Kayentapus*)

Lockley, M.G., Meyer, C.A., Moratalla, J.J. 1998. *Therangospodus*: trackway evidence for the widespread distribution of a Late Jurassic theropod with well-padded feet. *Gaia*, 15: 339–353.

Fig. 1A, B, C, E, F (*Therangospodus*)

Marty, D., Belvedere, M., Razzolini, N.L., Lockley, M.G., Paratte, G., Cattin, M., Lovis, C., Meyer,C.A. 2017. The true tracks of giant theropods (*Jurabrontes curtedulensis* ichnogen. & ichnosp. Nov.) from the Late Jurassic of NW Switzerland: palaeoecological and palaeogeographical implications. *Historical Biology,* DOI:10.1080/08912963.2017.1324438

Fig. 5B; Fig. 6K (*Jurabrontes*)

Niedzwiedzki, G. 2011. A Late Triassic dinosaur-dominated ichnofauna from the Tomanova Foramation of the Tatra Mountains, Central Europe. *Acta Palaeontologica Polonica*, 56: 291–300. https://doi.org/10.4202/app.2010.0027

Fig. 4A, C (*Kayentapus*)

Olsen, P.E., Smith, J.B., McDonald, N.G. 1998. Type material of the type species of the classic theropod footprint genera *Eubrontes*, *Anchisaurpus* and *Grallator* (Early Jurassic, Hartford and Deerfield Basins, Connecticut and Massachusetts, USA). *Journal of Vertebrate Paleontology*, 18: 586–601.

Fig. 7 (Anchisauripus); Fig. 8 (*Anchisauripus*); Fig. 10 (*Grallator*); Fig. 15C (*Anchisauripus*)

Rauhut, O.W.M., Piñuela, Castanera, D., Garcia-Ramos, J-C., Sachez Cela, I. 2018. The largest theropod dinosaurs: remains of a gigantic megalosaurid and giant theropod tracks from the Kimmeridgian of Austrias, Spain. *PeerJ*, DOI 10.7717/peerj.4963

Fig. 5A, D; Fig. 6A

Razzolini, N.L., Belvedere, M., Marty, D., Paratte, G., Lovis, C., Cattin, M., Meyer, C.A. 2017. *Megalosauripus trasjuranicus* ichnosp. Nov. A new Late Jurassic ichnotaxon from NW Switzerland and implications for tridactyl dinosaur ichnology and ichnotaxonomy. *Plose one*, 12(7): e0180289. https://doi.org/10.1371/journal.pone.0180289

Fig. 4A, B, C (*Megalosauripus*)

Smith, R.M.H., Marsicano, C.A., Wilson, J.A. 2009. Sedimentology and paleoecology of a diverse Early Jurassic tetrapod tracksite in Lesotho, southern Africa. *Palaios*, 24: 672–684.

Fig. 11 (*Grallator*)

Welles, S.P. 1991. Dinosaur footprints from the Kayenta Formation of northern Arizona. *Plateau*, 44: 27–38.

Fig. 2 (*Kayentapus*)

Xing, L., Peng, G-Z., Ye, Y., Lockley, M.G., McCrea, R.T., Currie, P.J., Zhang, J-P., Burns, M.E. 2014. Large theropod trackway from the Lower Jurassic Zhenzhuchong Formation of Weiyun County, Sichuan Province, China: Review, new observations and special preservation. *Palaeoworld*, 23: 285–293.

Fig. 4C, F (*Eubrontes*); Fig. 5A, B, C, D (*Eubrontes*)

Comparative ichnogenera database (reference material): Measurement-based PCA

The dimensions of tracks from the upper Stormberg Group considered in this study were compared to the dimensions of tracks with a global distribution from published literature. Below, are the sources of track data used for this comparative analysis. The data table numbers from the relevant publications are included.

Xing, L., Peng, G., Ye, Y., Lockley, M.G., Klein, H., Scott Persons IV, W., Zhang, J., Shu, C., Hao, B. 2014. Sauropod and Small Theropod Tracks from the Lower Jurassic Ziliujing Formation of Zigong City, Sichuan, China, with an Overview of Triassic–Jurassic Dinosaur Fossils and Footprints of the Sichuan Basin. *Ichnos*, 21: 119–30, DOI: 10.1080/10420940.2014.909352

Table 1

Cook, A.G., Saini, N., Hocknull, S.A. 2009. Dinosaur footprints from the Lower Jurassic of Mount Morgan, Queensland. *Memoirs of the Queensland Museum — Nature,* 55:135–146.

Table 1

Xing, L., Lockley, M.G., Zhanf, J-P., Klein, H., Kummelll, S.B., Scott Pearson IV, W., Kua ng, H-W. 2017. Theropod tracks from the Lower Jurassic of Gulin area, Sichuan Province, China. *Palaeoworld*, 26: 115–123.

Table 1

Olsen, P.E., Smith, J.B., McDonald, N.G. 1998. Type material of the type species of the classic theropod footprint genera *Eubrontes*, *Anchisauripus* and *Grallator* (Early Jurassic, Hartford and Deerfield Basins, Connecticut and Massachusetts, USA). *Journal of Vertebrate Paleontology*, 18: 586–601.

Table 2

Weems, R.E. 1992. A re-evaluation of the taxonomy of Newark Supergroup saurischian dinosaur tracks, using extensive statistical data from a recently exposed tracksite near Culpeper, Virginia. Publication 119.

Table 2

Demathieu, G., Gand, G., Sciau, J., Freytet, P. 2014. Les traces de pas de dinosaurs et autres archosaures du lias inferieur des Grands Causses, Sud de la France. *Palaeovertebrata, Montpellier,* 31: 1–143.

Table 30

10 Appendices

Appendix A: Track database

All datasets mentioned as Appendix A in the text of this thesis can be found at 10.6084/m9.figshare.12115521 an opensource online data repository hosted at Figshare. The available data on Figshare include:

five supplementary figures and ten supplementary table. The supplementary tables are within a single MS Excel spreadsheet, with each individual table saved on a separate tab.

1. Figure A.1– Track dimension-based PCA plots and accompanying loading plots for individual sites considering tracks with complete track datasets (excluding digit lengths and digit divarication angles; PDF file).
2. Figure A.2– Landmark-based PCA loading plots and accompanying vector deformation diagrams for select Stormberg Group tracks, within tracksites, that have a complete, defined tridactyl morphology (PDF file).
3. Figure A.3– Overview photographs and interpretive outlines or false depth maps of individual tracks from the Stormberg Group database (PDF file).
4. Figure A.4– Loadings from PCA of the upper Stormberg Group within stratigraphic groupings, A) PCA loadings using measurements with a correlation matrix applied, B) PCA loadings using log transformed, mean subtracted data with a variance-covariance matrix applied, C) PCA

loadings using Procrustes fitted landmarks with a variance-covariance matrix applied (PDF File).

5. Figure A.5– Loadings for measurement based PCA for upper Stormberg Group tracks by size class groupings. A) PCA loadings using raw measurements with a
   correlation matrix applied, B) PCA loadings using data normalised relative to TL with a variance-covariance matrix applied (PDF File).
6. Table A.1– Measured track dimensions, morphological grade and landmark-based ichnotaxonomic assignment for the upper Stormberg Group tracks considered in this study (MS Excel file).
7. Table A.2– Landmark co-ordinate data for select upper Stormberg Group tracks considered for land-mark based PCA (relates to Appendix Figure A.2; MS Excel file).
8. Table A.3– Correlation matrices for measured track parameters for the upper Stormberg Group database excluding considered ratios (MS Excel file).
9. Table A.4– Summary of statistical normality tests (Shapiro-Wilk, Anderson-Darling and Jarque-Bera tests). P-values highlighted in red reject the null hypothesis i.e., data does not follow a normal trend (MS Excel file).
10. Table A.5 Summary of statistical normality tests for normalised data by stratigraphic grouping (Shapiro-Wilk, Anderson-Darling and Jarque-Bera tests). P-values highlighted in red reject the null hypothesis i.e., data does not follow a normal trend (MS Excel file).
11. Table A.6 Summary of statistical normality tests for normailsed data by size groupings (Shapiro-Wilk, Anderson-Darling and Jarque-Bera tests). P-values highlighted in red reject the null hypothesis i.e., data does not follow a normal trend (MS Excel file).
12. Table A.7– Means and accompanying standard deviations, and medians with accompanying interquartile information for tracks within stratigraphic groupings from the Stormberg database with complete track dimension datasets (MS Excel file).
13. Table A.8– Means and accompanying standard deviations, and medians with accompanying interquartile information for tracks within track length groupings from the Stormberg database with complete track dimension datasets (MS Excel file).
14. Table A.9– Detailed discriminant analysis results distinguishing tracks by their stratigraphic position based on their individual linear measurements excluding digit lengths. Data has not been Jack-Knifed (MS Excel file).
15. Table A.10– Detailed discriminant analysis results distinguishing tracks by their stratigraphic position based on their individual linear measurements including digit lengths. Data has not been Jack-knifed (MS Excel file).

16. Table A.11– Detailed discriminant analysis results distinguishing tracks by their size class groupings based on their individual linear measurements excluding track length and digit lengths. Data has not been Jack-knifed (MS Excel file).
17. Table A.12– Detailed discriminant analysis results distinguishing tracks by their size class groupings based on their individual linear measurements excluding track length and including digit lengths. Data has not been Jack-knifed (MS Excel file).

Appendix B: U-Pb LA-ICPMS dating

All datasets mentioned as Appendix B in the text of this thesis can be found at 10.6084/m9.figshare.12115527 an opensource online data repository hosted at Figshare. The available data on Figshare include:

1. Figure B.1– Cathodolumisence images illustrating individual zircon crystal morphologies and internal structures for each sample collected for U-Pb LA-ICPMS dating (PDF file).
2. Table B.1– Complete dataset of geochronological measurements for each sample and standards (MS excel file).